6205
U58
and o NOV 9 - 1932
B97

U. S. DEPARTMENT OF COMMERCE

BUREAU OF STANDARDS JOURNAL OF RESEARCH

Vol. 9 SEPTEMBER, 1932 No. 3

CONTENTS

RP. No.	TITLE AND AUTHOR	Page
471.	A new determination of the atomic weight of osmium. Raleigh Gilchrist	279
472.	"Moisture expansion" of ceramic whiteware. R. F. Geller and A. S. Creamer	291
473.	Infra-red arc spectra photographed with xenocyanine. W. F. Meggers and C. C. Kiess	309
474.	Tensile properties of cast nickel-chromium-iron alloys and of some alloy steels at elevated temperatures. William Kahlbaum and Louis Jordan	327
475.	The comparison of high voltage X-ray generators. Lauriston S. Taylor and K. L. Tucker	333
476.	The structure of the chromic acid plating bath; the theory of chromium deposition. Charles Kasper	353
477.	Physical properties and weathering characteristics of slate. D. W. Kessler and W. H. Sligh	377
478.	Radiation from cæsium and other metals bombarded by slow electrons. C. Boeckner	413
479.	A simplified precision formula for the inductance of a helix with corrections for the lead-in wires. Chester Snow	419
480.	Register studies in offset lithography. C. G. Weber and R. M. Cobb	427
481.	Creep at elevated temperatures in chromium-vanadium steels containing tungsten or molybdenum. William Kahlbaum and Louis Jordan	441

BUREAU OF STANDARDS JOURNAL OF RESEARCH

CONTENTS OF RECENT NUMBERS

March, 1932 (Vol. 8, No. 3)

RP416. Heat vaporization of water at 50°, 70°, and 90° C. E. F. Fiock and D. C. Ginnings. Price, 5 cents.

RP417. Note on international comparison of X-ray standards. Lauriston S. Taylor. Price, 5 cents.

RP418. The course of the oxidation of the aldose sugars by bromine water. H. S. Isbell and C. S. Hudson. Price, 5 cents.

RP419. Fluctuations of the rate of emissions of α particles for weak sources and large solid angles. L. F. Curtiss.

RP420. Gases obtained from commercial feldspars heated in vacuo. G. R. Shelton and H. H. Holscher. Price, 5 cents.

RP421. Experiments on the emission and absorption of radiation by metallic silver. F. L. Mohler.

RP422. Accelerated weathering tests of soldered and tinned sheet copper. Peter R. Kosting. Price, 10 cents.

RP423. The chromium oxide and the vanadium oxide band spectra. W. F. C. Ferguson. Price, 5 cents.

RP424. Air density corrections for X-ray ionization chambers. Lauriston S. Taylor and George Singer.

RP425. The arc spectrum of phosphorus. C. C. Kiess. Price, 10 cents.

RP426. Some physical properties of levulose and its estimation by copper reduction methods. Richard F. Jackson and Joseph A. Mathews. Price, 10 cents.

April, 1932 (Vol. 8, No. 4)

RP427. The optical requirements of airplane mapping. I. C. Gardner. Price, 5 cents.

RP428. Note on the moving boundary method for measuring transference numbers. A pycnometer for determining the volume change occurring at an electrode and its application to a cathode of silver chloride in a solution of potassium chloride. E. R. Smith. Price, 5 cents.

RP429. Radio field intensity measurements at frequencies from 285 to 5,400 kilocycles per second. S. S. Kirby and K. A. Norton. Price, 5 cents.

RP430. The photographic emulsion: Silver ion and hydrogen ion concentrations and sensitivity. Burt H. Carroll and Donald Hubbard. Price, 10 cents.

RP431. Capacitance and power factor of a mica capacitor as measured at the Bureau of Standards and the National Physical Laboratory. Harvey L. Curtis, C. Matilda Sparks, L. Hartshorn, and N. F. Astbury. Price, 5 cents.

RP432. Isolation and determination of normal heptane and of methylcyclohexane in a mid-continent petroleum. Including a determination of the phase equilibrium diagram for the condensed system normal heptane-methylcyclohexane. Mildred M. Hicks-Bruun and Johannes H. Bruun. Price, 5 cents.

RP433. The spectral erythemic reaction of the untanned human skin to ultra-violet radiation. W. W. Coblentz, R. Stair, and J. M. Hogue.

May, 1932 (Vol. 8, No. 5)

RP434. A contribution relative to the structure of collagen. John Beek, jr.

RP435. Graphical determination of polar pattern of directional antenna systems. G. L. Davies and W. H. Orton.

RP436. Manufacture of calcium gluconate by the electrolytic oxidation of dextrose. Horace S. Isbell, Harriet L. Frush, and F. J. Bates.

RP437. Simplified automatic Wilson chamber. L. F. Curtiss.

RP438. Ionization of normal decane from petroleum by distillation and equilibrium melting. Johannes H. Bruun and Mildred M. Hicks-Bruun.

RP439. A laboratory apparatus for the continuous extraction of liquids by low boiling solvents. R. T. Leslie.

RP440. Volume changes of cast irons during casting. E. J. Ash and C. M. Saeger, jr.

RP441. A study of the delta lactones by the oxidation of aldoses with bromine water. Horace S. Isbell.

RP442. Effect of antimony on the mechanical properties of a bearing bronze (Cu 80 : Sn 10 : Pb 10). C. E. Eggenschwiler.

Research papers, where price is given, are already available, and others will be available in the near future as separates for purchase from the Superintendent of Documents, United States Government Printing Office, Washington, D. C.

U. S. DEPARTMENT OF COMMERCE
ROY D. CHAPIN, Secretary
BUREAU OF STANDARDS
LYMAN J. BRIGGS, Acting Director

BUREAU OF STANDARDS JOURNAL OF RESEARCH

September, 1932
Vol. 9, No. 3

UNITED STATES
GOVERNMENT PRINTING OFFICE
WASHINGTON : 1932

For sale by the Superintendent of Documents, Washington, D. C. - - Price 25 cents; $2.50 per year on subscription

For a partial list of previous research papers appearing in BUREAU OF STANDARDS JOURNAL OF RESEARCH see pages 2 and 3 of the cover

A NEW DETERMINATION OF THE ATOMIC WEIGHT OF OSMIUM [1]

By Raleigh Gilchrist

ABSTRACT

A method for the preparation of pure osmium is described. The value of the atomic weight of osmium is calculated from the average percentage of osmium found in carefully prepared samples of ammonium chloroosmate and of ammonium bromoosmate. The value obtained from the ratio $(NH_4)_2OsCl_6$: Os is 191.53, and from the ratio $(NH_4)_2OsBr_6$: Os is 191.57, based upon the values for nitrogen, hydrogen, chlorine, and bromine given in the International Table of Atomic Weights for 1932. The weighted average value is 191.55.

The densities of ammonium chloroosmate and of ammonium bromoosmate at 25° C. were found to be 2.93 g/cm³ and 4.09 g/cm³, respectively.

CONTENTS

	Page
I. Introduction	279
II. Preparation of pure osmium	280
1. Extraction of osmium from crude material	280
2. Purification of the osmium	280
III. Preparation of reagents	281
IV. Preparation of ammonium chloroosmate	282
V. Preparation of ammonium bromoosmate	284
VI. Determination of the osmium content of ammonium chloroosmate and of ammonium bromoosmate	285
1. Apparatus	285
2. Balances, weights, and weighing	285
3. Analysis	287
4. Densities of the substances weighed	288
5. Results	289
VII. Discussion of results	289
VIII. Acknowledgments	290

I. INTRODUCTION

Osmium was first identified as a new element by Tennant,[2] who discovered it in the portion of crude platinum which is not attacked by aqua regia. Osmium occurs as a constituent of a natural alloy with iridium known as osmiridium or iridosmine. The name osmium, which was chosen for the element, was taken from the Greek, *οσμή*, a smell, suggestive of the pronounced odor of the volatile tetroxide, the formation of which is the most outstanding property of the metal.

The earliest attempt to determine the atomic weight of osmium was made by Berzelius,[3] who analyzed potassium chloroosmate, K_2OsCl_6, and obtained the value 198.94 from the ratio Os:2 KCl.

Seubert,[4] 60 years later, undertook to make careful analyses of potassium chloroosmate and of ammonium chloroosmate, $(NH_4)_2\ OsCl_6$,

[1] Submitted as partial fulfillment of the requirements for the degree of doctor of philosophy, The Johns Hopkins University, June 1922.
[2] Smithson Tennant, Phil. Trans., vol. 94, p. 411, 1804.
[3] J. J. Berzelius, Ann. Physik (Pogg.), vol. 13, p. 530, 1828.
[4] K. Seubert, Ber., vol. 21, p. 1839, 1888; Ann., vol. 261, p. 258, 1891.

and it is upon his experiments that the value of the atomic weight was based which has appeared in the International Table of Atomic Weights for many years. Seubert used the ratios $(NH_4)_2OsCl_6$:Os; $6AgCl:(NH_4)_2OsCl_6$; K_2OsCl_6:Os; K_2OsCl_6:2 KCl; and $4\ AgCl:K_2OsCl_6$. The values obtained for the atomic weight range from 190.27 to 192.22 when recalculated on the basis of the International Table of Atomic Weights for 1932. The value calculated from Seubert's experiments on the osmium content of ammonium chloroosmate is 191.24.

In the last 41 years only one published account of new work on the atoic mweight of osmium has appeared, that of Seybold[5], describing the determination of the osmium content of ammonium chloroosmate. The value calculated from a set of three experiments is 191.09, while that from five other experiments is 189.33.

II. PREPARATION OF PURE OSMIUM

1. EXTRACTION OF OSMIUM FROM CRUDE MATERIAL

The osmium used in the experiments reported in this paper was obtained from two sources. That used in ammonium chloroosmate, Series VI, was obtained from one of the platinum companies, while that used in the other experiments was recovered from the osmiridium residues from grain platinum.

The crude material was fused with sodium hydroxide and sodium nitrate in a gold dish. The aqueous extract of this melt was acidified with nitric acid and distilled. The osmium tetroxide thus obtained was absorbed in a 10 per cent solution of sodium hydroxide and again distilled as just described. The remaining platinum metals,[6] under these conditions, do not appear in the distillate. The osmium was recovered by electrolysis from the alkaline solution, into which the tetroxide had been distilled the second time, using platinum electrodes. The osmium separated at the cathode as a black, loosely adherent deposit which, according to Moraht and Wischin,[7] is the dioxide. The precipitated material was washed as free from alkali as possible, dried, and ignited to metal in hydrogen. Spectrographic examination of the metal thus obtained showed that it was free from the other platinum metals, but that it did contain traces of sodium and of iron.

2. PURIFICATION OF THE OSMIUM

In considering possible reactions feasible for the preparation of pure osmium, it appeared highly desirable to employ volatile reagents. The reaction between osmium tetroxide and hydrochloric acid had been studied by Milbauer,[8] who observed that osmium tetroxide was decomposed by concentrated hydrochloric acid at room temperature with the evolution of chlorine. Ruff and Mugdan,[9] however, using acid of specific gravity 1.124, stated that the reaction reported by Milbauer did not take place. A few years later, Remy[10] made a careful study of the reaction at room temperature and concluded that the reaction depends considerably upon the concentration of the

[5] F. Seybold, Inaugural-Dissertation, 1912, Friederich-Alexanders Universität, Erlangen.
[6] R. Gilchrist, B. S. Jour. Research, vol. 6, p. 421, 1931.
[7] H. Moraht and C. Wischin, Z. anorg. Chem., vol. 3, p. 153, 1893.
[8] J. Milbauer, J. prakt. Chem. (2), vol. 96, p. 187, 1917.
[9] O. Ruff and S. Mugdan, J. prakt. Chem. (2), vol. 98, p. 143, 1918.
[10] H. Remy, J. prakt. Chem. (2), vol. 101, p. 341, 1921.

hydrochloric acid. He found that with hydrochloric acid of specific gravity greater than 1.160 the osmium tetroxide was decomposed with appreciable velocity, with the evolution of chlorine. He further found that the osmium was converted to the quadrivalent state and not to the bivalent, as asserted by Milbauer. Krauss and Wilken[11] later substantiated Remy's conclusion regarding the quadrivalent state.

In a recent study by Crowell[12] of the reaction between octavalent osmium and hydrobromic acid at 100° C., it was found that the products formed are quadrivalent osmium and bromine and that an equilibrium is reached. It was also found that in concentrated hydrobromic acid (about 8 normal) the reaction goes to practical completion in the direction of the formation of quadrivalent osmium and bromine, while in dilute acid solutions (about 0.1 normal) the reaction goes to completion in the reverse direction.

In 1920, previous to the appearance of Remy's paper, the author observed that reaction occurred when a mixture of osmium tetroxide and 20 per cent[13] hydrochloric acid (constant-boiling acid) was heated to incipient boiling and that the presence of a small quantity of ethyl alcohol assisted in the decomposition of the tetroxide. After about three hours the odor of osmium tetroxide disappeared and the solution, which had gradually turned deep brown in color, became reddish yellow and transparent. This solution, when evaporated to sirupy consistency, appeared to suffer no decomposition. Ammonium chloride, added to an acid solution of the sirupy residue, precipitated the brick red ammonium chloroosmate, $(NH_4)_2OsCl_6$. Ignition of the precipitate in hydrogen produced metallic osmium in the spongy form. It was further observed that the reaction between osmium tetroxide and 20 per cent hydrobromic acid proceeded with greater ease and rapidity than that between osmium tetroxide and hydrochloric acid. Considerable bromine was produced. Enough alcohol was added just to destroy the bromine vapor in the refluxing flask. The resulting solution was deep brown in color and likewise appeared to suffer no decomposition on evaporation to a sirup. Ammonium bromide precipitated the deep brownish black ammonium bromoosmate, $(NH_4)_2OsBr_6$, from an acid solution of the sirupy residue.

The osmium metal obtained by reduction of the product of electrolysis previously described was converted in turn into osmium tetroxide, chloroosmic acid, ammonium chloroosmate, and osmium sponge as will be described in detail in connection with the preparation of the compounds for analysis. This cycle of operations was repeated twice, using purified reagents. The resulting metal was found on spectrographic examination to be free from impurities and was used in the final preparation of the compound ammonium chloroosmate.

III. PREPARATION OF REAGENTS

Hydrochloric acid.—Chemically pure hydrochloric acid of commerce (specific gravity 1.18) was diluted with an equal volume of distilled water and distilled three times from a ground-glass stoppered Pyrex flask whose side arm extended a considerable distance into the tube of a condenser. In each case the first and last fractions were discarded.

[11] F. Krauss and D. Wilken, Z. anorg. allgem. Chem., vol. 137, p. 349, 1924.
[12] W. R. Crowell, J. Am. Chem. Soc., vol. 54, p. 1324, 1932.
[13] Here and elsewhere in this paper the percentage of acid is percentage by weight.

Bromine and hydrobromic acid.—Chemically pure bromine of commerce was purified by the procedure described by Baxter and Grover.[14] Hydrobromic acid was prepared by reducing bromine with hydrogen in the presence of a catalyst consisting of pumice impregnated with platinum. The hydrogen was produced by electrolysis in a cell described later. The first portion of the hydrobromic acid was discarded. The remainder was dissolved in water and distilled once.

Ammonium chloride.—Ammonium hydroxide, which had been freshly prepared by saturating distilled water with ammonia from a cylinder of liquid ammonia, was gently heated and the ammonia conducted into the purified hydrochloric acid until the acid was neutralized. A slight excess of acid was then added to the solution of ammonium chloride.

Ammonium bromide.—Ammonium bromide was prepared in the same manner as the ammonium chloride.

Alcohol.—Ethyl alcohol of commerce (95 per cent) was allowed to remain in contact with lime for several days, after which it was distilled three times. The first and last portions from each distillation were discarded.

Water.—In the preliminary work, the water used was purified by distilling from an alkaline permanganate solution and then from a

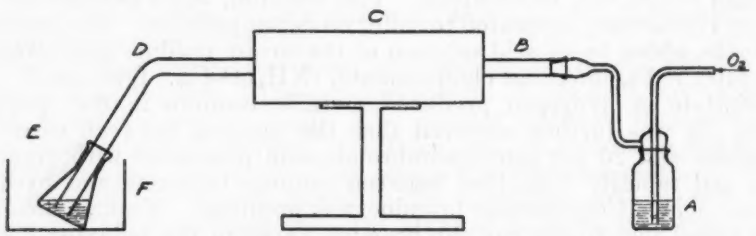

FIGURE 1.—*Apparatus for the preparation of osmium tetroxide*

dilute sulphuric acid solution, using a Pyrex distilling flask and a block-tin condenser. The preparation reported as ammonium chloroosmate, Series VI, was likewise made with water thus prepared. In the other three preparations reported, the water used was that which was regularly supplied to the chemical laboratories at the Bureau of Standards from a still by a pipe of block tin. This water gave no test for halides and had a specific conductance of about 1×10^{-6} reciprocal ohm at room temperature.

IV. PREPARATION OF AMMONIUM CHLOROOSMATE

Preparation VI.—Osmium, which had been prepared from the material obtained from one of the platinum companies as described in Section II, was converted to osmium tetroxide by heating it in a current of oxygen. Figure 1 shows the apparatus used. A bottle, *A*, containing water, served to indicate the flow of oxygen. A tube, *B*, of combustion glass, having a diameter of about 2.5 cm, was bent at an angle and the end inserted into a Pyrex flask which contained purified constant-boiling hydrochloric acid. The flask and contents were cooled by immersion in crushed ice in order to prevent too great a loss of osmium tetroxide. The combustion tube was heated by a

[14] G. P. Baxter and F. L. Grover, J. Am. Chem. Soc., vol. 37, p. 1029, 1915.

12-inch Hoskins electric furnace of the split type. When heated to a temperature of from 220° to 230° C. the osmium, contained in porcelain boats, absorbed oxygen rapidly and reached a glowing temperature. This rapid absorption of oxygen was repeatedly observed and probably indicated the formation of osmium dioxide. As the temperature was raised the oxidized osmium was converted to tetroxide which condensed to a pale yellowish mass, as well as to white crystals, in the cooler portion of the combustion tube. Gentle warming of the tube with a flame loosened the solidified tetroxide, while a jet of hot hydrochloric acid solution from a wash bottle completely removed all tetroxide from the tube as it was lifted from the flask.

The contents of the flask, consisting of osmium tetroxide and hydrochloric acid, were quickly transferred [15] to a refluxing flask to which a water-cooled condenser was attached by a ground joint. A U tube containing a solution of sodium hydroxide was attached to the top of the condenser to prevent the escape of any tetroxide vapor. A quantity of purified constant-boiling hydrochloric acid, four times the amount necessary to form chloroosmic acid, H_2OsCl_6, was added to the refluxing flask. From 3 to 5 ml of purified alcohol was added, and the mixture gently heated for one hour. During this time the color changed from faint yellow to deep brown. As heating was continued, droplets of osmium tetroxide gradually ceased to appear on the walls of the flask and the solution finally became reddish yellow in color and transparent. The total time of heating was about three hours, during the last hour of which the solution was kept at incipient boiling. The solution of chloroosmic acid which had been formed was evaporated to a sirup on the steam bath. On cooling, the sirupy solution solidified to a mass of crystals. These crystals were dissolved in purified constant-boiling hydrochloric acid and the resulting solution diluted with water so as to form a solution containing 4 per cent of osmium and 7 per cent of hydrochloric acid. This solution was filtered first through hardened paper, in a Gooch crucible, and then through blue ribbon paper (S. and S. No. 589).

A 15 per cent solution of purified ammonium chloride, in slight excess, was added slowly to the constantly stirred solution of chloroosmic acid at room temperature. The precipitate of ammonium chloroosmate, brick red in color, was caught on a hardened filter in a Gooch crucible and washed with a 15 per cent solution of purified ammonium chloride until the wash waters were colorless. The ammonium chloroosmate thus prepared was recrystallized by making a saturated solution of the compound in a solution containing 7 per cent of hydrochloric acid at about 90° C. The hot saturated solution was quickly filtered through a hardened filter and cooled to about 5° C. while being stirred. The supernatant liquid was decanted and the crystals of ammonium chloroosmate stirred with several portions of 7 per cent hydrochloric acid. The crystals were then caught on a hardened filter, in a Gooch crucible, drained by suction, washed with a dilute solution of hydrochloric acid, and finally washed with purified alcohol. The crystals were drained free from alcohol, spread on a watch glass and dried in a partially evacuated desiccator containing phosphorus pentoxide. The dried salt was thoroughly mixed by grinding in an agate mortar and kept in a desiccator until used.

[15] It is, perhaps, needless to mention that an operation of this kind should be conducted with care and that it is preferable to wear a mask to prevent the vapor of the tetroxide from attacking the eyes, nose, and throat of the operator.

Preparation VII.—Osmium, which had been prepared from osmiridium residues from grain platinum as described in Section II, was converted into chloroosmic acid. A solution of the chloroosmic acid was made which contained 1.5 per cent of osmium and 1.7 per cent of hydrochloric acid. This solution was slowly added, at room temperature, to a dilute solution (approximately 2 per cent) of purified ammonium chloride which was constantly stirred, according to one of the procedures used by Archibald [16] in the preparation of ammonium chloroplatinate. The precipitate of ammonium chloroosmate was not recrystallized, but was washed, dried, and mixed as described under Preparation VI.

V. PREPARATION OF AMMONIUM BROMOOSMATE

Preparation VI.—The ammonium bromoosmate was made from the osmium sponge [17] resulting from the analyses of ammonium chloroosmate. The source of the osmium was the osmiridium residues from grain platinum. This osmium was first converted into tetroxide as previously described, then into bromoosmic acid, ammonium bromoosmate, and again into metal using purified reagents. The metal prepared by this cycle of reactions was again converted into bromoosmic acid. The resulting solution of bromoosmic acid was evaporated to a sirup on the steam bath, then evaporated twice more with 20 per cent hydrobromic acid. The crystalline mass was dissolved in 20 per cent hydrobromic acid and diluted with water to form a solution containing 1.5 per cent of osmium in 7 per cent of hydrobromic acid. This solution was filtered twice through filter paper (S. and S. No. 589, blue ribbon). A 2 per cent solution of purified ammonium bromide, in slight excess, was added slowly to the constantly stirred solution of bromoosmic acid at room temperature. The precipitate of ammonium bromoosmate, deep brownish black in color, was caught on a hardened filter and washed with a 15 per cent solution of ammonium bromide until the wash waters were colorless. The compound thus prepared was recrystallized by making a saturated solution of it in a solution containing 15 per cent of hydrobromic acid at about 90° C. The hot saturated solution was quickly filtered through a hardened filter and cooled to about 10° C. while being stirred. The supernatant liquid was decanted and the crystals washed with 7 per cent hydrobromic acid. The crystals were then caught on a hardened filter, in a Gooch crucible, drained by suction, washed with a dilute solution of hydrobromic acid and finally washed with purified alcohol. The crystals were drained free from alcohol and dried over phosphorus pentoxide. The dried salt was then thoroughly mixed by grinding it in an agate mortar and kept in a desiccator over phosphorus pentoxide until used.

Preparation VII.—This preparation was made from another portion of the same sponge as Preparation VI and in the same manner except that the compound was recrystallized from 10 per cent hydrobromic acid.

---

[16] E. H. Archibald, Proc. Roy. Soc., Edinburgh, vol. 29, p. 721, 1908–9.

[17] A portion of this sponge was used by Meggers to measure the spectral lines of osmium. W. F. Meggers, Arc Spectra of the Platinum Metals, B. S. Sci. Papers No. 499, Jan. 23, 1925.

VI. DETERMINATION OF THE OSMIUM CONTENT OF AMMONIUM CHLOROOSMATE AND OF AMMONIUM BROMOOSMATE

1. APPARATUS

The apparatus used in determining the osmium content of the preparations just described is shown in Figure 2. It consisted of an electrolytic cell for the generation of hydrogen; two series of scrubbing and drying towers; and a reaction tube, electrically heated.

The electrolytic cell was equipped with platinum electrodes and contained a dilute solution of potassium hydroxide. An electrically heated porcelain combustion tube, containing asbestos and quartz both impregnated with palladium, was inserted in the line to convert to water any oxygen which might have diffused into the hydrogen chamber of the cell. The series of five towers for the purification of the hydrogen contained silver sulphate, sulphuric acid which had previously been heated to heavy fumes, soda-lime, sulphuric acid, and phosphorus pentoxide which had been sublimed into the tower. Glass beads were used in all liquid towers, and several layers of beads were used in the soda-lime tower.

The nitrogen was the commercial gas produced by the fractionation of liquid air. The method used to remove the small amount of oxygen present was based upon the experiments of Badger, [18] who found that a solution of ammonium hydroxide (1 volume of ammonium hydroxide, specific gravity 0.90, diluted with 1 volume of water), when saturated with ammonium chloride and kept in contact with metallic copper, absorbed oxygen quantitatively. In order to insure the complete removal of oxygen a tube 6 feet in length, containing copper and the ammoniacal solution, was placed between the wash bottle and the first tower, which also contained the same solution. The second tower in this series contained 50 per cent sulphuric acid to absorb ammonia. The last five towers were similar to the set of towers described for the purification of hydrogen.

The reaction tube of combustion glass was fitted to the purification train by a carefully ground joint. Two U tubes, containing glass beads and sulphuric acid, sealed the exit of the reaction tube. The Hoskins electric furnace which was previously mentioned was used to heat the reaction tube. At a few places in the apparatus where it was not possible to make sealed-glass connections, the ends of the rigid tubes were held flush by rubber tubing. A heavy coating of De Khotinsky cement was then applied so that the rubber tubing was completely covered. In order to make certain that no oxygen reached the reaction chamber, either from the hydrogen or from the nitrogen, these gases were alternately passed through the heated tube in the presence of spongy metallic osmium. A tube containing phosphorous pentoxide, attached directly to the reaction tube, indicated no formation of water.

2. BALANCES, WEIGHTS, AND WEIGHING

The experiments on ammonium chloroosmate, Series VI, were made at The Johns Hopkins University. The balance used in these experiments was a new analytical balance known as Ainsworth QA.

The experiments on ammonium chloroosmate, Series VII, and on ammonium bromoosmate, Series VI and VII, were made at the

[18] W. L. Badger, J. Ind. Eng. Chem., vol. 12, p. 161, 1920.

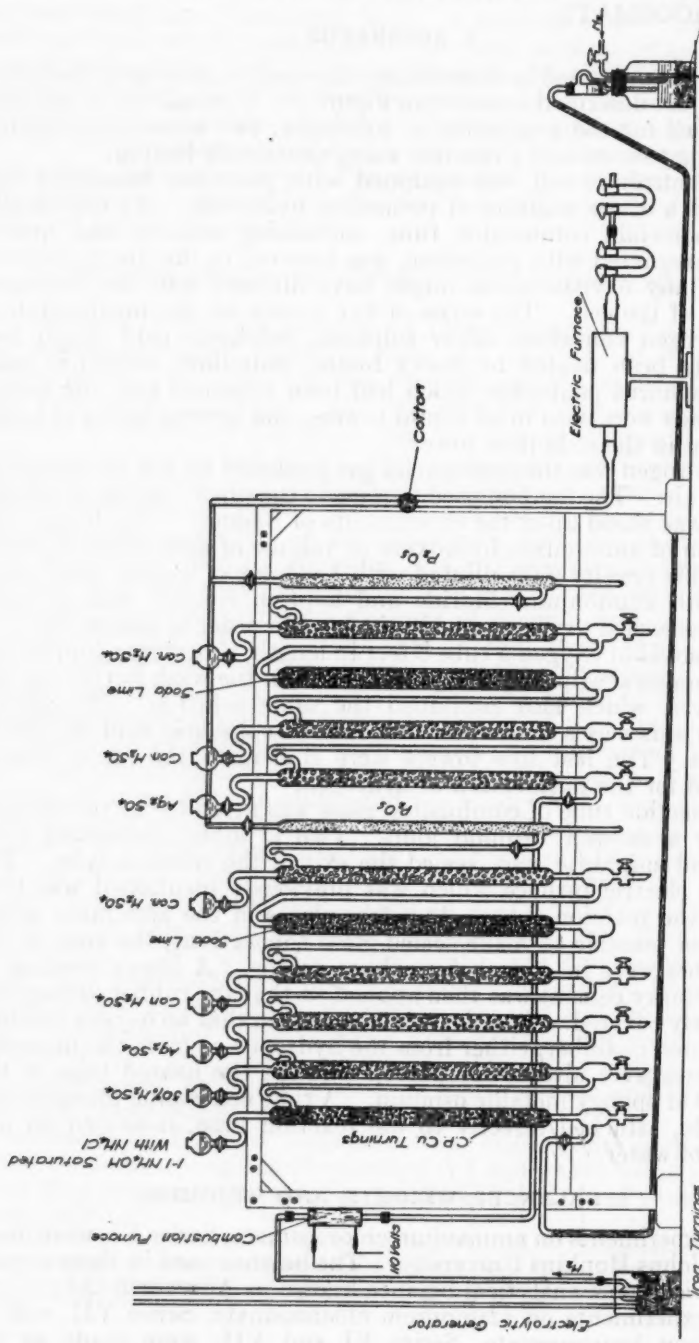

FIGURE 2.—*Apparatus for the analysis of the osmium salts*

Bureau of Standards. The balance used in these experiments was made by Ruprecht,[19] of Vienna, and was designed to carry a maximum load of 1 kg on each pan. This balance was inclosed in a case of blackened copper which served as a radiation screen. The weights used were carefully calibrated by the Bureau of Standards just previous to use.

Two glass weighing tubes of nearly the same size and weight, each fitted with a ground-glass stopper, were used. The boats were of porcelain. Weighing was done by the method of substitution, the vessels being allowed to remain in the balance case for three hours previous to weighing.

3. ANALYSIS

One is led to infer that Seubert [20] dried his compounds only over phosphorous pentoxide in a desiccator. Seybold,[21] cognizant of Seubert's procedure, in addition heated his preparations at 105° C., most likely in air so far as one is able to tell from his description.

Archibald,[22] in the analysis of ammonium chloroplatinate and of ammonium bromoplatinate, found that the purest samples which he was able to prepare began to decompose slightly at a temperature above 185° C. and that all hydrochloric acid and hydrobromic acid seemed to be driven off below 150° C.

With ammonium chloroosmate and ammonium bromoosmate it was found that slight decomposition occurred, in an atmosphere of dry purified nitrogen, if the temperature was above 170° C. At temperatures up to 150° C. no evidence of decomposition was observed. In experiment No. 1, ammonium chloroosmate, Series VII, the sample was heated for three 2-hour periods at 156° to 160° C. There was no change in weight during the second and third heating periods. When the temperature was raised to 166° to 170°, however, a faint white sublimate was formed and the sample continually decreased in weight. A solution of the sublimate in water gave a precipitate with silver nitrate. The weight recorded for the sample was that obtained at 156° to 160° C. These same temperature limits were also observed with ammonium bromoosmate.

Experiments previously made on other preparations, in which the drying was done at about 175° C., gave values for the atomic weight about 0.5 of a unit higher than those reported here. These values must be in error for the reason stated above and were rejected.

In the experiments reported here, the samples taken for analysis were dried to constant weight in a current of dry purified nitrogen. The samples in Series VI, ammonium chloroosmate, were dried from 3 to 5 hours at 140° to 145° C. Those in Series VII, ammonium chloroosmate, with the exception of No. 1 discussed above, were dried from 4 to 7 hours at 145° to 150° C. The samples in Series VI, ammonium bromoosmate, were dried from 10 to 14 hours at 150°, while in Series VII the first sample was dried for 14 hours at 145° and the second for 12 hours at 150° C. During the heating of the sample in experiment No. 2, ammonium chloroosmate, Series VII, a tube containing phosphorous pentoxide showed no increase in weight after the first heating period of 3 hours, although the sample was heated during two additional periods of 2 hours each.

---

[19] W. A. Noyes, Bulletin of the Bureau of Standards, vol. 4, p. 179, 1907.
[20] See footnote 4, p. 279.
[21] See footnote 5, p. 280.
[22] See footnote 16, p. 284.

The decomposition of the compounds was accomplished as follows: The porcelain boat with its contents was placed in the reaction tube. The tube was swept with dry purified nitrogen for one hour. The nitrogen was displaced by pure dry hydrogen for one and one-half hours, at the end of which time the temperature of the tube was gradually raised. When the decomposition appeared to be complete, the temperature was increased to 700° to 725° C. and maintained at this point for two hours. While at this temperature the hydrogen was displaced by dry purified nitrogen for one hour. The boat, now containing metallic osmium, was allowed to cool to room temperature in nitrogen, the furnace having been removed. The boat was placed in the glass-stoppered weighing tube and allowed to remain in the balance case for three hours before being weighed.

This procedure for the very gradual decomposition of the osmium compounds had been found, in previous experiments, to give a metal sponge which remained constant in weight upon reignition in hydrogen. No mechanical loss of material could be detected during the decomposition. With the exception of four instances where the metal sponges were returned to the cleaned reaction tube for an additional heating period of three hours in hydrogen at 700° to 725° C., the weights recorded in this paper were those obtained after the above treatment. The metal sponges in experiments Nos. 1 and 2, ammonium chloroosmate, Series VII, lost 0.00091 and 0.00051 g, respectively, on reheating in hydrogen. In these two cases the time of the first reduction had been cut somewhat short owing to the late hour of the night, so that all traces of volatile matter had apparently not been completely eliminated. The weight of the metal sponge in experiment No. 2, ammonium bromoosmate, Series VI, remained unchanged on reheating, while that in experiment No. 2, ammonium bromoosmate, Series VII, lost 0.00006 g. The weights recorded for these four sponges were those after the second heating period.

It had been repeatedly observed that metallic osmium, which had been ignited and cooled in hydrogen, was rapidly attacked by the air with the formation of osmium tetroxide. When the reaction tube was opened, the surface of the metal sponge usually glowed and a distinct odor of the tetroxide was noticeable. When the atmosphere of hydrogen was displaced as described in the experiments reported here, no odor of osmium tetroxide was detected either on opening the reaction tube or several days later when the boat was finally removed from the weighing tube. The limiting quantity of osmium tetroxide which von Wartenberg[23] could detect by the sense of smell was 2×10^{-5} mg/cm.

4. DENSITIES OF THE SUBSTANCES WEIGHED

In order to reduce the weights obtained to vacuum, the densities of the two osmium compounds and of the resulting osmium sponge were determined at 25° C. by displacement of toluene which had been dried and redistilled.

Two determinations of the density of ammonium chloroosmate were made, using 6.2303 and 8.7552 g of the compound. The values found were 2.941 and 2.908 g/cm^3. The average value was 2.93 g/cm^3.

Two determinations of the density of ammonium bromoosmate were made, using 10.2161 and 10.5552 g of the compound. The

[23] H. von Wartenberg, Ann., vol. 440, p. 97, 1924.

values found were 4.102 and 4.084 g/cm³. The average value was 4.09 g/cm³.

One determination of the density of the osmium sponge was made, using 6.7478 g. The value found was 19.13 g/cm³.

A correction of +0.00026, +0.00014, and −0.00009 g was applied to each gram of ammonium chloroosmate, ammonium bromoosmate, and osmium sponge, respectively.

5. RESULTS

The results of the determinations are given in Tables 1 and 2.

TABLE 1.—*Results of the analysis of ammonium chloroosmate*

	Experiment No.	Weight of $(NH_4)_2OsCl_6$ in vacuum	Weight of osmium in vacuum	Percentage of osmium	Atomic weight
		g	g		
$(NH_4)_2OsCl_6$, Series VI	1	3.81131	1.65758	43.491	
	2	3.46016	1.50505	43.496	
	3	1.11090	.48320	43.497	
				43.495	191.53
$(NH_4)_2OsCl_6$, Series VII	1	7.80602	3.39547	43.499	
	2	7.21775	3.13949	43.496	
	3	7.04888	3.06644	43.502	
	4	7.54170	3.27946	43.484	
				43.495	191.53

TABLE 2.—*Results of the analysis of ammonium bromoosmate*

	Experiment No.	Weight of $(NH_4)_2OsBr_6$ in vacuum	Weight of osmium in vacuum	Percentage of osmium	Atomic weight
		g	g		
$(NH_4)_2OsBr_6$, Series VI	1	5.85596	1.58647	27.091	
	2	5.59080	1.51471	27.093	
	3	3.91834	1.06117	27.082	
				27.089	191.55
$(NH_4)_2OsBr_6$, Series VII	1	4.98331	1.35016	27.093	
	2	4.53546	1.22899	27.097	
				27.095	191.61

The average percentage of osmium in ammonium chloroosmate, combining the results of the two series, was 43.495. The average percentage of osmium in ammonium bromoosmate, again combining the results of the two series, was 27.091. Using the values

N	14.008
H	1.0078
Cl	35.457
Br	79.916

the ratio $(NH_4)_2OsCl_6$: Os yields the value 191.53 for the atomic weight while the ratio $(NH_4)_2OsBr_6$: Os yields 191.57. The weighted average value is 191.55.

VII. DISCUSSION OF RESULTS

It is recognized that complex compounds of the platinum metals, of the type considered here, sometimes undergo a change of composition through hydrolysis. Such is known to be the case with

potassium chloroplatinate when formed under the conditions which obtain in the usual analytical separation of potassium from sodium. The change of composition comes about through the partial replacement of halogen by the hydroxyl group. The effect of such a change would be to raise the percentage of osmium and hence the apparent atomic weight. Except by accidental compensation the effect would be to produce a divergence in the values of the atomic weight calculated from similar ratios on analogous compounds. The probability that such change occurred in the compounds examined here is held to be highly unlikely, since the compounds were precipitated and recrystallized from solutions containing varying quantities of acid, and the value of the atomic weight as calculated from one compound agrees so closely with that calculated from the other analogous compound.

No impurities were detected in the metallic osmium used to prepare the compounds for analysis. The compounds were made by using only volatile reagents.

In the present work the samples of ammonium chloroosmate and of ammonium bromoosmate were dried to constant weight at temperatures of 140° to 150° C. A loss of weight was always observed in the first drying period when the salts, which had merely been desiccated over phosphorus pentoxide, were heated at 140° to 150° C. No evidence of decomposition was detected below 170° C. The probability that the compounds so treated still retained significant amounts of volatile impurities is held to be unlikely because of the close agreement of the values of the atomic weight calculated from the two ratios. The net effect of such impurities would be, of course, to lower the percentage of osmium and hence the apparent atomic weight, but a divergence in the ratios would result unless the relative amounts of the impurities in the two compounds happened to be such as to compensate for it.

The decomposition of the compounds in hydrogen was accomplished so gradually that the possibility of mechanical loss appears improbable.

The formation of only volatile products upon decomposition and the constancy of weight of the resulting metallic osmium, when heated in hydrogen at an elevated temperature, make it highly improbable that any impurity contaminated the final metal. The removal of hydrogen at an elevated temperature by nitrogen undoubtedly prevented the attack of the metal sponge by atmospheric oxygen during the time necessary to make the weighings.

The identical agreement of the average determinations of the osmium content of the two preparations of ammonium chloroosmate, when different quantities of the substances were taken and when different balances were used, makes it improbable that significant errors were introduced in weighing.

VIII. ACKNOWLEDGMENTS

The author wishes to express his gratitude for the help and encouragement received from Prof. J. C. W. Frazer, of The Johns Hopkins University, under whose supervision the research was conducted, and for the many valuable suggestions received from Edward Wichers.

WASHINGTON, June 8, 1932.

"MOISTURE EXPANSION" OF CERAMIC WHITE WARE

By R. F. Geller and A. S. Creamer

ABSTRACT

This report supplements the reports of a number of investigations of "moisture expansion." The relative susceptibility of various materials, individually and as consituents of bodies, was studied, as was also the effect of the temperature to which the specimens had been heated. The relative susceptibility to moisture expansion of the principal ingredients of ceramic bodies appears to be approximately as follows: Fused feldspar, 2.4; calcined clay, 0.40; unfused feldspar, 0.20; calcined flint, 0.06. The expansion caused by reaction with moisture may be decreased at temperatures as low as 120° C. The removal of the moisture is relatively sluggish at 120° C., proceeds faster as the temperature is raised, and apparently may be completed at 250° C. The marked difference is susceptibility to moisture expansion of fused and unfused feldspar has an important effect on ceramic bodies. The data indicate that at temperatures below approximately "cone 8" and absorptions above 10 per cent the ratio of fused to unfused feldspar is the predominating factor determining the resistance to moisture expansion while at higher temperatures and lesser absorptions the relative absorption is the predominating factor. The data obtained offer no evidence regarding the nature of the reaction involved.

CONTENTS

	Page
I. Introduction	291
II. Materials and methods	292
1. Commercial bodies	292
2. Experimental bodies	292
3. Individual materials	293
III. Results	295
1. Commercial bodies	295
(a) Moisture expansion of unautoclaved specimens	295
(b) Moisture expansion of autoclaved specimens	295
(c) Effect of various drying treatments on the length of autoclaved specimens	296
2. Experimental bodies	299
(a) Effect of composition, heat treatment, and absorption on moisture expansion	299
3. Individual materials	305
(a) Relative reaction to moisture	305
(b) Effect of particle size	306
(c) Petrographic examinations	306
4. Nature of reaction termed moisture expansion	306
IV. Conclusions	307

I. INTRODUCTION

This report supplements the reports of many investigations [1] which have been made during the past six years on the general subject of moisture expansion or expansion due to the action of water. It was undertaken primarily to determine which of the usual constituents of white-ware bodies are most susceptible to moisture expansion.

[1] G. E. Merritt and C. G. Peters, J. Am. Ceram. Soc., vol. 9 (6), p. 332, 1926; H. G. Schurecht, vol. 11 (5), p. 271, 1928, and vol. 12 (2), p. 118, 1929; H. G. Schurecht and G. R. Pole, vol. 12 (9), p. 596, 1929; R. G. Mills, vol. 13 (12), p. 903, 1930; H. H. Holscher, vol. 14 (3), p. 207, 1931; H. G. Schurecht and G. R. Pole, vol. 14 (4), p. 313, 1931, and B. S. Jour. Research, vol. 3 (RP98), August, 1929; O. S. U. Eng. Exp. Sta. Cir. Nos. 18, J. Otis Everhart, and 22, H. H. Holscher.

II. MATERIALS AND METHODS

1. COMMERCIAL BODIES

Dinner plates of the same quality as supplied regularly to the trade, and representing the product of 16 manufacturers of earthenware, were available for the study of commercial bodies. The specimens for water-absorption determinations were irregularly shaped pieces broken from the plates and tested without removing the glaze, using three specimens of each brand. The determinations were made by the so-called 5-hour boiling test in accordance with the method prescribed in Federal specification No. 243a for vitrified chinaware. Indirect moisture-expansion measurements were made by means of the interferometer according to the method described by Schurecht.[2] These indirect measurements are based on the assumption that the difference in total thermal expansion obtained at 400° C. (or at a higher temperature) in the first and second tests of specimens which have had the opportunity of reacting with moisture, either during prolonged storage or in an autoclave, is a measure of the moisture expansion.

2. EXPERIMENTAL BODIES

The compositions of the experimental bodies, together with the heat treatment received, are given in Table 1 and in part A, Table 2. The potter's flint and the feldspar (No. 3)[3] were composed of particles varying in size from 10μ to 80μ, the separation from coarser and finer particles having been made by means of a No. 325 United States standard sieve and an air elutriator.[4] The clay (Georgia kaolin) was not sized in the elutriator because it "balled" in the apparatus and made the separation of any particular range of particle sizes impracticable.

The mixtures were made into specimens 6 inches long and one-half inch in diameter. The extrusion method was used to form the specimens of bodies containing clay, while the flint-feldspar series, containing gum tragacanth as a binder, were tamped. The specimens which had been heated as described in section B, Table 1, were dried at $115° \pm 5°$ C., weighed, measured, and autoclaved at 150 lbs./in.^{2} steam pressure (183° C.) for one and one-half hours while submerged in water. They were then removed from the autoclave, reweighed and remeasured before and after drying (constant in weight to 0.01 g) at $115° \pm 5°$ C. and at $270° \pm 5°$ C. to determine changes in weight and length due to these drying treatments. The absorption was taken as the percentage gain in weight during the autoclave treatment.[5] The changes in length resulting from the autoclave treatment and subsequent drying were measured by means of a comparator using a graduated invar bar as reference.[6] Reference points in the specimens were obtained by cementing capillary Pyrex glass tubes in small holes approximately 12 cm apart, using a hydraulic high alumina cement. The precision in these length measurements was found to be approximately ± 0.01 per cent of the length measured. Room temper-

[2] H. G. Schurecht, J. Am. Cer. Soc., vol. 11 (5), p. 271, 1928.
[3] H. Insley, J. Am. Cer. Soc., vol. 10 (9), p. 651, 1927.
[4] J. C. Pearson and W. H. Sligh, B. S. Tech. Paper No. 48.
[5] This method of determining water absorption is believed to be fully as effective as the 5-hour boiling method because it has been shown by the authors that a 10-hour autoclave treatment at 150 lbs./in.^{2} steam pressure is as effective as 240 hours boiling. See B. S. Tech. News Bull. No. 167, March, 1931.
[6] J. C. Pearson, J. Am. Concrete Inst., 1921.

atures were noted at all readings, but did not vary sufficiently to justify correcting the measurements for this factor.

TABLE 1.—*Experimental bodies and heat treatments*

A. BODIES

[Three specimens of each mixture for each heat treatment]

Series A			Series B			Series C			Series D			
Body No.	Flint	No. 3 Feldspar	Body No.	Clay	No. 3 Feldspar	Body No.	Clay	Flint	Body No.	Clay	Flint	No. 3 Feldspar
	Per cent	*Per cent*		*Per cent*	*Per cent*		*Per cent*	*Per cent*		*Per cent*	*Per cent*	*Per cent*
A1	80	20	B1	80	20	C1	80	20	D1	20	40	40
A2	60	40	B2	60	40	C2	60	40	D2	40	30	30
A3	50	50	B3	50	50	C3	50	50	D3	50	25	25
A4	40	60	B4	40	60	C4	40	60	D4	60	20	20
A5	20	80	B5	20	80	C5	20	80	D5	80	10	10

B. HEAT TREATMENT

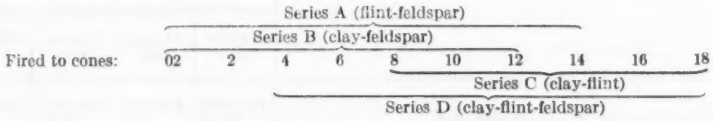

3. INDIVIDUAL MATERIALS

The individual raw materials included: (*a*) Feldspars Nos. 3 and 18; (*b*) pulverized quartz obtained by crushing a sample of standard Ottawa sand; (*c*) washed kaolin from Georgia containing about 4 per cent of impurities, such as mica and quartz; (*d*) two samples of lepidolite;[7] (*e*) Cornwall stone as supplied to the pottery trade; and (*f*) Lemoor china clay. Three samples of the china clay were available: (*a*) The original clay; (*b*) a granular separate containing particles larger than 1μ in diameter; and (*c*) a "colloidal" separate containing particles less than 1μ in diameter.[8] With the exception of the feldspar and the Lemoor china clay used in the determination of the effect of particle size, each of the individual materials tested as powders was heated at approximately 1,225° C.[9] in a small gas-fired furnace, cooled rapidly, and crushed to pass a No. 120 United States standard sieve. It is realized that differences in particle size (or ratio of surface to unit weight) introduce an unmeasured variable which may lessen appreciably the significance of the values. For this reason the materials were ground with a mortar and pestle and sieved repeatedly as the grinding progressed so as to produce a minimum of fines.

[7] The following chemical compositions were obtained from the concerns furnishing the lepidolite:

	SiO_2	Al_2O_3	Fe_2O_3	MnO	K_2O	Li_2O	Na_2O	F	H_2O
	Per cent	*Per cent*	*Per cent*	*Per cent*	*Per cent*	*Per cent*	*Per cent*	*Per cent*	*Per cent*
Sample A	49	27	0.9	0.5	8–10	4–5	2	--------	1.5
Sample B	63	24	.05	.35	6.8	2.9	1.5	1.5	.2

[8] The fractions were obtained by K. Langenbeck during the course of an investigation at the Bureau of Standards, the results of which have not been published.

[9] This temperature was chosen because it lies between the temperatures used by earthenware and vitrified chinaware manufacturers to mature their ware.

The determination of the relative degree of reaction of individual materials with moisture was based on weight change, assuming that expansion (or volume change) would be proportional to weight change. The crushed samples were dried to constant weight [10] at 115° ± 5° C., exposed to water vapor at 150 lbs./in.² steam pressure for five hours (precautions being taken to prevent condensation of moisture on the samples), weighed immediately on removal from the autoclave and again after drying at 115° ± 5° C. and at 250° ± 10° C.

TABLE 2.—*Effect of autoclave treatment on individual materials*

A. 1 BY 1 BY 5 INCH BARS (THREE SPECIMENS OF EACH BODY) AUTOCLAVED FOR THREE HOURS AT 150 LBS./IN.² STEAM PRESSURE (183° C.)

	Temperature of heating			
	Cone 5 to 6 (approximately 1,180° C.)		Cone 8 to 9 (approximately 1,230° C.)	
	Expansion	Absorption	Expansion	Absorption
	Per cent	*Per cent*	*Per cent*	*Per cent*
50 per cent feldspar No. 18—50 per cent flint	0.03	6.0	0.00	.4
50 per cent feldspar No. 3—50 per cent flint	.15	15.1	.03	3.9
Florida kaolin [1]	.04	14.8	.02	13.3
Georgia kaolin [1]	.63	20.7	.02	17.8

B. POWDERED SPECIMENS HEATED AT 1,225° C., RECRUSHED AND AUTOCLAVED FOR FIVE HOURS AT 150 LBS./IN.² STEAM PRESSURE

		Weight gain during autoclave treatment	Percentage of water absorbed during autoclave treatment which was removed by drying at—	
			115°± 5° C.	250°± 10° C.
		Per cent	*Per cent*	*Per cent*
Feldspar No. 3	1	2.4	32	84
	2	2.4	30	95
	3	2.5	30	93
	4	2.5		
Quartz	1	.06	67	92
	2	.06	69	86
	3	.05	17	81
	4	.05	15	78
Kaolin	1	.46	64	100
	2	.34	37	91
Lepidolite	A 1	1.7	35	84
	A 2	1.6	33	83
	B 1	1.3	27	78
	B 2	2.0	29	77
Cornwall stone	1	1.4	23	76
	2	1.4	22	74
	3	1.3	20	73

[1] Taken from Table 7 of H. H. Holscher's paper. (See footnote 12, p. 299.)

[10] In this phase of the work the specimens were considered to have reached constant weight when the weight difference after 2-day intervals of drying did not exceed 0.5 mg.

III. RESULTS

1. COMMERCIAL BODIES

(a) MOISTURE EXPANSION OF UNAUTOCLAVED SPECIMENS

As a preliminary study, specimens of five brands (Nos. 1, 5, 6, 14, and 16) were taken from glazed plates which had been stored in the laboratory for several months. The moisture expansion was found to vary from 0.03 to 0.06 per cent for four brands which had water absorptions of from 9.4 to 12.5 per cent; the other brand (No. 1) showed no moisture expansion and the water absorption was 2.0 per cent. Typical curves are given in Figure 1 and the values in Table 3.

Since the moisture expansion tests of unautoclaved glazed plates were made on specimens of the body immediately after being taken from the plates, it is indicated that the expansion noted had taken place regardless of the supposedly impervious coating of glaze.[11] The data, therefore, justify the conclusion that glazed earthenware may be subject to crazing caused by penetration of moisture through the glazed and the resultant moisture expansion of the body.

(b) MOISTURE EXPANSION OF AUTOCLAVED SPECIMENS

One specimen of each of the 16 brands was autoclaved at 150 lbs./in.^{2} steam pressure for one hour, the pieces being immersed. Typical results are shown by the curves in Figure 1. For any one specimen the expansions during the second and third heatings were practically identical. The curves in Figure 2 show also that the contraction during the cooling, following the first heating of an autoclaved specimen, is practically along the same curve as the expansion during the second heating. The data indicate that the first heating and the first cooling are sufficient to give the desired information. Pertinent data obtained in this phase of the investigation are summarized in Table 3 and the calculated moisture expansions are plotted against percentage water absorption in Figure 3. Although the bodies are all of one type and probably had been matured at about the same temperature, there are undoubtedly sufficient differences in composition and structure to affect the porosity-expansion relation. As shown by data given in this paper, feldspar alone may be an important factor.

TABLE 3.—*Effect of moisture on specimens either stored in laboratory air or autoclaved*

Brand No.	Water absorption	Moisture expansion after storage [1]	Moisture expansion after autoclave [2]	Brand No.	Water absorption	Moisture expansion after storage [1]	Moisture expansion after autoclave [2]
	Per cent	*Per cent*	*Per cent*		*Per cent*	*Per cent*	*Per cent*
1	2.	0	0.05	9	11	----	0.12
2	7.5	----	.07	10	11	----	.11
3	9.	----	.07	11	11	----	.14
4	9.5	----	.08	12	11	----	.09
5	9.5	0.03	.11	13	12	----	.08
6	10	[3] .04	.10	14	12	0.06	.12
7	10	----	.10	15	12	----	.09
8	10	----	.08	16	12	.03	.09

[1] Difference in total expansion at 400° C. between first and second heating of unautoclaved specimen which had been taken from a whole plate stored in the laboratory under normal atmospheric conditions for several months.

[2] Difference in total expansion at 400° C. between first and second heating of specimen autoclaved for one hour in steam at 150 lbs./in.^{2} pressure.

[3] Especially selected and tested for unbroken glaze before specimen was taken from plate.

[11] It was shown by Schurecht (footnote 1, p. 291) that glazes may undergo moisture expansion. This is further evidence that they are not impervious to moisture.

(c) EFFECT OF VARIOUS DRYING TEMPERATURES ON THE LENGTH OF AUTOCLAVED SPECIMENS

A number of observations were made by holding autoclaved specimens at several temperatures (maintaining the temperatures as nearly constant as possible) and observing length changes. Seventeen tests

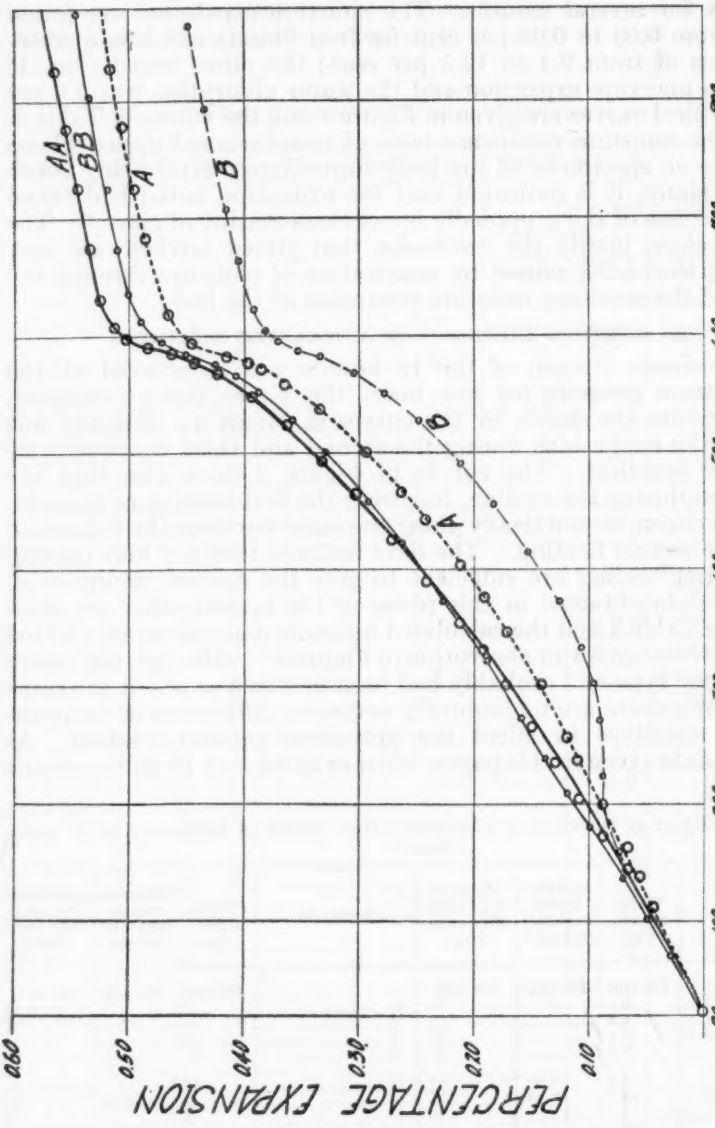

FIGURE 1.—*Thermal expansion determinations on specimens of two pieces of Brand No. 6*

Plate A had been stored in the laboratory for several months and plate B had been autoclaved for one hour at 150 pounds per square inch steam pressure. Curves *A* and *B*, first heating; curves *AA* and *BB*, second and third heating. Estimated percentage moisture expansions are given in Table 3.

were made on three different bodies. These tests were modifications of the following, the results of which are typical and are discussed in detail:

1. A specimen of brand No. 5 was "autoclaved" for two hours at 150 lbs./in.^{2} steam pressure while immersed in water. Length changes

were then observed while the specimen was heated in a furnace to approximately 118° C. and held for 5½ hours, reheated to approximately 180° C. and held for 1½ hours and again heated to 246° C. and held for 1½ hours and finally heated to 600° C. The specimen was permitted to cool to room temperature after each heat treatment.

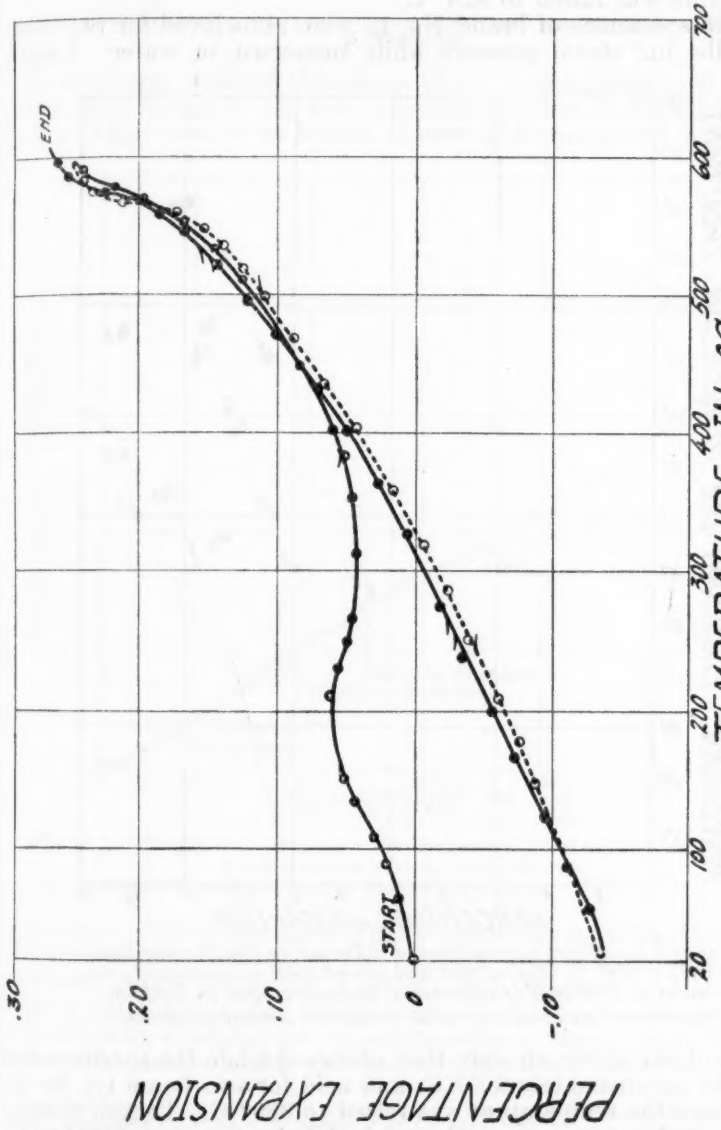

FIGURE 2.—*Thermal expansion curves showing that the contraction of an autoclaved specimen when cooled after the first heating is practically the same as the expansion during the second and third heating*

Test made on a specimen of commercial body No. 3 autoclaved for two hours at 150 pounds per square inch steam pressure.

The results obtained are shown by the curves in Figure 4. The specimens were held at each temperature until further length changes were negligible.

2. Length changes of a second specimen of brand No. 5 were observed while the specimen was held at approximately 245° C. for

five hours. As is evident from the curve in Figure 5, the rate of contraction had decreased considerably at the end of the 5-hour period, but conditions had not reached equilibrium. The specimen, after cooling to room temperature, was again heated to approximately 245° C. and held for four and one-half hours, after which the temperature was raised to 325° C.

3. Two specimens of brand No. 15 were autoclaved for two hours at 150 lbs./in.^{2} steam pressure while immersed in water. Length

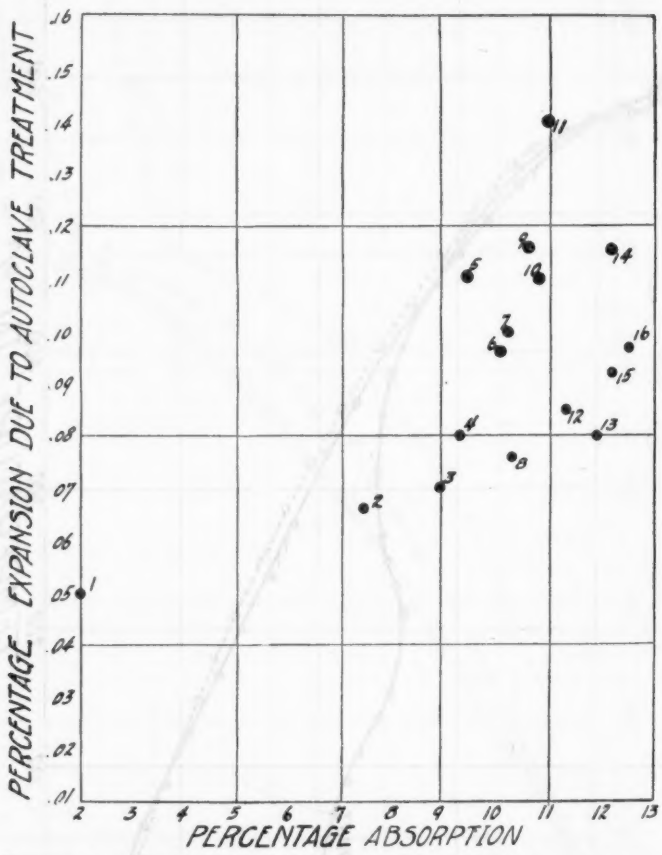

FIGURE 3.—*Water absorption and difference in total thermal expansion at 400° C. (during first and second tests) of autoclaved specimens of 16 brands of commercial whiteware (data in Table 3)*

The difference in total expansion at 400° is considered as moisture expansion.

changes of one specimen were then observed while the specimen was heated to approximately 260° C. and held for two hours (*A*, fig. 6), after which the temperature was raised to 380° C. Length changes of the second specimen were observed while heating it to 680° C. at a constant rate of temperature increase (*B*, fig. 6) permitting it to cool to room temperature, and again heating to 680° C. at a constant rate of 3° C. per minute.

The information given in Figures 4, 5, and 6 indicates that the reactions induced by heating autoclaved specimens, and evidenced by contraction, are relatively sluggish at 120° C., proceed faster as the temperature is raised, and are markedly accelerated at temperatures above 230° C.

2. EXPERIMENTAL BODIES

(a) EFFECT OF COMPOSITION, HEAT TREATMENT AND ABSORPTION ON MOISTURE EXPANSION

As originally outlined this phase of the investigation included the making and testing of 435 specimens representing 20 different bodies, each of which was to be heated at several temperatures as specified

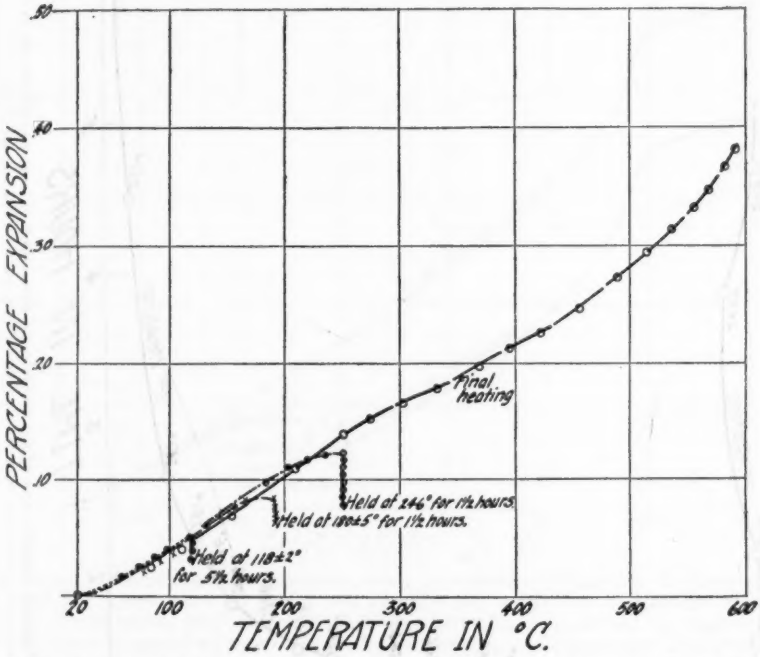

FIGURE 4.—*Length changes of an autoclaved specimen of commercial body No. 5 when held at various temperatures*

All tests made on the same specimen after one autoclave treatment.

in Table 1. Three specimens were prepared for each heat treatment of each body.[12] Because of the extreme weakness of many of the specimens, particularly the *A* series (flint feldspar), and the specimens of the *B* series (clay feldspar) heated at the lower temperatures, only 215 were available for the entire series of tests. Had this been anticipated, fewer bodies and more specimens of each would have

[12] It has been shown by previous investigators (footnote 1, p. 291) that the relative porosity is an important factor in determining the extent of the reaction of ceramic bodies with moisture. Obviously the relative moisture expansions of two bodies varying in composition are not comparable unless the porosity is the same both in extent and in nature. Not only is the nature of the pore space difficult of determination (ratio of fine to coarse pores, etc.), but it would be practically impossible to develop the same porosity in two bodies of the whiteware type, varying in composition, without using a different heat treatment for each. This introduces a third variable which, it was anticipated, would be a significant factor. It was this practical difficulty of changing only one variable at a time that prompted the study of such a large number of specimens in the hope that the data could be studied as group averages which might indicate the effect to be expected by changing either composition, porosity, or heat treatment.

been made. However, such values as could be determined are presented in Table 4. This table gives the average percentage moisture expansion and water absorbed for each body during the autoclave treatment, but only the group averages of each series of bodies for the determinations which were made after the drying treatments.

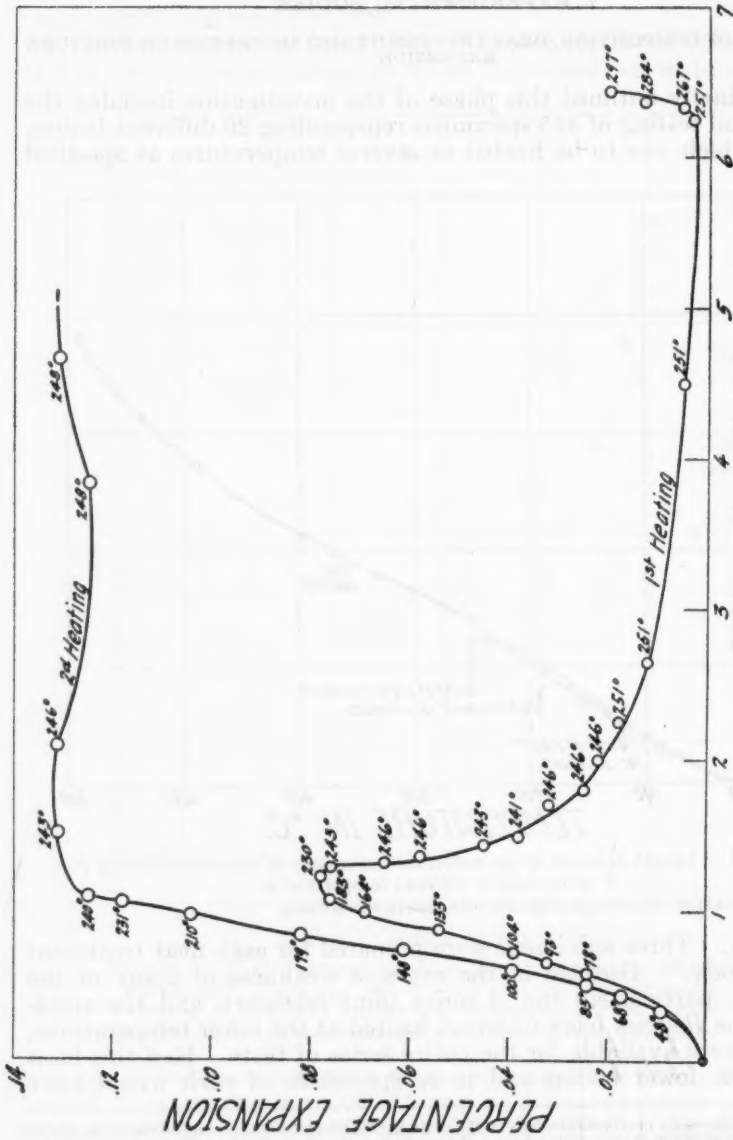

FIGURE 5.—*Thermal expansions of an autoclaved specimen of commercial body No. 5*

The curve obtained during the first heating indicates that the vapor pressure or dissociation pressure of that water in an autoclaved specimen which causes moisture expansion (the removal of which is accompanied by contraction) increases sharply as the temperature is raised above 180° C.

As stated in footnote 12, the analysis of data, obtained by heating a number of different ceramic bodies to a series of temperatures and subjecting them to moisture in an autoclave at elevated temperatures, is made difficult by the fact that one factor can not be changed without changing others. In studying the data (Table 4) it should

be remembered that only one clay, one feldspar, and one flint were investigated. Also, little significance can be attached to certain irregular absorption-temperature relations because the bodies were heated by the draw-trial method, which is comparatively rapid and not suitable for a study of absorption-temperature relations.

The length measurements show that autoclaved specimens of earthenware which have expanded due to reaction with moisture apparently return to their original length when held for a reasonably short time at 250° to 270° C. in air and under atmospheric pressure. However, the most noticeable development is the unique behavior of the *C* (or clay-flint) series of bodies. Although the compositions

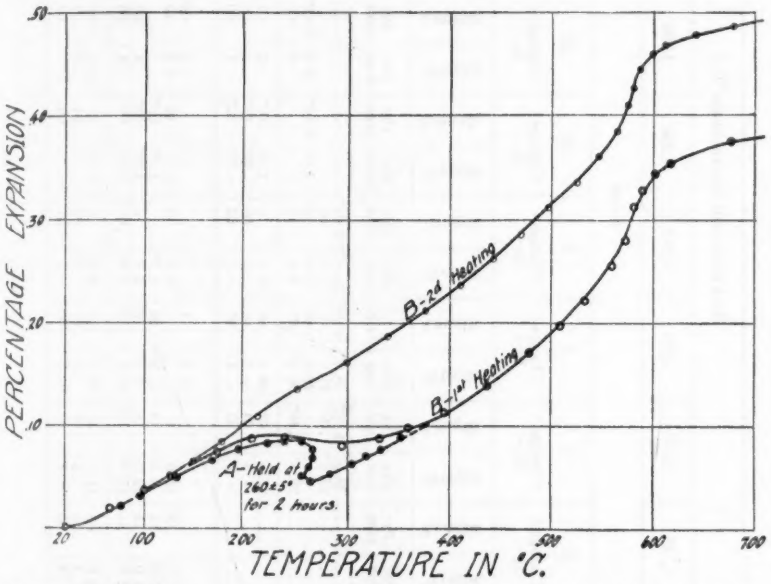

FIGURE 6.—*These thermal expansion curves for commercial body No. 15 (together with the curves given in figs. 4 and 5) show that subjection to a temperature of approximately 250° C. for a relatively short time is sufficient to overcome the effect of autoclave treatment on length change, while prolonged treatment at lower temperatures is not*

are very refractory, and the specimens highly porous, even after heating to cone 18, the only specimens showing a significant length change, or moisture expansion, after autoclaving are those heated to cone 8. This indicates that a body composed of the clay used in this investigation (Georgia kaolin) and of flint would be very resistant to moisture expansion even though the porosity was relatively high. The data obtained by Holscher [13] would indicate that this might not be true for all clays.

[13] J. Am. Cer. Soc., vol. 14 (3), p. 207, 1931.

TABLE 4.—*Percentage change in weight and length after autoclave treatment and also after subsequent drying*

Body	Heat treatment (approximate °C.)																	
	1,100		1,125		1,170		1,190		1,215		1,250		1,300		1,380		1,440		1,490	
	Cone																			
	02		2		4		6		8		10		12		14		16		18	
	Change[1] in—		Change[1] in—		Change[1] in—		Change[1] in—		Change[1] in—		Change[1] in—		Change[1] in—		Change[1] in—		Change[1] in—		Change[1] in—	
	Weight	Length	Weight	Length	Weight	Length	Weight	Length	Weight	Length	Weight	Length	Weight	Length	Weight	Length	Weight	Length	Weight	Length
	Per cent	*Per cent*	*Per cent*	*Per cent*	*Per cent*	*Per cent*	*Per cent*	*Per cent*	*Per cent*	*Per cent*	*Per cent*	*Per cent*	*Per cent*	*Per cent*	*Per cent*	*Per cent*	*Per cent*	*Per cent*	*Per cent*	*Per cent*
Flint-feldspar:																				
A1					29.5*	0.04*	28.0*	0.06*	21.5*	0.05*										
A2					27.5*	.07*	27.5	.07	17.0	.08										
A3							29.0	.05	15.0*	.14*	7.5*	0.06*	0.0*	0.00*						
A4					25.5*	.10*	30.0*	.05*	8.0	.12			.0	.02	0.0	0.00				
A5																				
Average after autoclave[2]					27.5	.07	28.6	.06	15.4	.10	7.5*	.06*	.0	.01						
Average after first drying[3]					−.3	.04	−.2	.04	.1	.06	.0*	.05*	.0	.00						
Average after second drying[4]					−.5	.02	−.4	.01	−.1	.02	−.3*	−.02*	−.1	.00						
Clay-feldspar:																				
B1	25.0*	0.10*					19.5	.11					7.0*	.08*						
B2	25.0	.08	21.5*	.13*	12.0	.17			7.0	.12	6.5	.12	4.0	.10						
B3	20.5	.09	20.0	.14	9.5	.18	11.0	.20	4.5*		4.0*	.05*								
B4	20.0	.06	15.0	.15	10.0	.18	9.0	.18	5.0	.14	4.0*	.05*	.0	.00						
B5	23.5*	.10*	22.0	.11	15.0*	.14*	16.0	.13	3.0*	.01*	0.0	.00	.0	.00						
Average after autoclave[2]	22.8	.09	20.0	.13	11.5	.17	14.0	.16	5.0	.09	3.5	.06	3.0	.09						
Average after first drying[3]	.0	.03	.2	.05	.3	.07	.2	.07	.3	.05	.1	.04	.1	.02						
Average after second drying[4]	−.2	.00	−.2	.00	−.2	.01	−.1	.00	−.1	−.01	−.2	.00	−.1	.00						
Clay-flint:																				
C1									22.0	.08	17.5	.02	15.0	.00	13.5	.02	12.0	0.01	8.5	0.00
C2																				

Clay-flint:																				
C1									22.0	.08	17.5	.02	15.0	.00	13.5	.02	12.0	0.01	8.5	0.00
C2									22.0	.07			20.0	.00	17.5	.00	17.0*	.00*	13.5*	*.00
C3									22.5	.04	21.0	.00	19.5	.02	18.9	.00	18.5	.01	14.5	.00
C4									22.5	.09	21.5*	.00*	20.5	.00	20.0	.00	20.0	.00	16.5	.00
C5																	22.5*	.03*	23.5	.00
Average after autoclave [2]									22.5	.07	19.0	.01	19.0	.00	23.5	.00	18.0	.01	15.5	.00
Average after first drying [3]									−.1	.03	−.1	.01	.0	.00	−.1	.00	−.1	.00	.0	.00
Average after second drying [4]									−.2	.00	−.2	.00	−.1	.00	−.1	.00	−.1	.00	−.1	.00
Clay-flint-feldspar:																				
D1					19.5	.17	20.0*	.27*	16.0	.13	11.0	.07	3.0		1.0	.06				
D2					17.0	.11	17.0*	.21*	14.0	.14	11.5*	.06	8.5	.08	5.0	.09				
D3					17.0	.17	15.5	.15	13.0	.12	11.5	.09	7.0	.09	5.5	.10*	.3	.00	.1	.00
D4					15.5*	.13*	16.0*	.15*	13.0	.13	12.0	.10	8.5	.04	6.0	.02	.2	.03	.2	.00
D5					23.0	.09			13.5	.09	12.0	.06	9.0	.05	6.5	.04	.1	.02	.0	.00
Average after autoclave [2]					18.5	.13	17.0	.19	14.0	.12	11.5	.08	7.0	.06	5.0	.06	.2	.02	.1	.00
Average after first drying [3]					.1	.06	.1	.09	.0	.04		.02	.2	.03	.0	.03	.0	.00	.0	.00
Average after second drying [4]					−.3	.00	−.2	.02	−.2	−.02		−.02	−.1	.00	−.2	.01	−.1	.00	.0	.00

[1] The negative values for averages 3 and 4 indicate that the specimens were lighter, or shorter, than after the preliminary drying (115° ±5° C.) before autoclave treatment.
[2] The individual values in the table of which these values are the average, represent determinations on from 1 to 3 specimens of each body and each heat treatment after autoclaving for 1½ hours at 150 lbs./in.² steam pressure (183° C.). The asterisk (*) identifies values representing determinations on 1 specimen only.
[3] Average difference in weight and length, from weight and length before autoclaving, after drying at 115°±5° C.
[4] Average difference in weight and length, from weight and length before autoclaving, after drying at 270°±5° C.

A point of interest concerning the B series is the progressively decreasing resistance to expansion which was shown by the bodies fired to cones 02, 2, and 4 even though the percentage absorption also decreased. (Table 4 and fig. 7.) This led to the supposition that crystalline or unaltered feldspar is less susceptible to moisture expansion than feldspar glass. Therefore, a specimen of raw feldspar No. 3 and one of the same sample fused at 1,225° C., both ground to pass a No. 325 United States standard sieve ($<80\mu$), were subjected to identical autoclave treatment. Also, specimens of body B4 heated to cones 02, 6, and 10 were examined petrographically.[14] It was found that the body heated to cone 02 was composed of two phases—unmelted feldspar (index of refraction = 1.52) and dehydrated clay

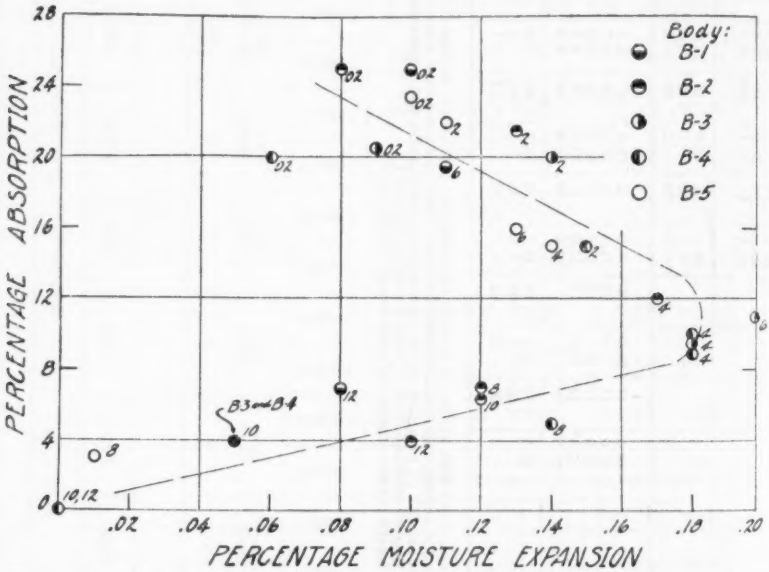

FIGURE 7.—*Relation between water absorption and moisture expansion of the clay-feldspar series of bodies (B, Table 4)*

The numbers indicate the temperatures, in terms of cones, to which the specimens were heated.

(index of refraction = 1.53 to 1.54). The specimen fired to cone 6 contained three phases—melted feldspar (index of refraction = 1.49), unmelted feldspar (index of refraction = 1.52), and dehydrated clay (index of refraction = 1.53 to 1.54). The cone 10 specimen contained the same phases as that fired to cone 6, but much more of the feldspar had melted. The absorption values obtained for raw and fused feldspar, which are given in Table 5 and supported by the other values for fused feldspar in Table 2 when considered in connection with the phase compositions of the B bodies examined may be accepted as supporting the supposition. Therefore, commercial earthenware, which is matured at about cone 6 and has an absorption averaging 10 per cent, may have a structure peculiarly susceptible to moisture expansion.

[14] Examinations made by R. H. Ewell.

3. INDIVIDUAL MATERIALS

(a) RELATIVE REACTION TO MOISTURE

Holscher [15] found that a body composed of feldspar, clay, and flint showed greater length changes after autoclave treatment than the pure clay although the absorptions were lower. This indicates that the other constituents of the bodies he investigated, namely, the feldspar or flint, may be even more reactive to moisture than the clay. Schurecht [16] investigated a series of bodies in which ball clay, feldspar and flint were varied between wide limits. He found that a mixture of 40 per cent feldspar and 60 per cent flint showed the greatest percentage length change in the series (0.188 per cent), while 60 per cent feldspar and 40 per cent flint showed only 0.100 per cent. The absorptions, however, were 13.4 per cent for the former and 5.0 per cent for the latter mixture. Whether the relatively high moisture expansion of the former mixture was induced by a reaction between the flint and feldspar, as Schurecht surmised, or because the presence of the flint produced sufficient porosity to permit the water vapors to react with a greater portion of the body had not been proven. It is worthy of note that the three bodies of Schurecht's series which showed unusually low expansions, considering their high absorptions, concontained no feldspar. The data indicate feldspar to be a material highly reactive to water vapor. This indication was strengthened by the results of preliminary tests given in part A of Table 2. The values given in part B of Table 2 are for individual powdered materials heated, recrushed and autoclaved as described in Part II.

TABLE 5.—*Effect of particle size on percentage gain in weight during autoclave treatment (samples exposed to vapor only)*

Material	Particle size	Gain in weight		
		Sample 1	Sample 2	Sample 3
	μ	*Per cent*	*Per cent*	*Per cent*
Feldspar No. 3:[1]				
Fused	<80	2.8		
Raw	<80	.18	0.22	
	80–10	.27	.28	0.28
	<10	1.7	1.2	1.2
Lemoor china clay [2]	Original.	2.3	2.2	
	>1	1.7	1.7	
	<1	3.2	3.3	

[1] Autoclaved at 500 lbs/in.² steam pressure for 1 hour (250° C.).
[2] Autoclaved at 320 to 350 lbs./in.² steam pressure for 16 hours (225°±5° C.).

The relative reactions of individual materials with moisture (Table 2) lead to conclusions similar to those indicated by the results of the much longer series of tests with experimental bodies. The weight increase of the feldspar glass investigated was the greatest, that of dehydrated clay was considerably less, and that of the calcined flint almost negligible. This is in accord with the observed fact that the bodies containing no feldspar (series C, Table 4) showed the least expansion. No lepidolite or Cornwall stone having been used in the experimental bodies, the data obtained with them are of general

[15] See footnote 13, p. 301. [16] J. Am. Ceram. Soc., vol. 12 (9), p. 596, 1929.

interest only. However, they are of possible value, when compared with those for feldspar, to those concerns using lepidolite or Cornwall stone in their bodies and glazes.

(b) EFFECT OF PARTICLE SIZE

The values obtained by autoclave treatment of fractions of one feldspar and of one clay, the fractions differing in the range of particle sizes comprised, are given in Table 5. They may be taken as further evidence that reactions with moisture in an autoclave will increase with increase in the surface exposed per unit mass. This is to be expected since there is no breaking down of the structures and the reaction is confined to the original surfaces or must proceed from these surfaces.

(c) PETROGRAPHIC EXAMINATIONS

These petrographic examinations and the following report were made by Dr. H. Insley.

Georgia clay (heated to 1,225° C., recrushed to pass a No. 120 sieve, and autoclaved at 760 to 800 lbs./in.^{2} steam pressure or at approxmiately 275° C., for 22 hours). Mean index of refraction of grains about 1.57. No difference between autoclaved and unautoclaved samples.

Cornwall stone (same treatment as Georgia kaolin). No apparent difference between autoclaved and unautoclaved samples.

Mica and quartz (same treatment as Georgia kaolin). No perceptible effect of autoclaving.

Lepidolite (same treatment as Georgia kaolin). Some etching marks on surfaces of grains, but otherwise indistinguishable from lepidolite which has been heated but not autoclaved.

Raw feldspar No. 3 ($<10\ \mu$; autoclaved at 800 lbs./in.^{2} steam pressure or 275° C., for 16 hours). Identical with untreated material.

Raw feldspar No. 3 (10 to 80 μ; same treatment as other raw feldspar). Identical with untreated feldspar.

Feldspar No. 3 (heated at 1,225° C.; recrushed to pass a No. 120 sieve and autoclaved for 24 hours at 700 to 1,000 lbs./in.^{2} steam pressure or approximately 265° to 290° C.). The feldspar is fused. Index of grains is slightly but unmistakably higher than the unautoclaved sample. (Unautoclaved=1.493, autoclaved=1.496.) Autoclaved sample shows a slight etching of the surface of the grains. The unautoclaved sample shows an extremely narrow layer on each grain somewhat higher in index than the body of the grain. The higher index of the autoclaved sample may be due to the annealing action during the autoclave treatment.

4. NATURE OF REACTION TERMED MOISTURE EXPANSION

While the results obtained in this investigation throw further light on the factors affecting the resistance of ceramic whiteware to moisture expansion, they offer no evidence regarding the nature of the reaction involved. Any of the observed facts can apply equally well, whether this expansion is caused by adsorption, absorption, or solid solutions. It is possible that the nature of the reaction could be proven using the method described by Washburn [17] for studying the dissociation equilibrium of autoclaved material at different temperatures. This method has been used by Schwarz [18] and Huttig [19] in a study of silica and its hydrates.

---

[17] J. Franklin Inst., p. 753, June, 1922.
[18] Ztschr. Elektrochem., vol. 32, p. 415, 1926.
[19] Ztschr. anor. Chem., vol. 121, p. 243, 1922.

IV. CONCLUSIONS

The most important conclusions justified by the data obtained in this investigation may be summarized briefly as follows:

1. Fused feldspar is the most susceptible to moisture expansion of the materials investigated.

2. The increasing content of fused feldspar and the decreasing absorption of whiteware bodies heated to progressively higher temperatures are counteracting influences which apparently result in least resistance to moisture expansion for those bodies matured at cone 6 to 8 and having an absorption of about 10 per cent.

3. Glazed earthenware may be subject to crazing caused by penetration of moisture through the glaze and the resultant moisture expansion of the body.

4. Reactions induced by heating autoclaved specimens and evidenced by contraction are relatively sluggish at 120° C., proceed faster as the temperature is raised, and are markedly accelerated at temperatures above 230° C.

5. Autoclaved specimens of whiteware which have expanded due to reaction with moisture apparently return to their original length when cooled to room temperature after holding for a reasonably short time at 250° to 270° C. in air and under atmospheric pressure.

WASHINGTON, June 21, 1932.

INFRA-RED ARC SPECTRA PHOTOGRAPHED WITH XENOCYANINE

By W. F. Meggers and C. C. Kiess

ABSTRACT

A new sensitizing dye, xenocyanine, has made possible the preparation, by the Eastman Kodak Co., of plates highly sensitive to infra-red light ranging in wave length from 8,000 to 11,000 A. With such plates the infra-red arc spectra of about 50 elements have been observed at the Bureau of Standards. New wavelength measurements have been made for Ti, Fe, Co, Ni, and Zr, and are presented in this paper. Many of these new lines have been accounted for as combinations between previously known terms of the neutral atoms. In the case of Ti a new term, a^5D, has been found. Both Ti and Fe are rich in strong lines in the region investigated and are recommended as suitable comparison spectra for the measurement of wave lengths in the infra-red.

CONTENTS

	Page
I. Introduction	309
II. Apparatus and methods	310
III. Results	310
1. Titanium	310
2. Iron	314
3. Cobalt	318
4. Nickel	322
5. Zirconium	324
IV. Conclusion	325

I. INTRODUCTION

More than a decade has passed since the authors [1] published several papers on the infra-red emission spectra of various metallic arcs. Use was made of photographic plates bathed in solutions of dicyanin which was the best photographic sensitizer then known for the infra-red. Dicyanin exhibits its maximum sensitivity in the red at wave length 7,000 A, but it is characterized by a broad band which made it possible to record, with prolonged exposures, the strongest lines between 9,000 and 10,000 A. It appears now that the practical limit of dicyanin as employed by us is about 9,800 A, and nearly all of the lines observed with apparently greater wave length have been explained as Lyman ghosts produced by the diffraction grating when very long exposures are used.

A new infra-red sensitizer, called neocyanine,[2] was discovered in 1926; its sensitizing action is a maximum at 8,100 A and it has been used extensively for the photography of spectra. However, its sensitizing band is much narrower than that of dicyanin, the action falling off very rapidly beyond 9,000 A, so that no appreciable advance was made in the study of infra-red spectra.

[1] W. F. Meggers, B. S. Sci. Papers, vol. 14 (S312), p. 371, 1918. W. F. Meggers and C. C. Kiess, B. S. Sc. Papers, vol. 14 (S324), p. 637, 1918. C. C. Kiess and W. F. Meggers, B. S. Sci. Papers, vol. 16 (S372) p. 51, 1920.

[2] M. L. Dundon, A. L. Schoen, and R. M. Briggs, J. Opt. Soc. Am. and Rev. Sci. Inst., vol. 12, p. 397, 1926.

The recent discovery, in the Eastman Kodak research laboratories, of a new infra-red sensitizer, xenocyanine, is now recognized as beginning a new era in infra-red spectroscopy. Photographic emulsions containing xenocyanine have two remarkable properties—(1) a very broad sensitizing band which ranges from about 8,000 to 11,000 Å with a maximum at 9,600 A, (2) extraordinary speed, which is estimated at one hundred to one thousand times that of the best materials heretofore available for the interval 9,000 to 10,000 A. At the Bureau of Standards more than 50 spectra have now been explored in the infra-red with these new plates, and in nearly all cases many new lines have been discovered. In this paper results are presented for titanium, iron, cobalt, nickel, and zirconium.

II. APPARATUS AND METHODS

The light source in each case was a direct-current arc carrying 6 to 8 amperes with an applied potential of 220 volts. Rods of iron, cobalt, and nickel served as arc electrodes, while in the cases of titanium and zirconium, pieces of metal were used in a copper arc.

The spectrograms were made with a concave grating, mounted stigmatically, as described elsewhere,[3] the dispersion being 10.4 A/mm in the first-order spectrum. The infra-red spectra were photographed in the first order with exposures of 20 to 60 minutes and adjacent portions of the plate were exposed for 1 minute to the second-order spectrum of iron for the purpose of wave-length measurements. For titanium and iron the stronger lines were photographed also with the grating ruled with 20,000 lines per inch, giving a dispersion of 3.6 A/mm.

The xenocyanine plates were hypersensitized in a dilute ammonia bath just before use in the spectrograph, and they were developed in Eastman Kodak X-ray developer at about 18° C. immediately after exposure.

Wave-length determinations in the infra-red spectra involved careful measurement of the position of the lines relative to lines in the blue and green portions of the iron spectrum recorded in juxtaposition. The values of the iron lines were those adopted as secondary standards by the International Astronomical Union,[4] their apparent values for the interpolation of wave lengths corresponding to infra-red lines being assumed to be exactly double their actual values.

III. RESULTS

1. TITANIUM

In Table 1 are presented the new wave lengths measured in the arc spectrum of Ti and extending it 1,000 A beyond the longest line previously recorded. The most complete list of Ti I lines published to date is that compiled by Prof. H. N. Russell [5] from various sources and giving the classifications of nearly 1,400 lines as combinations between terms of the singlet, triplet, and quintet systems. Our list overlaps Russell's by nearly 1,500 A, and a comparison of the two well illustrates the advantage of the new photographic materials over

[3] W. F. Meggers and K. Burns, B. S. Sci. Papers (No. 441), 18, p. 191, 1922.
[4] Trans. Internat. Astron. Union, vol. 3, p. 77, 1928.
[5] Astrophys. J., vol. 66, p. 347, 1927.

those formerly used. Not only are the intensity estimates of the lines greatly increased but many faint lines, predictable from term combinations and heretofore unobserved, are now recorded.

In addition to wave length and intensity estimates, Table 1 records for each line its vacuum wave number and its term combination. Most of the classifications are based on the terms given by Russell which we have expressed in the current standard notation.[6] A key for translating Russell's notation into that used at present is to be found in a recent paper by Miss Moore.[7]

As shown in Russell's analysis of Ti I a group of metastable terms is to be expected arising from the electron configuration $3d^4$. Of this group of terms we have found a^5D which actually lies higher in the energy diagram than the lowest odd terms ($z^5D°$ and $z^5F°$) of the middle group with which it combines. The values of the components of a^5D relative to $a^3F_2 = 0$ are given in Table 2.

TABLE 1.—*Wave lengths in the infra-red spectrum of titanium*

λ_{air} I. A.	Intensity	ν_{vac} cm^{-1}	Term combination
10, 774. 82	1	9, 278. 36	a^5F_2–$z^5G_2^\circ$
10, 732. 84	1	9, 314. 65	a^5F_3–$z^5G_3^\circ$
10, 731. 11	0	9, 316. 15	$x^5D_3^\circ$–f^5F_4
10, 726. 27	4	9, 320. 35	a^5F_1–$z^5G_2^\circ$
10, 689. 33	1	9, 352. 56	$x^5D_4^\circ$–f^5F_5
10, 676. 90	2	9, 363. 44	a^5F_4–$z^5G_4^\circ$
10, 661. 50	8	9, 376. 98	a^5F_2–$z^5G_3^\circ$
10, 607. 71	1	9, 424. 52	a^5F_5–$z^5G_5^\circ$
10, 584. 57	12	9, 445. 12	a^5F_3–$z^5G_4^\circ$
10, 552. 87	1	9, 473. 50	a^3H_5–$y^3G_4^\circ$
10, 496. 08	15	9, 524. 76	a^5F_4–$z^5G_5^\circ$
10, 459. 98	3	9, 557. 63	a^3H_6–$y^3G_5^\circ$
10, 396. 78	20	9, 615. 72	a^5F_5–$z^5G_6^\circ$
10, 145. 40	5	9, 853. 98	
10, 120. 87	7	9, 877. 87	a^3D_3–$x^3D_2^\circ$
10, 066. 47	8	9, 931. 25	a^3D_2–$x^3D_1^\circ$
10, 059. 87	12	9, 937. 77	b^3F_2–$z^3G_3^\circ$
10, 057. 69	25	9, 939. 92	a^3D_3–$x^3D_3^\circ$
10, 050. 11	5	9, 947. 41	
10, 048. 78	12	9, 948. 73	b^3F_3–$z^3G_4^\circ$
10, 034. 45	15	9, 962. 94	b^3F_4–$z^3G_5^\circ$
10, 011. 72	15	9, 985. 56	a^3D_1–$x^3D_1^\circ$
10, 003. 02	25	9, 994. 24	a^3D_2–$x^3D_2^\circ$
9, 997. 94	15	9, 999. 32	a^5G_3–$y^3F_2^\circ$
9, 981. 16	5	10, 016. 13	
9, 948. 98	8	10, 048. 53	a^3D_1–$x^3D_2^\circ$
9, 941. 33	8	10, 056. 26	a^3D_2–$x^3D_3^\circ$
9, 930. 30	1	10, 067. 44	$y^1G_4^\circ$–e^1G_4
9, 927. 35	20	10, 070. 42	a^3G_4–$y^3F_3^\circ$
9, 923. 25	2	10, 074. 58	a^3D_2–$y^3G_3^\circ$ a^3D_3–$y^3G_4^\circ$ $y^3G_5^\circ$–e^3F_4

[6] Phys. Rev., vol. 33, p. 900, 1929.

[7] Astrophys. J., vol. 75, p. 235, 1932.

TABLE 1.—*Wave lengths in the infra-red spectrum of titanium*—Continued

λ_{air} I. A.	Intensity	ν_{vac} cm^{-1}	Term combination
9, 879. 41	3	10, 119. 29	a^3G_3–$y^3F_3^0$
9, 832. 15	25	10, 167. 93	a^3G_5–$y^3F_4^0$
9, 813. 45	5	10, 187. 30	$z^5D_4^0$–a^5D_3
9, 787. 67	50	10, 214. 14	a^5F_3–$z^5F_2^0$
9, 783. 59	20	10, 218. 40	a^5F_2–$z^5F_1^0$
9, 783. 30	40	10, 218. 70	a^5F_4–$z^5F_3^0$
9, 770. 28	40	10, 232. 32	a^5F_5–$z^5F_4^0$
9, 768. 22	5	10, 234. 47	$z^5D_3^0$–a^5D_2
9, 746. 86	15	10, 256. 91	$z^5D_4^0$–a^5D_4
9, 743. 60	50	10, 260. 34	a^5F_1–$z^5F_1^0$
9, 737. 77	5	10, 266. 48	$z^5D_2^0$–a^5D_1
9, 728. 36	60	10, 276. 41	a^5F_2–$z^5F_2^0$
9, 718. 96	25	10, 286. 35	a^1G_4–$z^1F_3^0$
9, 717. 00	10	10, 288. 42	$z^5D_3^0$–a^5D_3
9, 715. 51	3	10, 290. 00	$z^5D_1^0$–a^5D_0
9, 705. 64	80	10, 300. 47	a^5F_3–$z^5F_3^0$
9, 702. 86	3	10, 303. 42	$z^5D_2^0$–a^5D_2
9, 690. 62	2	10, 316. 43	a^3D_2–$z^5P_2^0$
9, 688. 86	30	10, 318. 31	a^5F_1–$z^5F_2^0$
9, 678. 98	3	10, 328. 85	$z^5D_0^0$–a^5D_1
9, 675. 55	90	10, 332. 50	a^5F_4–$z^5F_4^0$
9, 663. 19	3	10, 345. 72	$z^5D_1^0$–a^5D_2
9, 661. 42	10	10, 347. 61	a^3D_3–$z^5P_3^0$
9, 652. 38	1	10, 357. 30	$z^5D_2^0$–a^5D_3
9, 651. 66	1	10, 358. 07	$z^5D_3^0$–a^5D_4
9, 647. 91	1	10, 362. 10	
9, 647. 40	50	10, 362. 65	a^5F_2–$z^5F_3^0$
9, 638. 28	100	10, 372. 45	a^5F_5–$z^5F_5^0$
9, 606. 77	3	10, 406. 48	$y^5F_5^0$–f^5F_4
9, 602. 38	1	10, 411. 23	$y^5D_3^0$–e^5F_4
9, 599. 53	50	10, 414. 32	a^5F_3–$z^5F_4^0$
9, 590. 15	3	10, 424. 51	$y^5D_4^0$–e^5F_5
9, 588. 77	4	10, 426. 01	$y^5F_4^0$–f^5F_3
9, 570. 08	4	10, 446. 37	$y^5F_3^0$–f^5F_2
9, 550. 11	2	10, 468. 21	$y^5F_2^0$–f^5F_1
9, 546. 07	50	10, 472. 64	a^5F_4–$z^5F_5^0$
9, 511. 80	8	10, 510. 37	$y^5F_3^0$–f^5F_2
9, 511. 55	10	10, 510. 65	$y^5F_1^0$–f^5F_1
9, 510. 81	12	10, 511. 47	$y^5F_2^0$–f^5F_3
9, 508. 49	20	10, 514. 03	$y^5F_4^0$–f^5F_4
9, 506. 04	25	10, 516. 76	$y^5F_5^0$–f^5F_5
9, 473. 51	2	10, 552. 86	$y^5F_1^0$–f^5F_2
9, 453. 22	3	10, 575. 51	$y^5F_2^0$–f^5F_3
9, 431. 77	3	10, 599. 56	$y^5F_3^0$–f^5F_4
9, 409. 69	2	10, 624. 44	$y^5F_4^0$–f^5F_5
9, 312. 48	4	10, 735. 34	$x^3F_2^0$–e^3F_2
9, 305. 04	1	10, 743. 92	$y^3F_4^0$–e^3G_4
9, 285. 04	5	10, 767. 06	$x^3F_3^0$–e^3F_3
9, 257. 62	7	10, 798. 95	$x^3F_4^0$–e^3F_4
9, 246. 14	10	10, 812. 36	$y^3F_4^0$–e^3G_5

TABLE 1.—*Wave lengths in the infra-red spectrum of titanium*—Continued

λ_{air} I. A.	Intensity	ν_{vac} cm^{-1}	Term combination
9, 170. 38	2	10, 901. 68	$v^3D_3^\circ$–g^3F_4
9, 167. 53	8	10, 905. 07	$y^5F_5^\circ$–e^5G_4
9, 135. 92	2	10, 942. 80	c^3P_1–$w^3D_2^\circ$
9, 123. 14	5	10, 958. 13	$y^3F_2^\circ$–e^3G_3
9, 090. 70	25	10, 997. 24	a^5P_3–$z^5S_2^\circ$
9, 087. 67	2	11, 000. 90	c^3P_2–$w^3D_3^\circ$
9, 086. 94	2	11, 001. 79	a^5P_3–$y^3F_2^\circ$
9, 027. 32	15	11, 074. 45	a^5P_2–$z^5S_2^\circ$
9, 023. 65	2	11, 078. 95	a^5P_2–$y^3F_2^\circ$
8, 989. 44	12	11, 121. 11	a^5P_1–$z^5S_2^\circ$
8, 985. 80	2	11, 125. 62	a^5P_1–$y^3F_2^\circ$
8, 863. 09	3	11, 279. 64	$x^5G_5^\circ$–f^5G_3
8, 821. 14	12	11, 333. 29	a^5P_3–$y^3D_2^\circ$
8, 819. 39	8	11, 335. 54	a^3P_2–$z^3D_1^\circ$
8, 794. 40	8	11, 367. 75	$z^1H_5^\circ$–e^1G_4
8, 778. 66	30	11, 388. 13	a^5P_3–$z^3P_2^\circ$
8, 766. 64	75	11, 403. 75	a^3P_2–$z^3D_2^\circ$
8, 761. 44	15	11, 410. 52	a^5P_2–$y^3D_2^\circ$
8, 737. 31	7	11, 442. 03	$x^5G_5^\circ$–f^5G_5
8, 734. 70	75	11, 445. 45	a^3P_1–$z^3D_1^\circ$
8, 725. 76	6	11, 457. 18	a^5P_1–$y^3D_2^\circ$
8, 719. 56	30	11, 465. 33	a^5P_2–$z^3P_2^\circ$
8, 692. 34	100	11, 501. 23	a^3P_0–$z^3D_1^\circ$
8, 682. 99	125	11, 513. 61	a^3P_1–$z^3D_2^\circ$
8, 675. 38	150	11, 523. 71	a^3P_2–$z^3D_3^\circ$
8, 641. 47	40	11, 568. 93	
8, 636. 38	18	11, 575. 75	
8, 629. 33	18	11, 585. 20	
8, 618. 44	20	11, 599. 85	b^3P_1–$w^3D_1^\circ$
8, 618. 14	15	11, 600. 25	
8, 612. 91	7	11, 607. 29	a^5P_2–$y^5D_1^\circ$
8, 600. 98	25	11, 623. 39	b^3P_2–$w^3D_2^\circ$ a^5P_1–$y^5D_0^\circ$
8, 598. 18	60	11, 627. 18	b^1G_4–$x^3G_3^\circ$
8, 578. 40	15	11, 653. 99	a^5P_1–$y^5D_1^\circ$
8, 569. 72	50	11, 665. 79	b^3P_0–$w^5D_1^\circ$
8, 565. 45	25	11, 671. 61	a^5P_2–$y^5D_2^\circ$
8, 550. 54	25	11, 691. 96	a^5P_3–$y^5D_3^\circ$
8, 548. 07	100	11, 695. 34	a^3G_3–$x^3F_2^\circ$
8, 539. 36	60	11, 707. 26	b^3P_1–$w^3D_2^\circ$
8, 531. 36	15	11, 718. 25	a^5P_1–$y^5D_2^\circ$
8, 526. 36	8	11, 725. 11	
8, 525. 99	8	11, 725. 63	
8, 518. 37	100	11, 736. 11	a^3G_4–$x^3F_3^\circ$
8, 518. 05	60	11, 736. 55	$z^5F_5^\circ$–a^5D_4
8, 496. 03	60	11, 766. 97	b^3P_2–$w^3D_3^\circ$ a^1F_3–$v^1F_3^\circ$
8, 495. 51	15	11, 767. 69	
8, 494. 42	30	11, 769. 20	a^5P_2–$y^5D_3^\circ$
8, 483. 16	25	11, 784. 83	a^3G_3–$x^3F_3^\circ$
8, 468. 46	100	11, 805. 28	a^3G_5–$x^3F_4^\circ$
8, 467. 15	75	11, 807. 11	$z^5F_4^\circ$–a^5D_3

TABLE 1.—*Wave lengths in the infra-red spectrum of titanium*—Continued

λ_{air} I. A.	Intensity	ν_{vac} cm^{-1}	Term combination
8, 460. 96	7	11, 815. 74	
8, 457. 10	40	11, 821. 14	a^5P_3–$y^5D_4^?$
8, 450. 89	75	11, 829. 74	a^3H_5–$x^3G_4^?$
8, 442. 98	20	11, 840. 91	b^3P_2–$x^5D_3^?$
8, 438. 93	75	11, 846. 60	a^3H_6–$x^3G_5^?$
8, 435. 68	300	11, 851. 15	a^5F_4–$z^5D_3^?$
8, 434. 98	300	11, 852. 14	a^5F_5–$z^5D_4^?$
8, 426. 50	200	11, 864. 07	a^5F_3–$z^5D_2^?$
8, 424. 41	50	11, 867. 01	$z^5F_3^?$–a^5D_2
8, 423. 10	20	11, 868. 86	a^3G_4–$x^3F_4^?$
8, 418. 70	10	11, 875. 06	
8, 417. 54	25	11, 876. 70	$z^5F_4^?$–a^5D_4
8, 416. 97	60	11, 877. 50	a^3H_4–$x^3G_3^?$
8, 412. 36	150	11, 884. 01	a^5F_2–$z^5D_1^?$
8, 407. 87	4	11, 890. 37	
8, 402. 54	5	11, 897. 90	a^3H_5–$x^3G_5^?$
8, 396. 93	90	11, 905. 84	a^5F_1–$z^5D_0^?$
8, 389. 48	25	11, 916. 42	$z^5F_3^?$–a^5D_1
8, 382. 82	90	11, 925. 89	a^5F_1–$z^5D_1^?$
8, 382. 54	100	11, 926. 29	a^5F_2–$z^5D_2^?$
8, 377. 90	100	11, 932. 90	a^5F_3–$z^5D_3^?$

Table 2.—The term a^5D

J	ν	$\Delta\nu$
4	28, 952. 10	69. 66
3	28, 882. 44	53. 93
2	28, 828. 51	36. 89
1	28, 791. 62	18. 76
0	28, 772. 86	

2. IRON

The arc spectrum of iron is of exceptional interest because it is the main source of internationally adopted secondary standards of wave length. Furthermore, it is the spectrum in which the largest number of lines have been classified on the basis of modern theories of spectral structure, more than 2,400 lines now being accounted for as combinations of established atomic energy levels characteristic of the neutral atoms of iron.

Extensive analyses of the arc sprectrum of iron have been published by Burns and Walters [8] and by Catalán,[9] the former being based on new measurements of wave lengths in the vacuum arc, while the latter uses all available data for the arc in air and presents the most complete list of energy levels. Since our observations were also made at atmospheric pressure, we are quoting term combinations from the latter paper in Table 3 below. The results for the infra-red arc spectrum of iron appearing in Table 3 include measured wave lengths, estimated relative intensities, computed wave numbers in

[8] K. Burns and F. M. Walters, jr., Pub. Allegheny Obs., vol. 6, No. 11, 1930.
[9] M. A. Catalán, Anales Soc. Esp. Fis. y Quim., vol. 28, p. 1239, 1930.

vacuum, and spectral term combinations. In the range covered by these photographic observations lines were observed radiometrically by Randall and Barker.[10] Without disparaging the excellent quality of the radiometric results as such, a comparison, nevertheless, shows the enormous advantage of the photographic method for recording details and improving precision of the measurements.

TABLE 3.—*Wave lengths in the infra-red spectrum of iron*

λ_{air} I. A.	Intensity	ν_{vac} cm $^{-1}$	Term combination
10, 863. 4	1	9, 202. 68	$b^3D_3'-\alpha^5F_4$
10, 817. 9	1	9, 241. 38	
10, 783. 0	1	9, 271. 36	
10, 532. 12	10	9, 492. 17	
10, 469. 55	20	9, 548. 89	
10, 452. 60	5	9, 564. 38	
10, 423. 55	3	9, 591. 04	
10, 395. 75	8	9, 616. 68	$a^5P_3-a^3F_4'$
10, 353. 7	2h	9, 655. 77	$d^5D_1'-\beta^3D_2$
10, 348. 16	4h	9, 660. 91	
10, 345. 2	1	9, 663. 70	
10, 340. 77	4	9, 667. 81	$a^5P_2-a^3F_3'$
10, 218. 36	3	9, 783. 63	$c^5F_4'-20C_5$
10, 216. 42	100	9, 785. 48	$b^3D_3'-\alpha^3F_4$
10, 195. 11	2	9, 805. 94	$a^5G_4-a^3F_3'$
10, 187. 4	1	9, 813. 35	
10, 167. 4	1	9, 832. 64	$a^5P_2-a^5F_2'$
10, 145. 64	80	9, 853. 75	$b^3D_2'-\alpha^3F_3$
10, 142. 82	2	9, 856. 49	$c^5F_3'-29C_3$
10, 115. 18	1	9, 883. 42	
10, 113. 86	2	9, 884. 71	
10, 071. 88	2	9, 925. 91	
10, 065. 09	60	9, 932. 61	$b^3D_1'-\alpha^3F_2$
10, 057. 64	3	9, 939. 97	$c^5F_4'-24C_3$
9, 996. 85	1h	10, 000. 41	
9, 980. 55	2h	10, 016. 74	
9, 977. 52	1	10, 019. 78	$c^5F_3'-35C_3$
9, 944. 13	3h	10, 053. 43	
9, 917. 93	1p?	10, 079. 99	
9, 897. 69	1p?	10, 100. 59	
9, 889. 11	40	10, 109. 36	$c^5F_4'-30C_5$
9, 881. 4	1	10, 117. 2	
9, 868. 09	3	10, 130. 90	$c^5F_4'-46C_3$
9, 861. 83	30	10, 137. 33	$c^5F_3'-39C_3$
9, 839. 38	1	10, 160. 46	
9, 834. 04	3h	10, 165. 97	$c^5F_5'-21C_{5,4}$
9, 811. 36	2	10, 189. 47	
9, 800. 42	20	10, 200. 85	$c^5F_2'-49C_3$
9, 794. 91	1	10, 206. 59	
9, 786. 62	2	10, 215. 24	$b^3F_3'-\alpha^5F_4$
9, 783. 96	3	10, 218. 01	$c^5F_5'-22C_5$
9, 763. 91	15	10, 238. 99	$c^5F_4'-33C_4$
9, 763. 34	15	10, 239. 59	$c^5F_1'-56C_2$
9, 753. 15	10	10, 250. 29	$b^3D_2'-\alpha^3F_2$
9, 747. 24	2	10, 256. 50	

[10] H. M. Randall and E. F. Barker, Astrophys. J., vol. 49, p. 42, 1919.

TABLE 3.—*Wave lengths in the infra-red spectrum of iron*—Continued

λ_{air} I. A.	Intensity	ν_{vac} cm^{-1}	Term combination
9, 738. 73	200	10, 265. 47	$c^5F_5'-23C_6$
9, 699. 70	6h	10, 306. 77	
9, 693. 69	1	10, 313. 16	$a^5S_2'-48C_2$
9, 683. 57	1	10, 323. 94	$a^5S_2'-49C_3$
9, 676. 42	1	10, 331. 57	
9, 673. 16	1h	10, 335. 05	
9, 666. 59	2	10, 342. 07	
9, 658. 94	3	10, 350. 26	$c^5F_3'-47C_{4,3}$
9, 657. 30	4	10, 352. 03	$c^5F_2'-56C_2$
9, 653. 18	20	10, 356. 44	$b^3D_3'-\alpha^3F_3$
9, 637. 55	2	10, 373. 25	
9, 634. 22	5	10, 376. 82	$c^5F_3'-49C_3$
9, 626. 60	30h	10, 385. 00	$c^5F_4'-39C_2$
9, 602. 07	2	10, 411. 57	
9, 569. 95	40h	10, 446. 51	$c^5F_5'-30C_5$
9, 556. 56	1	10, 461. 14	
9, 550. 90	2	10, 467. 35	$c^5D_2'-29C_3$
9, 529. 31	4h	10, 491. 06	$b^5G_6'-\beta^5F_5$
9, 527. 7	1	10, 492. 8	$c^5F_3'-54C_4$
9, 513. 21	10h	10, 508. 82	$c^5F_4'-45C_5$ $b^5G_2'-\beta^5F_3$
9, 462. 97	2	10, 564. 61	$c^5D_3'-24C_3$
9, 454. 24	4h	10, 574. 37	$c^5F_1'-61C_2$
9, 452. 45	2	10, 576. 37	$c^5F_5'-33C_4$
9, 443. 98	10h	10, 585. 85	$c^5F_2'-60C_3$
9, 437. 91	2	10, 592. 66	$b^3F_3'-\alpha^5F_3$
9, 430. 07	4	10, 601. 47	
9, 414. 14	20h	10, 619. 41	$c^5F_3'-58C_2$
9, 410. 1	1h	10, 624. 0	
9, 401. 09	10h	10, 634. 15	$c^5F_4'-50C_4$
9, 394. 71	3h	10, 641. 37	
9, 388. 28	3h	10, 648. 66	$c^5D_2'-36C_1$
9, 382. 83	3h	10, 654. 84	
9, 372. 84	6	10, 666. 20	$b^3F_4-a^3F_4'$ $c^5D_1'-43C_2$
9, 362. 36	4	10, 678. 13	$a^3P_2-a^5P_3'$
9, 359. 37	3	10, 681. 55	$b^3F_4-a^3D_3'$
9, 350. 52	10	10, 691. 66	$b^3F_4'-\alpha^5F_4$
9, 343. 40	3	10, 699. 80	$c^5F_4'-\alpha^3D_3$
9, 333. 94	2	10, 710. 65	$c^5F_5'-38C_6$
9, 318. 13	3	10, 728. 82	$c^5D_3'-29C_3$
9, 307. 94	2	10, 740. 57	$c^5F_4'-54C_4$
9, 294. 66	2	10, 755. 92	$c^5F_4'-\beta^5D_4$
9, 259. 05	15	10, 797. 29	$c^5D_4'-21C_{5,4}$
9, 258. 40	20	10, 798. 04	$b^3F_3'-\alpha^3F_4$
9, 246. 54	2	10, 811. 89	$b^3F_2-a^3D_2'$
9, 242. 32	2	10, 816. 82	$b^5F_1'-\alpha^5D_1$
9, 233. 2	1	10, 827. 5	$b^5G_5'-\alpha^3G_3$
9, 217. 54	5h	10, 845. 91	$c^5F_5'-45C_5$
9, 214. 45	6	10, 849. 54	$c^5D_4'-22C_5$
9, 210. 02	6	10, 854. 76	$b^3P_1-b^5D_2'$
9, 199. 52	2h	10, 867. 15	

TABLE 3.—*Wave lengths in the infra-red spectrum of iron*—Continued

λ_{air} I. A.	Intensity	ν_{vac} cm^{-1}	Term combination
9, 178. 57	1h	10, 891. 96	$c^5D_2'-35C_3$
9, 173. 46	4h	10, 898. 02	$b^5F_2-a^3D_1'$
9, 166. 44	3h	10, 908. 74	$c^5D_4'-24C_3$
9, 156. 9	2	10, 917. 7	$c^5D_2'-46C_3$
9, 155. 9	1	10, 918. 9	
9, 147. 91	5h	10, 928. 46	$c^5F_3'-\beta^5D_3$
9, 146. 11	3	10, 930. 61	$b^3F_3-a^3F_3'$
9, 121. 1	1	10, 960. 6	
9, 118. 87	20	10, 963. 26	$b^3P_2-b^5D_2'$
9, 117. 10	2	10, 965. 39	$c^5D_1'-\alpha^5F_2$
9, 116. 14	2	10, 966. 55	
9, 103. 64	1	10, 981. 60	$b^5F_5'-\alpha^5D_4$
9, 100. 50	5h	10, 985. 40	$c^5D_4'-26C_3$
9, 089. 40	30	10, 998. 81	$b^3G_5-a^5G_5'$
9, 088. 22	40	11, 000. 24	$b^3P_1-a^3P_2'$
9, 084. 2	1	11, 005. 1	$b^5F_3'-\alpha^5D_2$
9, 080. 48	3h	11, 009. 62	$c^5D_3'-39C_3$ $c^5F_4'-60C_3$
9, 079. 65	8	11, 010. 62	$b^3F_2'-\alpha^3F_3$
9, 070. 42	2	11, 021. 82	$b^5F_4'-\alpha^5D_3$ $c^5F_2'-\alpha^3D_1$
9, 062. 24	2	11, 031. 77	$c^5F_2'-\beta^5D_2$
9, 052. 6	1	11, 043. 5	$b^3G_5'-\alpha^3G_4$
9, 044. 63	1	11, 053. 25	
9, 036. 9	1	11, 062. 7	$c^5D_2'-\alpha^3D_3$
9, 030. 67	1	11, 070. 34	$b^3P_1-b^5D_1'$
9, 024. 47	15	11, 077. 94	$c^5D_4'-30C_5$
9, 019. 84	2	11, 083. 63	$c^5F_1'-\beta^5D_1$
9, 013. 90	1	11, 090. 93	$a^3P_2-a^5P_2'$
9, 012. 10	30	11, 093. 15	$c^5F_5-\beta^5D_4$
9, 010. 55	2	11, 095. 06	$b^3F_2-a^3F_2'$
9, 008. 37	2	11, 097. 84	$c^5D_2'-52C_{3,2}$
9, 006. 72	1	11, 099. 78	$c^5D_2'-53C_2$
8, 999. 54	100	11, 108. 63	$b^3P_2-a^3P_2'$
8, 995. 20	1p?	11, 113. 99	
8, 984. 87	3	11, 126. 77	$c^5F_1'-\beta^5D_0$
8, 975. 36	15	11, 138. 56	$b^3G_4-a^5G_4'$ $c^5D_2'-\alpha^5F_2$
8, 946. 25	1	11, 174. 80	$b^3P_1-b^5D_0'$
8, 945. 15	20	11, 176. 17	$c^5F_4'-\beta^5D_3$
8, 943. 00	3	11, 178. 86	$b^3P_2-b^5D_1'$ $c^5D_2'-46C_3$
8, 929. 04	5	11, 196. 34	$c^5F_2'-\beta^5D_1$
8, 919. 95	10	11, 207. 75	$c^5D_4-33C_4$ $c^5F_3'-\beta^5D_2$
8, 916. 26	1	11, 212. 39	$a^3F_2-a^7P_3'$
8, 876. 13	2	11, 263. 08	
8, 868. 42	3	11, 272. 97	$b^3G_3-a^5G_3'$
8, 866. 92	150	11, 274. 78	$b^3F_4'-\alpha^3F_4$
8, 863. 64	1p?	11, 278. 95	

TABLE 3.—*Wave lengths in the infra-red spectrum of iron*—Continued

λ_{air} I. A.	Intensity	ν_{vac} cm^{-1}	Term combination
8, 846. 82	5	11, 300. 40	$c^5D_1'-61C_2$
8, 838. 36	30	11, 311. 21	$b^3P_0-a^3P_1$
8, 824. 18	200	11, 329. 39	$a^5P_2-a^5P_3'$
8, 814. 5	2	11, 341. 8	
8, 812. 0	1p?	11, 345. 0	
8, 809. 1	2	11, 348. 8	
8, 808. 3	4h	11, 349. 8	
8, 804. 56	10	11, 354. 64	$a^3P_2-a^5P_1'$
8, 801. 98	1p?	11, 357. 96	
8, 796. 42	2	11, 365. 14	$c^5D_3'-54C_4$
8, 793. 38	120	11, 369. 07	$b^3F_3'-a^3F_3$
8, 790. 62	10h	11, 372. 64	$c^5D_2'-60C_3$
8, 784. 44	5	11, 380. 64	$c^5D_3'-\beta^5D_4$
8, 764. 02	100	11, 407. 16	$b^3F_2'-a^3F_2$
8, 757. 16	50	11, 416. 09	$b^3P_1-a^3P_1'$
8, 747. 32	2	11, 428. 94	$b^3G_3-a^3G_4'$
8, 729. 1	2	11, 452. 8	
8, 713. 19	10	11, 473. 70	$b^3G_5-a^5G_4'$
8, 710. 29	20h	11, 477. 53	$c^5D_4-45C_5$

3. COBALT

About 1,200 lines of the cobalt arc have been classified by Catalán and Bechert,[11] but only 10 of these have wave lengths exceeding 8,648 A. Our results for cobalt are shown in Table 4, the construction of which is identical with that of the preceding wave-length tables. The line classifications have all been derived from Catalán's term tables without any effort to extend these. A considerable number of lines, including some very strong ones, remain unclassified, indicating that the term analysis for cobalt is less complete than for iron. The arc spectrum of cobalt has also been explored radiometrically in the infra-red by Randall and Barker.[12] In the interval 9,000 to 11,000 A the wave lengths and relative intensities were measured for 10 lines, all but two of which are identifiable with the strongest ones in our list. Here again the superior advantages of photographic over bolometric methods of studying complex spectra are strikingly exemplified.

[11] M. A. Catalán and K. Bechert, Zeit. f. Phys., vol. 32, p. 336, 1925. M. A. Catalán, Zeit. f. Phys., vol. 47, p. 89, 1927.
[12] H. M. Randall and E. F. Barker, Astrophys. J., vol. 49, p. 54, 1919.

TABLE 4.—*Wave lengths in the infra-red spectrum of cobalt*

λ_{air} I. A.	Intensity	ν_{vac} cm^{-1}	Term combination
11, 091. 94	2	9, 013. 09	$b^2D_3'-\alpha^4F_4$
10, 805. 97	1	9, 251. 61	$c^4F_4'-[^4F_5]$
10, 681. 80	4	9, 359. 15	
10, 660. 15	5	9, 378. 16	
10, 584. 99	2	9, 444. 75	
10, 521. 36	2	9, 501. 87	$b^2D_2-b^4D_3'$
10, 471. 96	10	9, 546. 69	$b^2F_3'-\alpha^4F_3$
10, 447. 40	3	9, 569. 14	$b_5-[^4F_5]$
10, 442. 10	15	9, 574. 00	
10, 398. 37	4	9, 614. 26	$c^4G_6'-[H_7]$
10, 382. 22	30	9, 629. 26	$b^2D_2-a^2F_3'$
10, 374. 65	1	9, 636. 24	$c^4F_3'-[F_3]$
10, 369. 12	2	9, 641. 38	$c^4G_6'-[^4F_5]$?
10, 367. 95	2	9, 642. 47	$c^4F_4'-[D_3]$
10, 364. 43	1	9, 645. 74	$c^4G_6'-[H_6]$
10, 354. 45	60	9, 655. 04	$b^2F_4'-\alpha^4F_4$
10, 348. 00	1	9, 661. 1	$c^4F_3'-[F_4,D_3]$
10, 335. 40	4	9, 672. 84	
10, 332. 65	3	9, 675. 41	$c^4G_6'-[^4G_6,^4F_5]$
10, 327. 32	2	9, 680. 40	
10, 276. 80	5h	9, 727. 99	$(m^2F_3')-[F_3]$
10, 265. 4	1h	9, 738. 8	
10, 244. 64	1	9, 758. 52	
10, 239. 1	1h	9, 763. 8	$^2G_5-^6G_4'$
10, 222. 12	1	9, 780. 03	$a^2D_2-^6D_1'$
10, 195. 3	1	9, 805. 75	
10, 172. 83	20h	9, 827. 41	$c^4F_5'-[^4D_4]$
10, 167. 58	200	9, 832. 49	$b^2D_3'-\alpha^2F_2$
10, 154. 90	2	9, 844. 77	
10, 152. 93	4	9, 846. 68	
10, 131. 38	2	9, 867. 63	$b^4P_1-^6D_2'$
10, 128. 05	150	9, 870. 87	$b^2D_2'-\alpha^2F_3$
10, 111. 1	1h	9, 887. 4	
10, 105. 40	2	9, 892. 99	
10, 092. 0	2h	9, 906. 1	$c^4G_4'-[F_4]$
10, 078. 62	100	9, 919. 34	
10, 052. 96	8	9, 944. 60	$c^4F_5'-[^4F_5]$
10, 048. 80	3	9, 948. 71	$c^4F_5'-[H_6]$
10, 046. 31	150	9, 951. 18	$b^2D_2-a^2F_4'$
10, 031. 44	5	9, 965. 93	$b^4P_2-^6D_3'$
10, 021. 48	4h	9, 975. 83	
10, 019. 05	30h	9, 978. 25	$c^4F_5'-[^4G_6,^4F_5]$
10, 007. 78	3	9, 989. 49	
9, 999. 7	2h	9, 997. 6	$b^2D_2-b^4D_2'$?
9, 952. 2	3h	10, 045. 3	$b^2F_3'-\alpha^4F_2$
9, 940. 69	2	10, 056. 91	
9, 918. 1	1	10, 079. 8	$(a^2P_2')-[F_3,D_2]$
9, 912. 73	10	10, 085. 27	$b^4P_3-^6D_4'$
9, 909. 52	1h	10, 088. 54	
9, 890. 92	30	10, 107. 51	$b^2D_3-b^4D_4'$

TABLE 4.—*Wave lengths in the infra-red spectrum of cobalt*—Continued

λ_{air} I. A.	Intensity	ν_{vac} cm^{-1}	Term combination
9, 859. 90	1	10, 139. 31	
9, 852. 5	1	10, 146. 9	
9, 847. 7	2	10, 151. 9	c^4F_4'–[F_3]
9, 823. 52	4h	10, 176. 87	c^4F_4'–[F_4,D_3]
9, 798. 37	2h	10, 202. 99	c^4F_4'–[F_4,D_3]
9, 785. 39	40	10, 216. 52	
9, 769. 0	1h	10, 233. 7	
9, 764. 53	5h	10, 238. 34	
9, 746. 02	100	10, 257. 79	
9, 738. 46	2	10, 265. 78	
9, 735. 53	2	10, 268. 84	
9, 729. 54	3	10, 275. 16	
9, 696. 60	5	10, 310. 06	b^2D_2–a^2D_3'
9, 694. 0	2	10, 312. 8	
9, 678. 21	10h	10, 329. 66	
9, 670. 20	2	10, 338. 21	
9, 659. 94	3	10, 349. 20	
9, 638. 21	1	10, 372. 53	
9, 629. 83	3h	10, 381. 56	
9, 626. 72	1	10, 384. 91	
9, 618. 32	2	10, 393. 98	
9, 613. 46	4	10, 399. 23	
9, 606. 52	5	10, 406. 75	
9, 597. 90	200	10, 416. 09	b^2F_3'–a^2F_3
9, 592. 3	2h	10, 422. 2	
9, 585. 28	2	10, 429. 80	
9, 580. 63	3	10, 434. 87	
9, 569. 00	5h	10, 447. 55	c^4G_5'–[F_4]
9, 548. 66	4	10, 469. 80	
9, 544. 52	300	10, 474. 34	b^2F_4'–a^2F_4
9, 527. 17	10h	10, 493. 42	
9, 517. 33	1	10, 504. 27	
9, 513. 42	1	10, 508. 59	
9, 500. 01	1	10, 523. 42	
9, 482. 75	1	10, 542. 57	
9, 470. 74	2	10, 555. 94	b^4P_3–$^6D_3'$
9, 454. 23	3h	10, 574. 38	
9, 442. 34	4h	10, 587. 69	
9, 435. 70	3	10, 595. 14	c^4G_5'–[$^4F_5$]
9, 428. 8	1	10, 602. 9	
9, 425. 8	1	10, 606. 3	
9, 422. 60	3h	10, 609. 88	
9, 406. 12	4h	10, 628. 46	
9, 395. 11	2	10, 640. 92	
9, 356. 98	200	10, 684. 28	
9, 351. 06	3	10, 691. 04	
9, 347. 88	2h	10, 694. 68	
9, 344. 93	20	10, 698. 06	
9, 340. 54	3h	10, 703. 08	
9, 319. 53	2	10, 727. 21	

TABLE 4.—*Wave lengths in the infra-red spectrum of cobalt*—Continued

λ_{air} I. A.	Intensity	ν_{vac} cm^{-1}	Term combination
9, 280. 42	5	10, 772. 42	$b^2F_4'-a^6F_5$
9, 269. 90	1	10, 784. 64	
9, 262. 5	2	10, 793. 3	$b^2D_2-b^4F_3'$
9, 258. 18	4	10, 798. 30	$c^4F_4'-[F_4]$
9, 245. 60	1	10, 812. 99	$b^2D_3-a^2G_4'$
9, 233. 64	1	10, 827. 00	$a^2P_2-a^4F_3'$
9, 217. 80	2h	10, 845. 60	
9, 207. 96	1	10, 857. 19	
9, 204. 11	5	10, 861. 73	$b^2D_3-a^2F_3'$
9, 197. 29	1	10, 869. 79	$c^4F_5'-[F_4D_3]$
9, 185. 95	2	10, 883. 21	
9, 181. 75	5	10, 888. 18	
9, 177. 93	20	10, 892. 72	
9, 165. 52	2	10, 907. 47	
9, 150. 65	2h	10, 925. 19	
9, 133. 24	6	10, 946. 02	$c^4F_4'-[^4F_5]$
9, 130. 50	2	10, 949. 30	
9, 111. 64	1	10, 971. 96	
9, 095. 37	50	10, 991. 58	
9, 071. 35	4h	11, 020. 69	
9, 057. 29	2h	11, 037. 80	
9, 052. 44	2	11, 043. 72	$b^2D_2-b^4F_2'$
9. 040. 0	1	11, 058. 9	
9, 037. 87	50	11, 061. 52	
8, 997. 3	1	11, 111. 4	
8, 986. 51	3	11, 124. 74	
8, 972. 89	7	11, 141. 62	
8, 958. 37	15	11, 159. 68	$b^4F_3'-a^4F_4$
8, 953. 72	2	11, 165. 48	
8, 939. 14	5	11, 183. 69	
8, 926. 21	50	11, 199. 89	$b^2D_2-a^2D_2'$
8, 904. 63	30	11, 227. 03	
8, 892. 49	1	11, 242. 36	$c^4D_2'-[F_3]$
8, 888. 70	8h	11, 247. 15	
8, 886. 28	2	11, 250. 22	
8, 878. 28	3	11, 260. 35	
8, 872. 59	1	11, 267. 58	$c^4D_2'-[F_4D_3]$
8, 870. 70	8	11, 269. 98	
8, 856. 56	3	11, 287. 97	
8, 850. 70	30	11, 295. 44	$b^2F_4'-a^2F_3$
8, 837. 90	4h	11, 311. 80	
8, 835. 21	20	11, 315. 25	$b^4F_4'-a^4F_5$
8, 819. 10	100	11, 335. 92	$c^4G_6'-\pi_5$
8, 779. 20	3	11, 387. 44	
8, 774. 71	2	11, 393. 26	$c^4D_4'-[^4D_4,^4P_3]$
8, 772. 04	2	11, 396. 73	
8, 766. 55	4h	11, 403. 87	$c^4D_4'-[^4D_4]$
8, 759. 58	3	11, 412. 94	
8, 750. 13	60	11, 425. 27	$c^4F_4'-[F_3D_2]$

TABLE 4.—*Wave lengths in the infra-red spectrum of cobalt*—Continued

λ_{air} I. A.	Intensity	ν_{vac} cm^{-1}	Term combination
8, 745. 56	8	11, 431. 24	$b^4G_3'-\alpha^4F_4$
8, 744. 37	10	11, 432. 79	
8, 733. 27	40	11, 447. 32	
8, 728. 5	2	11, 453. 6	
8, 722. 12	2	11, 461. 96	
8, 678. 65	3	11, 519. 37	
8, 675. 02	20	11, 524. 19	$a^2D_2'-\alpha^4F_3$
8, 673. 02	2	11, 526. 85	
8, 661. 06	80	11, 542. 76	$b^2D_3-a^2D_3'$
8, 658. 14	3	11, 546. 66	$b^2D_3-b^4F_4'$
8, 655. 73	3h	11, 549. 85	
8, 648. 79	4	11, 559. 14	$a^2P_2-a^4D_3'$

4. NICKEL

All of the known and classified lines (1,071) of Ni I were published by Russell in 1929,[12] but only a dozen lines had been observed photographically beyond 8,700 A. The new results obtained with xenocyanine plates appear in Table 5, in which the combinations have all been derived from Russell's term tables. The infra-red, as well as other portions of the Ni I spectrum, appears to be less complex than Co I, and relatively simple compared with Fe I. Almost all of the new lines have been accounted for, and the analysis of the Ni I spectrum may be regarded as very nearly completed.

The infra-red arc spectrum of nickel was investigated radiometrically by Randall and Barker,[13] and in the range 9,520 to 10,980 A six lines coincide, within the errors of measurement, with the strongest we have recorded photographically. Comparison of our intensity estimates with their galvanometer deflections indicates that the photographic sensitivity of xenocyanine plates for wave length 11,000 A is approximately 5 per cent that for wave lengths below 10,300 A.

[12] H. N. Russell, Phys. Rev., vol. 34, p. 821, 1929.
[13] H. M. Randall and E. F. Barker, Astrophys. J., vol. 49, p. 55, 1919.

TABLE 5.—*Wave lengths in the infra-red spectrum of nickel*

λ_{air} I. A.	Intensity	ν_{vac} cm^{-1}	Term combination
10, 979. 87	5	9, 105. 09	$y^3D_3^0$–e^3D_3
10, 891. 25	2	9, 179. 17	$y^3F_2^0$–e^3D_2
10, 762. 24	2	9, 289. 20	$y^3D_2^0$–e^3D_2
10, 530. 53	20	9, 493. 60	$y^3F_3^0$–e^3D_3
10, 378. 62	100	9, 632. 56	$y^3F_4^0$–e^3D_3
10, 330. 23	50	9, 677. 68	$y^3F_3^0$–e^3D_2
10, 321. 10	5	9, 686. 23	$w^3F_3^0$–g^3F_3
10, 302. 61	50	9, 703. 62	$y^3D_1^0$–e^3D_1
10, 295. 05	5	9, 710. 75	
10, 226. 15	4	9, 776. 18	$w^3D_2^0$–g^3F_3
10, 193. 25	100	9, 807. 73	$z^1P_1^0$–e^3D_2
10, 145. 37	20	9, 854. 01	$y^3D_1^0$–e^1D_2
10, 061. 29	10	9, 936. 36	$y^3G_2^0$–g^3F_3
10, 048. 60	10	9, 948. 91	$y^3D_2^0$–e^3D_1
9, 898. 90	40	10, 099. 36	$y^3D_2^0$–e^1D_2
9, 842. 04	2	10, 157. 71	
9, 710. 1	1	10, 295. 74	$y^3D_3^0$–f^1F_3
9, 689. 35	3	10, 317. 78	$x^1D_2^0$–g^3F_3
9, 520. 06	100	10, 501. 26	$y^3F_2^0$–e^3D_1
9, 447. 29	5	10, 582. 15	$x^3F_3^0$–g^3F_4
9, 396. 57	20	10, 639. 26	
9, 385. 62	10	10, 651. 68	$y^3F_2^0$–e^1D_2
9, 258. 47	5	10, 797. 96	
9, 196. 18	2	10, 871. 10	a^1G_4–$y^3F_4^0$
9, 106. 40	30	10, 978. 28	w^3F_4–g^3F_4
9, 085. 25	3	11, 003. 84	$z^3G_3^0$–e^3D_2
9, 078. 70	10	11, 011. 77	$w^3F_3^0$–f^1F_3
9, 058. 56	6	11, 036. 25	
9, 005. 14	5	11, 101. 72	$w^3D_2^0$–f^1F_3
8, 982. 35	2	11, 129. 89	$z^1P_1^0$–e^3D_1
8, 968. 20	30	11, 147. 45	$y^3G_3^0$–g^3F_4
8, 965. 94	50	11, 150. 26	$y^3F_3^0$–e^1D_2
8, 954. 65	2	11, 164. 32	$z^1D_2^0$–e^3D_3
8, 877. 07	10	11, 261. 89	$y^3G_4^0$–f^1F_3
8, 862. 59	100	11, 280. 29	$z^1P_1^0$–e^1D_2
8, 824. 2	1	11, 329. 4	
8, 809. 47	30	11, 348. 30	$z^1D_2^0$–e^3D_2
8, 770. 68	10	11, 398. 50	a^1G_4–$y^3D_3^0$
8, 716. 58	3	11, 469. 24	$w^3D_3^0$–g^3F_4
8, 706. 05	1	11, 483. 12	
8, 702. 49	6	11, 487. 81	a^1G_4–$z^1G_4^0$
8, 688. 64	3	11, 506. 12	
8, 680. 2	1	11, 517. 3	
8, 661. 85	2	11, 541. 71	
8, 637. 04	15	11, 574. 86	$z^1F_3^0$–e^3D_3
8, 606. 45	10	11, 616. 00	$x^3D_3^0$–g^3F_4
8, 598. 84	2	11, 626. 29	$z^3G_4^0$–e^3D_3
8, 586. 2	1	11, 643. 40	$x^1D_2^0$–f^1F_3
8, 580. 04	2	11, 651. 76	$y^3G_3^0$–h^3F_4

5. ZIRCONIUM

About a year ago Kiess and Kiess [14] published an analysis of Zr I based on a list of approximately 1,600 wave lengths measured at the Bureau of Standards. To this list, which terminated at 9,276 A, we are now able to add the lines given in Table 6. All of the strong lines and many of the fainter ones are accounted for as combinations between the terms given in the paper cited above. No new terms have been revealed by these supplementary observations, although several metastable terms arising from the configuration $4d^4$ are still to be found.

A conspicuous feature of the infra-red Zr spectrum is a group of bands, shaded toward longer wave lengths, lying between 9,300 and 9,500 A. No regularities have been detected among these bands that will relate them to the systems recently described by Miss Lowater.[15] The wave lengths, estimated intensities, and wave numbers of the heads of these bands are given in Table 7.

TABLE 6.—*Wave lengths in the infra-red spectrum of zirconium*

λ_{air} I. A.	Intensity	ν_{vac} cm^{-1}	Term combination
10, 738. 94	1	9, 309. 36	a^3D_3–$y^3F_4^\circ$
10, 696. 67	1	9, 346. 14	a^3G_3–$z^3G_3^\circ$
10, 654. 11	1	9, 383. 48	a^3G_4–$z^3G_4^\circ$
10, 551. 46	1	9, 474. 77	a^3D_1–$y^3F_2^\circ$
10, 515. 86	1	9, 506. 84	b^3F_4–$z^3G_3^\circ$
10, 433. 73	1	9, 581. 67	
10, 328. 41	1	9, 679. 38	a^3D_3–$y^5D_4^\circ$
10, 242. 85	2	9, 760. 24	a^5F_2–$z^5G_2^\circ$
10, 210. 44	10	9, 791. 21	a^3G_5–$z^3G_5^\circ$
10, 199. 42	4	9, 801. 80	b^3F_4–$z^3G_4^\circ$
10, 105. 30	1	9, 893. 08	b^3F_3–$z^3G_3^\circ$
10, 084. 70	12	9, 913. 30	a^5F_1–$z^5G_2^\circ$
10, 045. 15	3	9, 952. 33	a^5F_3–$z^5G_3^\circ$
10, 028. 68	2	9, 968. 67	c^3P_2–$x^3D_3^\circ$
10, 016. 97	2	9, 980. 33	
9, 990. 44	1	10, 006. 83	
9, 958. 58	2	10, 038. 84	
9, 928. 53	1	10, 069. 22	
9, 909. 76	3	10, 088. 30	
9, 822. 30	20	10, 178. 12	a^5F_2–$z^5G_3^\circ$
9, 820. 42	3	10, 180. 07	a^5F_4–$z^5G_4^\circ$
9, 812. 85	10	10, 187. 93	b^3F_3–$z^3G_4^\circ$
9, 792. 74	6	10, 208. 85	b^3F_2–$z^3G_3^\circ$
9, 780. 40	18	10, 221. 73	b^3F_4–$z^3G_5^\circ$
9, 773. 30	0	10, 229. 15	
9, 666. 82	1	10, 341. 83	
9, 547. 26	25	10, 471. 34	a^3F_3–$z^3G_4^\circ$
9, 493. 47	1	10, 530. 67	c^3P_2–$y^3P_2^\circ$
9, 483. 35	3	10, 541. 91	
9, 441. 26	1	10, 588. 90	

[14] B. S. Jour. Research (RP296), vol. 6, p. 621, 1931.
[15] Proc. Phys. Soc. (London), vol. 44, p. 51, 1932.

TABLE 6.—*Wave lengths in the infra-red spectrum of zirconium*—Continued

λ_{air} I. A.	Intensity	ν_{vac} cm^{-1}	Term combination
9, 438. 35	1	10, 592. 17	
9, 419. 36	1	10, 613. 53	$c^3P_1-y^3P_2^\circ$
9, 405. 00	2	10, 629. 73	
9, 358. 32	2	10, 682. 74	
9, 352. 43	1	10, 689. 48	
9, 318. 19	4	10, 728. 76	
9, 290. 30	0	10, 760. 96	
9, 276. 89	25	10, 776. 52	$a^5F_4-z^5G_5^\circ$
9, 251. 17	5	10, 806. 48	$a^3G_4-y^3F_3^\circ$
9, 242. 65	5	10, 816. 44	$c^3P_1-w^3F_2^\circ$, $a^3G_3-y^3D_2^\circ$
9, 229. 33	3	10, 832. 05	
9, 182. 30	0	10, 887. 53	
9, 171. 50	3	10, 900. 35	$a^3G_4-y^3D_3^\circ$
9, 140. 40	0	10, 937. 44	
9, 139. 36	10	10, 938. 69	$a^5H_4-y^3G_3^\circ$
9, 134. 23	1	10, 944. 83	
9, 099. 90	2	10, 986. 12	$c^3F_3-x^3F_3^\circ$, $a^3G_3-y^5D_2^\circ$
9, 069. 41	15	11, 023. 05	$a^3H_5-y^3G_4^\circ$
9, 015. 16	20	11, 089. 39	$a^5F_5-z^5G_6^\circ$
9, 011. 34	2	11, 094. 09	$a^3G_3-y^3F_2^\circ$
8, 975. 78	0	11, 138. 05	$c^3F_4-x^3F_4^\circ$

TABLE 7.—*Infra-red zirconium bands*

λ_{air} I. A.	Intensity	ν_{vac} cm^{-1}	λ_{air} I. A.	Intensity	ν_{vac} cm^{-1}
9, 483. 55	2	10, 541. 69	9, 397. 21	2	10, 638. 54
9, 476. 65	1	10, 549. 36	9, 387. 26	2	10, 649. 82
9, 453. 55	1	10, 575. 14	9, 370. 74	3	10, 668. 59
9, 443. 93	1	10, 585. 91	9, 360. 34	3	10, 680. 45
9, 438. 24	1	10, 592. 29	9, 358. 33	1	10, 682. 74
9, 431. 75	2	10, 599. 58	9, 356. 12	3	10, 685. 26
9, 412. 03	2	10, 621. 79	9, 343. 19	4	10, 700. 05
9, 408. 92	1	10, 625. 30	9, 329. 93	5	10, 715. 26
9, 402. 84	2	10, 632. 17	9, 315. 87	5	10, 731. 43
9, 401. 09	2	10, 634. 15	9, 299. 56	5	10, 750. 25

IV. CONCLUSION

The data presented in the tables of this paper furnish ample proof of the effectiveness of xenocyanine in bringing into the domain of precise measurement a region of the spectrum heretofore accessible only with radiometric devices. Their application to the investigation of the structure of near-infra-red band spectra, a problem in which great efforts are being made to secure the advantages of increased resolving power, is obvious. In astrophysics the identification of unknown lines in the spectra of the sun and stars is advanced by each extension of our knowledge of the emission spectra of the elements. Reference to the Revision of Rowland's Preliminary Table of Solar

Spectrum Wave-Lengths [16] will show that several of the unidentified infra-red solar lines are due to the five elements whose spectra are described above. Both Ti and Fe are rich in strong lines in the region from 9,000 to nearly 11,000 A and may be used to supply comparison spectra for observations made with dispersing systems other than concave gratings. However, the values of the Fe wave lengths to be used as standards of reference may be calculated from the terms determined by interference methods more accurately than the observed values given in Table 3.

As stated above, we have completed a survey of the infra-red spectra of about 50 elements. We shall present the new wave lengths in subsequent papers in this Journal as soon as the data have been compiled for publication.

WASHINGTON, June 21, 1932.

[16] Carnegie Institution of Washington, Publ. No. 396, 1928.

TENSILE PROPERTIES OF CAST NICKEL-CHROMIUM-IRON ALLOYS AND OF SOME ALLOY STEELS AT ELEVATED TEMPERATURES

By William Kahlbaum[1] and Louis Jordan

ABSTRACT

The tensile properties as measured in "short-time" tests were determined for a medium-manganese steel at 900° F.; for a series of cast nickel-chromium-iron alloys containing about 0.5 per cent carbon, 35 per cent chromium and from 10 to 45 per cent nickel, at a temperature of 1,550° F.; and for three tungsten-chromium-vanadium steels and four molybdenum-chromium-vanadium steels at temperatures of 850° and 1,000° F.

CONTENTS

	Page
I. Introduction	327
II. Materials	327
III. Method of testing	328
IV. Results and discussion	328
1. Medium-manganese steel	328
2. Nickel-chromium-iron alloys	329
3. Tungsten-chromium-vanadium steels	330
4. Molybdenum-chromium-vanadium steels	331
V. Summary	332

I. INTRODUCTION

The most recently published report by the Bureau of Standards on the so-called short-time tensile properties (that is, the strength under relatively rapid loading) of steels at elevated temperatures [2] gave data on several groups of low-alloy steels. Among these were tungsten-chromium-vanadium steels with and without the addition of silicon or aluminum. Tests were also reported on wrought chromium-nickel-iron alloys containing approximately 10 per cent chromium and from 25 to 60 per cent nickel. The present report deals with the tensile properties, as determined by short-time tests, of some additional similar steels and alloys.

II. MATERIALS

The materials tested consisted of (1) a steel in some respects similar to the 0.45 per cent carbon "boiler drum" steel included in the preceding paper,[3] but containing in the present case 1.08 per cent manganese; (2) a series of five cast nickel-chromium-iron alloys, all containing about 35 per cent chromium and from 10 to 45 per cent of nickel; (3) a series of three tungsten-chromium-vanadium steels and (4) a series of four molybdenum-chromium-vanadium steels. The chemical compositions of these materials are given in Table 1.

[1] Research associate, The Midvale Co., Philadelphia, Pa.
[2] William Kahlbaum, R. L. Dowdell, and W. A. Tucker, The Tensile Properties of Alloy Steels at Elevated Temperatures as Determined by the "Short-time" Method, B. S. Jour. Research, vol. 6 (RP 270), p. 199, 1930.
[3] See footnote, 2.

TABLE 1.—*Chemical composition*

Type of alloy	Designation	C	Mn	P	S	Si	Cr	Ni	V	W	Mo
		Per cent	*Per cent*	*Per cent*	*Per cent*	*Per cent*	*Per cent*	*Per cent*	*Per cent*	*Per cent*	*Per cent*
Carbon steel (medium manganese).	8/1819	0.40	1.08	0.037	0.034	0.23					
Nickel - chromium - iron (cast).	EE1522	.57	.59			1.04	36.2	10.2			
	EE1523	.59	.65			1.07	35.2	21.0			
	EE1524	.54	.63			1.13	36.9	30.1			
	EE1525	.47	.71			1.08	34.5	38.4			
	EE1526	.36	.53			1.15	33.5	45.2			
Tungsten - chromium-vanadium steels.	HF-1/169	.29	.51			.58	2.28		0.36	1.70	
	HF-1/167	.26	.86			.69	2.25		.33	2.26	
	HF-1/168	.32	1.02			.17	1.63		.26	2.17	
Molybdenum - chromium-vanadium steels.	HF-1/166	.20	.45			.55	1.55		.26		0.87
	HF-1/165	.29	.88			.18	1.47		.22		.52
	HF-1/177	.31	1.38			.49	2.34		.29		.33
	HF-1/178	.21	2.23			1.33	1.28		.17		1.00

III. METHOD OF TESTING

The equipment and the method used for the short-time tension tests have been described and illustrated previously.[4, 5] All of the tests were made with a hydraulic testing machine, and measurements of strain were made with a Tuckerman optical strain gage.[6]

As in one previous work, a thermocouple mounted in the fillet of the 0.505-inch diameter test bar was used for measuring the temperature of the specimen. The temperature gradient from the center to either end of the gage length of the test bar was approximately 13° F. (7° C.).

Proportional limits were determined by plotting the differences between observed and calculated strain and taking a strain of 1×10^{-5} as indicating departure from a straight line.[7]

IV. RESULTS AND DISCUSSION

1. MEDIUM-MANGANESE STEEL

The data from tests of the 0.4 per cent carbon medium manganese (1.08 per cent) steel at room temperature and at 900° F. are given in Table 2. The point of chief interest in these results lies in the comparison they afford with similar tests made in previous work [8] on a 0.4 per cent carbon steel (boiler-drum steel) containing only a normal proportion of manganese, namely, 0.55 per cent. These previous tests of the lower manganese steel showed that it maintained a proportional limit of approximately 15,000 lbs./in.^{2} from 600° to 750° F., but that its proportional limit decreased noticeably, to 11,000 or 12,000 lbs./in.^{2}, at a temperature of 800° F. The higher manganese steel had a proportional limit of 15,000 to 16,000 lbs./in.^{2} at 900° F., fully 150° F. higher than the temperature at which the lower-manganese steel had an equivalent proportional limit. The higher manganese steel did not, however, show a corresponding superiority in tensile strength over the lower manganese steel at the elevated temperature.

[4] H. J. French, Methods of Test in Relation to Flow in Steels at Various Temperatures, Proc. Am. Soc. Test. Materials, vol. 26, Pt. II, p. 7, 1926; also Eng. News Record, vol. 97, p. 22.
[5] H. J. French, H. C. Cross, and A. A. Peterson, Creep in Five Steels at Different Temperatures, B. S. Tech. Papers, No. 362, 1928.
[6] L. B. Tuckerman, Optical Strain Gages and Extensometers, Proc. Am. Soc. Test. Materials, vol. 23, Pt. II, p. 602, 1923.
[7] L. B. Tuckerman, Discussion of paper by R. L. Templin, Proc. Am. Soc. Test. Materials, vol. 29, Pt. II, p. 538, 1929.
[8] See footnote 2, p. 327.

TABLE 2.—*Tensile properties of a medium manganese steel at elevated temperatures as determined by short-time tests*

Designation [1]	Temperature of test	Proportional limit	Tensile strength	Modulus of elasticity	Elongation in 2 inches	Reduction of area	Heat treatment prior to testing
	°F.	Lbs./in.²	Lbs./in.²	Lbs./in.² ×10⁶	Per cent	Per cent	
8/1819	70	[2] 32,000	86,000		27.5	53.9	1,600° F., 12 hours, air cooled; 1,200° F., 10 hours, cooled slowly.
	900	16,000	59,500	21.7	25.5	61.3	
	900	15,000	61,000	20.7	25.0	60.6	

[1] See Table 1 for chemical composition.
[2] Determined by the Midvale Co. A strain of 5×10^{-5} taken as indicating departure from a straight line.

2. NICKEL-CHROMIUM-IRON ALLOYS

The results of short-time tensile tests at 1,550° F. of cast nickel-chromium-iron alloys are given in Table 3. These alloys contained from 0.4 to 0.6 per cent carbon and about 1 per cent silicon and 35 per cent chromium. The nickel content of EE1522 was approximately 10 per cent and this increased to about 45 per cent in the last alloy of the series, EE1526.

This series showed no significant differences in the proportional limits of the various alloys at 1,550° F. There was, however, a progressive increase in the ductility of the alloy as the nickel content increased from 10 to 45 per cent, and above 30 per cent nickel there was a noticeable decrease in tensile strength.

It is in this case also of interest to recall the results of short-time tensile tests given in a previous report [9] for nickel-chromium-iron alloys containing 10 per cent chromium and either 35 or 57 per cent nickel. Only a very general correlation is possible as the earlier tests were made with maximum testing temperatures of only 1,360° F. as compared with 1,550° F. for the more recent tests; the alloys tested in the earlier work were rolled material and in the later work were "as cast"; and also the high-nickel alloy of the earlier work contained over 3 per cent tungsten.

TABLE 3.—*Tensile properties of cast nickel-chromium-iron alloys at 1,550° F. as determined by short-time tests*

Designation [1]	Proportional limit	Tensile strength	Modulus of elasticity	Elongation in 2 inches	Reduction of area
	Lbs./in.²	Lbs./in.²	Lbs./in.² ×10⁶	Per cent	Per cent
EE1522	7,000	49,000	11.6	2.5	3.4
	5,000	41,500	9.4	2.5	5.1
EE1523	5,000	49,000	14.4	3.0	4.2
		54,500		4.0	5.0
EE1524	6,000	49,000	13.2	4.0	7.3
	7,000	55,000	13.1	5.0	6.5
EE1525	6,000	44,000	14.4	8.5	13.3
	6,000	41,500	12.7	8.5	16.2
EE1526	6,000	33,500	11.0	15.5	34.0
		39,000		14.0	23.7

[1] See Table 1 for chemical compositions.
[2] See footnote 2, p. 327.

Nevertheless, it is to be noted that the tensile strengths of the cast alloys of the present series, containing 35 per cent chromium and either 10, 20, or 30 per cent nickel, were of the order of 50,000 lbs./in.² and the proportional limits of the order of 5,000 to 7,000 lbs./in.² at 1,550° F. as compared with tensile strengths of only 35,000 to 40,000 lbs./in.² and proportional limits of 5,000 to 6,000 lbs./in.² at 1,360° F. for rolled alloys containing 35 per cent nickel and 10 per cent chromium.

Increased proportional limits and tensile strengths in alloys of this type at temperatures of 1,300° to 1,500° F. appear to result from an increased chromium content rather than an increased nickel content. With this increase in strength, there is also noticeably less ductility as measured by elongation and reduction of area.

3. TUNGSTEN-CHROMIUM-VANADIUM STEEL

The chief differences in the chemical compositions of the three tungsten-chromium-vanadium steels (Table 1) were that the first of the series (HF–1/169) had a tungsten content of only 1.70 per cent, which was somewhat below the normal composition of the series; the second of the series (HF–1/167) may be considered of the normal composition, namely, about 2¼ per cent each of chromium and tungsten; the last steel of the group was low in chromium (1.63 per cent) but also had a manganese content (1.02 per cent) distinctly higher than the normal for the group.

All of these steels were tested after normalizing from 1,700° F., hardening, and tempering at 1,200° F. The hardening treatment consisted of air quenching from a temperature 50° F. above the upper critical temperature of the individual steel. The exact temperatures are shown in Table 4.

The results of the short-time high-temperature tests of these steels (Table 4) did not show any very striking differences in the behavior of the three steels. On the whole, the steel containing 1 per cent manganese (HF–1/168), with the lower chromium and the normal tungsten content, appeared to be superior with respect to the maintenance of a high proportional limit at elevated temperatures.

TABLE 4.—*Tensile properties of tungsten-chromium-vanadium steels at elevated temperatures as determined by short-time tests*

Designation [1]	Temperature of test	Proportional limit	Tensile strength	Modulus of elasticity	Elongation in 2 inches	Reduction of area	Hardening heat treatment [2]
	°F.	Lbs./in.²	Lbs./in.²	Lbs./in.² ×10⁶	Per cent	Per cent	
HF–1/169	70	[3] 92,000	128,000	----------	20.2	62.6	1,515° F., 30 minutes, air cooled.
	850	32,000	86,000	25.2	22.0	64.7	
	1,000	26,000	71,500	22.1	23.5	72.9	
HF–1/167	70	[4] 107,000	139,500	----------	19.2	59.9	1,510° F., 30 minutes, air cooled.
	850	30,000	98,500	23.6	21.5	62.3	
	1,000	16,000	77,500	22.1	23.0	70.1	
HF–1/168	70	[3] 109,000	136,500	----------	18.2	55.7	1,480° F., 30 minutes, air cooled.
	850	43,000	99,500	24.3	19.0	54.9	
	1,000	24,000	84,500	19.9	22.5	65.6	

[1] See Table 1 for chemical compositions.

[2] All specimens were normalized before the hardening treatment and tempered after the hardening treatment indicated in the last column of this table. In all cases the normalizing treatment consisted of heating at 1,700° F. for 30 minutes and cooling in air; the tempering treatment, of heating at 1,200° F. for 30 minutes and cooling in air.

[3] Determined by The Midvale Co. A strain of .5×10⁻³ taken as indicating departure from a straight line.

4. MOLYBDENUM-CHROMIUM-VANADIUM STEELS

The molybdenum-chromium-vanadium steels are listed in both Table 1 and Table 5 in the order of increasing manganese content. The second steel of the series differed from the first in that it had slightly higher carbon (0.29 per cent) and manganese (0.88 per cent) contents than the first steel of the series (0.20 per cent carbon, 0.45 per cent manganese). This difference in composition apparently accounted for a distinctly higher proportional limit and tensile strength in the steel of higher carbon and manganese contents at temperatures of 850° and 1,000° F. Further increase in the proportion of manganese, and also of chromium, in the third steel of the series (HF–1/177) resulted in a still higher proportional limit at 850° F., but produced no increase in either proportional limit or tensile strength at 1,000° F. The fourth and last steel of this series had the highest manganese content of all (2.23 per cent), about double the molybdenum content (1.00 per cent) of the other steels, and a high silicon content (1.33 per cent). This steel had tensile strengths, at the high temperatures, equivalent to or higher than the other steels of the series. Its proportional limit at 850° F. was also high. Its proportional limit at 1,000° F., however, failed to show an equivalent increase and was only of the order of the proportional limit of the first steel of this series, the low-carbon, low-manganese composition, at the corresponding temperature. In previous work [10] it has been observed that 1.25 per cent silicon had a very marked effect in lowering the proportional limit of a tungsten-chromium-vanadium steel at about 1,000° F.

TABLE 5.—*Tensile properties of molybdenum-chromium-vanadium steels at elevated temperatures as determined by short-time tests*

Designation [1]	Temperature of test	Proportional limit	Tensile strength	Modulus of elasticity	Elongation in 2 inches	Reduction of area	Hardening heat treatment [2]
	°F.	Lbs./in.²	Lbs./in.²	Lbs./in.² ×10⁻⁶	Per cent	Per cent	
HF-1/166	70	[3] 60,000	104,000	----------	24.7	66.2	1,490° F., 30 minutes, air cooled.
	850	25,000	83,000	24.7	23.5	67.5	
	1,000	19,000	71,000	22.6	24.0	71.6	
HF-1/165	70	[3] 80,000	118,000	----------	20.7	65.0	1,460° F., 30 minutes, air cooled.
	850	32,000	96,000	24.0	21.5	67.5	
	1,000	26,000	81,000	21.7	23.5	74.5	
HF-1/177	70	[3] 75,000	112,000	----------	23.0	63.3	1,460° F., 30 minutes, air cooled.
	850	37,000	97,000	24.8	20.5	60.1	
	1,000	25,000	71,500	20.2	25.0	73.3	
HF-1/178	70	[3] 74,000	124,000	----------	21.5	54.4	1,460° F., 30 minutes, air cooled.
	850	36,000	104,000	23.3	23.5	63.5	
	1,000	20,000	78,500	18.9	27.0	77.4	

[1] See Table 1 for chemical compositions.

[2] All specimens were normalized before the hardening treatment and tempered after the hardening treatment indicated in the last column of this table. In all cases the normalizing treatment consisted of heating at 1,700° F. for 30 minutes and cooling in air; the tempering treatment, of heating at 1,200° F. for 30 minutes and cooling in air.

[3] Determined by The Midvale Co. A strain of 5×10^{-3} taken as indicating departure from a straight line.

[10] See footnote 2, p. 327.

V. SUMMARY

1. Short-time tensile tests at elevated temperatures were made of a medium-manganese steel; of a series of cast nickel-chromium-iron alloys containing about 0.50 per cent carbon, 35 per cent chromium, and nickel from 10 to 45 per cent; and of two series of low-alloy steels, namely, tungsten-chromium-vanadium and molybdenum-chromium-vanadium steels, all normalized, hardened, and tempered at 1,200 ° F.

2. The medium-manganese steel (1.08 per cent) had a proportional limit of 15,000 to 16,000 lbs./in.^{2} at 900° F. This is fully 150° F. higher than the temperature at which a 0.55 per cent manganese boiler-drum steel of the same carbon content (0.4 per cent carbon) possessed the same proportional limit.

3. The nickel-chromium alloys showed no marked change in proportional limit at 1,550° F. over the range of composition studied. With nickel contents over 30 per cent tensile strengths of the alloys decreased noticeably and the ductility increased.

4. A medium-manganese content (1.02 per cent) in one of the steels of the tungsten-chromium-vanadium series was accompanied by proportional limits as high as or higher than in the other steels of the series.

5. Increased manganese contents (up to 1.4 per cent) in the molybdenum-chromium-vanadium steels resulted in higher proportional limits at 850° and 1,000° F. A steel having a still higher manganese content (2.23 per cent) accompanied by high silicon (1.33 per cent) and 1.00 per cent molybdenum had a high proportional limit at 850° F., but a comparatively low proportional limit at a temperature of 1,000° F. Similarly, low proportional limits at 1,000° F. were observed in previous work with tungsten-chromium-vanadium steels having a high silicon content (1.25 per cent Si).

WASHINGTON, July 6, 1932.

RP475

THE COMPARISON OF HIGH VOLTAGE X-RAY GENERATORS

By Lauriston S. Taylor and K. L. Tucker[1]

ABSTRACT

It is shown that when measurements are made in the customary manner, the X-ray emission of a tube operated on two mechanical rectifiers may differ by ±20 per cent, although the electrical indications are the same. This also applies to quality evaluations whether of the full absorption curve, half-value layer or effective wave-length type.

Determinations of percentage depth dose do not show any such marked differences since this is a comparatively insensitive indicator. It is seen, moreover, that there is little gain in percentage depth dose in going from 160 to 200 kv peak; the only change of significance being in the actual 10 cm depth dose.

It is shown on the other hand, when the potential of three generators including constant potential is measured in "effective kilovolts," that for the same effective voltage the outputs for a given filter are all very nearly the same, both as regards intensity and quality.

CONTENTS

		Page
I.	Introduction	333
II.	Apparatus	334
III.	Intensity measurements in air	336
IV.	Quality measurements in air	338
V.	Depth dose measurements	340
VI.	Half-value layers and true effective wave lengths	345
VII.	Voltage measurements	347
VIII.	Conclusion	351

I. INTRODUCTION

In the technical and clinical use of high voltage X rays, a wide variety of generators have come into common use. To save strain on the X-ray tube, unidirectional voltage, obtained by mechanical or by thermionic rectifiers, is usually applied. Since the rectification characteristics of such generators differ widely, there has been considerable confusion as to their relative effectiveness in producing the desired therapeutic or technical results.

Experience in this laboratory has led us to the conclusion that, due largely to the lack of properly controlled experimental conditions, comparisons between X-ray generators which have been made in the past, are of questionable soundness. For example, we have found that a different X-ray emission, as expressed in terms of the ionization produced in air, is obtained from a given tube and generator when either the aerial system or the tube inclosure is changed.

It was decided, therefore, to make a careful comparison of several typical X-ray generators having as few variables as possible and yet under as nearly clinical operating conditions as obtainable in a labora-

[1] Research associate, Radiological Research Institute. This work was started by K. L. Tucker, who, by reason of illness, was obliged to withdraw from active participation before the experimental work was complete.

tory. For the most part, the various quantities were measured in the same units and in the same manner as in the clinic so that the results may be readily interpreted in commonly used terms.

The physical equality of X-ray beams produced by different generators, so far as concerns therapeutic application, has been shown to be based on 10 or more factors.[2] Included in these are tube current, tube voltage (peak), filter, quality (H. V. L. or λ_e),[3] Röntgens per minute delivered by tube,[4] and percentage depth dose.[5]

II. APPARATUS

Three generators, *A*, *B*, and *C*, were chosen as typical. *A* and *B* were rated to deliver full wave 220 to 230 kv (peak) at 30 ma (milliamperes). *C* was rated to deliver 200 kv (peak) at 10 ma. *A* was a mechanical rectifier having a single high-tension transformer and rectifying approximately 30° of the cycle. *B* was a mechanical rectifier having a divided secondary high-tension transformer and rectifying approximately 20° of the cycle. *C* was a valve tube and condenser ripple potential generator (so-called constant potential) having a ripplage[6] of only about 1.5–2 per cent per milliampere, and hence an X-ray emission not differing appreciably from strictly constant potential.

Any one of the three generators could be connected to the same overhead system without changing its capacitance. As will be shown, this is essential. The X-ray tube was of the Coolidge type, having thin walls. Since tubes of the same design vary slightly, a single tube was left in position for the six months during which the measurements were made. It was inclosed in a rectangular ¼-inch lead box, 4 by 4 by 7 feet, having forced ventilation. Previous experience indicated that X-ray tubes operate more smoothly in unconfined space than in some of the conventional tube drums. For example, it was found that for a tube operating at 200 kv (peak) a spacing of about 12 inches from center to ground wall produced unsteadiness, whereas an 18-inch spacing appeared sufficient to avoid such difficulty. Accordingly, we used the 24-inch spacing and had no difficulty with tube unsteadiness at voltages up to 230 kv (peak).

Control of the tube with generators *A* and *B* was observed by means of a d. c. milliammeter in the high-tension circuit and a wide-

---

[2] E. A. Pohle, Am. J. Roent., vol. 18, p. 55, 1927.

[3] The half-value layer (H. V. L.) in copper or aluminum is a measure of the "penetrating power" of an X-ray beam. It is defined as the thickness of copper (or aluminum) which interposed in an X-ray beam reduces its intensity to one-half its initial value (as measured in terms of air ionization).

The effective wave length of an X-ray beam is the wave length of the homogeneous radiation having the same absorption coefficient in copper (or aluminum) as the heterogeneous radiation in question. (See discussion of various methods of expressing X-ray qualities in a paper by L. S. Taylor, B. S. Jour. Research, vol. 5 (RP212), p. 517, 1930.)

[4] The "Röntgen" (r), is defined as the quantity of radiation which, when the secondary electrons are fully utilized and the wall effect of the chamber is avoided, produces in 1 cm^3 of atmospheric air at 0° C., and 76 cm mercury pressure such a degree of conductivity that one electrostatic unit charge is measured at saturation current.

[5] The "percentage depth dose" is the ratio of the X-ray intensity as measured at a given depth in a body of homogeneous material, to the intensity as measured at the irradiated surface. It must be recognized that these intensities are measured in terms of Röentgens per minute and hence do not give true indications of the energy absorbed in a given volume element.

[6] Up to the present the term "constant potential" has been used carelessly in describing the potential supplied by kenotron or other valve tube rectification. We will use a more accurate designation of voltages which are actually not constant but fluctuate about a certain average value. Thus by a "ripple quantity" (potential or current) is meant a simple periodic quantity

$$y = V_0 + V_1 \sin(\omega x + \alpha_1) + V_2 \sin(2\omega x + \alpha_2) + \ldots$$

in which the constant term (V_0) is so large that all values of the quantity are positive (or negative). The amount of ripple ("ripplage" or "ripplance") in a ripple quantity is the ratio of the difference between the maximum and minimum values of the quantity to the average value.

scale voltmeter connected directly across the transformer primary. Duplication of results over a period of months indicated that this control method was sufficient. In the case of the generator *C* ("constant potential") the control was effected by means of a shielded high-tension voltmeter [7] connected directly across the tube leads.

Peak voltage was measured with a sphere gap in all cases. Average voltages were measured by means of the high-tension voltmeter, which in the case of generator *C* gave readings very slightly less than those of the sphere gap, depending upon the tube current. Since the rectification characteristics of generators *A* and *B* vary with load, this was kept constant at 4 ma (average) throughout the entire work.

The rectifying switch of generator *B* was fixed in a permanent position on the synchronous motor shaft, so measurements made with

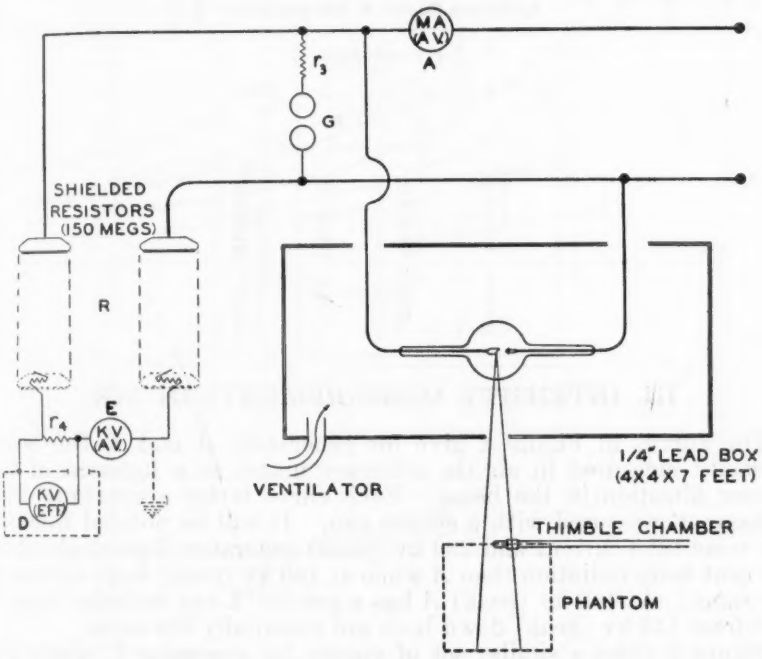

FIGURE 1.—*Diagram of apparatus showing current and voltage measuring systems*

B were arbitrarily chosen as a basis in comparing with *A*. The switch on *A* was so arranged that its phase position could be readily changed. The positions of the switches were at the points set by the agents of the respective manufacturers—presumably best suited for use at 200 kv (peak).

Ionization measurements were made with a calibrated thimble ionization chamber arranged according to the diagram in Figure 1. The distance from focal spot to center of the chamber was 104 cm. The ionization chamber system was tested for leakage by covering the thimble chamber cap with lead and then exposing it to the X-ray beam. No leakage was detectable in an exposure time double the longest used in the measurements.

[7] L. S. Taylor, B. S. Jour. Research, vol. 5 (RP217), p. 609, 1930.

For depth dose measurements a cubical wax phantom about 35 cm on a side was used. Wax was selected instead of water largely for convenience since its difference from water has been shown [8] to be insignificant. The wax was carved out so that the chamber in the surface position was half submerged leaving no air pockets between it and the wax. The focal spot-surface distance was likewise 104 cm. A beam area of 10 cm diameter (78 cm^2) at the position of the chamber was chosen in order to work with a clearly defined field receiving little stem radiation. Table 1 from Grebe and Nitzge shows that within wide limits variations of depth dose with quality are independent of the field area.

TABLE 1.—*Relationship between radiation quality and percentage depth dose for two different field areas*

A, field area 400 cm^2; *B*, field area 50 cm^2

H. V. L.	Per cent depth dose		Ratio
	A	*B*	
mm Cu			*A/B*
2.00	52	30	1.73
1.6	51	30	1.70
1.0	50	29	1.72
.8	48	28	1.72
.6	47	27	1.74
.4	40	24	1.67
.2	28	16	1.75
.1	16	9	1.78
.05	7	4	1.75

III. INTENSITY MEASUREMENTS IN AIR

The curves in Figure 2 give for generators *A* and *B* the beam intensity measured in air (in arbitrary units) as a function of the copper filtration in the beam. Each curve is for a constant peak voltage as measured with a sphere gap. It will be noticed that, for the same tube current and 200 kv (peak) generator *B* gives about 20 per cent more radiation than *A* while at 180 kv (peak) both are about the same. At 160 kv (peak) *A* has a greater X-ray emission than *B* and from 140 kv (peak) down both are essentially the same.

Figure 3 gives a similar set of curves for generator *C* where the voltages are expressed in kilovolts average. The curve for 150 kv (average), replotted as the broken line on Figure 2, approximates very closely the curve for 200 kv (peak) on generator *B*. Similarly, it will be found for the conditions used here that the other approximate intensity equivalents given in Table 2 are obtainable for radiation filtered through 0.5 mm of copper.

Thus to obtain an X-ray intensity of 178 units from any of the three generators, through 0.5 mm copper filter, would require that *A* be operated at 200 kv (peak), *B* at 189 kv (peak), and *C* at 142 kv (average). This is, of course, for the same tube current in all cases. Similarly, an intensity of 80 units is obtained at 138 kv (peak), 140 kv (peak), and 99 kv (average), respectively.

[8] Grebe and Nitzge, Strahlen (Sonderbände), vol. 14, 1930.

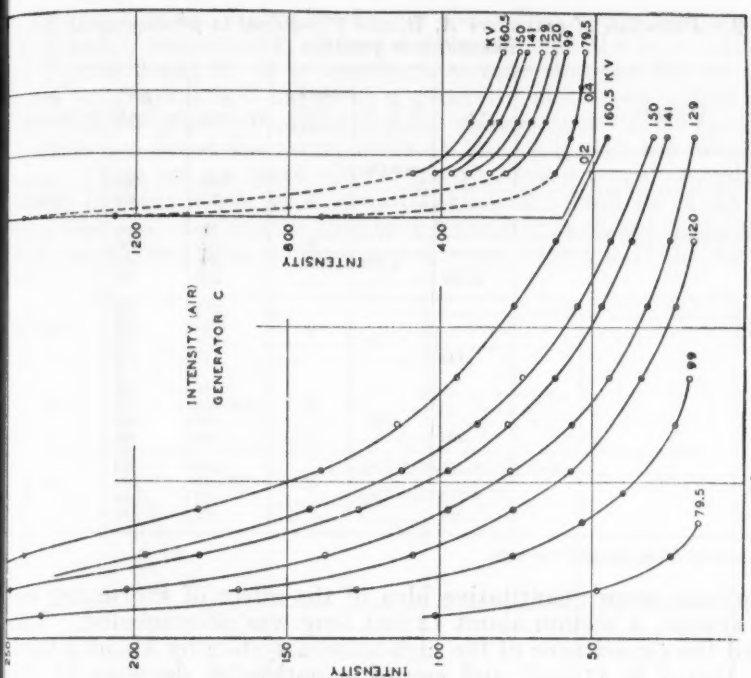

FIGURE 3.—*Beam intensities for generator C measured in air*

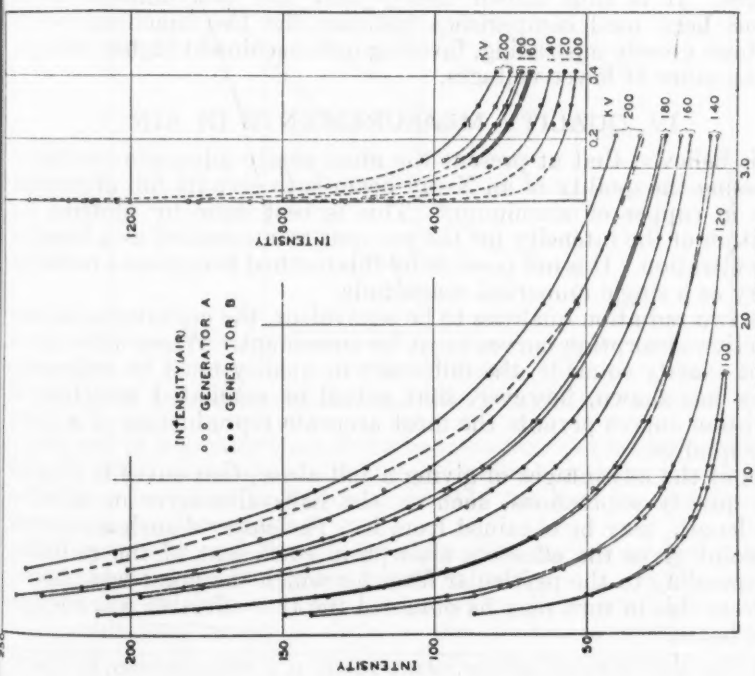

FIGURE 2.—*Beam intensities for generators A and B measured in air*
broken curve is for 150 kv (average) on generator *C*, taken from Figure 2.

TABLE 2.—*Potentials of generators A, B, and C required to produce equal X-ray intensities or qualities*

Intensity	λ_e	H. V. L.	Absorption curve	*A* kv (peak)	*B* kv (peak)	*C* kv (average)
	A.	*mmCu*				
215				[1] 237	200	152
			X	(215)	200	(155–160)
178				200	189	142
			X	200	(190)	(150)
		0.775		200	195	161
	0.192			200	195	159
151				173	180	132
			X	(180)	180	(135–140)
		.68		178	180	147
	.199			177	180	146
122				154	160	122
			X	(150–155)	160	(125–130)
		.60		153	160	124
	.208			154	160	126
80				138	140	99
			X	(133–140)	140	(105–110)
		.525		132	140	112
	.218			134	140	110

[1] Extrapolated value, probably too high.

To obtain some quantitative idea of the effect of shortening the aerial system, a section about 12 feet long was disconnected. This reduced the capacitance of the high-tension system by about a third (from 158$\mu\mu$f to 110$\mu\mu$f) and caused a noticeable decrease of the X-ray emission at the higher voltages and a slight increase at lower voltages. It is thus shown clearly that had two different aerial systems been used comparisons between the two machines would have been grossly misleading, favoring one machine at higher voltages and the other at lower voltages.

IV. QUALITY MEASUREMENTS IN AIR

It is believed that at present the most nearly adequate method of expressing the quality of an X-ray beam is to give its full absorption curve in copper or aluminum.[9] This is best done by plotting the logarithm of the intensity (or the per cent transmission) as a function of the filtration. It is not possible by this method to express a radiation quality as a single numerical magnitude.

For two radiation qualities to be equivalent, the curvatures of their respective absorption curves must be coincident. Where two curves do not exactly coincide, the difference in quality must be estimated. Wilsey has shown, however, that actual or estimated matching of absorption curves permits the most accurate reproduction of a given X-ray quality.

One of the advantages of giving a full absorption curve is that all other quality expressions, such as the half-value-layer or effective wave length, may be obtained from it. The slope of such a curve at any point gives the effective absorption coefficient of the radiation corresponding to the particular filter for which the point was chosen, and from this in turn may be obtained the true effective wave length of the beam.[10]

[9] E. A. Pohle, and C. S. Wright, Radiology, vol 14, p. 17, 1930. R. B. Wilsey, Radiology, vol. 17, p. 700, 1931.

[10] L. S. Taylor, B. S. Jour. Research, vol. 5, p. 517, 1930. This corresponds to Mutscheller's "average wave length."

Figures 4, 5, and 6 give the copper absorption curves for generators *A*, *B*, and *C* respectively. These curves are from the same data used for Figures 2 and 3. It is significant to note that the 200 kv (peak) curve for generator *B* indicates a generally more penetrating radiation than for generator *A* at the same voltage. At 180 kv (peak) the qualities are about the same, while at 150 kv (peak) the reverse obtains. From 140 kv (peak) down, the qualities are again roughly the same. In other words, as shown in Table 2, the qualities of the radiations bear a similar relationship to one another as do the intensities so that, for a given peak voltage, and a given filtration, if the radiation

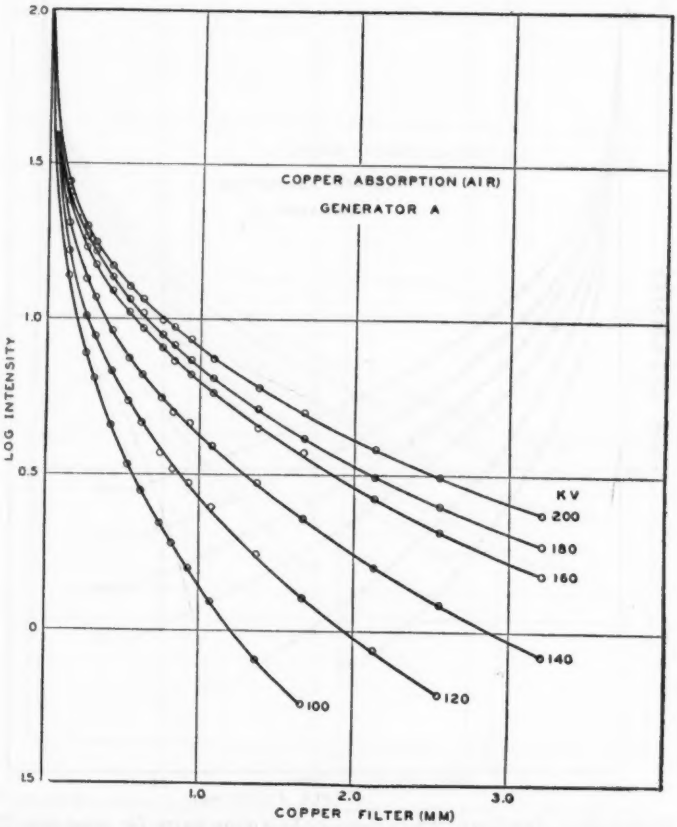

FIGURE 4.—*Semilogarithmic copper absorption curve for generator A*

emission of *A* is greater than *B* the penetration of *A* is likewise greater than *B*. It is unsafe to draw any generalization from these results, but it may be noted that such is roughly the case for all conditions thus far encountered in this work.

In Figure 6, giving the copper absorption curves for generator *C*, the broken lines are transposed from Figures 4 and 5. It will be noted that the 200-kv (peak) curve for generator *B* (upper broken curve) corresponds very nearly in slope to the 150-kv. (average) curve for generator *C*. (It will be recalled that the corresponding intensity curves also nearly coincide.) Similarly, it is found possible to match

the other absorption curves for the different generators and we find that Table 2 above for intensity equivalents holds approximately true for quality equivalents, also.

V. DEPTH DOSE MEASUREMENTS

Measurements of the percentage depth dose were made over the whole range of radiation qualities used. Figures 7, 8, and 9 give, respectively, the surface and 10-cm depth intensities for generators *A*, *B*, and *C*. Comparison of the curves for the two mechanical rec-

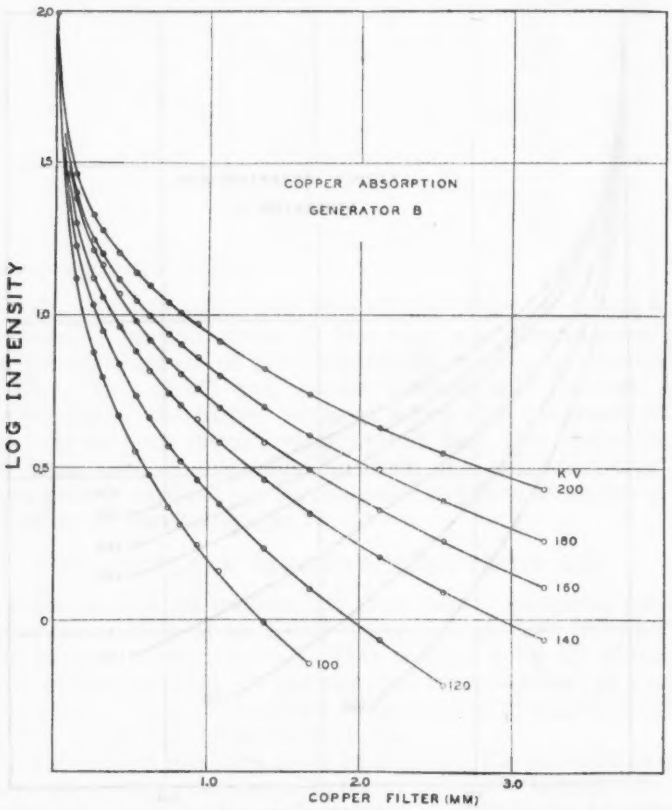

FIGURE 5.—*Semilogarithmic copper absorption curve for generator B*

tifiers shows the same general similarities as were evidenced by the air intensity curves given in Figures 2 and 3. Thus the 200-kv curve for generator *B* (broken line curve in fig. 7) shows a considerably greater surface dose than the 200-kv curve for generator *A*.

Again the intensities measured at 10 cm depth for the two machines are related in the same manner as the air intensities.

The broken line curves in Figure 8 are intensities for generator *B* when used with the shortened aerial system. As noted for the air intensity measurements, the long aerial system has a greater X-ray emission at 200 and 180 kv and a smaller emission at 160 kv than the short aerial system. Below 160 kv there appears to be no significant difference between generators.

In comparing generator C with A and B, it is found (fig. 9) that 160.5 kv (average) on C produces slightly greater air and surface intensities than 200 kv (peak) on generator B while 150 kv (average) on C is about equivalent to 200 kv (peak) on generator A. Also 140 kv (average) on C is seen to be equivalent to 180 kv (peak) on either A or B.

Quality measurements as here carried out, with the thimble chamber at the phantom surface and at 10 cm depth, have no real

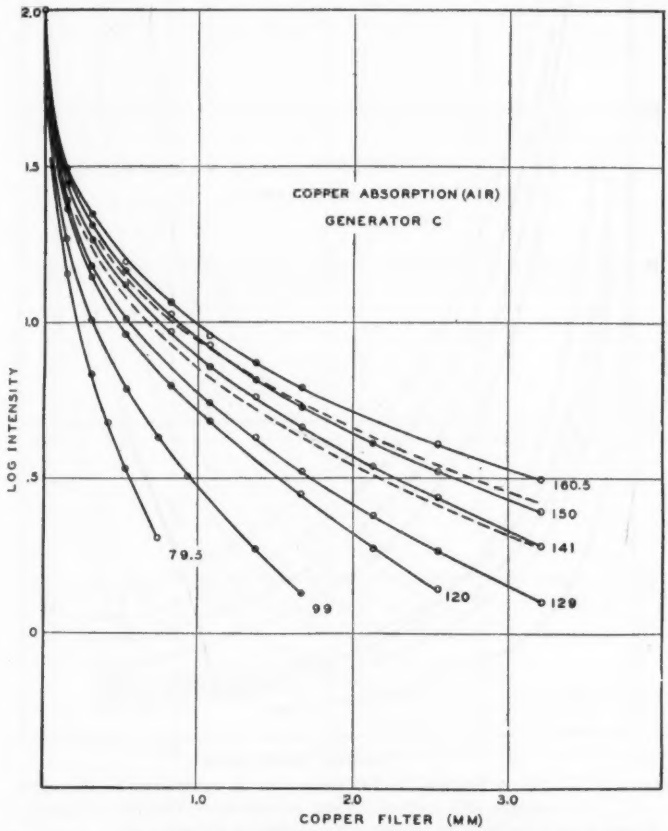

FIGURE 6.—*Semilogarithmic copper absorption curve for generator C*
Upper broken line curve for generator B at 200 kv. Lower broken line curve for generator A at 180 kv.

significance in relating the radiation quality in a phantom to that in air. This is because radiation under such conditions contains a major proportion of very soft scattered X rays that introduce a large and unknown wall correction into the measurements. Since it is impossible to reproduce such radiations entering a standard chamber, the thimble chamber can not be calibrated for equivalent radiation qualities.

Such curves have significance, however, in comparing radiation qualities measured under identical experimental conditions, and as such have been used to compare depth dose qualities.

Figures 10, 11, and 12 give the copper absorption (corresponding to the intensity curves of figs. 7, 8, and 9) measured at the surface and 10 cm depth for generators *A*, *B*, and *C*, respectively. On the assumption that similar absorption curves, obtained under identical conditions, imply equivalent radiations, these curves show precisely the same relation between the 10 cm depth radiation qualities for the

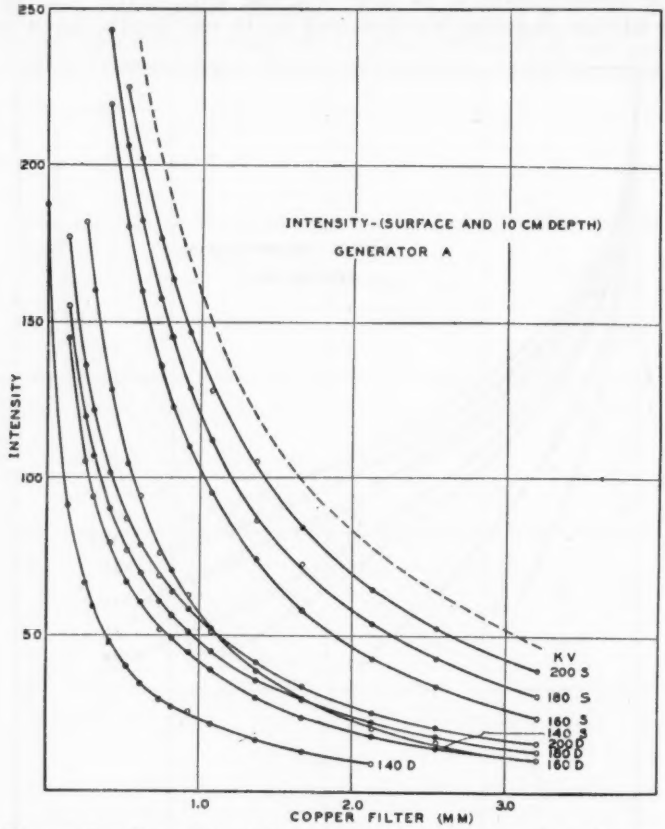

FIGURE 7.—*Beam intensities for generator A measured at phantom surface (S) and at 10 cm phantom depth (D)*

Broken curve is for 200 kv on generator *B* measured at surface.

three generators as was indicated by the absorption curves measured in air.

Percentage depth doses for all the conditions here used may be obtained directly from the curves in Figures 7, 8, and 9. It happens that the percentage depth dose changes but very slowly with increasing hardness of radiation after one or two tenths of a millimeter copper filtration. It also changes but slightly with increase of voltage above 160 kv (peak). Consequently, the change in percentage depth dose is an insensitive indicator of radiation equalities. It can not, however, be neglected; since, if two radiations, having otherwise similar properties, should differ materially in percentage depth dose, there would be no justification for saying that they were equivalent.[11]

[11] It should be noted that a percentage depth dose is the ratio between two measurements and hence its error may be considerably larger than the individual errors of the original measurements.

The change of depth dose with filtration for the three generators is given in Table 3. It is seen that, while the accuracy is none too good, the percentage depth dose with generators *A* and *B* are about the same at equal voltages. The depth doses at 160 kv appear to be slightly greater than at higher voltages which is probably unreasonable but may be due to small cumulative errors. In comparing generator *C* with the mechanical rectifiers, it is found that the depth doses at 160

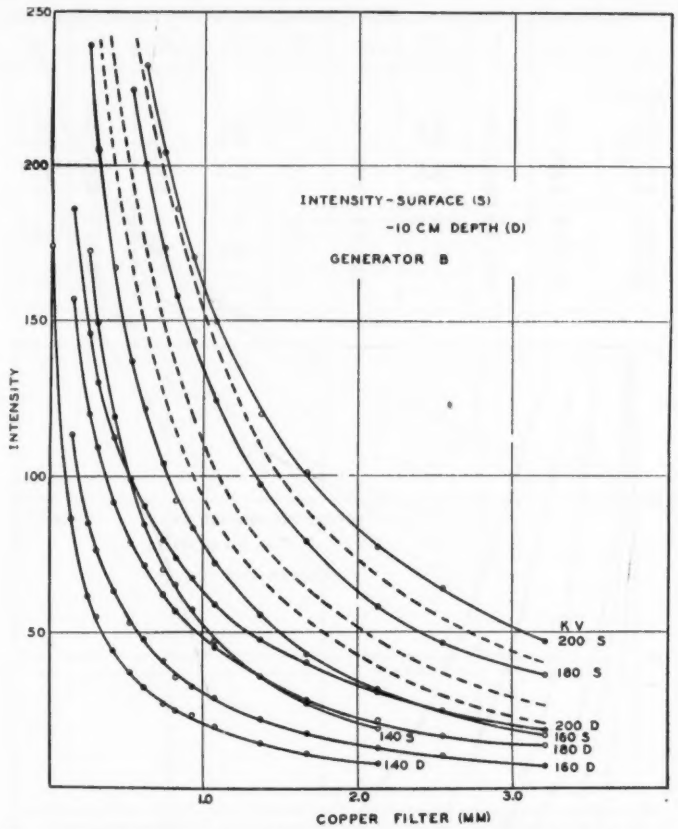

FIGURE 8.—*Beam intensities for generator B measured at phantom surface (S) and at 10 cm phantom depth (D)*

Broken line curves (top to bottom) for surface intensities for same generator except with shortened aerial operating at 200, 180, and 160 kv (peak).

kv (average) for *C* slightly exceed those at 200 kv (peak) for *A* and *B* and likewise the depth doses at 140 kv (average) for *C* are slightly greater than those at 180 kv (peak) for *A* and *B*. At 160 kv (peak) generators *A* and *B* give a slightly greater depth dose than *C* operating at 120 kv (average). The importance of these depth-dose measurements rests in their agreement and no inference should be drawn from the small differences found.

TABLE 3.—*Percentage depth doses in wax phantom (field 10 cm diameter) for different copper filtrations*

Filter	kv (peak)		kv (average)	kv (peak)		kv (average)	kv (peak)		kv (average)
	200	200	160.5	180	180	140	160	160	120
	Machine								
	A	*B*	*C*	*A*	*B*	*C*	*A*	*B*	*C*
mm Cu									
0	18	18	------	17	16	------	16	16	------
0.14	35	34	34.8	34	31	34.2	34	33	29.3
0.304	------	------	36.9	------	------	37.5	------	0	35.9
0.415	37	38	------	37	35	------	37	38	------
0.6	38	38	38.3	37	37	38.4	37	39	37.7
0.8	38	39	------	38	37	------	39	39	------
1.0	38	39	40.0	38	37	38.9	40	39	------
1.5	39	40	------	39	38	------	40	40	38.7
2.0	39	40	41.3	40	38	40.4	40	39	------
2.5	38	39	------	38	37	------	40	40	------
3.0	39	39	------	40	38	------	------	------	40.0

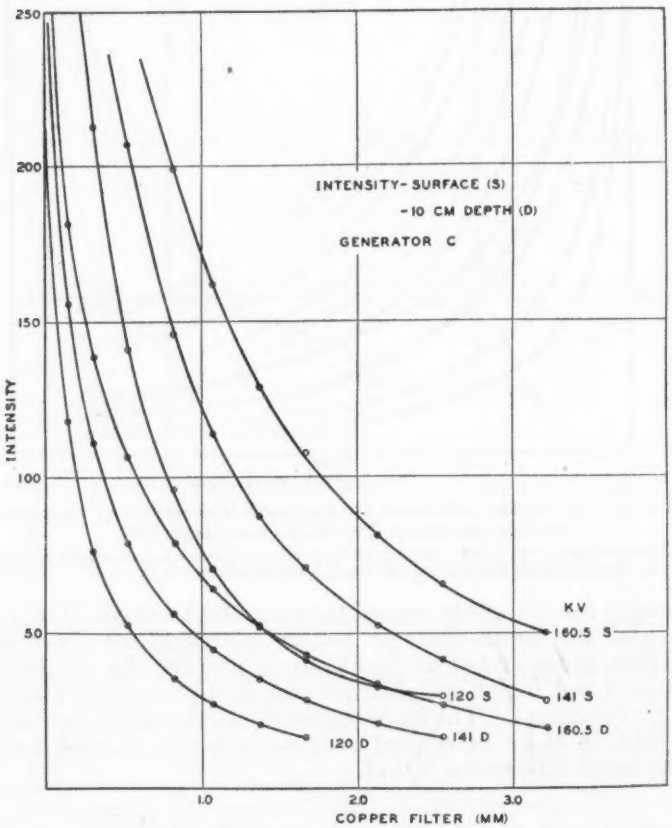

FIGURE 9.—*Beam intensity for generator C measured at phantom surface (S) and at 10 cm phantom depth (D)*

VI. HALF-VALUE LAYERS AND TRUE EFFECTIVE WAVE LENGTHS

The results above have shown that the copper absorption curves for the three generators give a fairly reasonable comparison of the resulting tube emission as regards quantity, quality, and depth dose. From the curves given, effective wave lengths or half-value layers in copper for any desired beam of radiation may be obtained directly. In practice, radiation qualities have been variously expressed by either

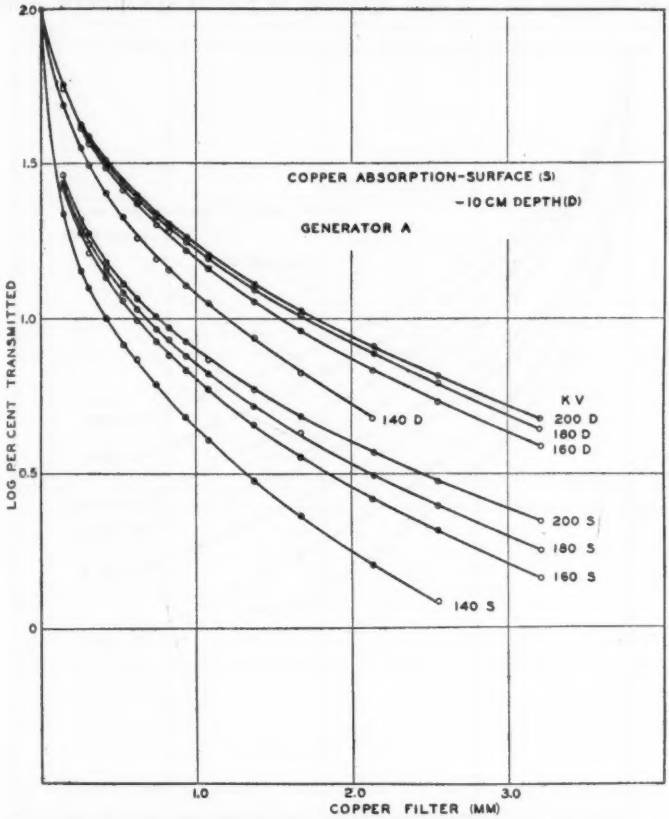

FIGURE 10.—*Semilogarithmic copper absorption curves for radiation measured at surface (S) and 10 cm depth (D) on phantom for generator A*

of these two methods. Hence, for facilitating comparisons of the radiation output of generators, values of the copper half-value layer (H. V. L.) and true effective wave length (λ_e), covering all the radiations used in this study, have been plotted in Figures 13 and 14. It should be emphasized that the values for mechanical rectifiers are likely to vary somewhat between machines and that the values here given hold strictly only for our generators. They should, however, serve as a fairly close guide.

Values of H. V. L. and λ_e also depend upon the thickness of the tube wall, this probably accounting for the differences in H. V. L. for "constant potential" reported by several workers. Probably a more

serious source of difference between workers lies in their method of voltage measurement and in the amount of ripplage present in their generator. When using generator *C* the ripplage was found to be about 8 per cent and to vary slightly with voltage. Voltage measurements were made by means of a shielded high resistance "voltmeter multiplier" in series with a d. c. microammeter.[12] Thus the potentials are expressed in average kilovolts whereas the potentials used by other workers in measuring H. V. L. were usually, if not always, in peak kilovolts. To show how various observers agree, their results are plotted in Figure 15. There appears to be no systematic difference

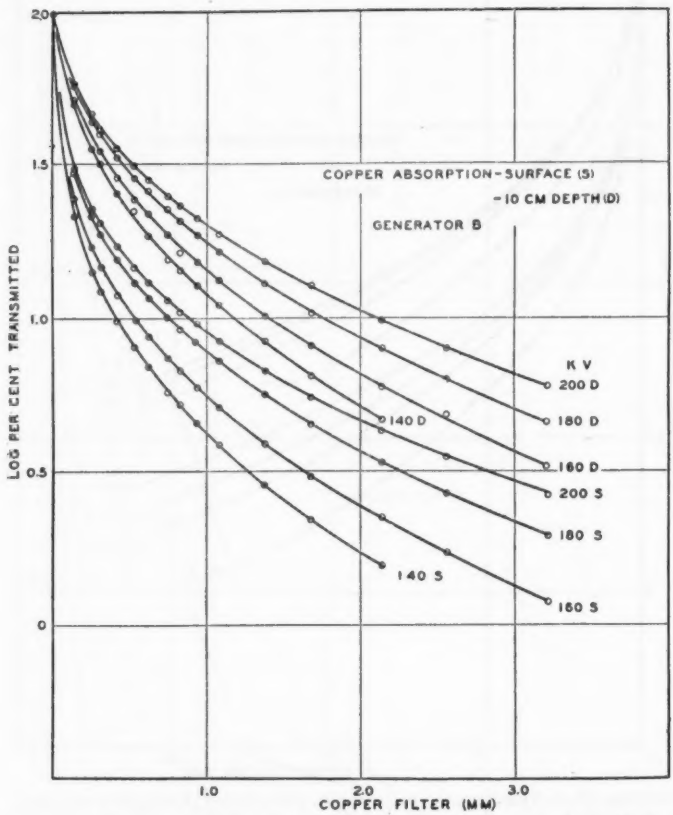

FIGURE 11.—*Semilogarithmic copper absorption curves for radiation measured at surface (S) and 10 cm depth (D) on phantom for generator B*

except that Holthusen's are consistently higher than all others. Our measurements fall between the others over a large portion of the range covered.

The "quality" comparisons of the three generators, made from the full absorption curves, are borne out very well by the H. V. L. and λ_e curves of Figures 13 and 14. For example, an X-ray beam, filtered with 0.5 mm copper and having an H. V. L. of 0.75 mm Cu, may be obtained with 200 kv on generator *A*, 195 kv on *B*, and 160 kv on *C*.

[12] See footnote, 7 p. 335.

Again a beam filtered with 0.25 mm copper and having an H. V. L. of 0.50 mm copper may be obtained with 210 kv on *A*, 202 kv on *B*, and 150 kv on *C*. We find a similar relationship from the effective wavelength curves. Thus a beam filtered with 0.5 Cu and having a value of $\lambda_e = 0.195$ Angstrom may be obtained with 200 kv on *A*, 196 kv on *B*, and 160 kv on *C*. Again a 0.25 mm copper filtered beam having $\lambda_e = 0.235$ Angstrom is obtained by 212 kv on *A*, 203 kv on *B*, and 150 kv on *C*. The agreement of these with the results obtained from the H. V. L. curves is probably within the experimental error.

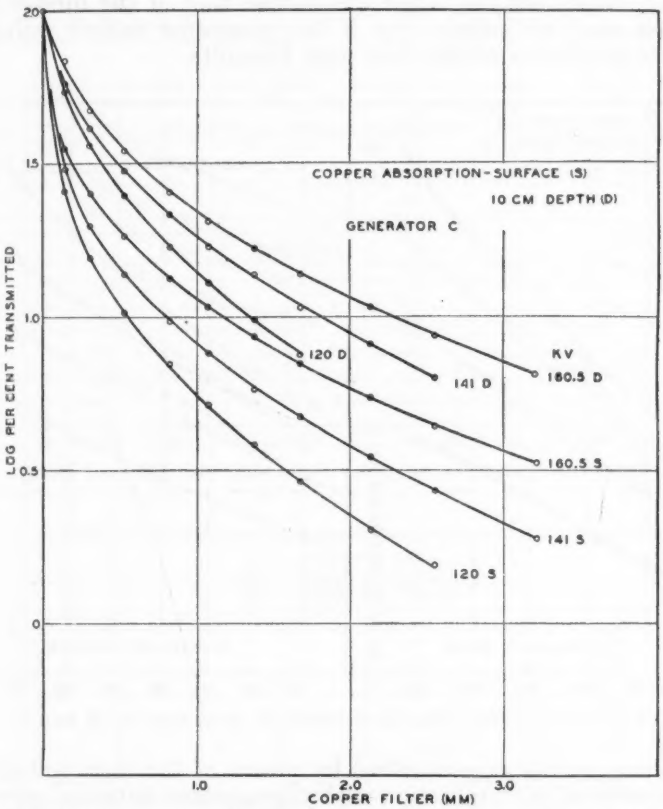

FIGURE 12.—*Semilogarithmic copper absorption curves for radiation measured at surface (S) and 10 cm depth (D) on phantom for generator C*

VII. VOLTAGE MEASUREMENTS

A partial explanation, at least, for the variation in X-ray emission under apparently identical conditions, is found to lie in the method of voltage measurement. The emission of an X-ray tube operating on a mechanically rectified generator depends upon the wave form of the voltage and the voltage-space current characteristic of the tube. If the tube current saturation is reached at a comparatively low voltage, then the voltage wave form of the generator is the predominant factor in determining the tube output. The wave form in turn depends upon current load drawn from the generator, the voltage, and the

setting of the rectifying switches. It happens that, in general, no single setting of the rectifiers will suffice to yield the maximum output for all current and voltage combinations. In practice a single rectifier setting is used for all operating conditions and as a consequence the optimum output is realized only for a narrow range of conditions.

In measuring the voltage with a sphere gap the peak of the wave is the quantity determined, regardless of the wave form. Thus while the peak voltage of two waves may be the same, if one is a sharp-topped wave form while the other is broad-topped, it is obvious that the tube output for the latter will exceed that of the former. This condition may be largely met if the generator output voltage be measured in *effective* rather than peak kilovolts.

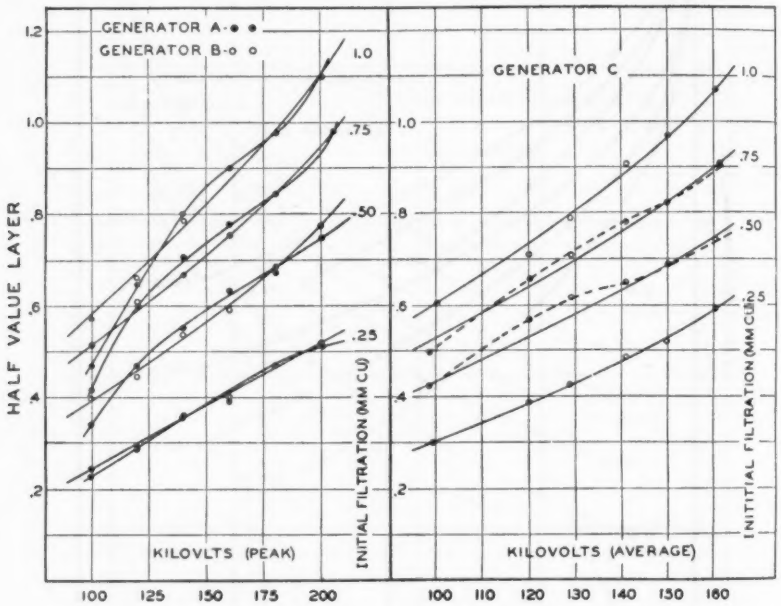

FIGURE 13.—*Half-value layer curves for generators A, B, and C*

This was readily accomplished by means of the high voltage voltmeter described in conjunction with the constant potential generator. As used up to the present, the 150 megohm noninductive shielded resistor [13] was in series with a d. c. microammeter and thus measured *average* voltage. When the d. c. instrument is replaced by an a. c. microammeter the potential is measured in *effective* kilovolts. In this work, the latter instrument not being readily available, we used a Kelvin multicellular electrostatic voltmeter to measure the potential drop across 75,000 ohms placed in series with the main high resistance. The meter then read the voltage across the line.

In the case of generator *C* the effective and average voltages are nearly identical. However, for mechanically rectified potentials,

[13] These have been described in paper referred to in footnote 7, p. 335. It was found that the separate units making up the final resistor had a very slight negative reactance at 1,000 cycles.

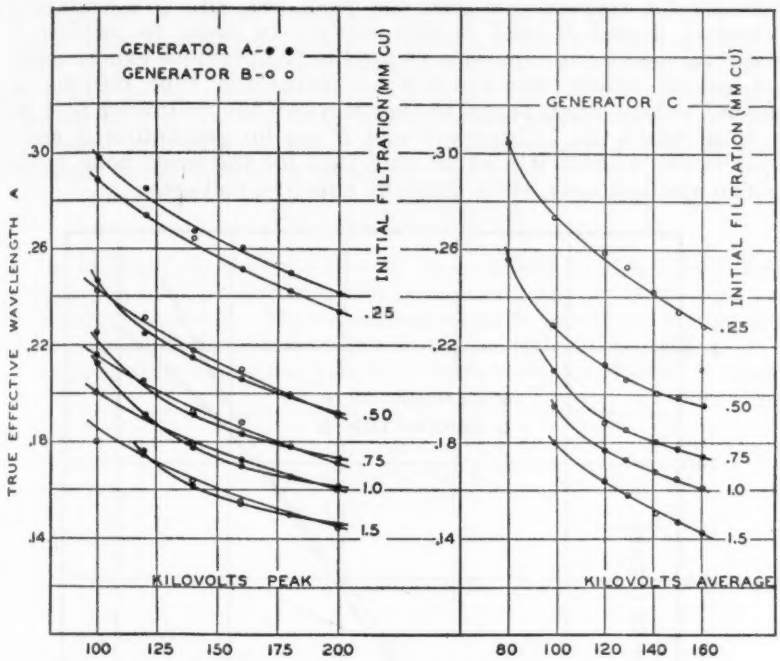

FIGURE 14.—*Effective wave length curves for generators A, B, and C*

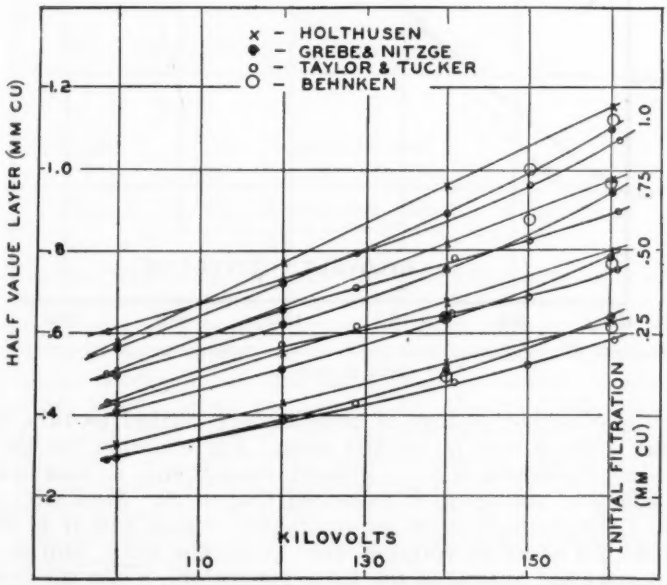

FIGURE 15.—*Comparison of half-value layer measurements by different observers*

the effective voltage is considerably higher than the average. Figure 16 shows the relation between the peak and effective voltage for generators *A* and *B* used in this study. In order to produce the same total load on the rectifier as used in the previous experiments—thus having nearly the same wave form—the tube current was adjusted so that when added to that through the voltmeter (0–1 ma) the total was 4 ma. Curves *A* and *B* are for generators *A* and *B*, respectively, whence it may be seen that for the same peak voltage the two systems have quite different effective voltages.

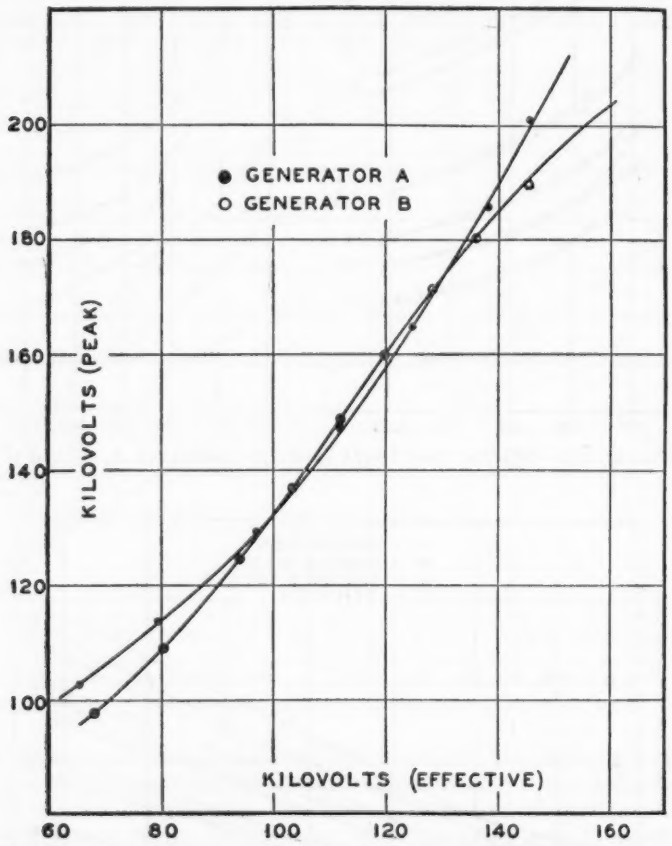

FIGURE 16.—*Effective and peak voltage measurements on generators A and B*

That the effective voltage is more closely related to tube output than peak voltage may be readily seen. For example, for the same 200 kv peak, generator *B* had a greater output; and, as seen in Figure 16, the effective voltage of *B* exceeded that of *A*. Similarly, at 180 kv (peak) the outputs were approximately equal and it is likewise found that the effective voltages were about the same, and so on.

To compare the output of the three generators, when the potential is measured in effective kilovolts, the curve in Figure 17 shows the relationship between the beam intensity (filtered through 0.525 mm.

of copper) and the effective kilovoltage. Curve *C* is for generator *C* ("constant potential") and the other points are as indicated. It is seen at once that the output at a given voltage is of the same order of magnitude for all three generators. Since the radiation quality was found to be roughly proportional to the intensity for a given tube current, it follows that the effective voltage also presents a fairly close indication of the quality. These results will be discussed in greater detail in a later paper.

VIII. CONCLUSION

It is believed that any value to be ascribed to this study lies in showing physical similarities, and not differences, between high voltage X-ray generators. Care has been taken to avoid any comparisons of the biological effectiveness per se of the radiations used. One of the outstanding biological problems is how to administer a desired

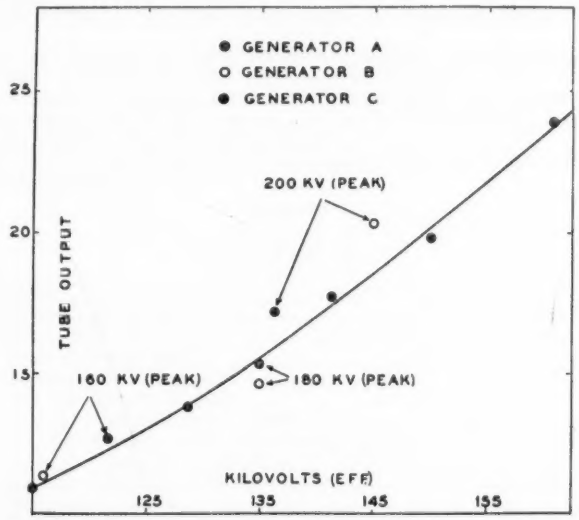

FIGURE 17.—*Plot showing tube output as a function of effective voltage for generators A, B, and C*

dose of radiation within the body without at the same time producing a dangerous skin erythema or destroying intervening tissue. It has been shown here how equivalent depth dose may be obtained with different generators and a wide range of qualities and intensities. The clinical application of this wide range of radiations depends on two factors which must be decided by the clinician, not by the physicist. The first, is the relationship between quality and the erythema dose. The second is the economics of administering radiation,[14] for obviously it would not be economical to use highly filtered low-voltage radiation for deep therapy when there is available a much greater intensity of less filtered radiation—assuming the biological effect to be the same.

[14] G. Failla, Dissert. L'Univ. de Paris, Serie A, No. 1776, 1923.

It is hoped that the results of the present study will enable the clinician to better compare his technique with that of others using different generators and making his measurements by different methods.

This study has been made possible through the support and the generous cooperation of the Radiological Research Institute and the X-ray manufacturers of this country, for which we express our appreciation. In addition, we thank G. Singer and C. F. Stoneburner, of this laboratory, for their assistance, particulary with the effective voltage measurements.

WASHINGTON, June 6, 1932.

THE STRUCTURE OF THE CHROMIC ACID PLATING BATH; THE THEORY OF CHROMIUM DEPOSITION

By Charles Kasper

ABSTRACT

The structure of solutions that are of importance to the theory of chromium deposition from the chromic acid bath was investigated by cryoscopic and conductivity measurements, and absorption spectra. It was shown that the first step in the reduction of chromic acid is the formation of chromium dichromate, $Cr_2(Cr_2O_7)_3$, a strong electrolyte which forms negative molecular ions. This compound is found not to exist in the "green" form. The next product of reduction is the basic chromium chromate, $Cr(OH)_3 \cdot Cr(OH)CrO_4$. This compound is a colloid, which may exist in relatively acid solutions. If sulphate is present, it forms chromic sulphate only the green form of which exists in chromic acid solutions.

If the basic colloid does not have its electrophoretic velocity reduced, it coats the cathode and prevents further reduction of chromic acid. The beneficial action of the sulphate is caused by the fact that it lowers that velocity by adsorption. The sulphate reaches the cathode film by being transported as a nonreactive positive molecular ion, $[Cr_4O(SO_4)_4(H_2O)_n]^{++}$.

The above theory was confirmed by employing it to correlate facts and principles of chromium plating.

CONTENTS

	Page
I. Introduction	353
II. Materials and solutions	354
III. Structure of solutions	355
1. Pure chromic acid	355
2. Chromium dichromate	355
(*a*) Previous work	355
(*b*) Cryoscopic evidence	355
(*c*) Conductivity measurements	356
(*d*) Absorption spectra	357
3. Highly reduced solutions	362
4. State of sulphate	364
5. Conclusions	365
IV. The theory of chromium deposition	366
1. Survey of theories	366
2. Possible reduction processes	367
3. Reactions in the cathode film	368
4. Action of negative ions, such as sulphate	369
5. Conclusions	372
V. Applications of the proposed theory	372
VI. Acklowledgments	374
VII. Bibliography	374

I. INTRODUCTION

Chromium is electrodeposited commercially from baths containing chromic acid (2 to 4 *M*), a small amount of sulphate (0.02 to 0.05 *N*), and a variable concentration of trivalent chromium (derived from the partial reduction of the chromic acid). No entirely satisfactory explanation has been offered for the mechanism of this process, and in particular for the function of the sulphate.

The research naturally divided itself into two parts—first, the structure of the initial solution and of any system to which it may give rise on electrolytic reduction, and, second, the deportment of such systems in an electric field.

By the structure of a solution is meant the type and extent of the linkages existing between the various species present. Two types of such bonds are now recognized (23),[1] although modern research indicates that an indefinite number may exist (29).

Unless otherwise stated, all strong electrolytes [2] will be regarded as completely ionized at all concentrations. This characteristic is associated with systems in which only the ionic type of linkage exists.

The structure of the solutions was studied by measuring their freezing point lowerings, conductivities, and absorption spectra. From a consideration of published data on the systems of interest and admittedly similar ones, and from new experimental evidence, a theory of the electrodeposition of chromium has been developed. This theory correlates and explains practically all known facts concerning the process and also permits valid predictions to be made.

II. MATERIALS AND SOLUTIONS

A special lot of pure chromic acid was employed which had the composition (on a dry basis) shown in Table 1. The methods of analysis were the same as those employed by Moore and Blum (26).

TABLE 1.—*Composition of chromic acid*

Material	Per cent
Chromic acid (CrO_3)	99.75
Trivalent chromium (Cr_2O_3)	.15
Sulphate (SO_4)	.01
Alkali (Na_2O+K_2O)	.01
Insoluble	.01
Total	99.93

A number of methods were employed to prepare chromic acid solutions containing trivalent chromium and practically no other substances. Reduction with alcohol gave solutions from which the resultant acetic acid could not be readily removed. By dissolving pure Cr_2O_3 (produced by igniting CrO_3) in strong chromic acid, solutions with compositions corresponding to degrees of reduction up to 20 per cent [3] were obtainable. Dissolving of basic chromate, calcined at 200° C., in chromic acid yielded the same result. The more highly reduced solutions were prepared by the addition of concentrated hydrogen peroxide. These will be described and discussed in a subsequent section.

The solutions for the cryoscopic measurements were prepared, as customary, on a weight basis (moles per 1,000 g of water). Those for the measurement of conductivity and light absorption were prepared

[1] The numbers in the text here and throughout the text refer to the bibliography at the end of the paper.

[2] In this paper the term electrolyte is used in the same sense as ionogen; that is, a substance which when dissolved in a specified medium produces a conducting solution (which latter is frequently called the "electrolyte").

[3] The relative content of trivalent chromium in these solutions may be conveniently expressed in terms of the total chromium content. For example, a solution corresponding to $Cr_2(Cr_2O_7)_3$, chromium dichromate, has one-fourth of its chromium content in the trivalent state, and, hence, represents a solution that is 25 per cent reduced. Similarly, the basic-chromate, $(Cr(OH)_2 \cdot Cr(OH)CrO_4$ represents a reduction of about 67 per cent.

on a volume basis (moles per liter of solution). The stated concentrations of free chromic acid are based on the assumption that the trivalent chromium is present as the dichromate, $Cr_2(Cr_2O_7)_3$. Sulphate was introduced as dilute sulphuric acid, which was added at room temperature, and, therefore, produced no appreciable heating.

III. STRUCTURE OF SOLUTIONS

1. PURE CHROMIC ACID

The published data analyzed by Abegg (7) show conclusively that chromic acid is a strong acid, which at moderate concentrations exists principally as dichromic acid, $H_2Cr_2O_7$, of which both hydrogens are strongly dissociated. In more concentrated solutions trichromic acid, $H_2Cr_3O_{10}$, and possibly tetrachromic acid, $H_2Cr_4O_{13}$, exist. In very dilute solutions the monochromate ions, $HCrO_4^-$, and CrO_4^{--}, are the principal forms. The content of CrO_4^{--} ions at any finite acid concentration is extremely low.

2. CHROMIUM DICHROMATE

As it appeared probable from chemical evidence that the first step in the reduction of chromic acid results in the formation of chromium dichromate, the structure of partly reduced solutions was first investigated.

(a) PREVIOUS WORK

Some investigators (13), (16), and (19) have considered chromium dichromate as a colloid, while others (22) have regarded it as a very weak electrolyte. In all cases the evidence is unsatisfactory. The principal arguments were based upon ultramicroscopic observations. In order that a colloid be detectable by this means it must possess a certain size, a certain refractive index, and a certain transmittancy. It is difficult to see how scattered (not reflected) light could be observed in such highly absorbing solutions as these, if the dispersoid is not a metal. Some solutions like those previously investigated were examined with the ultramicroscope. From these experiments the conclusion was reached that the variable results (and hence the variable interpretations) were caused by dust. No great weight should be attached to ultramicroscopic observations on these solutions.

In addition to obtaining negative results with the ultramicroscope, Ollard (22) cited the qualitative evidence of the migration of the trivalent chromium toward the cathode in these solutions. This observation does not prove that chromium dichromate is a very weak electrolyte. It might be a strong electrolyte or a lyophilic colloid (a micelle).

(b) CRYOSCOPIC EVIDENCE

The measurements were made with the usual type of apparatus; in the 1F series a platinum resistance thermometer was used, and in the 2F series a Beckmann. The results are given in Table 2.

TABLE 2.—*Freezing-point depressions*

Solution No.	Moles per 1,000 g H_2O					Depression
	Cr^{VI}	Cr^{III}	$Cr_2(Cr_2O_7)_3$	Free CrO_3	H_2SO_4	
						° C.
1FI	4.340	1.108	0.554	1.016		13.72
1FII	4.340	1.108	.554	1.016	0.04	13.97
1FIII	4.340	1.108	.554	1.016	.20	15.47
1FIV	1.016			1.016		2.98
2FI	1.084	.278	.139	.249		1.72
2FII	1.084	.278	.139	.249	.05	2.17
2FIII	.249			.249		.66

In the designation of a given solution, for example 2FI, the Arabic numeral (2) refers to the apparatus employed, the letter (F) denotes the type of measurement (in this case freezing point), and the Roman numeral (I) refers to the number of the solution in that series. These three symbols define the composition of the solution. Sometimes it was found necessary to heat the solutions for one hour at 100° C.; such solutions are designated with an additional symbol, B.

The data relating to solutions 1FI and 1FIV show that the depression produced by 0.554 mole of chromium dichromate is 13.72° − 2.98° = 10.74°, or 19.40° per mole. If this salt were completely ionized into chromic and dichromate ions, and "perfect" in the Arrhenius sense, there would be a molar depression of 9.3°. The solute is a "superperfect" one, and most certainly is not a colloid or a very weak electrolyte. This point is shown even more conclusively by the data for the more dilute solutions. In the same manner the molal depression calculated from the data for the 0.139 *M* chromium dichromate is 7.6°; the value for violet chromic sulphate (7) (a comparable solute) at the same dilution is 4.15°.

Heating the above solutions for one hour at 100° C. caused no change in the depressions. As practically all inorganic chromic compounds exhibit changes in properties (from the violet to the green form[4]) when they are heated, this observation is important. This evidence is indicative that the "green" form of chromium dichromate did not exist in these solutions. In this respect this salt is similar to chromic nitrate and perchlorate. The absence of a change in solutions containing sulphate shows that the state of the sulphate is the same in the heated as in the unheated solutions.

(c) CONDUCTIVITY MEASUREMENTS

A solution that was 1.086 *M* in Cr^{VI} and 0.277 *M* in Cr^{III}, and which was, therefore, 0.255 *M* in free CrO_3, had at 25° C. a conductivity of 0.666 mho–cm. This is about 15 per cent higher than the interpolated value of 0.579 of Moore and Blum (26) for 0.255 *M* CrO_3. The increase in conductivity caused by 0.138 *M* chromium dichromate is 0.086 mho–cm, which corresponds to a molal conductance of $\frac{1,000 \times 0.086}{0.138} = 623$ mho–cm. The data in Abegg (7) show that the molal conductance of violet chromic sulphate at the same

[4] For example, the violet chloride $[Cr(H_2O)_6]Cl_3$, is transformed by heat into the green compound $[Cr(H_2O)_5Cl]Cl_2$ and $[Cr(H_2O)_4Cl_2]Cl$.

dilution is about 800 mho–cm. The difference is of the order expected in view of the greater mobility of the sulphate ion ($\mu_\infty = 136$) as compared with the dichromate ion ($\mu_\infty = 50$).

The cryoscopic and conductimetric measurements that we have made indicate that chromium dichromate is similar in structure to violet chromic sulphate; that is, it is an electrolyte that does not form molecules or molecular ions that include the negative radical. The spectrophotometric measurements to be described indicate that, while this conclusion is in the main correct, true molecular ions do exist.

(d) ABSORPTION SPECTRA

The cells for these measurements were made entirely of glass and were usually 1 mm thick. Thin cells were necessary on account of the high absorbencies of most of the solutions. The measurements were limited to wave lengths from 500 to 700 mμ. The 1P series were measured on a Koenig-Martens visual spectrophotometer.[5] The 2P series were executed on a Bausch & Lomb visual spectrophotometer. Although the accuracy of our measurements with the latter instrument is not quite as high as with the former, the results are sufficiently precise for our purposes.

In expressing the results the nomenclature of the Optical Society of America (12) is followed as closely as possible. The transmittancy, T, is equal to I/I_o, where I is the light intensity through a cell filled with the solution, and I_o that through a similar cell filled with the solvent. The absorbency, A, is equal to $-\log_{10} T$. Also, A is equal to $\Sigma(a_i c_i)1$, where 1 is the length in centimeters of the path traversed, c_i is the concentration of species i in moles per cubic centimeter, and a_i is the molal absorbency of i. If the values of a_i are independent of those of c_i, the system is said to obey Beer's law.

All measurements were made at about 25° C. The composition of the solutions upon which spectrophotometric measurements were made is given in Table 3.

TABLE 3.—*Composition of solutions for spectrophotometric measurements*

Designation No.	Moles per liter							
	Cr^{VI}	Cr^{III}	Free CrO_3	Al^{III}	Y^{III}	$Cr(SO_4)_{3/2}$	$Cr(NO_3)_3$	H_2SO_4
1PI	1.086	0.277	0.254					
1PII	1.086	.277	.254					0.01
1PIII	1.086	.277	.254					.10
1PIV	1.086		1.086					
1PV	.254		.254					
1PVI								
1PVII	1.086		.254		0.277		0.544	
2PI						0.066		
2PII	1.086		.254	0.277				
2PIII	.0225	.00519	.00635					
2PIV	.518	.277						
2PV	.255	.185						

[5] These measurements were made by Mabel E. Brown, of the colorimetry section.

The first five solutions (and the corresponding heated ones) were so selected that the following salient facts could be determined: First, the absorbency of $Cr_2(Cr_2O_7)_3$ as such; second, the apparent absorbency of Cr^{III}; third, the possible existence of the "green"

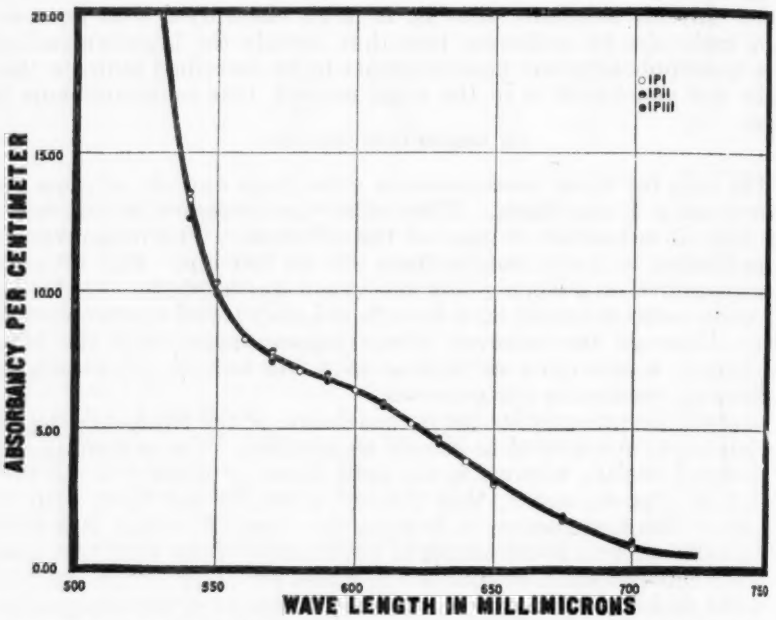

FIGURE 1.—*Effect of sulphuric acid on absorbency of solutions containing free chromic acid (0.254 M) and chromium dichromate (0.139 M)*

	Sulphuric acid
	M
1PI	0
1PII	.01
1PIII	.10

form of chromium dichromate; fourth, the state of the sulphate in cold solutions; and fifth, the state of the sulphate in heated solutions. The data are reported in Table 4 and are plotted in Figures 1, 2, and 3.

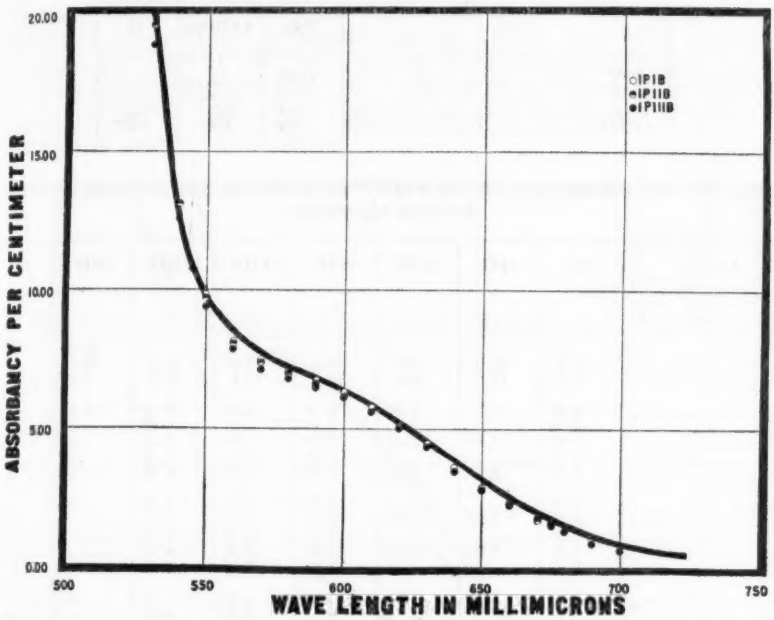

FIGURE 2.—*Effect on absorbency produced by heating solutions of Figure 1 to 100° C. for one hour*

(Curve same as in fig. 1)

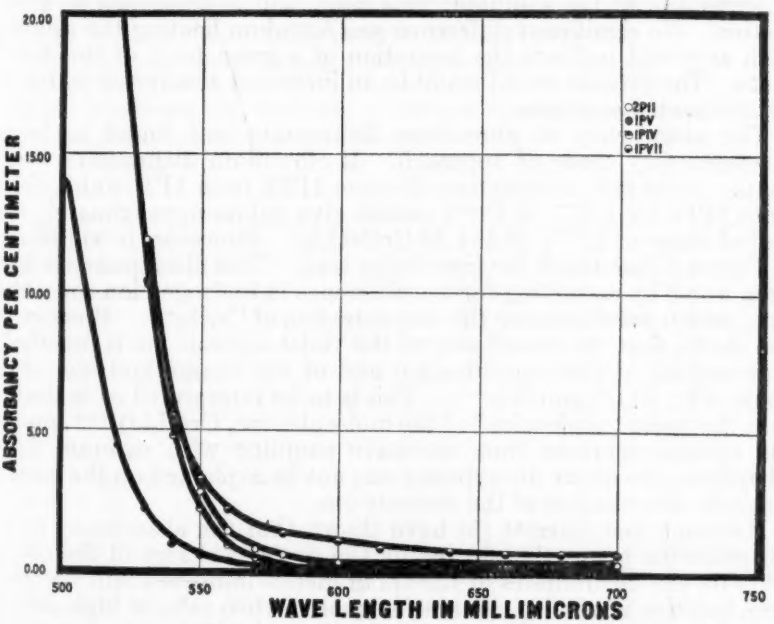

FIGURE 3.—*Effect of trivalent ions on absorbency of chromic acid*

	CrO_3	Addition	*M*
1PIV	1.086		
1PV	.254		
1PII	.254	Al^{+++}	0.277
1PVII	.254	Y^{+++}	.277

TABLE 4.—*Absorbency per centimeter at 25° C. of chromic acid solutions containing trivalent chromium*

λ in mμ	1PI	1PII	1PIII	1PIB	1PIIB	1PIIIB	1PIV	1PV
500								14.0
10								8.24
20							21.0	4.42
30	19.6	20.0	19.6	19.6	19.6	18.9	10.4	2.13
40	13.3	13.6	12.6	13.1	13.1	12.6	4.84	.88
550	9.91	10.3	9.87	9.79	9.67	9.36	2.15	.42
60	8.24			8.18	8.07	7.83	.84	
70	7.57	7.83	7.45	7.50	7.38	7.13	.36	.11
80	7.10			7.08	6.95	6.78	.16	
90	6.80	6.97	6.78	6.76	6.60	6.48	.10	
600	6.40			6.33	6.22	6.13	.04	.03
10	5.78	5.97	5.80	5.78	5.62	5.58		
20	5.20			5.12	5.02	5.00		
30	4.51	4.69	4.49	4.47	4.32	4.33		
40	3.83			3.63	3.55	3.55		
650	3.03	3.18	3.10	2.90	2.79	2.79	.02	.02
60				2.33	2.26	2.28		
70				1.71	1.72	1.79		
75	1.69	1.86	1.76		1.51	1.56		
700	.67	.87	.87	.90	.62	.59	.03	.00

In Figures 1 and 2 it will be noted that there are only small differences due to the sulphate; this point will be discussed in a later section. No significant difference was found on heating the solutions such as would indicate the formation of a green form of the dichromate. The process would result in an increased absorption in the red by the heated solutions.

The absorbency of chromium dichromate was found to be an unsatisfactory mode of approach. If chromium dichromate were a simple violet salt, subtraction of curve 1PIV from 1PI (which differs from 1PIV by 0.277 *M* Cr^{III}) should give values approximately one-half of those of *1PVI* (0.554 *M* $Cr(NO_3)_3$). However, it will be seen in Figure 4 that this is far from being true. This discrepancy is made even worse by correcting for the difference in hydrogen ion concentration, which would change the concentration of $Cr_3O_{10}^{--}$. Bjerrum (3) has shown that the absorbency of the violet chromic ion is practically independent of the concentration and of the charge and size of the anion (Cl^-, NO_3^-, and SO_4^{--}). This is to be interpreted as indicating that the water "molecules" of the molecular ion, $Cr(H_2O)_6^{+++}$, protect the optical electrons from excessive coupling with external fields. Therefore, the above discrepancy can not be explained on the basis of a simple deformation of the chromic ion.

Hantszch and Garrett (5) have shown that the absorbency of the chromate ion is greatly affected by the size and charge of the cation. Data on the dichromates of the alkali metals indicate slight deformation, but this possiblity can not be ignored when salts of high valence types are involved. To obtain the desired information regarding deformation of the dichromate ion, the absorbencies of solutions

2PII and 1PVII were measured. In each there is exactly the same content of hexavalent chromium as in 1PIV, but 2PII contains aluminum and 1PVII yttrium, each in a concentration equivalent to that of trivalent chromium in 1PI. The data are reported in Table 5, and are plotted in Figure 3. Table 5 also includes solutions that will be discussed later in this paper.

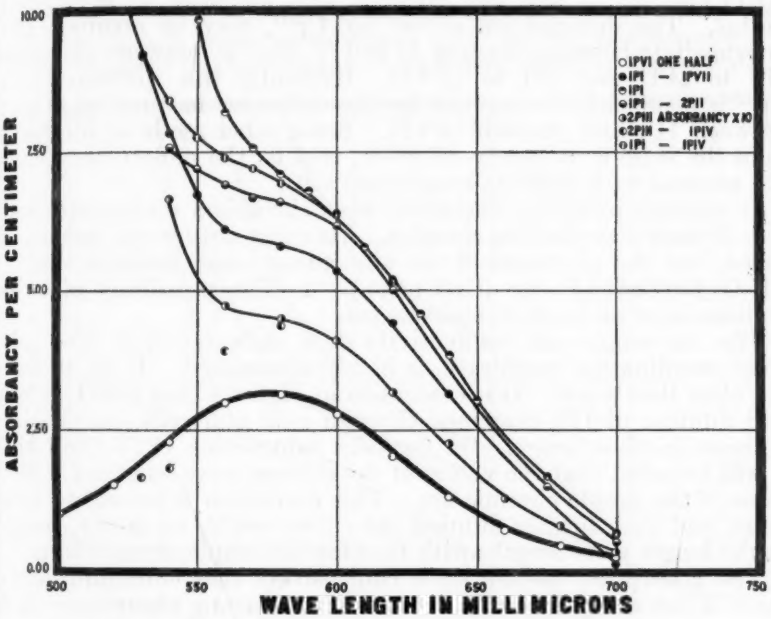

FIGURE 4.—*Absorbencies of various chromium solutions*

TABLE 5.—*Absorbency per centimeter of various chromium solutions at 25°C.*

λ in mμ	2PI	2PII	2PIII [1]	1PVI	1PVII
500	0.67			1.95	
510					
520				3.05	19.6
530		11.9	12.00		10.3
540	.97	5.68	6.64	4.56	5.4
550		2.73			3.16
560		1.32	4.75	5.99	2.12
570	1.31	.50	4.50	6.35	1.30
580		.23	4.10	5.56	1.04
590	1.31		3.19	4.09	.78
600			2.26	2.63	.67
610	.92		1.28	1.41	.62
620			.79	.89	.60
630	.41	.17	.38	.41	.58

[1] Absorbency ×10.

It is well known that in ionic systems deformation effects can be related to the size and charge of the "companionate" ions. Only relative sizes of the bare (not hydrated) ions are involved. The available data indicate that no simple analysis is possible, but it is legitimate to employ the conception for interpolative purposes.

Crystal structure data (28) indicate that the radii of the trivalent ions of Al, Cr, and Y are, respectively, 0.55, 0.70, and 0.90 A°. So, from a knowledge of the deformation produced by aluminum and yttrium, we can estimate that to be expected from chromium. The data plotted in Figure 3 show that the deformation is, as demanded by the above discrepancy, greater with the increasing charge (H^+ (1PIV) to Al^{+++}) and for trivalent ions increases with increasing radius. The deformation caused by Cr^{III}, may be assumed to be intermediate between those of Al and Y (that is, between the curves 1PI to 2PII and 1PI to 1PVI). Evidently this deformation by Cr^{III} is insufficient to account for the difference in question; that is, between 1PI and one-half 1PVII. Some other mode of interaction than the ionic is evidently effective; that is, the molecular. This is not unusual with chromic compounds (29).

It appears probable, therefore, that chromium dichromate exists as a Werner coordination complex. Its exact nature was not investigated, but the character of the absorption bands indicate that it is $[(H_2O)_2Cr(Cr_2O_7)_2]^-$ or $[Cr(Cr_2O_7)_3]^{---}$. The possibility of a true undissociated molecule is not excluded.

The cryoscopic and conductivity data indicated that this, unlike most coordination complexes, is highly dissociated. If so, it should not obey Beer's law. It is evident from Figure 4 that 2PIII (a forty-fold dilution of 1PI examined through a 40 mm cell) shows a large decrease in absorbency. On formally subtracting 1PIV from 2PIII it will be noted that the values at the shorter wave lengths fall below those of the simple chromic ion. This correction is known to be too large, and with further dilution the curve would, no doubt, coincide at the longer wave lengths with that for the simple chromic ion.

The absorption spectra show conclusively that chromium dichromate is not a colloid, as this would have a strong absorbency in the red and would obey Beer's law strictly (34). All experiments were consistent with the interpretation made, and inconsistent with any other that was entertained. No variations in absorbency occurred on standing for long periods.

3. HIGHLY REDUCED SOLUTIONS

Ollard (22) reported that by treating chromic acid solutions with concentrated hydrogen peroxide, a reduction up to 50 per cent ($Cr(OH)CrO_4$) could be effected, but that beyond that point a precipitate of $Cr(OH)_3Cr(OH)CrO_4$, (9) (14) (67 per cent reduction) was produced. In our experiments it was found that a reduction as high as 60 per cent could be thus effected without immediate precipitation. On standing one or more days the above precipitate appeared in which the ratio of the trivalent to hexavalent chromium was 2 to 1 and the filtrate corresponded to about 37 per cent reduction. The precipitation occurred with all solutions more highly reduced than 37 per cent. The rate of precipitation varied directly as the degree of reduction; it was accelerated by heating. These observations indicate that the system is a mixture of a sol, whose dispersoid is $Cr(OH)_3Cr(OH)CrO_4$, and a true solution of an electrolyte, chromium dichromate. The reason that solutions with 37 per cent reduction are stable is that then the hydrogen ion concentration is so high that the particles of the basic sol become sufficiently electropositive to remain in suspension. This hypothesis was confirmed by precipitat-

ing the basic chromate out of partially reduced solutions (42 per cent) with sodium sulphate.

Liebreich (9) and Müller (14) prepared colloidal solutions of the basic chromate by digesting the precipitate with water for a long time. The method employed in the present research was to take an unstable, highly reduced solution and dilute it strongly. Sols prepared in this manner exhibited a strong Tyndall beam and a dichroic appearance. They were quite murky and hence had fairly large particles, though none were visible with the ultramicroscope. As previously noted this instrument is not well adapted for these solutions.

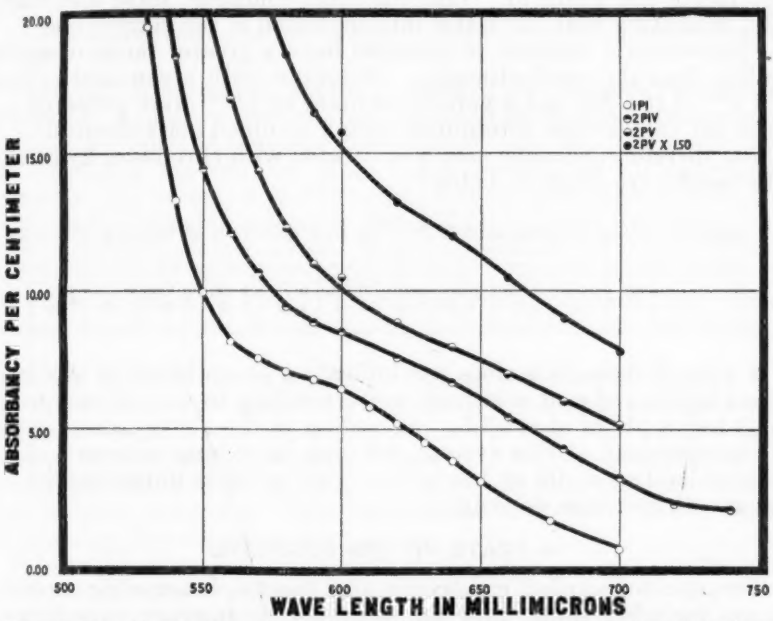

FIGURE 5.—*Absorbencies of solutions with equal contents of trivalent chromium and decreasing contents of hexavalent chromium*

The absorbency data for the highly reduced solutions, 2PIV and 2PV (prepared in the cold), are recorded in Table 6 and shown in Figure 5.

TABLE 6.—*Absorbency per centimeter of highly reduced solutions*

λ in mμ	2PIV	2PV	2PV×1.5
540	18.5		
50	14.4		
60	12.1	17.0	
70	10.7	14.3	21.6
80	9.43	12.4	18.6
90	8.89	11.0	16.5
600	8.51	10.5	15.8
20	7.56	8.86	13.3
40	6.68	7.98	12.0
60	5.42	7.00	10.5
80	4.30	6.00	9.00
700	3.20	5.16	7.80
20	2.37		
40	2.07		

The data in the last column have been recalculated to correspond to the same concentration of trivalent chromium as the other two. It will be noted that an increase in reduction causes an increased absorption over the entire range. The increase at the shorter wave length is probably caused in part by the deformation of the chromate radical. The increase in absorption in the red could be caused either by a complex (green) electrolyte, or a colloid, or both.

An effort to settle the question by freezing point measurements was only partially successful in that the data could be interpreted equally well in terms of a weak electrolyte or a mixture of a strong electrolyte and a colloid. Like the other solutions, these also coagulate, indicating that the latter interpretation is the correct one.

Electrometric methods of titration have a greater range of applicability than the conductimetric. Solutions with a constant content of Cr^{VI} (0.184 *M*) and a variable content of Cr^{III} were prepared and their pH values were determined with a modified glass electrode. In effect, therefore, chromic acid was titrated with chromium hydroxide. The results are given in Table 7.

TABLE 7.—*pH of chromic acid (0.184 M) with additions of trivalent chromium*

Cr^{III} *M*	0.000	0.033	0.058	0.061	0.065	0.079	0.118	0.123	0.125	0.129	0.133	0.137
pH	1.08	1.20	1.26	1.31	1.32	1.47	2.22	2.30	2.42	2.54	2.66	2.82

A plot of these data does not indicate a sharp break of any kind. More highly reduced solutions (corresponding to 60 per cent reduction) had a pH of about 3.5. According to the above interpretation of the structure of this system, we may have large amounts of the basic colloid at a pH as low as 3. This point is important for the theory of chromium deposition.

4. STATE OF THE SULPHATE

The above recorded cryoscopic and spectrophotometric measurements included some data on solutions containing chromic acid, chromium dichromate, and sulphuric acid. As noted before, the cryoscopic measurements indicated that there was no difference in the state of the sulphate in the heated and unheated solution. This behavior would be impossible with the violet chromic sulphate, so the green salt must be present.

The spectrophotometric measurements confirm this conclusion. It will be noted in Figures 1 and 2 that the absorbencies of the solutions with the largest content of sulphate are lower at the shorter, and (usually) higher at the longer, wave lengths than those with no sulphate, whether the solutions are heated or not. This is to be expected if green chromic sulphate replaces some chromium dichromate. The difference can be calculated [6] from the data on 1PI and 2PI, which latter is a solution of green chromic sulphate that was

[6] As this is rather involved, a sample calculation, that at 540$\mu\mu$ is given. According to Table 1 the absorbence per centimeter of the chromium dichromate in 1PI is 13.30−0.88=12.4. 1PIII contains in addition 0.1 *M* of sulphate. If the complex is $[Cr_4O(SO_4)_4(H_2O)_n]^{++}$, then according to Tables 3 and 5 the expected absorbency of the green chromic sulphate will be $0.97\times\frac{3}{2}\cong 1.5$;

There will be a loss in absorbency corresponding to $\frac{1}{2.77}\times 12.4\cong 4.1$. So the change in absorbency will be 4.1−1.5−1.3=1.3. The minus 1.3 denotes the increase due to the formation of free chromic acid.

heated for one hour at 100° C. The effects, though small, are quite definite and beyond experimental error; the interpretation explains why only a small change is found. The results are given in Table 8.

TABLE 8.—*Change in absorbency produced by addition of sulphate to solutions containing* Cr^{VI} *and* Cr^{III}.

λ in mμ	540	570	580	590	620	650	700
A_c[1]	1.3		0.37		0.06	−0.51	−0.40
A_f	.68	0.12		0.02			−.23
A_{fs}	.50		.40		.12	.05	.04

[1] A_c is the calculated change in absorbency, A_f is that found for the unheated series, and A_{fs} that for the heated series.

The green complexes of chromic sulphate possess very remarkable properties. Some are true colloids, but most of them are electrolytes. The colloidal form is obtained only with drastic treatment. Part of the sulphate in the ordinary green forms is combined with the trivalent chromium to form a positive molecular ion $[Cr_4O(SO_4)_4(H_2O)_n]^{++}$. In the green chloride we have $[CrCl(H_2O)_5]^{++}$ and $[CrCl_2(H_2O)_4]^{+}$. These complexes are remarkable in that apparently there is absolutely no dissociation of the coordinated groups. Electron pair bonds are undoubtedly effective (29). These positive molecular ions furnish an ideal means of conveying the sulphate radical into the cathode film.

The pH of pure violet chromic sulphate solutions is about 2. It was noted previously that the maximum pH found in solutions containing colloidal basic chromium chromate was 3.5. These data indicate that, barring complex formation (which, however, is not favored at a intermediate pH like 3), free sulphate ions can exist in these colloidal solutions. This point is also important for the theory of chromium deposition.

In pure solutions the violet form is the more stable at room temperature and below; the green is more stable above room temperature. The rate of conversion of the green into the violet is low, especially in the presence of acid, which acts as a negative catalyst and may even shift the quasiequilibrium. Such a shift is recorded in this paper for the sulphate in chromic acid solutions; a similar case has been worked out by Bjerrum (2) for violet chromic chloride in hydrochloric acid solutions. The fairly high temperatures employed in chromium deposition probably assist in this shift of equilibrium.

5. CONCLUSIONS

1. Chromium dichromate is a strong electrolyte and forms true molecular ions.

2. The "green" form of chromium dichromate does not exist in the solutions investigated.

3. More highly reduced solutions than the dichromate contain, in addition to that compound, a sol of the basic chromium chromate $Cr(OH)_3Cr(OH)CrO_4$.

4. In partially reduced solutions with an excess of chromic acid, the sulphate exists principally as the green chromic sulphate.

IV. THE THEORY OF CHROMIUM DEPOSITION

1. SURVEY OF THEORIES

The principal theories of chromium deposition that have been advanced will be briefly considered, including that proposed by the author in this investigation.

1. Sargent (6) recognized a number of features that are extremely important; that the cathode film is only slightly acid at high current densities, that reduction of chromic acid at high current densities must occur through the medium of the chromic-chromous couple (see p. 369), that sulphate is necessary for metal deposition, and that pure chromic acid can be reduced at low but not at high current densities. The latter feature he attributed to a colloidal layer which he designated as nonpermeable, though he tacitly assumed it to be permeable to hydrogen ions. The mechanism of the action of the sulphate was not clearly set forth.

2. Liebreich (9) (10) measured polarization curves by means of which he endeavored to show the successive stages through which chromic acid must pass before being reduced to the metallic state. The existence of this "step-wise" reduction is the principal feature of Liebreich's theory. The action of the sulphate was not explained. He demonstrated that the cathode film is less acid than the solution, and that in it there probably is an electropositive colloid, $Cr(OH)_3$-$Cr(OH)CrO_4$.

3. Fink (11) advanced a theory in which the sulphate is designated as a catalyst, but he gave no clear conception of its action. He assumed that the hydrogen that is always evolved in chromium deposition protects the metal from oxidation.

4. E. Müller (14) recognized that pure chromic acid is not reducible at high current densities. He attributed this fact to the formation of a colloidal layer in the slightly acid cathode film as a result of the migration of an electropositive sol. The idea that the cathode layer is permeable to hydrogen ions was expressly set forth. His first explanation of the action of the sulphate was that it precipitated and destroyed the cathode layer, and thus made possible the reduction of chromic acid. Later (20), (21), (24), and (33) he abandoned this interpretation in favor of one which states that the bisulphate ion, HSO_4^-, can, on account of its relatively small size, pass through interstices in the colloidal layer, thus permitting the existence of a higher hydrogen ion concentration in the cathode film. This condition is less favorable for the formation of the basic colloid. It is important to note that he found it necessary to assume that the bisulphate ion is effective at a pH of 3 or 4, and that its attraction toward the cathode is secondary. Müller demonstrated that the basic dispersoid, $Cr(OH)_3Cr(OH)CrO_4$, is electropositive. This theory is somewhat similar to that developed in this paper.

5. Haring (13), (17), and later Piersol (27) suggested that the action of the sulphate is in accordance with the following equation:

$$\underset{\text{(colloid)}}{Cr_2(Cr_2O_7)_3} + \underset{\text{(strong electrolyte)}}{3H_2SO_4} \rightarrow \underset{\text{(strong electrolyte)}}{Cr_2(SO_4)_3} + \underset{\text{(strong electrolyte)}}{3H_2Cr_2O_7}$$

Chromium dichromate is not a colloid, and a pure metathesis (like the one represented) between a slightly soluble (or ionizable) salt and a strong electrolyte to produce two strong electrolytes in dilute solution is thermodynamically impossible.

6. Ollard's (22) theory denies that chromic acid can be reduced directly, and states that all reduction must proceed through the medium of the chromic-chromous couple. The action of the sulphate was explained by a reaction similar to that proposed by Haring and Piersol except that chromium dichromate was considered to be a very weak electrolyte.

7. In this research a theory of chromium deposition has been developed, which involves some features that have been expressed in previous theories, but that have been modified in the light of additional information and of a different viewpoint.

Deposition of bright chromium depends upon maintaining in the cathode film a definite hydrogen ion concentration. This must be sufficiently low to permit metal deposition and yet sufficiently high to prevent hydrolysis and thus yield oxide-free deposits.

At low current densities direct reduction of hexavalent to trivalent chromium undoubtedly occurs. At high current densities, which require cathode potentials sufficient to liberate hydrogen gas, the conditions are vastly different. On account of the tremendous migration velocity of the hydrogen ion in the cathode film, the latter becomes relatively alkaline. If the hydrogen ion concentration drops to 10^{-3}, a basic electropositive dispersoid of $Cr(OH)_3 \cdot Cr(OH)CrO_4$ exists. In the absence of the sulphate the dispersoid migrates toward the cathode and covers it with a colloidal layer which prevents reduction of everything except hydrogen ion, to which it is permeable.

The action of the sulphate is to decrease the electrophoretic velocity of the colloid by adsorption; which causes a reduction of the positive charge and prevents the formation of a dense, adherent colloidal layer. Other ions can then reach the cathode and be reduced. It is improbable, on account of the repulsive action of the cathode toward negative ions, that the simple sulphate ion can approach the cathode sufficiently close to be very effective. Some other means must be found for bringing it to the cathode.

It is well known that ordinary green chromic sulphate forms nondissociable, positive molecular ions like $[Cr_4O(SO_4)_4(H_2O)_n]^{++}$. This ion can, on account of its nonreactiveness, convey the sulphate to the cathode surface, and when the complex ion is discharged and reduced, the sulphate is set free to wander toward the anode. Before leaving the vicinity of the cathode, it may be adsorbed by the positive dispersoid and may thus limit the formation of the colloidal layer. While reduction at high current densities is made possible by the presence of sulphate, the actual reduction occurs mainly through the chromic-chromous couple.

2. POSSIBLE REDUCTION PROCESSES

It will be profitable to examine the principal reactions in terms of their standard electrode potentials (4). It will be seen that the conditions that are required for chromium deposition are those that inhibit certain undesirable reactions.

TABLE 9.—*Standard potentials of possible reactions in chromium deposition*

No.	Reaction	Standard potential
		Volts
1	$1/2\ Cr_2O_7^{--}+7H^+ +3\epsilon = Cr^{+++} +7/2\ H_2O$	1.1
2	$1/2\ Cr_2O_7^{--}+7H^+ +4\epsilon = Cr^{++} +7/2\ H_2O$	.9
3	$1/2\ Cr_2O_7^{--}+7H^+ +6\epsilon = Cr+7/2\ H_2O$	.4
4	$H^+ + \epsilon = 1/2\ H_2$	.0
5	$Cr^{+++} + \epsilon = Cr^{++}$	−.4
6	$Cr^{++} +2\epsilon = Cr$	−.1
7	$Cr^{+++} +3\epsilon = Cr$	−.8

ϵ denotes an electron.

According to reaction 3, it should be theoretically possible to arrange a cell having a chromium-coated metal as cathode and a hydrogen electrode as anode, and deposit chromium without the use of external electrical energy. In fact, there would be a gain of electrical energy that could be employed to generate some of the hydrogen used. The reason that this is impracticable is because reaction 1 is the more probable under any condition that is favorable for reaction 3. If instead of chromic acid a chromic salt were employed electrical energy would be required in order to effect chromium deposition.

3. REACTIONS IN THE CATHODE FILM

During deposition at appreciable current densities the solution close to the cathode, the cathode film, may differ greatly in composition from the body of the solution. However, a steady state is set up between the factors causing depletion and restoration of the various species in the film. The former include, first, the rates of discharge of the various ions present, and, second, the forces that exist between the ions and the cathode. The restorative factors include, first, migration of the ions toward the cathode, second, diffusion processes and, third, convection currents. The electrical forces very close to the cathode are relatively large and hence there is a large concentration gradient in the cathode film. The processes that actually occur at the cathode under specified conditions depend upon the composition and structure of the cathode film.

There are three imperative reasons why the cathode film must possess an intermediate pH (3 or 4) before deposition of metallic chromium can occur. First, the difference in free energy between the standard chromium-chromic ion potential and the standard hydrogen-hydrogen ion potential is 0.5 volt faraday per equivalent. This demands, first, that the hydrogen ion concentration be low for chromium to be deposited, although the permissible hydrogen ion concentration will be conditioned by the hydrogen overvoltage. Second, it must not be too low because the chromic ion is easily hydrolyzed and, if the film becomes too basic, oxides or basic compounds will be deposited. Third, in the reduction of chromic acid large amounts of oxygen are converted to oxygen ions or hydroxyl ions, which must be neutralized by hydrogen ions to prevent the formation of oxides and hydroxides.

If pure chromic acid is electrolyzed at such low current densities that the cathode potential is not sufficient to cause hydrogen evolution, the cathode film will have a higher hydrogen ion concentration than the solution. Under these conditions true undissociated mole-

cules of chromic acid can exist close to the cathode and may be reduced directly by the electrons to the trivalent state. The formation of metallic chromium is possible but improbable with the acidic conditions obtaining.

If the cathode potential and current density are raised so that hydrogen is discharged the conditions are vastly different. The hydrogen ion concentration in the cathode film tends to drop very rapidly on account of the tremendous migration velocity of the hydrogen ion within the film. The decrease in hydrogen ion concentration is favorable to the deposition of chromium, especially as large amounts of trivalent chromium must have been formed before this condition could arise. Reactions, 1, 2, and 3 show that the direct reduction of chromic acid will be tremendously affected by a variation in the hydrogen ion concentration. This leads to the conclusion that with increasing current density the chromic-chromous couple becomes the dominant process in effecting the reduction of chromic acid. This couple consists of having chromic ion reduced at the cathode to the chromous ion, which on escaping into the body of the solution reduces chromic acid to trivalent chromium. There is no justification for the suggestion that cathodic reduction is effected by atomic hydrogen. Such a process is in direct conflict with thermodynamic principles.

It has been shown above that when this system attains a hydrogen ion concentration of 10^{-3}, a sol of the basic chromium chromate, $Cr(OH)_3 \cdot Cr(OH)CrO_4$, exists. This sol and any other form of the colloid are probably permeable to hydrogen ions, in view of the fact that in migration and diffusion the radius of the bare hydrogen ion is effective and not that of the hydrated or hydronium ion. The chain theory (30) of the abnormally high migration velocity of the hydrogen ion indicates that although the colloid may permit hydrogen ions to pass through, it will hamper their motion. By this action the portions closer to the cathode will possess a still lower hydrogen ion concentration.

The amount of the colloid formed and the particle size will vary inversely, whereas the electrophoretic velocity will vary directly as the hydrogen ion concentration. The Brownian movement of the dispersoid of the sol, and hence the permeability of the sol, is greatest at the highest hydrogen ion concentration consistent with its existence. However, the high electrophoretic velocity under these conditions favors the formation of the colloidal layer, which would tend to exclude all ions but hydrogen and thus prevent reduction. As shown elsewhere in this paper the amount of colloid varies very rapidly with the hydrogen ion concentration, whereas the electrophoretic velocity does not vary in the range probably involved. No change in conditions is to be expected by varying the hydrogen ion concentration in the cathode film by means of the current density. It appears from this analysis that the formation of the objectionable colloidal layer is a precipitative effect and that any explanations of the beneficial action of the sulphate on the basis of a similar effect is illogical.

4. ACTION OF NEGATIVE IONS, SUCH AS SULPHATE

Müller's first theory that the sulphate coagulates the colloid and thus destroys the colloid layer is untenable because the resultant precipitate would probably hinder the reduction as completely as the

original sol. He abandoned this view in favor of one which states that the particles of the sol tend to arrange themselves in a more or less regular manner on the surface of the cathode. In consequence, there will be spaces with a certain average size through which relatively small negative ions may pass. This condition permits the existence of a higher hydrogen ion concentration at the cathode surface and is less favorable to the formation of the colloid.

A number of criticisms have been leveled against the conception of colloids and colloidal layers in chromium deposition. It is important to note that the sol is only a part of the cathode film; though it may under certain conditions constitute almost exclusively a definite section of it; that is, the colloidal layer. The colloidal layer and the sol are stable because the cathode film is low in hydrogen ions. The supposed difficulty of the discharged hydrogen breaking up the colloidal layer and destroying the film structure does not exist because the cathodic processes discussed are microscopic and not macroscopic. The rates of the reactions involved are undoubtedly much faster than bubble formation; furthermore, bubble formation would not involve the destruction of the film.

If electrophoretic migration is important in determining the reduction processes, adsorption is also. Since the sol is electropositive, the adsorbable ions must be negative. Theories of the structure of the cathode film (31) indicate that close to the cathode there is a paucity of negative ions, because they are repelled by the cathode. This is the most important region, hence means must be found for bringing negative ions into this forbidden territory.

The question naturally arises as to why the dichromate ion, $Cr_2O_7^{--}$, is ineffective (chromate ion, CrO_4^{--}, does not exist at a pH of 3 or 4). Being a negative divalent ion, it could be adsorbed by the sol and thus alter the electrophoretic velocity. It is admitted that this effect does exist in the outer fringes of the film, but apparently not close to the cathode proper. Only high-energy negative ions can penetrate the repulsive barrier and be adsorbed by the electropositive sol. It has been demonstrated above that chromium dichromate does not exist in the green form and hence does not form positive molecular ions like $[Cr(Cr_2O_7)\ (H_2O)_4]^+$, which on account of their nonreactive nature would be able to penetrate the film. Even if it were so conveyed, the dichromate would be reduced at the cathode and hence become ineffective. An effective addition agent must be nonreducible. The nonexistence of the "green" form of the dichromate favors, however, the formation of oxide-free deposits.

The action with the sulphate is vastly different. In consequence of its small size and high charge it will be readily adsorbed by the electropositive sol. It readily forms green complexes with trivalent chromium in which the sulphate is in an extremely nonreactive, positive molecular ion, possibly $[Cr_4O(SO_4)_4(H_2O)_n]^{++}$. This ion is capable of passing through the "forbidden" territory with little change. On reaching the cathode surface the ion is reduced so that the chromium is no longer trivalent and the sulphate ion is set free. While still in the cathode film it may either first, reform the green complex (which is improbable at the pH prevailing); second, exist in the free state (a possibility already demonstrated in this paper); or, third, it may be adsorbed by the particles of the sol. This latter action will lower the

electrophoretic velocity, and render the formation of a dense collodial layer improbable. The action of the chloride would be similar. The positive molecular ions that would then be effective are undoubtedly $[CrCl(H_2O)_5]^{++}$ and $[CrCl_2(H_2O)_4]^{+}$.

Evidence of the relative adsorption of ions by basic chromium chromate was obtained in migration experiments reported in Table 10. A suspensoid of the basic chromate, $Cr(OH)_3Cr(OH)CrO_4$, was prepared by grinding a precipitate in a colloid mill until the particles were of the order of 1 μ. The migration apparatus was of the type used by Abramson and Freundlich (16). Electrode effects were rendered negligible by having nonpolarizable electrodes. The electro-endosmose effect was eliminated in the manner advocated by Smoluchowski (8). Relative values only are reported, as absolute measurements were impracticable with the apparatus employed. Either sodium or potassium salts were used.

TABLE 10.—*Relative electrophoretic velocities of basic chromate in the presence of added ions at 25° C.*

Concentration in equivalent per ml×10⁷	SO_4^{--}	CrO_4^{--}	$Cr_2O_7^{--}$	NO_3^-	ClO_4^-	$H_2PO_4^-$	Cl^-	OH^-
0	+0.133	+0.133	+0.182	+0.133	+0.133	+0.133	+0.170	+0.173
1	+.122	+.120						
4								+.089
5	+.067	+.040						
8								+.050
10			+.100				+.106	
12								−.067
16								−.100
20			+.095					
40			+.076					
50	+.010	−.092					+.048	
100							+.009	
150			+.073					
200			+.050					−.204
500	±.000	−.127		+.095	+.130	+.099	±.000	
1,000	−.038	−.130		+.084	+.127	+.077		

It is obvious that three ions are outstanding in their adsorption; namely, the sulphate, chromate, and hydroxide. The effects of the latter two ions are undoubtedly specific, since we are dealing with a basic chromate. At a pH of 3 or 4 neither chromate nor hydroxide ions can exist in significant concentrations, hence they are unimportant in the cathode film. The dichromate and the chloride are adsorbed to about the same extent, but only the chloride is an effective addition agent. This difference must be due to the fact that the green form of chromic chloride exists, whereas that of chromic dichromate does not. The perchlorate ion is much less adsorbed than the nitrate or phosphate.

pH measurements with the glass electrode were made on solutions with hydroxide additions. It was established that the isoelectric point occurred at a pH of about 6. The maximum electropositive velocity was attained at a pH of 4.5 and remained constant with a further decrease in pH. The maximum electronegative velocity was attained at 7 and did not change with a further increase in pH.

5. CONCLUSIONS

(*a*) The processes of reduction at low and high current density are different.

(*b*) Metal deposition from the chromic acid bath depends on maintaining a definite pH in the cathode film.

(*c*) At high current densities pure chromic acid can not be reduced owing to the formation of a colloidal layer.

(*d*) The action of the sulphate is to lower the electrophoretic velocity of the particles of the sol and thus render the formation of a dense adherent layer improbable.

(*e*) The sulphate is effective because it is a negative ion that is nonreducible and strongly adsorbable, and that forms positive molecular ions with trivalent chromium.

V. APPLICATIONS OF THE PROPOSED THEORY

The utility of the proposed theory was tested by explaining the principal known facts of chromium deposition, and by making predictions that were verified experimentally. The data used in these considerations were derived principally from the curves of Haring and Barrows (17) and of Farber and Blum (25), whose experimental conditions were clearly defined. These data refer chiefly to the 2.5 *M* solutions of chromic acid.

1. The sulphate ion is the most effective addition agent tried. This is to be expected in view of the fact it forms positive molecular ions with trivalent chromium and that it is highly adsorbed by the basic chromate.

2. The effect of the sulphate is independent of the form in which it is added. This follows from the theory which involves only the sulphate ion or its complex with trivalent chromium.

3. A low concentration of sulphate is effective. This is in accordance with adsorption phenomena and with the migration experiments recorded in this paper.

4. The curve for the sulphate concentration versus the cathode efficiency passes through a maximum. The increase in the cathode efficiency up to the maximum represents the favorable effect of the sulphate in preventing the formation of a dense colloidal layer on the cathode. Beyond the maximum the adsorption is so great as to produce excessively large colloidal particles with a sluggish Brownian movement. This feature decreases the permeability and hence the efficiency. At the isoelectric point a colloidal layer is formed through precipitation. The deposits produced with excess sulphate are usually nonadherent, owing probably to the precipitated colloid. The beneficial action of the sulphate occurs on the positive side of the isoelectric point.[7]

5. At higher current densities the curve for the sulphate concentration versus the cathode efficiency becomes flatter. This is because at the higher current densities more colloid is formed and the effect of a given increase in sulphate content is proportionally less.

6. At higher temperatures the sulphate content is less critical, as was shown by Willink (32). This is because the sulphate is then not so strongly adsorbed, which tends to make the curve of current

[7] Compare Frölich (15).

efficiency versus sulphate concentration broad and similar to that obtained with the fluoride at lower temperatures. A higher concentration of sulphate is probably necessary in order to realize the maximum efficiency.

7. The curve for fluoride concentration versus cathode efficiency has a long flat maximum, in contrast to the sharp maximum of the sulphate curve. The adsorption of the divalent sulphate ion will be much greater than that of monovalent ions, such as fluoride and chloride. No electrophoretic measurements were made on the effect of the fluoride, but it is probably simular to that of the chloride. On this basis the difference in behavior can be explained.

8. The acetate ion is ineffective. Acetates and other organic anions do not form green chromic complexes.

9. The nitrate ion is ineffective. Carvath and Curry (1) reported that it produces black deposits with low efficiencies. The nitrate does not form green complexes under the conditions that obtain in these solutions and is not readily adsorbed by the sol.

10. According to Müller phosphates are completely ineffective. While the dihydrogen phosphate ion is adsorbed at least as much as the nitrate, chromium phosphate is very insoluble at the pH of the cathode film.

11. Perchlorate is ineffective according to Müller's polarization curves. As this is a stable radical it would appear ideal according to the theories of Haring, Ollard, and Piersol. However, the green form of chromium perchlorate does not exist, and the perchlorate ion is only slightly adsorbed; hence, according to the theory presented in this paper, it is ineffective. This was confirmed by numerous experiments. In all cases a brown powder or no deposit was obtained and the metal efficiencies were very low (compare (33)). The solutions contained 2.5 *M* CrO_3 and from 0.1 to 1 *M* $HClO_4$, the current densities ranged from 10 to 50 amp./dm^2, and the temperature was 45° C.

12. Pure chromic acid can be reduced to trivalent chromium at low but not at high current densities. This is because at low current densities the chromium compounds have access to the cathode, while at high current densities the semipermeable colloidal layer prevents reduction.

13. As the concentration of chromic acid is increased, the cathode efficiency is decreased. In view of the fact that the chromic ion is less readily reduced and slower than the hydrogen ion, the hydrogen ion concentration in the cathode film will be the most sensitive factor dependent on the rate of supply. With a greater concentration of acid in the body of the solution, the hydrogen ion concentration in the film will be greater, and hence the efficiency will be less.

14. The cathode efficiency does not change greatly if the acidity is decreased by neutralizing part of the chromic acid with alkali. This conclusion (Farber and Blum) is in apparent contradiction with No. 13. The two cases are not strictly comparable. In this case the slower and less reducible positive ion (sodium) would permit a larger concentration of dichromate ions to exist in the cathode film, and cause an even lower hydrogen ion concentration than would be expected on the basis of lowering the free acid. Apparently what occurs is that this condition favors the formation of excessive amounts of the colloid, which

counteracts the increase in efficiency due to lowering the hydrogen ion concentration.

15. At 25° C. the bright plating range is decreased by an increase in the trivalent chromium content (18). This behavior is readily explained by the theory. It was also predicted that this effect could be counteracted by an addition of sulphate. The trivalent chromium increases the cathode efficiency, but also increases the colloid formation at the cathode, especially at high current densities. By adding sulphate this effect should be eliminated. This was confirmed by experiments with 2.5 *M* CrO_3 in which the presence of about *N* trivalent chromium required an increase of sulphate from 0.05 *N* to 0.15 *N* to widen the plating range.

16. The cathode efficiency increases with an increase in current density. This is because at the higher current density the hydrogen evolution is greater (absolutely but not relatively) and hence the cathode film becomes less acid, and a higher potential is required for hydrogen evolution, which factor favors a higher efficiency for the reduction of chromic acid.

17. A still further increase in current density produces "burnt" deposits. These contain oxides derived from the hydrolysis of the chromic ion when the hydrogen ion concentration in the cathode film is too low.

18. The cathode efficiency decreases with an increase in temperature. The hydrogen overvoltage decreases with increase in temperature, and hence hydrogen evolution is increased. This effect partially results from the more rapid convection with increasing temperature, which brings a larger supply of chromic acid into the cathode film and increases the hydrogen ion concentration.

19. Although many of the factors that give rise to the widened plating range at higher temperatures are beyond the theory presented, there is one important factor that can be accounted for. The shift of the plating range at higher temperatures to higher current densities is due to the fact that then a higher current density is necessary to yield the intermediate hydrogen ion concentration necessary for chronium deposition.

20. The initial cathode efficiency is highest on metals with the highest hydrogen overvoltage. This feature is strictly beyond the theory, but is consistent with it.

A number of other features of the process have been analyzed by means of the theory and explained. Only those that are regarded as the most outstanding have been reported.

VI. ACKNOWLEDGMENTS

Appreciation is extended to W. Blum for his suggestion of the problem, his ever available assistance, and his able counsel. M. R. Thompson kindly made the pH measurements that disclosed important relationships.

VII. BIBLIOGRAPHY

1. H. R. Carveth and B. E. Curry, J. phys. chem., vol. 9, p. 353, 1905.
2. N. Bjerrum, Z. physik. chem., vol. 59, p. 596, 1907.
3. N. Bjerrum, Z. anorg. chem., vol. 63, p. 140, 1909.
4. R. Abegg, F. Auerbach and R. Luther, Abhandlungen der Deutschen Bunsengesellschaft No. 5 Halle, 1911.
5. A. Hantszch and P. Garrett, Z. physik. chem., vol. 84, p. 321, 1913.

6. G. J. Sargent, Trans. Am. Electrochem. Soc., vol. 37, p. 479, 1920.
7. R. Abegg, Handbuch der Anorganischen Chemie, Band IV, 1921.
8. M. Smoluchowski in Gratz, Handbuch der Elektrizität, Band II, p. 366, 1921.
9. E. Liebreich, Z. Elektrochem., vol. 27, pp. 94, 452, 1921.
10. E. Liebreich, Z. Elektrochem., vol. 29, p. 208, 1923.
11. C. G. Fink, United States Patent, 1581188, 1925.
12. Opt. Soc. Am., vol. 10, p. 169, 1925.
13. H. E. Haring, Chem. Met. Eng., vol. 32, p. 692, 1925.
14. E. Müller, Z. Elektrochem., vol. 32, p. 399, 1926.
15. P. K. Frölich, Trans. Am. Electrochem. Soc., vol. 69, p. 395, 1926.
16. H. Freundlich and H. A. Abramson, Z. physik. chem., vol. 126, p. 25, 1927.
17. H. E. Haring and W. P. Barrows, B. S. Tech. Paper No. 346, 1927.
18. R. Schneidewind, Univ. Michigan Eng. Res. Bull., No. 10, 1928.
19. D. T. Ewing, J. O. Hardesty, and T. H. Kao, Bull. No. 19, Michigan Eng. Exper. Station, 1928.
20. E. Müller and P. Eckwall, Z. f. Elektrochem., vol. 35, p. 84, 1929.
21. E. Müller and I. Stscherbakow, Z. f. Elektrochem., vol. 35, p. 222, 1929.
22. E. A. Ollard, Electroplaters' and Depositors' Tech. Soc., vol. 3, p. 5, 1929.
23. S. Freed and C. Kasper, J. Am. Chem. Soc., vol. 52, p. 2632, 1930.
24. E. Müller and O. Essin, Z. Elektrochem., vol. 36, p. 2, 1930.
25. H. L. Farber and W. Blum, B. S. Jour. Res., vol. 4, p. 27, 1930.
26. H. R. Moore and W. Blum, B. S. Jour. Res., vol. 5, p. 255, 1930.
27. R. J. Piersol, Metal Cleaning and Finishing, vol. 3, p. 207, 1931.
28. R. W. Wyckoff, Structure of Crystals, 2d ed., Chem. Catalogue Co., 1931.
29. L. Pauling, J. Am. Chem. Soc., vol. 53, p. 1396, 1931.
30. M. Huggins, J. Am. Chem. Soc., vol. 53, p. 3190, 1931.
31. R. W. Gurney, Proc. Roy. Soc., vol. 134A, p. 137, 1931.
32. A. Willink, Trans. Electrochem. Soc., preprint 61–5, 1932.
33. E. Müller, Z. Elektrochem., vol. 38, p. 205, 1932.
34. B. Lange, Z. physik. chem., vol. A 159, p. 277, 1932.

WASHINGTON, July 6, 1932.

PHYSICAL PROPERTIES AND WEATHERING CHARACTERISTICS OF SLATE

By D. W. Kessler and W. H. Sligh

ABSTRACT

Tests on 343 samples of slate from the various districts gave the following average values: Modulus of rupture, 11,700 lbs./in.^{2}; modulus of elasticity in flexure, 13,500,000 lbs./in.^{2}; toughness, 0.192; abrasive hardness, (H_a) 7.6; absorption, 0.27 per cent by weight; porosity, 0.88 per cent; bulk density, 2.771; weight per cubic foot, 172.9 pounds. The strength, elasticity, and toughness values given above were obtained on oven-dried specimens tested in the strongest grain direction. Strength determinations on specimens that had been soaked in water for several days showed considerably lower values. The average ratio of the modulus of rupture of soaked specimens to that of dry specimens was 0.69.

The examination of a considerable number of slate shingles which had been in service for periods varying from 12 to 130 years indicated that slate deteriorates mainly from a combination of chemical and physical causes. Slates containing both pyrite and calcite in appreciable amounts are subject to decay due to the conversion of a part of the calcite to gypsum. The increase in molecular volume causes scaling of the surface. Slate shingles exposed on the roof decay more rapidly on the downward surface, which is probably due to the leaching and concentration of gypsum. A similar type of decay can be produced by alternately soaking and drying the slate. The slates which are more subject to this type of weathering can be disintegrated by 40 or 50 cycles of this treatment.

Frost may cause deterioration, but the rate of this action is very slow. Aside from chipping off the scales near the edges already loosened in the trimming process, frost plays a very minor part in slate weathering. However, the freezing of water between shingles which are nailed down tightly may cause breakage.

CONTENTS

	Page
I. Introduction	378
II. General description of slate	378
1. Origin	378
2. Distribution	378
3. Classification	379
4. Cleavage	379
5. Grain	379
6. Texture	380
7. Colors	380
8. Color permanence	380
9. Ribbons	381
III. Factors affecting service	381
1. Service conditions	381
2. Fabrication processes	382
IV. Composition of slate	383
1. Mineral composition	383
2. Chemical	383
V. Physical determinations	384
1. Strength	384
2. Elasticity	389
3. Toughness	390
4. Abrasive hardness	393
5. Absorption	395
6. Porosity	397
7. Specific gravity	399
8. Weights per cubic foot	399
VI. Weathering characteristics	400
1. Weathering processes	400
2. Weathering test procedures	407
VII. Conclusions	410

I. INTRODUCTION

This paper embraces the results of laboratory studies on the commercial slates of this country and is a continuation of the general investigation relating to various types of stone.

The samples were from nine different States, and consist, mainly, of the materials now found on the market. Fifty samples in the form of large blocks and a large number in the form of shingles were collected especially for this work. Results are also given for numerous samples submitted for various Government buildings. Studies of slate weathering were made of shingles taken from buildings representing exposures of from 12 to 130 years.

While the scope of the paper is limited mainly to physical properties, a brief description of the general characteristics and uses of slate is included as an aid in the interpretation of the results.

The cooperation of the National Slate Association, Bangor Slate Association, Pennsylvania Slate Institute, The Structural Slate Co., and many individual producers was of great assistance and is gratefully acknowledged. The Albion Vein Slate Co. supplied samples from each bed in its quarry at a depth from 190 to 240 feet. The tests on these samples indicate the variations in a section across this quarry and may also be applicable to other quarries on the same "vein."

II. GENERAL DESCRIPTION OF SLATE

1. ORIGIN

All slates considered herein are assumed to have been formed from very fine argillaceous silts, originally deposited under water in horizontal beds. These beds were compacted by vertical pressures due to subsequent deposits of other sediments. Finally, horizontal pressures distorted the original beds into folds, some of which are now standing in a vertical position, while others are overturned and are resting in a horizontal position. The dynamic action which caused the folding of the beds also caused further consolidation and, by the aid of heat, a process of recrystallization took place which resulted in a marked change in the mineral constituents. The predominating mineral in slate is found to be mica in the form of fine flakes. These flakes are arranged in parallel order, with the flat faces roughly parallel to the axes of the folds. As the original silts were formed from decomposing igneous rocks, the chemical composition of slate bears some relation to that of the parent rock. The geologic age of the slates ranges from Cambrian to Silurian.

2. DISTRIBUTION

Although slate deposits are known to exist in 17 States, it is now being produced in only 5 or 6. The latest statistics indicate that 95 per cent of the roofing slate is supplied by Vermont, Pennsylvania, and Virginia. A large portion of the slate from Maine is used in electrical equipment. The Vermont-New York region supplies red, green, and purple slates for roofing, electrical, and structural purposes, as well as some dark and gray varieties for roofing only. Pennsylvania also produces a large amount of structural and blackboard slate, as well as a considerable quantity for electrical purposes.

3. CLASSIFICATION

Slate is broadly classified under the headings of mica, clay, and igneous slates. A mica slate is one formed from clay sediments, but the process of metamorphism is so complete that the clay content is very small. A clay slate is one in which clay still exists in appreciable quantities, while an igneous slate is one resulting from the metamorphism of a ledge of igneous rock. All materials included in this report are classified as mica slates. The slates of this country have sometimes been subdivided into fading and unfading varieties; but due to the misconceptions arising from such terms and difficulties involved in defining such terms, this phase of the subject will be discussed under a separate heading.

4. CLEAVAGE

The distinguishing characteristic of slate is its fissility. Most types of rock may be split more easily in one direction than in another, but in no other type is this property so prominent as in slate. The plane of splitting is commonly called the cleavage plane. Cleavage is evidently due to the parallel arrangement of the mica flakes and the elongation of other mineral constituents in the same general direction. As may be expected, the flattening of the mineral particles occurred on the sides exposed to the greatest pressure and the elongation in the direction of least resistance. The horizontal thrust which caused the folding of the original beds also caused the parallel arrangement of minerals; hence the cleavage is found to make various angles with the original direction of bedding, depending on the part of the fold being considered. At either the apex or trough of a fold the cleavage is commonly perpendicular, while on the sides of the folds it is roughly parallel to the bedding. Not all deposits of slate are as simple as the case just described, and it can not be definitely claimed that horizontal pressures are necessary for the formation of slate. Probably the only necessary conditions are pressures from two opposite directions on a clay stratum with a limited degree of freedom to flow or yield in some other direction. The direction of yielding will determine the cleavage.

5. GRAIN

A slab of slate having its broad faces parallel to the cleavage can be broken transversely in one direction more readily than at right angles to this direction. This direction of easiest breaking is called the "grain," and is caused by the arrangement of the minerals. This feature is assumed to be due to a greater elongation of the mineral in the grain direction than at 90°.

The grain or "sculp" of slate is advantageous in quarrying processes. Mill blocks, or pieces taken from the quarry in convenient size for handling, commonly have the largest faces in the cleavage planes, the next largest in the grain direction, and the least across grain. Likewise in the finished product, when in the form of rectangular slabs, the largest, next largest, and smallest faces will bear the same relation to the cleavage, grain, and cross-grain directions.

There are various ways of determining the grain direction in slate. Slate workers usually resort to the hammer and ascertain the easiest breaking direction in a slab. A means proposed by Jannetaz [1]

[1] Jannetaz, E., Memoire sur les clivages des roches et sur leur reproduction. Soc. Geol. France, Bul. 3d ser., vol. 12, p. 211, 1884.

depends on an assumed difference in thermal conductivity parallel and perpendicular to the grain. This means has not proven very satisfactory as applied to the slates of this country. A method used with considerable success in this study is as follows: A square slab of slate is laid on an asbestos mat with a hole in the center of the latter about 1 inch in diameter. The flame of a Bunsen burner is applied directly to the slate surface through the hole. In a few seconds the slate will usually break in the grain direction.

6. TEXTURE

The term "texture" is commonly used by geologists, and mineralogists in describing the state of aggregation of mineral components in rocks. This term in the slate trade has come into a somewhat more restricted use in describing the character of the split surface. A slate which presents a rough cleavage surface when split in the usual way is said to have more "texture" than one that splits evenly. Within recent years architects have often shown a preference for what they call "textural roofs." By using the rougher splitting slates in various sizes and thicknesses they obtain what is designated as "roof texture."

7. COLORS

The prevailing color of slates now being produced in Maine, Pennsylvania, and Virginia is dark gray with slight tinges of blue, green, or occasionally brown. Generally the slates from Maine and Virginia present a somewhat darker appearance than the Pennsylvania slates, although the Peach Bottom slates from Maryland and certain beds from Pennsylvania are quite dark. That known as "gray bed" from Pennsylvania, representing a minor part of the total production of that slate, is gray with a tinge of green. The production of red, green, and purple slate is now mainly limited to the Vermont-New York region. A purple slate was once worked in Maryland. Black, red, and green slate deposits occur in Arkansas, and green slates are now being worked to some extent in Georgia and Tennessee.

8. COLOR PERMANENCE

The apparent fading which occurs in some of the dark-gray slates seems to be due to an efflorescence of calcium sulphate which partially conceals the true color. During rains, when a slate roof is wet, such fading effects are not apparent, although the same roof may show considerable fading when dry. The source of the calcium sulphate will be discussed under the heading "Weathering processes."

Some of the dark-gray varieties change to a rusty color after a period of exposure. This appears to be due to decomposition of the sulphides of iron in the slate. The first change is probably the formation of sulphate of iron, which is finally oxidized on the exposed surface.

Some of the green varieties of slate also change to buff or rusty brown after a few months of exposure. Such slates have been called "sea green" or "weathering green" slates. This change has been ascribed to the conversion of finely divided particles of iron carbonate to the oxide.

The red, most of the purple, and some of the green varieties undergo no appreciable change of color during long periods of exposure.

As no satisfactory laboratory test for color permanence has been developed, it has been the practice to rely on past experience with the various deposits. Generally those slates which are low in carbonates undergo the least color changes.

9. RIBBONS

Bands of different color, texture, and composition in slate are commonly called "ribbons." The most common ribbons are darker in color than the main part of the slate and vary in width from a fraction of an inch up to several inches. Ribbons follow the original bedding planes of the clay deposits and represent periods of accumulated coarse particles in the sediments. The dark color is due to carbonaceous matter. Such ribbons are usually more absorptive and contain more calcite than the clear part of the slate. Fresh slate containing these ribbons usually shows no appreciable difference in strength whether broken through a ribbon or through the clear part. On account of having coarser particles of quartz the ribbon offers more resistance to cutting or grinding than other parts of the material. The cleavage surface is more uneven and is often deflected somewhat at the ribbon.

Fading effects as mentioned in section 8 above are more common along ribbons, and generally this part is less durable than the clear portion when exposed to the weather.

III. FACTORS AFFECTING SERVICE

1. SERVICE CONDITIONS

Since the most extensive use of slate is for roofing purposes, the foremost point of concern is durability. A roofing material is obviously exposed to the most severe weather conditions. Roof temperatures may often reach 140° F., and the exposure offers no protection against the lowest winter temperatures. Moisture, ice, snow, and hail all contribute to the severe conditions. Wind storms deflect the rafters, and where slates are nailed down too tightly may strain them to the breaking point. Besides the normal weather conditions, slate is exposed to flue gases and the leaching from deposits of soot. Evidently the durability of slate in such exposure depends upon the resistance of the mineral component; hence a study of the composition is important. Strength, elasticity, and density are also important characteristics.

Slate also finds extensive use in the form of heavier slabs for steps, floor tile, window sills, toilet stalls, tubs, sinks, etc. In such uses strength and density are important, but probably the most important property is resistance to abrasion. Where exposed to severe wear, as in floors or steps, the presence of hard veins is undesirable because they cause uneven wear.

For blackboards the material has few competitors. Color and texture are the main considerations. In this use of the material, physical tests afford little information of value.

Electrical slate is limited mainly to the products of those deposits which have high insulating values. A slate of high absorption is not apt to prove satisfactory for this purpose unless it is thoroughly dried and treated with some preparation to prevent the entrance of

moisture. Strength and toughness are important properties, but the final test is that of electrical resistance, and this test it of little value unless applied to the entire panel. The producers of switchboards should have appliances for conducting such tests.

2. FABRICATION PROCESSES

Certain processes used in quarrying and working slate into the finished product may have a bearing on its service. The use of explosives in quarrying is quite general. Considerable waste material results, due to shattering, and it seems inevitable that some of the finished product will contain portions of the injured material.

In splitting slabs from quarry blocks the practice is to separate the block into two equal parts by a middle split. The two halves are then divided into halves and so on until the desired thicknesses are obtained. In roofing slate, where no further finishing of the split face is required, there is necessarily a considerable variation in thickness. Slabs which are to be planed to definite thicknesses, as for structural or electrical purposes, must be split to a thickness considerably greater than the finished piece. Slates with curved cleavage are not suitable for such purposes.

The splitting process is varied somewhat according to the nature of the cleavage. Slates having an easy cleavage are split with a long-handled wedge driven into the block on one of the long edges and used as a lever. Slate blocks somewhat more reluctant to split are separated with one wedge, which is driven in the middle of one end and used as a lever. In the most difficult cases the driving of two or more wedges to start the crack is required, and the final separation is made by forcing a long thin blade, shaped like a spatula, down from one end. In all of these methods there is an unavoidable strain produced which is transverse to the slab and greatest in the weakest direction. Thin roofing slates occasionally find their way into the stacks of marketable material which have partially opened transverse cracks running the long way of the shingles. The presence of such cracks can usually be detected by supporting the shingle on the knuckles of one hand and striking it with a light tool or pencil. If free from cracks it should ring clearly.

Slate shingles are usually trimmed to size, after being split to the desired thickness, by shearing with heavy steel blades. Although this would seem to be a severe treatment for so brittle a material, no very appreciable injury appears to be caused by shearing. However, it probably accounts for the fact that small fragments of slate are often found on the ground near slate roofs. That the slight fracturing near the sheared edge does not affect the durability of the slate is indicated by the fact that decay is more rapid on other parts.

Nail holes are more frequently punched than drilled. Machine punching is usually considered to be more satisfactory than hand punching, although the process is about the same in both. The punch is driven from the side that is to be laid downward. Where the point comes through there is enough chipping around the hole to produce a recess that serves the purpose of countersinking for the nail head. Observations on old shingles seem to indicate that punching is more injurious than the shearing, as decay often begins around the hole before it does on other parts. Some trimming and punching

must be done by the roofer. As this is done under less favorable conditions than at the plant, it is more apt to prove injurious. Furthermore, slate is less brittle when fresh from the quarry than after it has become seasoned.

IV. COMPOSITION OF SLATE

1. MINERAL COMPOSITION

The prevailing mineral in the commercial slates of this country is sericite mica, which accounts for 30 to 40 per cent of its bulk. Next in order is usually quartz or carbonate of lime, although chlorite, kaolin, or carbon is occasionally found to be next in abundance. Pyrite, magnetite, and rutile are usually present, and occasionally talc, hematite, rhodochrosite, zirocon, tourmaline, pyrrhotite, apatite, limonite, and feldspar. These minerals occur as small scales, lenses, or crystals, the greatest dimension of which is generally a small fraction of a millimeter.

2. CHEMICAL COMPOSITION

Chemical analyses made in connection with this study have been confined mainly to weathered slates to determine what changes have occurred. Chemical analyses of various slates have been compiled by Dale in United States Geological Survey Bulletin No. 586. The variations shown for slates from different regions are as follows:

	Vermont	New York	Pennsylvania	Virginia
	Per cent	*Per cent*	*Per cent*	*Per cent*
SiO_2	59 to 68	56 to 68	55 to 65	54 to 62.
Al_2O_3	14 to 19	10 to 13	15 to 22	17 to 25.
Fe_2O_3	0.8 to 5.2	1.5 to 5.6	1.4 to 4.5	7.0 to 7.8.
FeO	2.5 to 6.8	1.2 to 3.8	2.3 to 9.0	
CaO	0.3 to 2.2	0.1 to 5.1	0.2 to 4.2	0.4 to 1.9.
MgO	2.2 to 3.4	3.2 to 6.4	1.5 to 3.8	1.5 to 3.9.
K_2O	3.5 to 5.5	2.8 to 4.4	1.1 to 3.7	
Na_2O	1.1 to 1.9	0.2 to 0.8	0.5 to 3.5	
CO_2	0.1 to 3.0	0 to 7.4	1.6 to 3.7	0.2 to 2.0.

The chemical composition of various minerals occurring in slate as given in textbooks on mineralogy are as follows:

Muscovite	$H_2KAl_3(SiO_4)_3$.
Biotite	$(HK)_2(Mg, Fe)_2(Al, Fe)_2(SiO_4)_3$.
Quartz	SiO_2.
Calcite	$CaCO_3$.
Chlorite (clinochlore)	$H_8(Mg, Fe)_5Al\ Si_3O_{18}$.
Pyrite	FeS_2.
Rutile	TiO_2.
Magnetite	Fe_3O_4.
Tourmaline	R_6SiO_5, R=Al, K, Mn, Ca, Li.
Kaolinite	$H_4Al_2Si_2O_9$.
Siderite	$FeCO_3$.

Due to the complex nature of some of these minerals, it is a very difficult, if not impossible, task to determine the true composition from a chemical analysis. Referring to the molecular formulas given above for the predominating minerals in slate, it is seen that silica (SiO_2) may be ascribed to muscovite, biotite, quartz, chlorite, tour-

maline, or kaolinite; iron oxides (Fe_2O_3 and FeO) to biotite, chlorite, magnetite, or siderite; alumina (Al_2O_3) to muscovite, biotite, chlorite, tourmaline, or kaolinite; lime (CaO) to calcite or tourmaline; magnesia to biotite or chlorite; potassia (K_2O) to muscovite, biotite, or tourmaline; soda (Na_2O) to muscovite; carbon dioxide to calcite or siderite; sulphur (S) to pyrite; titanium (TiO_2) to rutile. Water (H_2O) determined below 110° C. is considered to be present in the form of moisture within the pores, while water determined above 110° C., may form a part of the minerals muscovite, biotite, kaolinite, or one of the chlorite group. Sulphur anhydride (SO_3) is seldom present in appreciable quantities in fresh slate, but in weathered slates it indicates the presence of gypsum ($CaSO2_4H_2O$).

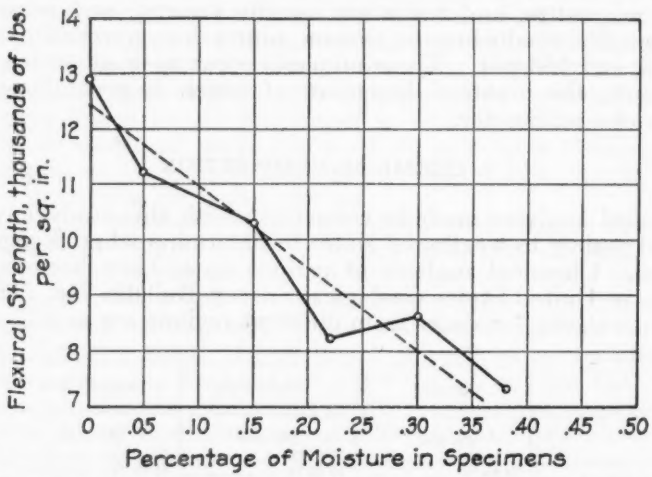

FIGURE 2.—*Relation of flexural strength to moisture content of slate*
Each point on the curve is the average of six strength tests.

V. PHYSICAL TESTS

1. STRENGTH

The flexural strength of slate is commonly determined instead of compressive, tensile, or shearing strength because of facility in preparing the specimens. In this work a specimen 12 inches long, 4 inches wide, and of thickness varying from one-eighth to one-half inch was generally used. These were tested on the apparatus shown in Figure 1. The pieces were supported on knife-edges of the rocker type spaced 10 inches and loaded at the middle through a third knife-edge. Loads were added in 10-pound increments. The strength was computed by means of the modulus of rupture formula $R = \frac{Wl}{bd^2}$ in which W = breaking load, l = length of span, b = width, and d = thickness, the load being in pounds and dimensions in inches.

The strength was usually determined "across the grain"; that is, the long dimension of the specimen was parallel to the grain direction, and hence the fracture was transverse to this direction. Several tests were also made "parallel to the grain" in which the fractural occur-

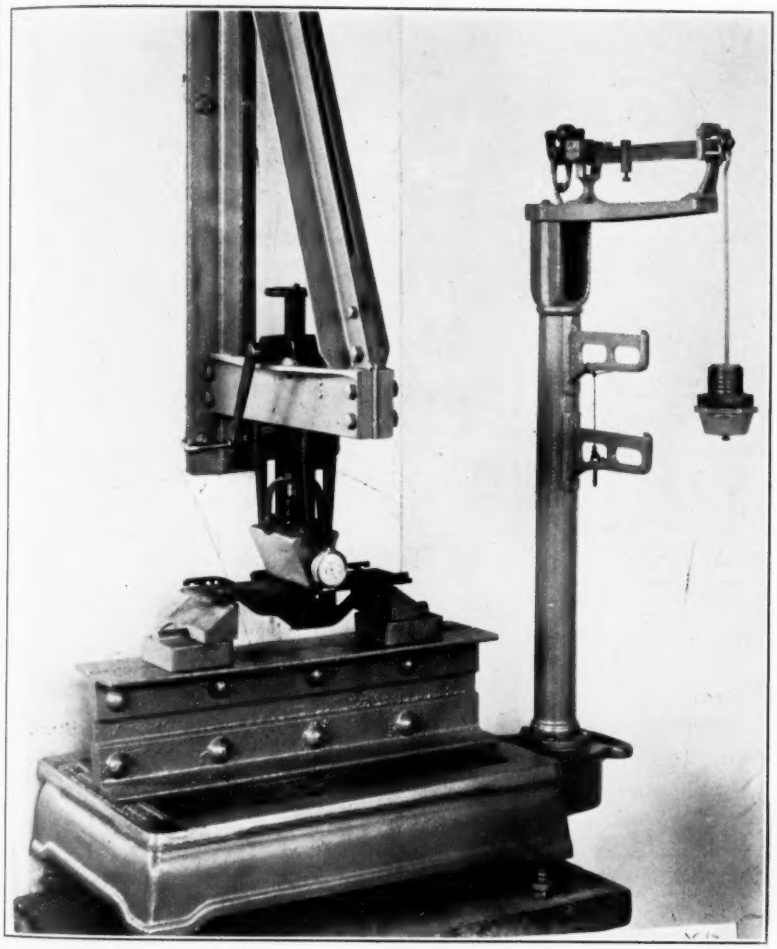

FIGURE 1.—*Apparatus used for determining the flexural strength and elasticity of slate*

UNIV. OF MICH.

red in the grain direction. Results of strength tests on slate in the dry condition are given in Table 1.

The effect of absorbed moisture on the strength was studied by tests on several samples after 14 days' soaking. The pronounced reduction in strength is shown in the last column of Table 2. Figure 2 shows strength determinations on several specimens of one slate tested with various amounts of absorbed water. This shows the importance of drying before the strength test if truly comparative results are desired.

TABLE 1.—*Modulus of rupture—specimens dry*

MAINE SLATES

Serial No.	Number of samples	Number of tests	Modulus of rupture, thousands of lbs./in.²			Source of sample	Variety
			Maximum	Minimum	Average		
1	1	[1]3	10.9	10.0	10.6	Portland Monson Co.	Blue black.
2	2	[1]7	12.1	10.2	11.0	Monson Maine Co.	Do.
	1	[2]3	9.0	7.6	8.3	do.	Do.
3	1	[1]6	15.3	9.8	13.3	Rising & Nelson Slate Co.	Do.

VERMONT-NEW YORK SLATES

4	4	[1]11	15.5	5.3	9.8	Norton Bros.	Sea green.
	2	[2]5	10.3	5.9	7.6	do.	Do.
5	2	[1]4	14.9	12.0	13.9	do.	Silver gray.
	1	[2]3	12.2	9.5	11.1	do.	Do.
6	2	[1]4	14.6	8.4	12.0	do.	Gray and black.
	1	[2]3	12.9	9.5	11.3	do.	Do.
7	2	[1]4	10.2	7.2	8.6	do.	Green and purple.
	1	[2]3	8.7	7.2	8.2	do.	Do.
8	2	[1]4	12.7	10.4	10.8	do.	Unfading green.
	1	[2]3	10.3	8.8	9.7	do.	Do.
9	1	[1]1			10.7	do.	Dark purple.
10	1	[1]2	12.2	11.6	11.9	Wells, Vt.	Green and purple.
13	1	[1]5	11.1	7.7	9.2	J. D. Emack	Colonial gray.
14	1	[1]3	12.3	11.1	11.8	Hydeville, Vt.	Green and purple.
	1	[2]3	9.4	9.0	9.2	do.	Do.
15	1	[1]3	8.4	7.5	7.8	do.	Purple.
	1	[2]2	8.2	7.5	7.85	do.	Do.
16	1	[1]3	13.3	8.6	10.9	do.	Green.
	1	[2]3	9.3	5.6	7.0	do.	Do.
17	1	[1]3	11.0	8.7	10.2	Fair Haven	Green and purple.
	1	[2]3	9.9	6.2	8.4	do.	Do.
18	1	[1]3	12.6	12.0	12.3	do.	Unfading green.
	1	[2]3	8.3	7.3	7.8	do.	Do.
19	1	[1]3	10.5	9.8	10.0	do.	Green and purple.
	1	[2]3	10.1	8.5	9.5		
20	1	[1]3	9.5	8.0	9.0	Granville	"Arabian red."
	1	[2]3	9.7	6.1	8.0	do.	Do.
21	1	[1]3	15.3	15.2	15.2	Poultney	Semiweathering gray.
	1	[2]3	14.2	9.0	12.2	do.	Do.
22	1	[1]2	11.5	11.4	11.4	Rupert, Vt.	Mottled purple.
		[2]3	14.2	9.5	11.1	do.	Do.

PENNSYLVANIA SLATES

HARD VEIN REGION

23	11	[1]44	16.5	10.0	13.8	Chapman	Smooth texture.
	1	[2]3	6.0	4.9	5.4	do.	Do.
24	5	[1]19	16.5	9.0	13.4	do.	Rough texture.
25	1	[1]6	12.7	8.4	10.8	Belfast	Smooth texture.

See footnotes at end of table.

TABLE 1.—*Modulus of rupture—specimens dry*—Continued

PENNSYLVANIA SLATES—Continued

BANGOR REGION

Serial No.	Number of samples	Number of tests	Modulus of rupture, thousands of lbs./in.² Maximum	Minimum	Average	Source of sample	Variety
26	3	[1] 8	16.2	9.6	13.7	Structural Slate Co	Bangor clear.
	3	[2] 5	10.8	6.1	7.8	do	Do.
27	3	[1] 8	14.8	8.2	11.5	do	Bangor ribbon.
	3	[2] 6	9.0	5.5	7.3	do	Do.
28	3	[1] 7	16.0	7.9	12.2	Vendor Slate Co	Bangor clear.
29	2	[1] 6	12.6	11.5	12.1	do	Bangor ribbon.
30	2	[1] 4	16.0	12.9	14.1	Wallace & Gale	Bangor clear.
31	1	[1] 4	14.6	12.3	13.4	Griffith Consumers Co	Do.
32	1	[1] 2	14.3	13.9	14.1	Starrett Equipment Co	Do.
33	6	[1] 18	13.9	9.9	12.2	N. Bangor Slate Co	Do.
	1	[2] 3	8.3	7.3	7.8	do	Do.
34	1	[1] 4	11.2	10.4	10.8	do	Bangor ribbon.
35	1	[1] 4	15.2	12.0	13.8	Bangor Quarry Co	Bangor clear.
36	2	[1] 8	13.8	11.0	12.6	do	Bangor ribbon.
	1	[2] 1			8.1	do	Do.
37	1	[1] 4	12.2	11.1	11.7	Old Bangor Quarries	Bangor clear.
38	2	[1] 10	14.7	10.6	12.9	do	Bangor ribbon.
39	1	[1] 4	12.5	10.4	11.2	Bangor Ideal Quarry	Bangor clear.
40	1	[1] 4	12.1	8.8	10.5	do	Bangor ribbon.
41	1	[1] 4	15.8	13.8	14.6	Columbia Bangor Quarry	Bangor clear.
42	1	[1] 4	16.1	12.6	13.8	do	Bangor ribbon.
43	1	[1] 4	13.1	9.7	11.7	E. Bangor Consolidated	Bangor clear.
44	1	[1] 4	12.4	10.9	11.5	do	Bangor ribbon.

PEN ARGYL REGION

45	8	[1] 31	14.3	8.8	11.7	Jackson Bangor	Deep bed clear.
46	6	[1] 18	12.9	8.6	11.1	do	Albion clear.
	1	[2] 3	11.8	8.4	10.5	do	Do.
47	1	[1] 4	11.9	10.8	11.6	do	Albion black bed.
48	1	[1] 4	12.0	10.0	11.0	do	Albion ribbon.
49	2	[1] 7	13.0	8.5	10.9	Parson Bros	Clear.
	1	[2] 5	11.7	6.4	8.9	do	Do.
50	2	[1] 12	14.1	9.6	11.1	do	Deep bed clear.
51	1	[1] 4	11.1	7.7	10.1	do	Ribbon.
52	54	[1] 212	15.9	6.8	12.0	Albion Vein Slate Co	Blue gray.
	38	[2] 134	12.6	4.6	7.4	do	Do.
52a	6	[1] 22	15.9	9.1	12.7	do	Blue gray, 300-foot level.
53	3	[1] 10	14.0	10.8	12.9	Albion Vein Slate Co	Gray Bed.
	1	[2] 4	8.6	7.8	8.1	do	Do.
54	2	[1] 8	12.1	9.7	11.0	do	Ribbon.
	1	[2] 4	7.9	6.8	7.2	do	Do.
55	1	[1] 2	11.8	11.1	11.4	Keenan Structural Slate Co.	Clear.
56	4	[1] 20	11.5	8.8	10.3	Doney Slate Co	Do.
57	3	[1] 11	11.7	9.1	10.7	Colonial Slate Co	Do.
58	4	[1] 12	11.1	9.0	10.4	Structural Slate Co	Do.
	3	[2] 9	9.5	8.2	8.5	do	Do.
59	4	[1] 12	12.1	9.0	10.6	do	Ribbon.
	5	[2] 16	10.3	7.1	8.0	do	Do.
60	1	[1] 4	13.4	11.2	12.2	do	Gray.
61	2	[1] 3	12.8	9.9	11.0	Vendor Slate Co	Clear.
62	2	[1] 10	14.2	11.3	12.7	Stephens-Jackson	Gray.
63	1	[1] 5	14.3	12.9	13.7	do	Blue gray.
64	2	[1] 6	12.1	10.6	11.4	Belmont Slate Co	Do.

See footnotes at end of table.

TABLE 1.—*Modulus of rupture—specimens dry*—Continued

PENNSYLVANIA SLATES—Continued

WIND GAP REGION

Serial No.	Number of samples	Number of tests	Modulus of rupture, thousands of lbs./in.² Maximum	Minimum	Average	Source of sample	Variety
65	1	[1] 2	11.4	11.3	11.35	Structural Slate Co	Clear.
	5	[2] 14	7.7	5.6	7.2	do	Do.
66	1	[1] 3	12.3	10.4	11.3	do	Ribbon.
	1	[2] 5	8.8	4.8	7.1	do	Do.
67	1	[2] 4	11.0	9.1	10.0	Phoenix Slate Co	Rough texture.
68	2	[1] 12	13.0	10.4	11.0	Imperial Slate Blackboard Co.	Clear.
	1	[2] 3	7.7	6.2	6.8	do	Do.

SLATINGTON REGION

70	2	[1] 4	13.3	11.6	12.4	Franklin Big Bed	Clear.
69	1	[1] 3	10.9	9.8	10.3	Structural Slate Co	Do.
	3	[2] 10	9.2	4.6	6.8	do	Do.
71	1	[1] 2	13.0	11.3	12.15	Vendor Slate Co	Rough texture.
72	5	[1] 17	14.4	9.4	12.1	Washington Big Bed	Clear.
73	2	[1] 5	12.5	9.2	11.7	Slatington Slate Co	Do.
74	2	[1] 7	11.1	9.7	10.4	Kern Slate Co	Rough texture.
75	1	[1] 4	9.7	7.5	8.5	Shenton Slate Co	Clear.

VIRGINIA

76	7	[1] 22	14.2	8.1	10.2	Arvonia	Blue black.
	1	[2] 3	13.3	11.3	12.5	do	Do.
77	7	[1] 19	12.9	7.3	10.6	Ore Bank	Do.
	1	[2] 2	8.2	6.4	7.3	do	Do.
78	1	[1] 3	9.4	5.8	7.5	Esmont	Greenish gray.
	1	[2] 2	2.9	2.8	2.85	do	Do.

MARYLAND

79	1	[1] 3	9.4	5.8	7.5	Ijamsville	Purple.
	1	[2] 2	2.9	2.8	2.85	do	Do.
80	1	[2] 3	4.1	3.4	3.4	do	Green.
81	2	[1] 3	15.4	15.2	15.3	Peach Bottom	Blue black.

TENNESSEE

82	1	[1] 2	10.6	9.2	9.9	Tellico Plains	Green.
	1	[2] 3	10.0	8.5	9.0	do	Do.

GEORGIA

83	1	[1] 3	14.5	7.9	11.0	Fairmont	Green.
	1	[2] 3	8.2	5.7	6.7	do	Do.

ARKANSAS

84	1	[1] 2	6.5	3.4	4.95	Missouri Mountain	Black.
85	3	[1] 13	11.4	5.2	8.1	do	Green.
86	2	[1] 5	7.6	3.7	5.4	do	Red.

[1] Specimens broken across the grain. [2] Specimens broken along the grain.

The remarkably high flexural strength of slate is probably due to its compactness and the reinforcing effect of the mica particles. The difference in strength between the two grain directions indicates the effect of the elongation of the mica flakes in the grain direction. The lubricating action of water in its effect on strength of stone has been emphasized by Julien [2] and by Baldwin-Wiseman and Griffith.[3]

Besides affording a ready means of comparing various slates, the flexural strength is of interest in connection with most of the uses of the material. When slate shingles are nailed down too tightly they may be strained to the breaking point due to wind pressures deflecting the rafters. Breakage of shingles on roofs due to workmen walking on the slate or placing ladders on the roof is an important consideration. The flexural strength is a factor in determining the thickness of slabs for various uses. There appears to be no general relation between the strength and durability of slates from different districts.

TABLE 2.—*Results of modulus of rupture tests—specimens wet*

Serial No.[1]	Number of specimens	Number of tests	Modulus of rupture, thousands of pounds/in.[2]			Ratio wet strength to dry strength
			Maximum	Minimum	Average	
2	1	[2] 3	8.0	7.2	7.7	0.93
14	1	[2] 3	7.4	7.0	7.2	.61
15	1	[2] 3	5.2	3.9	4.7	.60
16	1	[2] 3	10.9	6.2	9.1	.83
17	1	[2] 3	5.9	5.7	5.8	.57
18	1	[2] 3	6.3	4.4	5.1	.42
19	1	[2] 3	7.2	6.0	6.5	.65
20	1	[2] 3	7.4	6.8	7.1	.89
21	1	[2] 3	11.2	9.7	10 6	.89
22	1	[2] 3	9.6	6.6	8.1	.73
29	1	[2] 4	8.8	7.9	8.4	.69
52	38	[2] 141	12.3	4.9	7.7	.66
53	1	[2] 4	11.0	9.1	9.8	.74
54	1	[2] 4	9.1	7.8	8.3	.74
62	1	[2] 5	9.2	6.9	8.1	.66
63	1	[2] 5	9.3	8.2	8.6	.63
76	1	[2] 3	10.5	9.8	10.0	.80
81	1	[2] 3	10.1	9.4	9.8	.64
83	1	[2] 3	13.5	9.9	12.3	1.12

[1] Identification of serial numbers given in Table 1.
[2] Specimens broken along the grain.
[3] Specimens broken across the grain.

The average modulus of rupture and extreme values for slate from various regions obtained by tests on dry specimens broken across the grain are as follows:

District	Number of tests	Average	Maximum	Minimum
Maine	21	11,700	15,300	9,800
Vermont-New York	68	10,600	15,500	5,300
Hard Vein, Pa	73	13,600	16,500	8,400
Bangor, Pa	156	12,500	16,300	7,900
Pen Argyl, Pa	431	11,500	15,900	6,800
Wind Gap, Pa	21	10,900	13,000	8,500
Slatington, Pa	35	11,800	14,400	9,200
Virginia	62	10,500	14,200	6,700

[3] Building Stones, J. Franklin Inst., April, May, and June, 1899.
[4] Minutes of the Proc. Inst. of Civ. Eng., vol. 179, p. 290, 1909.

2. ELASTICITY

The modulus of elasticity in flexure is easily determined in connection with the modulus of rupture test by making deflection measurements at various loads. Determinations in connection with this work were made by suspending the deflectometer shown in Figure 1 from rods laid across the specimen above the supporting knife-edges. The gage used indicated deflections of 0.0001 inch. Usually deflection readings were recorded for each 20 pounds increment of load. The modulus of elasticity, E, was computed by means of the formula

$$E=\frac{W' l^3}{4\Delta b d^3}$$

in which Δ is the deflection corresponding to some chosen load W', and l, b, and d are the same dimensions used in the modulus of rupture test.

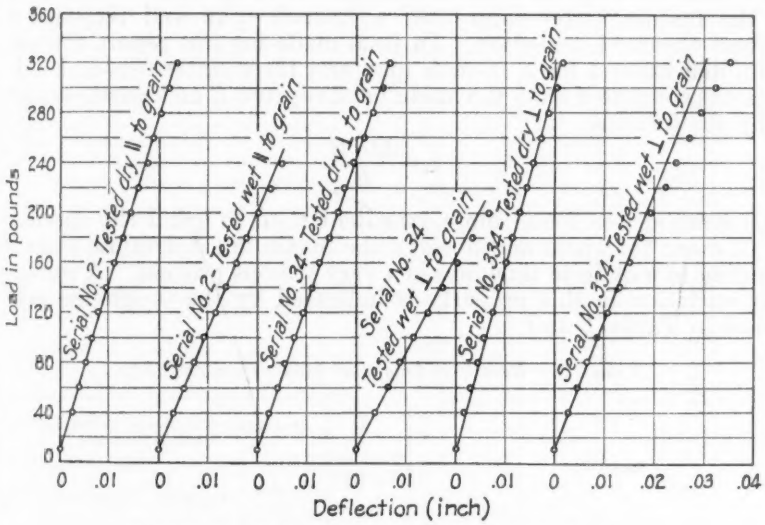
Load in pounds
360
320
280
240
200
160
120
80
40
0
Serial No. 2- Tested dry ∥ to grain
Serial No. 2- Tested wet ∥ to grain
Serial No. 34- Tested dry ⊥ to grain
Serial No. 34 Tested wet ⊥ to grain
Serial No. 334- Tested dry ⊥ to grain
Serial No. 334- Tested wet ⊥ to grain
0 .01 0 .01 0 .01 0 .01 0 .01 0 .01 .02 .03 .04
Deflection (inch)

FIGURE 3.—*Stress-strain curves for slate in flexure*

Figure 3 shows a few stress-strain relations for slate specimens in flexure. In general there is a small deviation from a straight line for loads above half of the breaking load, but no definite yield point is in evidence.

Elasticity determinations have been made in both grain directions on dried specimens and across the grain on several wet specimens. The modulus values are usually somewhat lower for tests on wet specimens, but show no appreciable difference for tests made in different grain directions on dry specimens. The average value of E obtained was 13,500,000, with a maximum of 18,000,000. There appears to be less variation in the E values for slates from different regions than in other properties. The average E and extreme values

determined across the grain on dry specimens for the main producing districts are:

District	Number of tests	Average	Maximum	Minimum
Maine	18	15,100,000	18,000,000	13,100,000
Vermont-New York	63	14,500,000	17,600,000	12,000,000
Hard Vein, Pa	45	15,300,000	16,700,000	13,000,000
Bangor, Pa	129	13,500,000	16,300,000	10,200,000
Pen Argyl, Pa	259	12,900,000	15,900,000	9,800,000
Slatington, Pa	29	13,400,009	15,200,000	11,300,000
Wind Gap, Pa	17	12,400,000	13,800,000	9,800,000
Virginia	56	14,700,000	16,400,000	12,400,000

3. TOUGHNESS

Merriman's test [4] for toughness with slight modifications has been employed in this work. This consists in determing the maximum deflection for a given span and thickness of specimen when loaded in the middle. Merriman used a 22-inch span and recorded the highest observed deflection. In tests made for this report the maximum deflection Δ for a 16-inch span and three-sixteenths-inch thickness was computed from the modulus of rupture R and elastic modulus E by the formula

$$\Delta = \frac{227\ R}{E}$$

This method was found more expedient than to grind the specimens to an exact thickness and observe the maximum deflection, since the grinding to a definite thickness is a very tedious process. A considerable variation in this property is indicated by the toughness values shown in Tables 3 and 4.

TABLE 3.—*Results of toughness tests—specimens dry*

Serial No.[1]	Number of samples	Maximum deflection of 16-inch span and 3/16 inch thickness			
		Number of tests	Maximum	Minimum	Average
			Inch	*Inch*	*Inch*
1	1	[2] 3	0.142	0.125	0.135
2	2	[2] 7	.192	.152	.174
	1	[3] 3	.139	.125	.131
3	1	[2] 6	.245	.159	.200
4	4	[2] 11	.212	.093	.143
	2	[2] 5	.164	.111	.130
5	2	[2] 4	.217	.212	.214
	1	[3] 3	.182	.144	.167
6	2	[2] 4	.226	.153	.193
	1	[3] 3	.202	.146	.174
7	2	[2] 4	.161	.119	.135
	1	[3] 3	.140	.116	.132
8	2	[2] 4	.194	.159	.172
	1	[3] 3	.153	.125	.142
9	1	[2] 1			.187
10	1	[2] 2	.182	.180	.181
13	1	[2] 2	.171	.131	.151

See footnotes at end of table.

[4] Strength and Weathering Qualities of Roofing Slates, Trans. Am. Soc. of Civ. Engrs., No. 551, vol. 27 September, 1892.

TABLE 3.—*Results of toughness tests—specimens dry*—Continued

Serial No.[1]	Number of samples	Maximum deflection of 16-inch span and 3/16 inch thickness			
		Number of tests	Maximum	Minimum	Average
			Inch	*Inch*	*Inch*
14	1	[2] 3	0.197	0.173	0.184
	1	[3] 3	.167	.155	.161
15	1	[2] 3	.117	.108	.111
	1	[3] 2	.130	.121	.126
16	1	[2] 3	.197	.125	.160
	1	[3] 3	.155	.105	.134
17	1	[2] 3	.180	.141	.166
	1	[3] 3	.163	.115	.142
18	1	[2] 3	.213	.204	.209
	1	[3] 3	.134	.117	.125
19	1	[2] 3	.181	.166	.172
	1	[3] 3	.169	.141	.159
20	1	[2] 3	.136	.113	.128
	1	[3] 3	.154	.096	.126
21	1	[2] 3	.230	.226	.228
	1	[3] 3	.208	.147	.184
22	1	[2] 2	.186	.182	.184
	1	[3] 3	.226	.155	.182
23	9	[2] 25	.249	.153	.208
24	4	[2] 10	.232	.154	.198
25	1	[2] 3	.189	.166	.175
26	3	[2] 8	.247	.173	.222
	5	[3] 14	.173	.099	.130
27	3	[2] 8	.233	.141	.187
	3	[3] 6	.166	.092	.122
28	3	[2] 5	.271	.190	.219
29	1	[2] 2	.199	.190	.194
30	2	[2] 4	.254	.237	.246
31	1	[2] 4	.238	.209	.225
32	1	[2] 2	.246	.227	.236
33	6	[2] 18	.223	.168	.197
	1	[3] 3	.148	.127	.140
34	1	[2] 4	.206	.184	.193
35	1	[2] 4	.240	.190	.216
36	2	[2] 8	.219	.189	.203
	1	[3] 1	----	----	.130
37	1	[2] 4	.209	.186	.196
38	2	[2] 7	.222	.172	.204
39	1	[2] 4	.233	.184	.206
40	1	[2] 4	.235	.191	.207
41	1	[2] 4	.231	.196	.212
42	1	[2] 4	.232	.185	.208
43	1	[2] 4	.236	.175	.207
44	1	[2] 4	.238	.198	.220
45	7	[2] 22	.244	.157	.212
46	11	[2] 33	.244	.160	.206
	1	[3] 3	.184	.137	.166
47	1	[2] 4	.218	.195	.210
48	1	[2] 4	.211	.189	.200
49	1	[3] 5	.205	.115	.160
50	2	[2] 12	.254	.170	.210
51	1	[2] 4	.195	.139	.179
52	47	[2] 104	.248	.127	.207
	1	[3] 2	.148	.138	.143
53	1	[2] 2	.250	.202	.226
54	2	[2] 6	.207	.174	.197
55	1	[2] 2	.202	.188	.195
56	3	[2] 10	.221	.177	.198
57	3	[2] 6	.211	.182	.199
58	4	[2] 12	.206	.161	.190
	3	[3] 8	.208	.139	.157
59	4	[2] 12	.220	.168	.193
	5	[3] 16	.179	.122	.152
60	1	[2] 2	.204	.187	.196

See footnotes at end of table.

TABLE 3.—*Results of toughness tests—specimens dry*—Continued

Serial No.[1]	Number of samples	Maximum deflection of 16-inch span and 3/16 inch thickness			
		Number of tests	Maximum	Minimum	Average
			Inch	*Inch*	*Inch*
61	2	[2] 3	0.211	0.191	0.201
62	2	[2] 6	.222	.183	.196
63	1	[3] 3	.219	.208	.213
64	2	[2] 6	.222	.191	.208
65	1	[2] 2	.195	.186	.190
	5	[3] 15	.140	.112	.122
66	1	[3] 3	.207	.182	.194
	1	[3] 3	.143	.103	.119
67	1	[3] 4	.211	.188	.200
68	2	[2] 8	.227	.151	.197
	1	[3] 3	.149	.123	.134
69	1	[3] 3	.180	.159	.169
	3	[3] 9	.163	.102	.122
70	2	[2] 2	.229	.199	.214
71	1	[2] 2	.224	.196	.210
72	4	[3] 11	.226	.160	.190
	1	[3] 3	.155	.146	.150
73	2	[2] 5	.229	.151	.206
74	2	[2] 7	.223	.178	.196
75	1	[2] 4	.193	.151	.169
76	7	[2] 22	.200	.130	.162
	1	[3] 3	.189	.153	.175
77	6	[3] 16	.198	.142	.170
78	1	[2] 3	.130	.110	.123
	1	[3] 2	.125	.110	.118
79	1	[2] 3	.158	.132	.144
	1	[3] 2	.103	.076	.090
80	1	[3] 2	.102	.092	.097
81	1	[2] 3	.198	.189	.193
	1	[3] 3	.137	.099	.123
82	1	[3] 2	.185	.162	.174
	1	[3] 3	.183	.149	.166
83	1	[2] 3	.180	.104	.140
	1	[3] 3	.136	.096	.113
84	1	[3] 1	----	----	.164
85	3	[2] 12	.160	.101	.137
86	2	[2] 5	.230	.084	.130

[1] Identification of serial numbers given in Table 1.
[2] Specimens broken across the grain.
[3] Specimens broken along the grain.

The average and extreme values from tests across the grain on dry specimens for various regions are:

District	Number of tests	Δ Average	Δ Maximum	Δ Minimum
Maine	18	0.178	0.245	0.125
Vermont-New York	63	.163	.230	.093
Hard Vein, Pa	45	.204	.249	.153
Bangor, Pa	125	.205	.271	.141
Pen Argyl, Pa	263	.205	.250	.127
Wind Gap, Pa	17	.196	.227	.151
Slatington, Pa	29	.197	.229	.151
Virginia	56	.164	.200	.106

TABLE 4.—*Results of toughness tests—specimens wet*

Serial No.[1]	Number of samples	Maximum deflection of 16-inch span and 3/16 inch thickness			
		Number of tests	Maximum	Minimum	Average
			Inch	*Inch*	*Inch*
2	1	[2] 2	0.126	0.120	0.124
14	1	[2] 3	.136	.131	.134
15	1	[2] 3	.089	.065	.080
16	1	[2] 3	.180	.131	.161
17	1	[2] 3	.134	.126	.130
18	1	[2] 3	.127	.090	.105
19	1	[2] 3	.150	.118	.131
20	1	[2] 3	.132	.121	.125
21	1	[2] 3	.183	.165	.176
22	1	[2] 3	.172	.113	.143
52	33	[2] 68	.202	.114	.168
53	1	[2] 2	.192	.169	.180
54	1	[2] 2	.185	.172	.178
62	2	[2] 4	.176	.132	.152
63	1	[2] 2	.184	.170	.177
76	1	[2] 3	.151	.140	.146
81	1	[2] 3	.180	.167	.172
83	1	[2] 3	.176	.127	.160

[1] Identification of serial numbers given in Table 1.
[2] Specimens broken along the grain.
[3] Specimens broken across the grain.

This test is of value in showing the flexibility of the material. Other properties being equal, a slate of high toughness is less apt to break under a given strain than one of lower toughness. This property is sometimes used as a specification requirement.

4. ABRASIVE HARDNESS

The apparatus used in determining the abrasive hardness values given in Table 5 is described in detail in the Proceedings of the American Society for Testing Materials, volume 28, part 2, 1928, pages 855–867. The result is expressed as a reciprocal of the volume abraded under controlled conditions in a given period of time. The specimens, which were 2 inches square and 1 inch thick, were weighed and subjected to the abrading process, after which they were weighed again. By means of the apparent specific gravity of the material the weight loss is converted to volume, since this gives a more definite basis of comparison. The reduction formula is

$$H_a = \frac{10\ (2{,}000 + W_s)G}{2{,}000\ W_a}$$

in which W_s is the weight of the specimen, G the apparent specific gravity, and W_a the loss of weight by abrasion. The constant load on the specimen during the grinding is 2,000 G which is augmented by the variable weight of the specimen. In applying the correction for the weight W_s the average of the original and final weights is used. The reciprocal relation is used in order to give values in conformity with the usual conceptions of hardness; that is, low values for soft materials and higher values to harder materials. The factor 10 in the numerator is used arbitrarily to avoid values less than unity for soft materials.

TABLE 5.—*Results of abrasive hardness tests*

Serial No.[1]	Number of samples	Hardness values (H_a)			
		Number of tests	Maximum	Minimum	Average
1	1	3	9.4	8.8	9.1
2	1	5	9.8	9.3	9.6
4	1	5	8.0	7.6	7.7
5	1	5	7.8	7.2	7.5
6	1	5	7.2	7.0	7.1
7	1	6	15.2	7.4	11.7
8	1	6	7.6	7.2	7.4
14	1	5	8.5	7.6	8.0
15	1	5	9.0	6.9	8.3
16	1	6	8.1	7.0	7.6
17	1	6	9.2	8.8	9.0
18	1	6	8.7	8.1	8.3
19	1	4	8.9	7.4	7.9
20	1	3	12.2	11.0	11.8
21	1	5	7.9	7.5	7.7
22	1	5	7.3	6.7	6.9
23	1	[2] 6	9.3	8.1	8.7
26	3	9	7.2	6.8	6.9
55	1	5	7.2	5.8	6.5
58	2	12	7.2	6.3	6.8
59	2	[3] 15	7.2	6.2	6.6
65	4	12	6.4	5.6	6.0
66	2	[2] 6	7.2	6.5	6.9
69	2	6	5.8	5.5	5.6
76	1	5	12.2	9.9	10.9
81	1	3	5.7	5.5	5.6
83	1	5	8.9	7.9	8.4

[1] Identification of serial numbers given in Table 1.
[2] All specimens contained ribbons.
[3] Nine specimens contained ribbons.

A comparison of the H_a values in Table 5 with the service records of various slates shows considerable evidence that hardness is directly proportional to durability. However, the very low H_a value for one slate, which has so thoroughly established its good weathering quality by long service, can be cited to prove that no general relation between hardness and durability exists.

The range in hardness values for slates from different districts was not found to be as great as for other materials of a given type, as marble, limestone, etc. The average and extreme H_a values for various regions were as follows:

District	Number of tests	H_a average	H_a maximum	H_a minimum
Maine	8	9.4	9.8	8.8
Vermont-New York	72	8.3	15.2	6.7
Hard Vein, Pa	9	8.2	9.3	7.0
Bangor, Pa	6	6.8	7.0	6.8
Pen Argyl, Pa	32	6.7	7.2	5.8
Wind Gap, Pa	18	6.3	7.2	5.6
Slatington, Pa	6	5.6	5.8	5.5
Virginia	5	10.9	12.2	9.9

The dark "ribbons" in the slates from Pennsylvania are usually more resistant to abrasion than the parts of the slate free from ribbons. According to Dale [5] and Behre,[6] this is due to the presence of coarser quartz particles in the ribbons.

The abrasive hardness of the material is of interest in cases where it is to be used in floors, steps, sills, sinks, table tops, etc., but probably has no significance in connection with roofing slate.

5. ABSORPTION

The absorption test is frequently used in roofing-slate specifications, and there appears to be a relation between absorption values and weathering qualities. The values given in Table 6 were determined on slabs from 4 to 6 inches square and from three-sixteenths to one-fourth inch thick. These were dried at 100° C. for 24 hours for the dry weight, and then completely immersed in water at room temperatures for 48 hours. Absorption results are given in percentage by weight, which were determined by dividing the weight of water absorbed by the weight of the dry specimen. The weight ratio is commonly used in specification tests, but the volume ratio is a more definite means of comparison. The errors arising from the use of the weight ratios are not as great for slate as for most other materials, since the variation in "bulk density" from one slate to another is comparatively small.

TABLE 6.—*Results of absorption tests*

Serial No.[a]	Number of samples	Absorption by weight			
		Number of tests	Maximum	Minimum	Average
			Per cent	*Per cent*	*Per cent*
1	1	9	0.08	0.05	0.06
2	2	7	.06	.02	.03
3	1	3	.04	.03	.04
4	4	26	.20	.06	.12
5	2	8	.11	.07	.09
6	2	8	.29	.08	.11
7	2	17	.23	.09	.13
8	2	8	.20	.11	.12
9	1	2	.17	.17	.17
10	1	2	.30	.29	.30
11	1	1			.25
12	1	1			.42
13	1	4	.15	.09	.11
14	1	6	.15	.12	.14
15	1	12	.18	.09	.12

[a] Identification of serial numbers given in Table 1.

[5] U. S. Geological Survey Bulletin No. 586.
[6] Slate in Northampton County, Pa., Bul. M9, Topographic and Geologic Survey of Pennsylvania, 1927.

TABLE 6.—*Results of absorption tests*—Continued

Serial No.	Number of samples	Absorption by weight			
		Number of tests	Maximum	Minimum	Average
			Per cent	*Per cent*	*Per cent*
16	1	9	0.18	0.14	0.16
17	1	6	.12	.11	.11
18	1	6	.14	.10	.12
19	1	6	.14	.12	.13
20	1	12	.15	.07	.12
21	1	5	.06	.05	.06
22	1	4	.13	.12	.13
23	10	43	.37	.10	.15
24	5	15	.20	.12	.15
25	1	4	.26	.21	.24
26	5	54	.35	.14	.18
27	3	34	.37	.11	.17
28	1	3	.35	.33	.34
29	1	4	.67	.58	.60
30	1	3	.27	.25	.26
31	1	4	.40	.29	.33
33	4	24	.43	.16	.26
34	1	4	.45	.43	.44
35	1	4	.30	.28	.29
36	2	12	.31	.23	.26
37	1	4	.44	.33	.38
38	2	10	.44	.24	.32
39	1	4	.34	.31	.32
40	1	4	.42	.31	.35
41	1	4	.23	.21	.22
42	1	4	.32	.28	.30
43	1	4	.33	.25	.30
44	1	4	.40	.35	.38
45	6	27	.38	.24	.30
46	10	57	.39	.11	.24
47	1	8	.50	.45	.47
48	1	7	.33	.29	.31
49	3	22	.46	.26	.36
50	2	13	.32	.26	.28
51	1	8	.32	.29	.30
52	53	244	.48	.19	.31
52a	6	34	.32	.19	.25
53	3	16	.21	.17	.19
54	2	12	.50	.27	.41
55	1	2	.32	.21	.26
56	4	28	.57	.26	.44
57	3	11	.56	.43	.50
58	5	61	.32	.20	.23
59	6	81	.34	.21	.25
60	1	4	.21	.19	.20
61	2	8	.49	.19	.44
62	2	12	.14	.10	.12
63	1	6	.21	.18	.20
65	4	35	.47	.28	.38
66	3	33	.43	.23	.34
67	1	8	.46	.42	.45
68	2	15	.58	.51	.54
69	3	40	.35	.21	.26
70	1	2	.20	.17	.18
71	4	25	.42	.19	.31
72	2	6	.45	.35	.41
73	2	14	.36	.30	.34
74	1	8	.93	.89	.91
75	3	21	.04	.00	.01
76	1	2	.03	.02	.02
77	1	13	.18	.13	.15
78	1	14	1.63	1.23	1.41
89	1	6	1.31	1.01	1.13
80	1	6	.21	.18	.20
81	1	4	.28	.25	.27
82	1	12	.13	.08	.10
83	1	4	.59	.54	.57
84	3	14	.55	.33	.40
85	2	6	1.54	1.09	1.27

A study of the relations between absorption and certain other properties of slate has been made by computing the correlation coefficients. A high degree of correlation would be expected to exist between absorption and porosity, but the correlation coefficient obtained for the results of these determinations was $r=0.70$. Two factors may be expected to influence this relation—first, the rate of absorption and, second, mineral composition. A better correlation between these properties might be obtained by determining the absorption values for a longer period of immersion and using the volume ratio instead of the weight ratio. The loss of strength due to soaking in water suggests that there may be a relation between the amount of water absorbed and the strength loss; however, the computation of the correlation coefficient for these values gave $r=0.25$, which indicates a very small relationship. In the acid tests, to be described below, the decay is caused by converting the particles of calcite to gypsum. Since the measurements are based on the depth below the surface to which the decay occurs, one might expect a relation to exist between the absorption values and the depth of softening for slates of similar composition. A study of such relations was made from 61 determinations on the slate from one quarry which gave $r=-0.18$. The negative value indicates a reciprocal relation, or that the more absorptive slates are more resistant to the acid action. The reason for this is believed to be due to a variation in the calcite content of the various samples rather than to differences in absorption.

The average absorption and the range (48 hours' immersion) in percentage by weight for various regions were as follows:

District	Number of tests	Absorption		
		Average	Maximum	Minimum
		Per cent	*Per cent*	*Per cent*
Maine	27	0.05	0.08	0.02
Vermont-New York	154	.13	.42	.05
Hard Vein, Pa	77	.16	.37	.10
Bangor, Pa	250	.28	1.24	.11
Pen Argyl, Pa	648	.30	.75	.11
Wind Gap, Pa	91	.38	.58	.23
Slatington, Pa	81	.29	.45	.17
Virginia	61	.06	.31	.00

6. POROSITY

The porosity of a material is usually expressed as a percentage of the void space to the total volume. Table 7 gives the results of several porosity determinations on slate. The values were deduced from the results of true and apparent specific gravity determinations as follows:

$$P=\frac{100\ (T-A)}{T}$$

where T and A are respectively the true and apparent specific-gravity values.

TABLE 7.—*True specific gravity, apparent specific gravity, porosity, and weight per cubic foot*

Serial No.[1]	True specific gravity					Apparent specific gravity					Porosity per cent by volume	Weight per cubic foot (dry)
	Number of samples	Number of tests	Maximum	Minimum	Average	Number of samples	Number of tests	Maximum	Minimum	Average		
1	1	5	2.833	2.816	2.823	1	9	2.809	2.806	2.807	0.57	175.2
2	1	3	2.831	2.826	2.829	1	6	2.822	2.820	2.821	.28	176.0
3						1	6	2.809	2.796	2.804		174.8
4	3	11	2.803	2.768	2.787	3	18	2.776	2.758	2.767	.74	172.6
5	1	3	2.782	2.778	2.780	1	6	2.773	2.770	2.772	.29	173.0
6	1	3	2.776	2.767	2.772	1	6	2.767	2.763	2.764	.29	172.4
7	1	3	2.812	2.806	2.809	1	6	2.803	2.790	2.796	.46	174.5
8	1	3	2.788	2.781	2.786	1	6	2.770	2.768	2.769	.61	172.8
14	1	5	2.814	2.810	2.812	1	6	2.803	2.791	2.798	.50	174.6
15	1	3	2.828	2.825	2.827	1	6	2.812	2.810	2.811	.57	175.4
16	1	3	2.808	2.805	2.806	1	6	2.786	2.782	2.784	.78	173.7
17	1	3	2.821	2.819	2.820	1	6	2.811	2.806	2.810	.35	175.4
18	1	3	2.808	2.802	2.804	1	6	2.795	2.780	2.788	.57	174.0
19	1	3	2.809	2.808	2.809	1	6	2.792	2.788	2.790	.68	174.1
20	1	3	2.805	2.802	2.803	1	6	2.795	2.794	2.795	.29	174.4
21	1	3	2.775	2.772	2.774	1	5	2.765	2.764	2.764	.36	172.5
22	1	3	2.810	2.805	2.808	1	4	2.791	2.774	2.783	.89	173.7
23						2	4	2.770	2.755	2.764		172.4
24						1	2	2.769	2.766	2.768		172.7
26	4	16	2.795	2.774	2.785	5	47	2.775	2.754	2.763	.79	172.4
27	2	6	2.775	2.769	2.772	2	23	2.771	2.751	2.758	.51	172.1
28						1	2	2.773	2.771	2.772		173.0
29						1	2	2.780	2.778	2.779		173.4
30						2	6	2.780	2.762	2.772		173.0
31						1	4	2.764	2.749	2.758		172.1
32						1	2	2.776	2.776	2.776		173.2
33	1	4	2.810	2.792	2.802	5	17	2.802	2.749	2.770	.50	172.9
36						1	5	2.791	2.774	2.783		173.7
45						3	10	2.769	2.760	2.764		172.5
46	1	5	2.781	2.760	2.771	5	15	2.784	2.739	2.763	.29	172.4
49	1	5	2.789	2.779	2.785	1	15	2.751	2.738	2.743	1.51	171.2
50						1	6	2.767	2.761	2.764		172.5
52						2	9	2.771	2.753	2.764		172.5
55						1	2	2.747	2.741	2.744		171.3
58	5	20	2.800	2.775	2.786	5	61	2.769	2.750	2.761	.84	172.3
59	6	22	2.808	2.775	2.791	6	64	2.789	2.753	2.768	.80	172.8
61						2	3	2.760	2.753	2.756		172.0
65	5	22	2.788	2.765	2.780	5	48	2.754	2.739	2.748	1.15	171.5
66	2	10	2.812	2.789	2.802	2	21	2.787	2.736	2.753	1.72	171.8
68						1	9	2.743	2.738	2.740		171.0
69	3	11	2.799	2.772	2.785	3	34	2.771	2.753	2.760	.94	172.2
70						2	6	2.773	2.770	2.771		172.9
71						1	2	2.761	2.761	2.761		172.3
72	1	4	2.783	2.778	2.780	2	9	2.760	2.742	2.752	1.15	171.8
73						1	4	2.750	2.750	2.750		171.6
76	1	3	2,802	2.789	2.795	5	17	2.796	2.777	2.788	.14	174.0
77						6	24	2.811	2.774	2.798		174.6
78	1	10	2.908	2.890	2.898	1	5	2.874	2.868	2.871	.93	179.2
79	1	4	2.883	2.869	2.878	1	7	2.757	2.742	2,754	4.31	171.8
80	1	5	2.854	2.839	2.848	1	3	2.769	2.743	2.758	3.16	172.1
81	1	3	2,889	2.887	2.888	1	6	2.903	2.878	2.888		180.2
82	1	3	2.813	2.806	2.810	1	4	2.778	2.777	2.778	1.14	173.4
83	1	3	2.832	2.821	2.827	1	6	2.814	2.809	2.811	.57	175.4
84						1	4	2.694	2.689	2.692		168.2
85						1	3	2.745	2.744	2.744		171.2
86						1	3	2.727	2.718	2.723		170.2

[1] Identification of serial numbers given in Table 1.

Porosity values are of interest in studying the weathering qualities of a material, but, in general, the determination is too difficult and tedious for specification purposes. A sufficiently accurate indication of porosity for comparative purposes is obtained by the absorption test. Evidently the porosity value for any material should be equal to or greater than the volume absorption value. In the specific-gravity determinations the true value was determined on one specimen of the sample and the apparent on another. The porosity values are so small that a slight error in either determination or a slight variation of the material will lead to erroneous porosity results.

Most of the porosity values found were between 0.3 and 1 per cent, although one value was 0.14 per cent and another over 4 per cent. The latter was obtained on a sample taken from the surface of the ground and hence is not representative of material below the weathered zone.

7. SPECIFIC GRAVITY

The "true specific gravity" of a porous material may be considered as the ratio of the weight of a certain volume of material to the weight of the same volume of water at the same temperature, assuming that the material has been compressed until the pores are entirely filled. It is not feasible to eliminate the pores by compression, but the material can be pulverized until the component particles are separated. Determinations given in Table 7 were made on material pulverized and passed through a 100-mesh sieve. Various types of specific-gravity apparatus were tried, but the most concordant results were obtained with the LeChatelier flask. As this apparatus requires a much larger sample than other types and the process is less tedious, it was employed for the tests. By using considerable care in removing the air from the powders and correcting for temperature differences between the initial and final volume readings it was found possible to obtain quite consistent results. A 95 per cent ethyl alcohol was used as the liquid, since there was no difficulty in immersing all of the powdered material in it, while other liquids had a tendency to float some of the fine powder.

The apparent specific gravity of a porous material is the ratio of weight of a certain volume of the material in its natural state to the weight of the same volume of water at the same temperature. The results given in Table 7 were determined from dry weights of regular-shaped specimens and the corresponding volumes obtained by weighing the saturated specimens immersed in water. The reduction formula was

$$A = \frac{w_1 d}{w_2 - w_3}$$

where w_1 = dry weight of specimen, d = apparent density of the water at the temperature of observation, w_2 = weight of the specimen after immersion in water for 48 hours, and w_3 = weight of saturated specimen suspended in water. It is necessary to use soaked specimens for determining the weight suspended in water to prevent errors due to absorption during the operation.

8. WEIGHTS PER CUBIC FOOT

Having determined the apparent specific gravity or "bulk density" of a material, it is only necessary to multiply this value by the weight of a cubic foot of water in order to deduce the weight per cubic foot

of the sample. The results in the last column of Table 7 were obtained by multiplying the average apparent specific-gravity value for each sample by 62.35. The average and extreme weights per cubic foot for slate from various districts were as follows:

Weight per cubic foot

District	Number of tests	Average	Maximum	Minimum
		Pounds	*Pounds*	*Pounds*
Maine	21	175.3	176.1	174.3
Vermont-New York	93	173.7	175.5	172.1
Hard Vein, Pa	16	172.7	173.2	171.9
Bangor, Pa	108	172.6	174.8	171.8
Pen Argyl, Pa	185	172.4	174.0	170.9
Wind Gap, Pa	78	171.5	173.9	170.7
Slatington, Pa	51	172.2	173.0	171.8
Virginia	52	174.8	179.3	173.1

The above values, considered in conjunction with service records of the slates, afford considerable evidence that a correlation exists between bulk density and durability. However, as will be shown later, the durability of slate is influenced to such a large extent by the presence of small amounts of certain minerals, it would not be logical to base judgment upon this determination alone.

VI. WEATHERING CHARACTERISTICS

1. WEATHERING PROCESSES

In the study of slate weathering, about 60 samples of old shingles were collected which had been exposed to the elements for various periods of time up to 131 years. Where an appreciable amount of decay was in evidence the decayed portion was subjected to a partial chemical analysis to determine if any alteration in composition of the less stable minerals had occurred. Specimens were also subjected to strength, toughness, and absorption tests to determine the physical alterations. A summary of these results is shown in Table No. 8.

TABLE 8.—*Summary of tests on weathered slate*

Producing region	Number of samples examined	Average weathering period	Average modulus of rupture		Average toughness values		Average absorption by weight		Indicated change per year due to weathering		
			Fresh slate	Weathered slate	Fresh slate	Weathered slate	Fresh slate	Weathered slate	Modulus of rupture	Toughness	Absorption
		Years	*Lbs./in.²*	*Lbs./in.²*	*Inch*	*Inch*	*Per cent*	*Per cent*	*Lbs./in.²*	*Inch*	*Per cent*
Maine	4	46	11,700	10,100	0.178	0.168	0.05	0.06	−35	−0.0002	+0.0002
Vermont-New York	3	40	10,600	8,700	.163	.160	.13	.23	−47	−.0007	+.0025
Hard Vein, Pa	12	54	13,600	9,000	.204	.168	.16	.85	−85	−.0006	+.0128
Soft Vein, Pa [1]	29	24	11,700	9,600	.201	.189	.31	.68	−100	−.0005	+.0154
Virginia	9	81	10,500	9,600	.164	.144	.06	.15	−11	−.0002	+.0011

[1] Slates from Bangor and Pen Argyl region.

A large range in the resistance of the various slates was evident from the examination of weathered samples. The chemical analysis revealed, in most cases, a considerable amount of gypsum in the weathered portion, while the fresh slates showed almost none. It

seemed probable, therefore, that some of the calcite in the slate was converted to gypsum in the weathering process. Two means were considered possible for this change—first, the action of sulphur acids from the air on the calcite, and, second, an interaction between the sulphide minerals and calcite. Sulphides of iron are usually present in slate.

If gypsum could be formed from an interaction of the constituent minerals of slate, it was assumed that the weathering process could be simulated in the laboratory by merely soaking and drying the material several times. The following experiments were made for that purpose: Three samples of slate were selected which were known to have poor weathering qualities. Determinations of SO_3 were made on each in the original condition and after the samples had been subjected to 30 cycles of soaking and drying. The following results were obtained:

	SO_3
	Per cent
Sample No. 1:	
(*a*) In original condition	0. 01
(*b*) After 30 cycles of soaking and drying	. 50
Sample No. 2:	
(*a*) In original condition	. 01
(*b*) After 30 cycles of soaking and drying	. 50
Sample No. 3:	
(*a*) In original condition	. 01
(*b*) After 30 cycles of soaking and drying	. 23

A portion of each of these three samples, after the soaking and drying process, was powdered and leached with distilled water. The leach was then filtered and evaporated. An abundance of crystals was obtained which was examined with the petrographic microscope and proven to be gypsum. In these experiments it was considered that the sulphur acids of the air could play no appreciable part and that the gypsum was due practically entirely to the reaction between the calcite and sulphide minerals, the oxygen necessary for completing the SO_3 radicle being drawn from the air.

It was desirable to study the reaction between iron sulphide and calcite alone as well as in the presence of carbon. For this purpose four mixtures were made, as follows: (1) Equal parts of calcite and pyrite; (2) equal parts of calcite and marcasite; (3) same as (1) with a small addition of carbon; (4) same as (2), with a small addition of carbon. The four mixtures were placed in open beakers, covered with distilled water, and allowed to stand for seven hours at room temperatures. The beakers were then set in a drying oven at 110° C. for 17 hours. The 7 hours' soaking and 17 hours' drying constituted a cycle which was repeated one hundred times. The water-soluble matter was then extracted and determined as follows:

Sample No.	$CaSO_4$
	Per cent
1	7.0
2	2.3
3	14.9
4	6.0

These experiments indicate that a chemical reaction between pyrite and calcite or between marcasite and calcite occurs under such conditions and results in the formation of gypsum. They also indicated that the presence of carbon accelerates the rate of reaction.

Since this chemical change has been found to occur in slates containing appreciable amounts of calcite and iron sulphides, it remains to be considered how this may produce decay. The gypsum molecule requires about twice as much space as the calcite molecule, hence the conversion to gypsum of a calcite crystal, which is embedded in another material, must produce stresses in the surrounding material. Slates containing considerable amounts of both pyrite and calcite, when subjected to several cycles of soaking and drying, disintegrated almost completely. Slates of the same kind in actual exposure on the roof of a building are found to decay more rapidly on the unexposed parts. This seems to indicate that in service the solubility of gypsum comes into consideration. As the rain water leaches downward through the slate some of the gypsum is carried in solution and deposited at a lower level. By this process the gypsum is concentrated on the lower sides of shingles and the recrystallization within the pores causes internal stresses. The analyses made on weathered shingles showed, in most cases, a concentration of gypsum in the decayed parts.

Soaking and drying tests have been made on numerous samples of slates which were known to have poor weathering qualities by drying at 110° C. for 17 hours and soaking 7 hours. Under such conditions some of the samples showed signs of decay in 30 cycles and an advanced state of disintegration in less than 50 cycles. Some producers contended that the drying temperatures were too high in these tests and out of proportion to those of service conditions. For this reason a series of tests was made in which the drying temperature was 50° C. This temperature was assumed to be about equivalent to roof temperatures on hot summer days. The results are given in Table 9, and show that the deterioration occurs under such conditions but at a much slower rate.

TABLE 9.—*Soaking and drying tests with absorption and weight determinations after 200 cycles* [1]

Serial No.[2]	Specimen No.	Average absorption by weight of specimens		Average change in weight of specimens	Final appearance of specimens
		Original condition	After 200 cycles		
		Per cent	*Per cent*	*Per cent*	
1	1	0.06	0.08	−0.05	No apparent change.
	2				Do.
	3				Do.
2	1	.02	.04	−.05	Do.
	2				Do.
	3				Do.
4	1	.09	.14	−.06	Do.
	2				Do.
	3				Do.
5	1	.08	.13	−.05	Do.
	2				Do.
	3				Do.
6	1	.08	.12	−.03	Do.
	2				Do.
	3				Do.
7	1	.14	.16	−.03	Do.
	2				Do.
	3				Do.

[1] In the first 100 cycles each cycle consisted of 17 hours drying at 50° C., followed by 7 hours immersion in water at room temperatures. In the second 100 cycles each cycle consisted of 24 hours drying at 50° C. and 24 hours immersion in water at room temperatures.

[2] For identification of serial numbers see Table 1.

TABLE 9.—*Soaking and drying tests with absorption and weight determinations after 200 cycles*—Continued

Serial No.	Specimen No.	Average absorption by weight of specimens		Average change in weight of specimens	Final appearance of specimens
		Original condition	After 200 cycles		
		Per cent	*Per cent*	*Per cent*	
8	1	0.11	0.16	+0.04	No apparent change.
	2				Do.
	3				Do.
14	1	.14	.15	−.01	Do.
	2				Do.
	3				Do.
15	1	.12	.12	−.04	Do.
	2				Do.
	3				Do.
16	1	.16	.22	+.05	Do.
	2				Do.
	3				Do.
17	1	.11	.12	−.03	Do.
	2				Do.
	3				Do.
18	1	.12	.15	−.03	Do.
	2				Do.
	3				Do.
19	1	.13	.19	−.04	Hair cracks on 2 edges.
	2				No apparent change.
	3				Do.
20	1	.10	.11	.00	Do.
	2				Do.
	3				Do.
21	1	.06	.07	−.02	Do.
	2				Do.
	3				Do.
22	1	.13	.18	−.05	Do.
	2				Do.
	3				Do.
23	1	.15	.32	−.04	Hair cracks on 4 edges.
	2				No apparent change.
	3				Do.
26	1	.17	.27	−.06	Do.
	2				Hair cracks on 1 edge.
	3				Cracks along 2 edges.
27	1	.14	.19	−.04	No apparent change.
	[1] 2				Hair cracks on 1 edge.
	[1] 3				No apparent change.
49	1	.39	.60	−.02	No apparent change.
	2				Hair cracks on 2 edges.
	3				Hair cracks on 1 edge.
58	1	.22	.33	−.02	No apparent change.
	2				Do.
	3				Do.
59	1	.27	1.54	−.02	Do.
	[1] 2				Ribbon badly cracked
	3				No apparent change.
65	1	.36	.70	+.03	Hair cracks on 4 edges.
	2				Hair cracks on 3 edges.
	3				Hair cracks on 4 edges.
66	1	.32	.77	−.50	No apparent change.
	[1] 2				Ribbon disintegrated.
	[1] 3				Do.
69	1	.26	.64	.00	Hair cracks on 4 edges.
	2				Do.
	3				Do.
76	1	.01	.02	−.04	No apparent change.
	2				Do.
	3				Do.
81	1	.20	.25	+.02	Do.
	2				Do.
	3				Do.
82	1	.27	.32	−.07	Do.
	2				Do.
	3				Do.
83	1	.10	.18	−.04	Do.
	2				Do.
	3				Do.

[1] Specimens contained a dark ribbon. Those not so marked are clear slate.

In order to determine if a relation exists between the results obtained in the soaking and drying tests and the resu ts of actual weathering it is necessary to have some definite measure of the deterioration. It is fair to assume that a decrease in strength or an increase in absorption is indicative of deterioration. In Table 9 is shown the computed rate of "strength loss" and "absorption increase" per year for weathered slate from five producing districts. These rates are based on the average strength and absorption results obtained on the fresh material as compared to the results obtained on slate shingles after exposure to the weather. It was found that these yearly rates of change were approximately one-twentieth part of the corresponding changes obtained in 200 cycles of the soaking and drying test when the specimens were dried at 50° C. Figure 4 shows the "absorption increases"

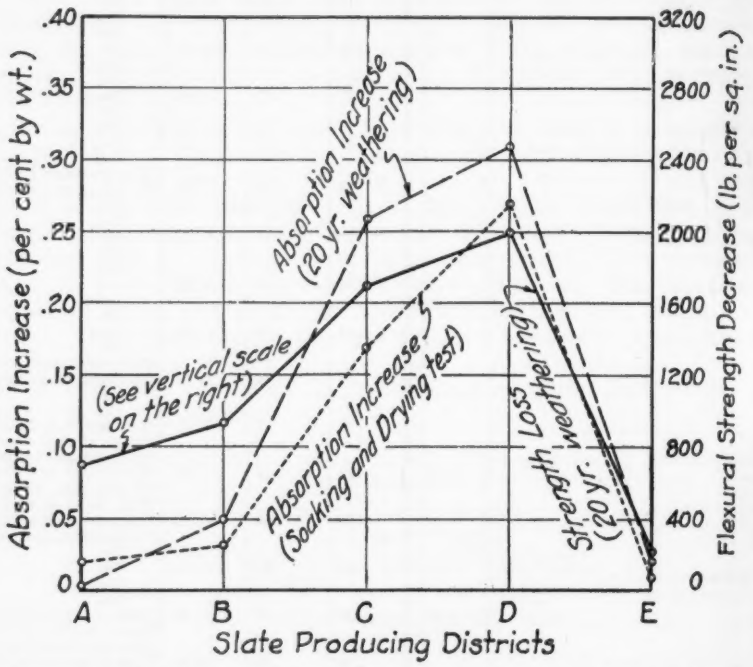

FIGTRE 4.—*Relation between strength loss for 20 years weathering, absorption increase for 20 years weathering and absorption increase in the soaking and drying test*

Plotted points are the respective averages of all specimens from five districts as follows: *A*, Maine; *B*, Vermont-New York; *C*, Hard Vein, Pa.; *D*, Soft Vein, Pa., *E*, Virginia.

obtained in the soaking and drying tests plotted with the computed "absorption increases" and "strength losses" for 20 years weathering. These curves indicate that the soaking and dry ng test gives results similar to those of actual weathering.

Thermal expansion and contraction of the component minerals has often been mentioned as a possible cause of deterioration. This was studied by means of a series of tests on samples from five districts. The samples were heated in an oven for 17 hours and laid out in the laboratory for 7 hours. Two of the samples were disintegrated by 63 cycles but the others were continued in the test to 554 cycles.

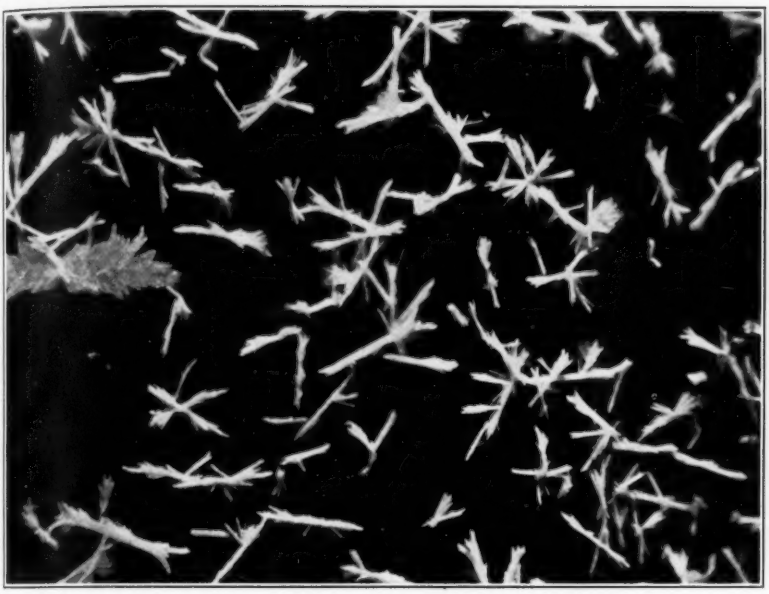

FIGURE 5.—*Photomicrograph of calcium sulphate crystals obtained by evaporating the leach from a sample of Pen Argyl (Pa.) slate which had been heated and cooled 310 cycles*

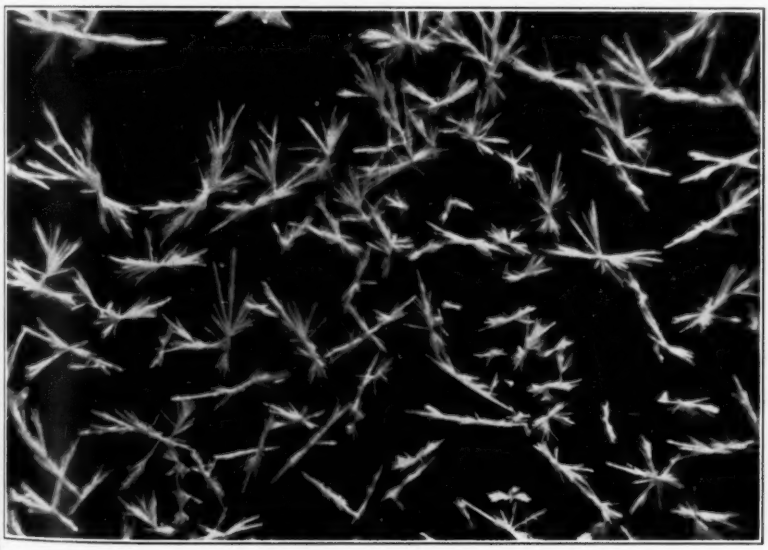

FIGURE 6.—*Photomicrograph of calcium sulphate crystals obtained by evaporating the leach from a sample of Bangor (Pa.) ribbon slate that had been heated and cooled 63 cycles*

UNIV. OF MICH.

The results were judged by means of inspection and by absorption tests after 25, 50, and 554 cycles. The detailed results are given in Table 10. The s ates which had previously shown a high resistance to the soaking and drying test showed little deterioration in the heating and cooling procedure. As those samples which decayed in this test presented about the same appearance as samples which decayed in the soaking and drying test, they were examined for gypsum and it was found in considerable amounts. Figures 5 and 6 are photomicrographs of the crystals obtained by leaching serial Nos. 58 and 27, respectively. Hence, it is probable that decay was caused mainly by the formation of gypsum. Most of the samples showed considerable resistance to the heating and cooling process, especially those of low calcite content, which seems to indicate that the effect of temperature changes on slate is slight unless it results in such chemical alterations as described above. The tests also indicate that considerable amounts of moisture are not necessary to bring about the reaction. Furthermore, they supply a c.ue to the cause of decay sometimes noted on interior slate installations.

TABLE 10.—*Effect of repeated heating and cooling on slates from five different regions*

Serial No.[1]	Observed condition of specimens				Per cent absorption by weight after 48-hour immersion			
	After 20 cycles	After 63 cycles	After 100 cycles	After 554 cycles	Original condition	After 25 cycles	After 50 cycles	After 554 cycles
2	No visible effect	No visible effect	No visible effect	No visible effect	0.04	0.04	0.02	0.04
15	do	do	do	do	.15	.16	.15	.16
23	do	do	do	Swelling at ribbons.[2]	.12	.12	.10	.40
26	do	do	do	No visible effect	.32	.24	.23	.48
27	Swelling at ribbon	Badly decayed			.48	1.76	(3)	
58	No visible effect	No visible effect	do	Considerable decay.	.37	.40	2.88	(3)
59	Swelling at ribbon	Badly decayed			.46	1.20	(3)	

[1] Identification of serial numbers given in Table 1.
[2] On 1 specimen the ribbons were crumbling at the surface.
[3] Specimens were too badly decayed for absorption determination. 1 specimen of No. 58 was in an advanced state of decay at 310 cycles.

Frost action is considered to be one of the common causes of stone weathering. Table 11 gives the results of freezing tests on 18 samples from the various districts. The samples were slabs 4 inches square and approximately one-half inch thick. They were soaked 14 days before freezing was started and then thawed each time by immersion in water at about 20° C. for 30 minutes. The temperature of the freezing chamber was maintained at approximately −10° C. and two freezings were made each day. In these tests only one sample failed and this occurred after 1,374 cycles. This sample was originally taken from the surface of the ground and showed signs of weathering when received. Five of the samples were continued in the test until 2,436 cycles were reached and the others were discontinued after 1,743 cycles. The results were judged by inspection and by absorption tests.

TABLE 11.—*Results of freezing tests*

Serial No.[1]	Specimen No.	Number of cycles[2]	Condition[3]	Average absorption by weight			Remarks
				A[4]	B[5]	C[6]	
				Per cent	*Per cent*	*Per cent*	
1	1 2 3 4 5 6	1,743	b b b d c c	0.15	0.08	0.06	Sharp corners chipped off in some places.
4	1 2 3 4 5 6	2,436	b b b b c c	.29	.22	.16	Corners chipped off in places and some cleavage cracks.
26	1 2 3 4 5 6	1,743	c c c c c c	.39	.33	.15	Corners chipped slightly and some scaling on cleavage faces.
27	1 2 3 4 5 6	1,743	c c c c c c	.34	.29	.14	Do.
33	1 2 3 4 5 6	2,436	d d e d c d	.46	.38	.19	Considerable scaling on cleavage faces; more in evidence at ribbons.
46	1 2 3 4 5 6	2,436	c c c d c d	.36	.28	.15	Effects mainly confined to scaling on cleavage faces.
58	1 2 3 4 5 6	1,743	c c c c c b	.43	.38	.24	Some scaling on cleavage faces.
59	1 2 3 4 5 6	1,743	d e c c c c	.46	.43	.25	Considerable scaling on cleavage faces; more pronounced at ribbons.
65	1 2 3 4 5	1,743	e e c e c	.69	.63	.35	Considerable scaling on cleavage faces and corners chipped.

[1] Identification of serial numbers given in Table 1.
[2] A cycle consisted of 1 freezing and 1 thawing as outlined on p. 405.
[3] The final state of the specimens was estimated by inspection and expressed in 8 stages as follows: "a" signifies no decay, "h" advanced state of decay. The intervening letters represent about equal stages of decay between "a" and "h."
[4] Percentage of water absorbed during the freezing and thawing process.
[5] Absorption obtained by drying the specimens after the freezing procedure and then immersing them for 48 hours.
[6] Absorption of samples in original condition.

TABLE 11.—*Results of freezing tests*—Continued

Serial No.[1]	Specimen No.	Number of cycles[2]	Condition[3]	Average absorption by weight			Remarks
				A[4]	B[5]	C[6]	
				Per cent	*Per cent*	*Per cent*	
66	1	1,743	c	0.65	0.56	0.32	Surface scaling on cleavage faces; corners chipped.
	2		c				
	3		c				
	4		c				
	5		d				
	6		d				
69	1	1,743	b	.54	.46	.26	Some specimens scaling considerably.
	2		d				
	3		d				
	4		c				
	5		c				
	6		d				
72	1	2,436	e	.73	.64	.36	Considerable surface scaling.
	2		e				
	3		d				
	4		d				
	5		c				
	6		c				
78	1	2,436	a	.61	.45	.15	No definite sign of decay.
	2		a				
	3		a				
	4		a				
	5		a				
	6		a				
79	1	1,374	h			1.41	Cracked and crumbled.
	2	1,469	h				
	3	1,374	h				
80	1	1,743	d	1.49	1.28	1.12	Surface scaling and some cleavage cracks.
	2		d				

See footnotes on p. 406.

While all of the samples showed an increase in absorption after repeated freezing and thawing, and while surface scaling was observed in most cases, it can not be said that any sample (except one mentioned above) had reached an advanced state of decay. In view of the large number of cycles of freezing it may be concluded that the action of frost on slate is not a very serious cause of decay. This is especially true of those slates which are subject to the chemical changes discussed above, since that action is several times as severe. However, it should be considered that when decay has started from any cause then frost action can proceed at a more rapid rate.

2. WEATHERING TEST PROCEDURE

The soaking and drying test requires a month or more to carry the weathering process to a definite visible stage. A more rapid acceptance test is often desirable. Several procedures, such as the change in strength or absorption, have been used to measure the effects of the weathering test at some intermediate stage of the process. The strength criterion has not proven very satisfactory, because one can not determine the original strength of the actual specimens used in the weathering test. Determinations on separate specimens of the sample may prove very misleading, due to the natural variation of the material. Figure 7 shows the average strength losses for a large number of specimens after 10, 20, and 30 cycles of soaking and drying. In this series of tests the specimens were dried

17 hours at 110° C. and soaked 7 hours at about 20°. This shows that the strength loss up to 20 cycles is slight and unless a large number of specimens are averaged the effect might not be discerned. Absorption tests can be made on the same specimens before and after the soaking and drying process, and such tests afford a more reliable criterion than strength determinations. An indirect means which offers considerable promise consists in determining the gypsum content of the sample before and after the weathering process, and using the gypsum increase as a measure of weathering.

A test procedure which has been used to some extent for judging the weathering qualities of slate consists of soaking the specimens for seven days in a 1 per cent solution of sulphuric acid. The depth of softening is then determined by gaging the thickness of the specimens at several points, scraping off the softened layer at these points and gaging again. By using a dull blade for the scraping and standardizing the conditions of the process it is possible to obtain fairly

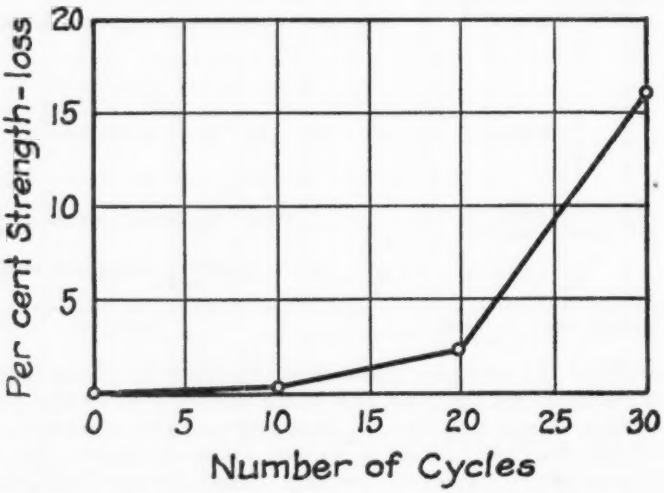

FIGURE 7.—*Average strength-loss for 16 samples of slate from 1 district after 10, 20, and 30 cycles of soaking and drying*

consistent results. This test converts the calcite near the surface to gypsum and causes decay similar to that obtained in the soaking and drying test. Slates which have a low calcite content are not appreciably affected by this test. The absorption of the slate may have a marked effect. Evidently this test would lead to erroneous conclusions if applied to slates containing considerable calcite, but very little sulphide of iron. All of the slates now being produced in this country contain considerable amounts of pyrite so the acid test is applicable to our present commercial materials.

Table 12 gives the results of such tests on several samples representing the various producing districts. Figure 8 shows the relations obtained by plotting the average acid resistances of slates from the various districts with absorption increases due to actual weathering as well as absorption increases noted in the soaking and drying test. This test indicates no appreciable difference between the durability of slates from districts *A*, *B*, and *E*, all of which are generally accepted

to be durable materials. It does show a greater difference between districts *C* and *D* than is indicated by either the soaking and drying test or by the examination of weathered samples. The test is advantageous in cases where the results must be had in a short period of time. It seems to be fairly reliable in distinguishing between the good and poor grades within certain districts but its general application to all types of slates is not justified by the results of this investigation.

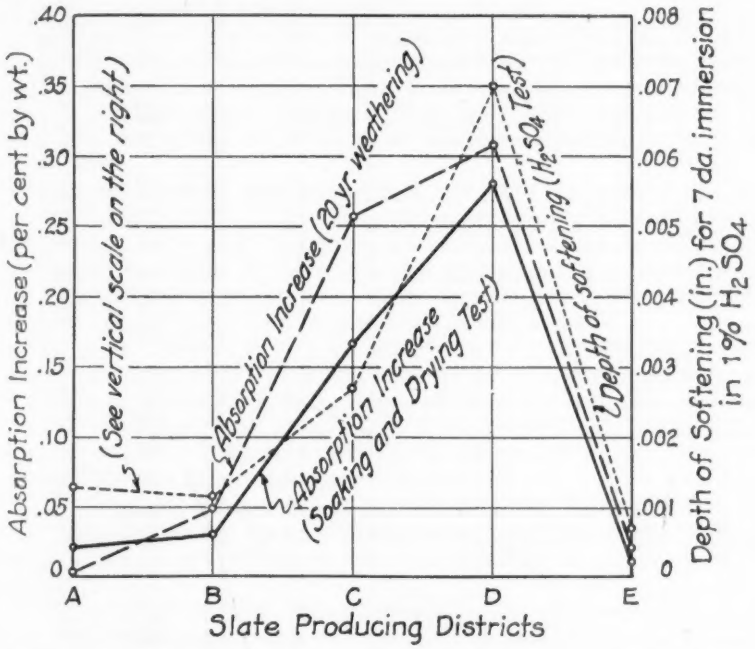

FIGURE 8.—*Relation between absorption-increase for 20 years weathering, absorption increase during soaking and drying test and depth of softening in sulphuric acid test*

Plotted points are the respective averages of all the specimens from five districts as follows: *A*, Maine; *B*, Vermont-New York; *C*, Hard Vein, Pa.; *D*, Soft Vein, Pa.; *E*, Virginia.

TABLE 12.—*Sulphuric acid tests with depth of softening measurements after seven days in 1 per cent H_2SO_4*

Serial No.[1]	Number of samples	Depth of softening			
		Number of tests	Maximum	Minimum	Average
			Inch	*Inch*	*Inch*
1	1	8	0.002	0.000	0.001
2	2	16	.003	.000	.002
3	1	4	.001	.000	.001
4	1	4	.001	.000	.001
5	1	8	.002	.000	.001
6	1	8	.003	.001	.002
7	1	8	.001	.000	.001
8	1	8	.003	.000	.002
13	1	6	.002	.001	.002
14	1	8	.002	.001	.001

[1] Identification of serial numbers given in Table 1.

TABLE 12.—*Sulphuric acid tests with depth of softening measurements after seven days in 1 per cent H_2SO_4*—Continued

Serial No.	Number of samples	Depth of softening			
		Number of tests	Maximum	Minimum	Average
			Inch	*Inch*	*Inch*
15	1	8	0.001	0.000	0.001
16	1	8	.002	.000	.001
17	1	8	.001	.000	.001
18	1	8	.001	.000	.000
19	1	8	.002	.001	.001
20	1	8	.001	.000	.001
21	1	8	.003	.000	.001
23	4	26	.005	.000	.002
24	2	12	.006	.001	.003
25	1	6	.007	.001	.004
29	2	14	.024	.008	.015
34	1	6	.018	.013	.016
36	1	3	.012	.010	.011
38	1	4	.017	.012	.015
40	1	6	.016	.007	.012
42	1	6	.016	.009	.013
45	1	9	.007	.001	.003
47	1	9	.024	.010	.016
49	1	9	.011	.006	.009
51	1	6	.004	.001	.002
52	40	150	.017	.001	.006
52a	2	4	.011	.002	.004
53	1	3	.003	.001	.002
54	2	10	.010	.001	.005
56	1	6	.004	.003	.004
57	3	15	.007	.001	.005
60	1	6	.003	.001	.002
61	1	6	.015	.002	.007
62	2	16	.005	.001	.003
63	1	8	.012	.007	.010
67	1	6	.017	.004	.010
72	1	2	.010	.007	.008
73	1	6	.014	.007	.012
74	1	6	.005	.002	.003
75	1	3	.020	.017	.018
76	3	20	.002	.000	.000
81	1	8	.002	.001	.002
82	1	8	.002	.001	.001
83	1	8	.002	.001	.001
85	2	24	.005	.000	.002

VII. CONCLUSIONS

1. The flexural strength of slate is much higher than other types of rock used for structural purposes. Although most slates are stronger across the grain than along the grain, this ratio varies greatly with different deposits. The effect of moisture in decreasing the strength is more marked than for other common types of rock.

2. The elastic modulus of slate is high in comparison with other types of rocks. The high flexural strength of the material enables it to be used in relatively thin slabs which have considerable flexibility.

3. Although the porosity determinations in some cases were of rather uncertain precision, they seem to indicate that the void spaces in slate are usually less than 2 per cent of the volume.

4. The bulk density (apparent specific gravity) of slate varies between the limits 2.74 and 2.89, the average being 2.78.

5. The abrasive hardness of slate is about equal to that of the harder oolitic limestones in present-day use in this country.

6. Slate is probably affected to some extent by frost and atmospheric acids, but the major weathering action is due to, first, chemical interaction between certain mineral constituents and second, internal stresses resulting from the newly-formed compounds.

7. The weather resistance is decreased by appreciable amounts of calcite and pyrite existing together. The presence of free carbon with these two minerals lessens weather resistance.

8. Tests on several samples of weathered slate shingles indicate that the early stages of decay are accompanied by an increase in absorption and decrease in strength. These facts may be found of value in deciding upon the use of shingles which have been exposed to the weather for a few years at the plant or the reuse of shingles removed from a building.

9. The most reliable weathering test for slate appears to be the soaking and drying test. For the slates now being produced in this country the sulphuric acid test gives a sufficiently accurate indication of weathering qualities for specification purposes. For slates containing a considerable amount of calcite but no pyrite the sulphuric acid test would probably lead to erroneous conclusions.

10. The possibility of injury to slate due to diurnal temperature changes alone is remote. The chemical transformations occurring in slates, containing considerable amounts of calcite and pyrite, proceed even in dry weather, but at a much slower rate than when more moisture is present. This fact probably accounts for the decay sometimes noted in cases of interior slate construction.

11. Color changes in slate are of two kinds: First, those due to concealment of the true color by an efflorescence giving the effect of fading, and, second, oxidation of ferrous minerals resulting in a more permanent color.

12. The so-called fading of dark-colored slate is confined mainly to those varieties containing considerable amounts of calcite and pyrite. This phenomenon accompanies the weathering process and is believed to be a result of the same chemical changes which produce decay. Color changes due to the oxidation of ferrous minerals are confined mainly to certain varieties of green slate and results in a change from green to brown. Occasionally dark-colored slates take on a brown color after exposure to the weather. This appears to be due to a decomposition of the pyrite and oxidation of the iron compounds.

WASHINGTON, June 21, 1932.

RADIATION FROM CÆSIUM AND OTHER METALS BOMBARDED BY SLOW ELECTRONS

By C. Boeckner

ABSTRACT

The absolute intensity and intensity wave-length distribution of the radiation from Cs, Cr, Ni, Mo., and W is measured and found to be similar for all five metals. Control measurements are also made allowing the effect of surface contamination to be estimated. It is found that the radiation from contaminated surfaces is usually much more intense than from clean metals. It is pointed out that the similarity between the radiation from cæsium and other metals makes it probable that the radiation is analogous to the continuous X rays and is not due to the excitation of electron levels characteristic of the metal.

CONTENTS

	Page
I. Introduction	413
II. Experimental	414
1. Method	414
2. Control measurements	414
3. Measurement of the cæsium radiation	414
III. Results	416
1. Absolute intensities	416
2. Experimental uncertainty	416
3. Radiation from contaminated surfaces	416
IV. Discussion	417

I. INTRODUCTION

It has been observed in this laboratory that a small metal electrode (Langmuir probe), drawing a heavy electron current in a gas discharge, emits radiation. The properties of this radiation, dependence upon the metal used as electrode, the energy of bombarding electrons, etc., have been set forth in two previous papers.[1]

The principal facts may be summarized as follows: The spectrum of radiation is continuous and of almost constant intensity throughout the visible and ultra-violet. Exceptions are silver and copper which possess intense selective emission bands. The absolute intensity of the radiation for most metals is about the same. For electron energies of 2 or 3 volts the spectrum has a short wave-length limit, the frequency of which is connected with the work function of the metal and the electron energy by the familiar Einstein photo-electric equation. The intensity of the radiation is of the order expected for the "bremsstrahlung" produced by electrons with energies of the order used, which suggests that the radiation is similar in orgin to the continuous X rays.

The present work is a continuation of the studies described in the first two papers in the earlier work. The absolute intensity measurements were few and the results discordant. It was therefore decided to make more extensive absolute measurements and at the same time look for unknown factors, such as surface contamination, which might influence the results.

[1] F. L. Mohler and C. Boeckner, B. S. Jour. Research, vol. 6 (RP297), p. 673, 1931; vol. 7 (RP371), p. 751, 1931.

It was also decided to measure the radiation from several metals not studied previously, namely, Cs, Cr, Mo, and Ni. The radiation from cæsium was considered of particular interest because of the exceptional properties of the metal and because a cæsium electrode surface in a cæsium discharge could be kept very clean.[2]

II. EXPERIMENTAL

1. METHOD

For information concerning the technique, the original papers should be referred to. Some details, however, will be mentioned.

The intensity measurements were made by the usual photographic methods, using an incandescent tungsten strip at various temperatures as a comparison source. An E2 Hilger quartz spectrograph was used to photograph the spectrum of the radiation and quartz fluorite achromats were used to focus the image of the electrodes on the slit.

A low-voltage hot cathode discharge in cæsium vapor was used as a source of electron current to the probe. The discharge tube was placed in a furnace at about 170° C. to maintain the required Cs vapor pressure (several thousandths of a millimeter).

The electrodes were usually in the form of cylinders 2 to 4 mm in diameter. The sides were insulated by glass tubing and the flat polished ends exposed to the discharge.

2. CONTROL MEASUREMENTS

A number of control measurements were made in order to locate possible sources of contamination of the probe surfaces. In the earlier work the probes had been placed in the negative glow of the discharge, near the barium oxide coated platinum cathode. It was suspected, however, that barium or oxygen evaporated from the cathode might contaminate the probe surface. Measurements were therefore made in the negative glow, using a tungsten cathode, and also in the positive column some 15 cm from the cathode.

In most of the work the probes were outgassed at 400° C. and the metal surface cleaned by several hours' bombardment with 100-volt Cs ions. To ascertain the effect of better outgassing and a possibly cleaner surface, a tungsten electrode was used in the form of a wire 0.4 mm in diameter and 1 cm long. The wire could be heated to incandescence and outgassed by current passed through it from insulated supporting leads.

3. MEASUREMENT OF THE CÆSIUM RADIATION

A specially designed tube was required for the measurement of the radiation from a cæsium electrode. A tungsten wire, 2 mm in diameter and several centimeters long, was sealed into the glass wall of a discharge tube, the inner end being flush with the glass wall. The other end projected from the tube and through the walls of the furnace into the air. Upon blowing air against the end of the wire the end in the discharge was cooled sufficiently to condense a bright layer of cæsium upon it. If the electron current to the probe was too large

[2] A cæsium vapor discharge was found to be most suitable as a source of current to the electrodes due to the relative scarcity of lines in its arc spectrum. Scattered light from the discharge is a serious difficulty in the type of work described here.

the cæsium evaporated; if too small it would spread over the surrounding glass wall. A current and voltage could easily be found for which the cæsium just covered the end of the wire. The cæsium could be evaporated and deposited many times during the observations, thus insuring a clean surface. The diameter of the cæsium

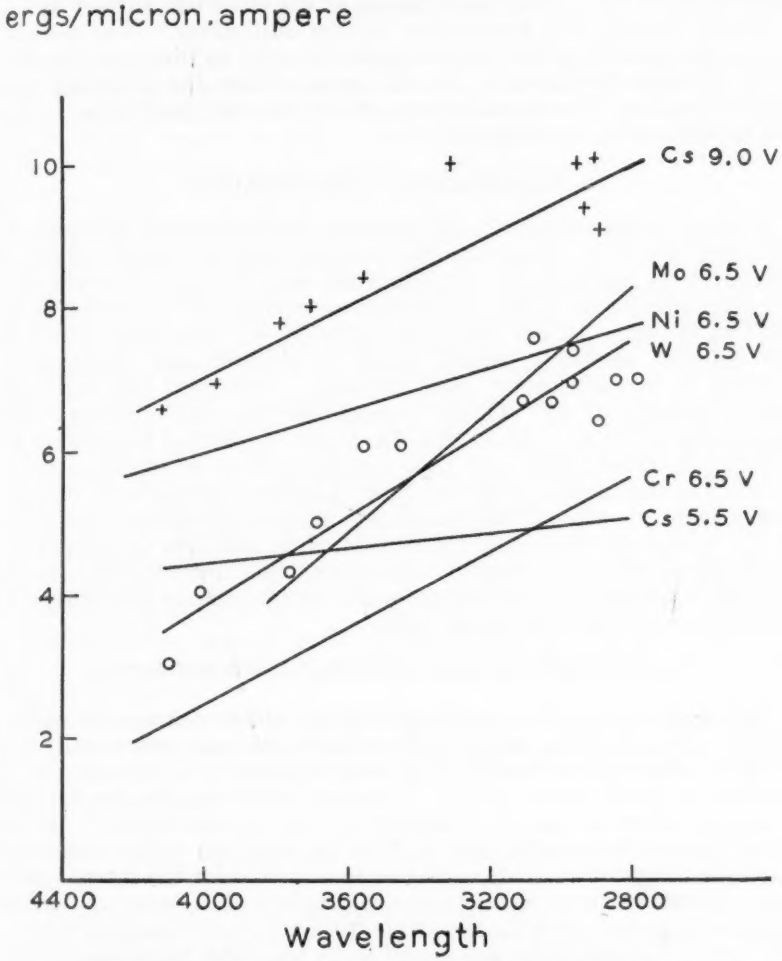

FIGURE 1.—*Absolute intensities of radiation from metals*
Ordinates, intensities in ergs per ampere in a micron wave-length range. "o" tungsten 6.5 volts; "+" cæsium 9 volts.

disk, a knowledge of which was necessary in order to determine the current density, was evaluated from the size of the image on the spectrograms. It may be mentioned that a monatomic adsorbed cæsium layer present on the other metals studied does not, of course, constitute a difficulty in the case of a cæsium electrode.

III. RESULTS

1. ABSOLUTE INTENSITIES

The curves of Figure 1 give the results of the intensity measurements. The intensities are given in ergs in a micron wave-length range emitted by a square centimeter of the electrode surface and for a current density of 1 ampere per square centimeter.[3] The measurements are given together in one figure in order to illustrate the similarity between the metals. It will be seen from the following paragraph that the differences between them are not much greater than the experimental uncertainty.

2. EXPERIMENTAL UNCERTAINTY

A series of measurements on tungsten electrodes will illustrate the influence of various factors on the intensity and the magnitude of the experimental uncertainty. An electrode near the cathode yielded 4.5 ergs per ampere at 3,700 A for electron energies of 6.5 volts; in the positive column, 15 cm from the cathode, 4.1 ergs were obtained; the filament electrode, which could be cleaned and outgassed by heating to incandescence, gave 5.6 ergs. The first two electrodes were outgassed at 400° C. and cleaned by ion bombardment. The agreement is fair and shows that the latter method of outgassing and cleaning is satisfactory and that contamination by material evaporated from the cathode is not serious. Fluctuations in check measurements were usually of the magnitude illustrated above. As causes of the variations there may be mentioned, in addition to surface contamination and photometric difficulties, the uncertainties in the current collecting area of electrodes due to variation in fit between the glass insulators and the metal cylinder.

3. RADIATION FROM CONTAMINATED SURFACES

Before cleaning by ion bombardment the electrodes were sometimes visibly stained. The radiation from such surfaces was usually very intense; after a few seconds ion bombardment the intensity would drop to a much lower value. Changes could usually be detected, however, after an hour's cleaning by ion bombardment.[4] It was suspected in some cases that a layer of tungsten oxide evaporated from the tungsten cathode might be responsible for the intense radiation. Measurements were, therefore, made with a layer of tungsten oxide evaporated upon the electrode from a near-by oxidized tungsten filament. The radiation was found to be ten times more intense than that from a metal, but to have about the same intensity distribution between 4,500 and 2,700 A. Measurements made at low voltage indicated a work function of about 2.4 volts, somewhat higher than that for a metal in cæsium vapor. The surface layer was, however, soluble in water and was probably a compound of cæsium and tungsten oxide formed during evaporation in the presence of cæsium vapor. A grayish white layer of oxide, formed during evaporation in the absence of cæsium, emitted radiation two or three times stronger than the metallic radiation.

[3] The variation of intensity with angle is supposed to be similar to that of a black body.

[4] Publishe l data on sputtering indicates that the ion current densities used here remove of the order of an atomic layer in a second.

The measurements of the radiation from aluminum previously reported were from a contaminating layer which seems to form upon an aluminum surface in a cæsium discharge. The peculiar minimum in the voltage intensity relation reported in the earlier paper is characteristic of this layer and not of aluminum.

IV. DISCUSSION

The fact that the radiation from cæsium is similar to that from other metals is of some interest in connection with the theory of its origin. One possibility is that the radiation is analogous to the continuous X-ray spectrum and is produced by the deceleration of the bombarding electrons in the fields of the metal atoms. Another suggestion supposes that the primary electron ejects a free electron from the metal and that another free electron then falls into the vacated level with emission of radiation. The latter explanation would predict that, for sufficiently great energy of the bombarding electrons, the spectrum would possess a fixed short wave-length limit, the frequency of which corresponds to the energy spread of the free electron levels. For most metals the width of these levels is of the order of 10 volts and the limit would lie in the far ultra-violet. For cæsium, however, this width, according to most writers,[5] is near 2 volts and the cæsium spectrum should have a high frequency limit in the red or yellow. Since this is not observed one may conclude that the "bremsstrahlung" explanation is probably the correct one.

This view is suggested by the observations of O. W. Richardson and his coworkers [6] that the total intensity of soft X rays produced by 300 to 6,000 volt electrons is very nearly independent of the metal from which the target is made. The extreme variation between 14 metals was less than twofold. This fact is analogous to the similarity of the radiative properties of metals in the low-voltage region described in the present paper, and suggests that the phenomena have a common origin.[7]

The observed intensity may be compared with that predicted by quantum theory for the continuous radiation generated by slow electrons impinging on protons.[8] The radiation emitted in ergs in frequency range $d\nu$ is

$$J(\nu) = g32\,\pi^2\,Z^2\,e^6\,d\nu/3\sqrt{3}c^3m^2v^2 \qquad (1)$$

The intensity is given in ergs per proton for a current of 1 electron passing through a square centimeter in a second. Z is the charge on the proton; e, m, and v are the charge, mass, and velocity of the electron; g is a numerical factor equal to unity classically, and also in the quantum theory for the case of slow electrons.

It is of interest to compute the intensity radiated by 6-volt electrons, for example, falling on a monatomic layer of protons (0.25×10^{16} on a square centimeter). In the units of Figure 1, one obtains at 3,000 A roughly 80 ergs, about ten times greater than is observed.

[5] Ig. Tamm, Phys. Rev., vol. 39, p. 170, 1932.
[6] O. W. Richardson and F. S. Robertson, Proc. Roy. Soc., vol. 124, p. 188, 1929.
[7] The similarity is surprising when one considers the extreme difference in the properties of tungsten and cæsium, for example: the atomic volume of cæsium is seven times that of tungsten; the spread of energies of the free electrons in tungsten is perhaps three or four times that of cæsium; tungsten has the highest melting point of the metals, while cæsium was a liquid under the conditions of the measurements.
[8] A. W. Maue, Ann. der Physik, vol. 13, p. 161, 1932.

When it is considered that many layers of charged centers contribute to the radiation in the experimental case of electrons striking a metal, the discrepancy becomes even greater.[9] "Z" was made unity in the computation because the field of the singly charged nucleus was thought to represent more nearly the fields actually encountered by the bombarding electrons.

Leo Neledsky [10] has computed the intensity to be expected when the nucleus is surrounded by its shielding electrons. Using a rough model of such a system of charges, he obtained values much lower than those given by equation (1) and in better agreement with the observed magnitudes. The classical explanation is of course that the external electrons prevent the bombarding electrons from approaching near the nucleus where most of the radiation is emitted.

WASHINGTON, June 20, 1932.

[9] The agreement with the theoretical intensity for thick targets reported in an earlier paper was due to the use of the Thomson-Whiddington formula for the depth of penetration of electrons into metals. This relation can not be applied to slow electrons.

[10] Leo Neledsky, Phys. Rev., vol. 39, p. 552, 1932. (Abstract.)

A SIMPLIFIED PRECISION FORMULA FOR THE INDUCTANCE OF A HELIX WITH CORRECTIONS FOR THE LEAD-IN WIRES

By Chester Snow

ABSTRACT

A precision formula is here given for the self inductance of a single-layer helix wound with ordinary round wire. This is neither more nor less accurate than that previously published, from which it has been derived by evaluating certain correction terms and replacing them by approximation formulas which are much simpler to compute.

CONTENTS

	Page
I. Introduction	419
II. Tranfsormation of $B_0(k)$	420
III. Transformation of $B_1(k)$	423
IV. Corrections due to lead-in wires	424

I. INTRODUCTION

The formula derived in this paper is a modification, without loss of precision, of the expression for the inductance of a single-layer helix of round wire, given in Bureau of Standards Scientific Paper No. 337 (vol. 21, p. 431, 1926–27). The notation has been changed, and the correction terms transformed so that the present formula is more simple from the point of view of the computer.

The diameter of the wire is d; the mean diameter of the solenoid is D; and its length l is the axial distance from the center of the wire at the begininng of the first turn to the center of the wire at the end of the N^{th} turn, N being the total turns so that the pitch of the winding is l/N. The modulus k of the complete ellipitic integrals K and E is given by

$$k^2=\frac{D^2}{l^2+D^2}$$

The principal term L_s is the current-sheet formula of Lorenz.

$$L_s=\frac{4\pi N^2}{3}\sqrt{l^2+D^2}\left[K-E+\frac{D^2}{l^2}\,(E-k)\right] \tag{1}$$

As one of the correction terms there appears M, the mutual inductance between the two end-circles of the solenoid, which is computed by

$$M=4\pi D\left[\frac{K-E}{k}-\frac{k}{2}K\right] \tag{2}$$

The inductance L of an actual helix is (to a precision which neglects terms of the order of $\left(\frac{l}{ND}\right)^3\log\frac{l}{ND}$)

$$L=L_s+\pi D\left[2N\left(ln\frac{l}{Nd}-0.89473\right)+\frac{1}{3}ln\frac{N\pi D}{l}\right]+lP\left(\frac{l}{D}\right)$$
$$-\frac{1}{6}M-\frac{2}{\pi}\sqrt{l^2+D^2}\,(E-k)\left[2\pm\left(\frac{N\pi d}{2l}\right)^2\right]$$
$$-\frac{l\pi}{2}\left[1-\frac{l}{D}sin^{-1}\frac{D}{\sqrt{l^2+D^2}}\right]$$

where

$$P(\eta)=\frac{1}{4\eta^2}+2ln4\eta \text{ when } \eta\geqq 1$$
$$=3\eta-\eta ln\eta \text{ when } \eta\leqq 1$$

The ambiguous sign is plus for the "natural" and minus for the uniform distribution of current over the section of the wires. A current density inversely proportional to the distance from the axis of the solenoid is called the natural distribution.

The formula for L here given is obtained by change of notation and by transformation of the function $A_2(k)$ in formula (114) of the paper cited. (This formula contains a misprint in the term $\frac{1}{3}\log$ which should be $\frac{1}{3}\log\frac{a}{p}$). In the present notation this formula is

$$L=L_s+\pi D\left[2N\left(ln\frac{l}{Nd}-0.89473\right)+\frac{1}{3}ln\frac{N\pi D}{l}\right]$$
$$+\pi DA_2(k)\mp\frac{2}{\pi}\sqrt{l^2+D^2}(E-k)\left(\frac{N\pi d}{2l}\right)^2$$

The function $A_2(k)$ is defined by formula (89)

$$A_2(k)=\frac{4}{\pi^2}[B_0(k)-B_1(k)+B_2]\ +0.66267-\frac{1}{3}ln\pi$$

The numerical quantity B_2 was defined in (90) as a series which has been found to be -0.60835. Hence

$$\pi DA_2(k)=D\left[\frac{4}{\pi}(B_0(k)-B_1(k))+0.11\right]$$

The term 0.11 in the parenthesis will be omitted since 0.1 D will be considered negligible in this small correction term. As most solenoids to be used as precision standards would have an inductance greater than 10 millihenries (10^7 cm), it is evident that with a diameter of say 30 cm, 0.1 D would be 3 cm, which is about 3 parts in 10,000,000. Hence, in the transformations of $B_0(k)$ and $B_1(k)$ which follow, terms of the order of 0.1 may be considered negligible.

II. TRANSFORMATION OF $B_0(k)$

On page 507 of the paper quoted, B_0 is given by

$$B_0(k)=1-\frac{E(k)}{k}+\frac{\sqrt{1-k^2}}{k}\int_k^1\frac{K(x)dx}{x\sqrt{1-x^2}}$$

If we let

$$\eta=\frac{\sqrt{1-k^2}}{k} \text{ and } x^2=\frac{1}{1+\lambda^2} \text{ and}$$

$$P(\eta)\equiv\frac{4}{\pi}\int_k^1\frac{K(x)dx}{x\sqrt{1-x^2}}=\frac{4}{\pi}\int_0^\eta\frac{d\lambda}{\sqrt{1+\lambda^2}}K\left(\frac{1}{\sqrt{1+\lambda^2}}\right)$$

$$=\frac{4}{\pi}\int_0^{\frac{\pi}{2}}d\theta\int_0^{\frac{\pi}{2}}\frac{d\lambda}{\sqrt{\lambda^2+sm^2\theta}}=\frac{4}{\pi}\int_0^{\frac{\pi}{2}}\log\left[\frac{\eta+\sqrt{\eta^2+\sin^2\theta}}{\sin\theta}\right]d\theta \tag{7}$$

then (6) gives

$$\frac{4D}{\pi}B_0(k)=-\frac{4}{\pi}\sqrt{l^2+D^2}\,[E(k)-k]+lP\left(\frac{l}{d}\right) \tag{8}$$

We may evaluate $P(\eta)$ first for the case where $\eta\geqq1$; that is, where $l\geqq D$. Using the formula

$$\int_0^{\frac{\pi}{2}}\log\sin\theta\,d\theta=-\frac{\pi}{2}\log 2$$

we may write (7) in the form

$$P(\eta)=2\log 2+\frac{4}{\pi}\int_0^{\frac{\pi}{2}}\log\,(\eta+\sqrt{\eta^2+\sin^2\theta})\,d\theta$$

$$=2\log 2\eta+\frac{4}{\pi}\int_0^{\frac{\pi}{2}}\log\left(1+\sqrt{1+\frac{\sin^2\theta}{\eta^2}}\right)d\theta$$

or since (for $\eta\geqq1$)

$$\log\left(1+\sqrt{1+\frac{\sin^2\theta}{\eta^2}}\right)=\log 2-\frac{1}{2\sqrt{\pi}}\sum_{n=1}^{\infty}\frac{(-1)^n}{n}\frac{\Gamma\left(n+\frac{1}{2}\right)}{\Gamma(n+1)}\frac{\sin^{2n}\theta}{\eta^{2n}}$$

$$P(\eta)=2\log 4\eta+\frac{1}{4\eta^2}-\sum_{n=2}^{\infty}\frac{(-1)^n}{n}\left[\frac{1.3.5\ \ldots\ (2n-1)}{2.4.6\ \ldots\ 2n}\right]^2\frac{1}{\eta^{2n}} \text{ if } \eta\geqq1 \tag{9}$$

Since the sum of this alternating series is numerically less than the value of its first term $\frac{9}{128\eta^4}$, which is never greater than about $\frac{1}{14}$ if $\eta\geqq1$, it is sufficient to take

$$P(\eta)=2\log 4\eta+\frac{1}{4\eta^2} \qquad \text{when } \eta\geqq1 \tag{10}$$

When $\eta=1$ this becomes $2\log 4+\frac{1}{4}=3.02$ while the exact expression (9) becomes 2.98. We may, therefore, take $P(1)=3$. On the other hand, when $0\leqq\eta\leqq1$, the approximation

$$P\,(\eta)=3\eta+\eta\log\frac{1}{\eta} \qquad \text{when } 0\leqq\eta\leqq1 \tag{10}'$$

will be in error by not more than 0.1. This may be seen from the fact that (10)′ is correct at $\eta=0$ and $\eta=1$, while the error between 0 and 1 is

$$Y(\eta)\equiv 3\eta+\eta\log\frac{1}{\eta}-P(\eta)$$

which has its greatest numerical value when

$$\eta=\frac{\sqrt{1-k^2}}{k}=0.34904$$

corresponding to $k^2=0.8914$. This is the root of the equation

$$Y'(\eta)=0=2+\log\frac{1}{\eta}-P'(\eta)=2+\frac{1}{2}\log\frac{k^2}{1-k^2}-\frac{4k}{\pi}K_{(k)}$$

To estimate this greatest error, we may obtain an upper and lower limit to $P(\eta)$ as follows:
Write

$$P(\eta)=\log 4+\frac{1}{\pi}\int_0^{\pi}\log\,(\eta+\sqrt{1+\eta^2-\cos^2\theta})^2 d\theta$$

$$=\log 4+\frac{1}{\pi}\int_0^{\pi}\log\,(1+2\eta^2-\cos^2\theta+2\eta\sqrt{1+\eta^2-\cos^2\theta})\,d\theta$$

Now

$$2\eta\sqrt{1+\eta^2-\cos^2\theta}=2\eta\sqrt{1+\eta^2}-\frac{\eta}{\sqrt{1+\eta^2}}\cos^2\theta-Z\,(\eta,\,\theta)$$

where

$$Z\,(\eta,\,\theta)=\frac{\eta\sqrt{1+\eta^2}}{\sqrt{\pi}}\sum_{s=2}^{\infty}\frac{\Gamma\left(s-\frac{1}{2}\right)}{\Gamma(s+1)}\,k^{2s}\cos^{2s}\theta$$

where

$$k^2=\frac{1}{1+\eta^2}$$

The function Z is never negative. It vanishes when $\theta=\frac{\pi}{2}$ and has its greatest value when $\theta=0$ and $\theta=\pi$ which is

$$Z\,(\eta,\,\theta)=\frac{\eta(\sqrt{1+\eta^2}-\eta)^2}{\sqrt{1+\eta^2}}$$

Hence $P(\eta)$ may be written in the form

$$P(\eta)=\frac{1}{\pi}\int_0^{\pi}\log 4\left\{(\sqrt{1+\eta^2}+\eta)^2-Z(\eta,\,\theta)-\left(\frac{\sqrt{1+\eta^2}+\eta}{\sqrt{1+\eta^2}}\right)\cos^2\theta\right\}d\theta$$

If in this integral we replace the variable function $Z(\eta,\,\theta)$ by its smallest value, zero, we get a function $F(\theta)$, which is an upper limit for $P(\eta)$ for all values of η.

$$F(\eta)\equiv\frac{1}{\pi}\int_0^{\pi}\log 4\left\{(\sqrt{1+\eta^2}+\eta)^2-\left(\frac{\sqrt{1+\eta^2}+\eta}{\sqrt{1+\eta^2}}\right)\cos^2\theta\right\}d\theta$$

If we replace $Z(\eta,\theta)$ by its greatest value, we get a function $f(\eta)$ which is a lower limit to $P(\eta)$ for all values of (η) where

$$f(\eta)\equiv\frac{1}{\pi}\int_\delta^\pi \log 4\left\{(\sqrt{1+\eta^2}+\eta)^2-\frac{\eta(\sqrt{1+\eta^2}-\eta)^2}{\sqrt{1+\eta^2}}-\left(\frac{\sqrt{1+\eta^2}+\eta}{\sqrt{1+\eta^2}}\right)\cos^2\theta\right\}d\theta$$

That is $f(\theta) < P(\eta) < F(\eta)$ if $\eta>0$.

Both of these functions may be evaluated by means of the definite integral formula

$$\frac{1}{\pi}\int_0^\pi \log 4\ (a^2-b^2\cos^2\theta)\ d\theta=2\log\ (a+\sqrt{a^2-b^2})\ \text{if}\ a\geqq b$$

which gives

$$F(\eta)=2\log\ (\sqrt{1+\eta^2}+\eta)\left(1+\sqrt{\frac{\eta}{\sqrt{1+\eta^2}}}\right)$$

$$f\ (\eta)=2\log\left(2\eta+\sqrt{1+4\eta^2+\frac{\eta}{\sqrt{1+\eta^2}}}\right)$$

This gives

$$F(0)=0,\ F(1)=2.984$$

$$f(0)=0,\ f(1)=2.958$$

At the point of maximum error in the range $0<\eta<1$, which is at $\eta_1=0.349$, we find

$$\left.\begin{matrix}F(\eta_1)=1.581\\ f(\eta_1)=1.431\end{matrix}\right\}\text{whence}\ P(\eta_1)=1.506\ \pm 0.075$$

and

$$3\ \eta_1+\eta_1\log\frac{1}{\eta_1}=1.415$$

which shows that the maximum error made by using (10)′ for $P(\eta)$ is approximately 0.1 in the range $0\leqq\eta\leqq 1$.

III. TRANSFORMATION OF $B_1(k)$

The function $B_1(k)$ is defined in the paper quoted, on page 453, by

$$kB_1(k)=\frac{\pi^2}{12}\ E(k)-\int_0^{\frac{\pi}{2}}\theta^2\sqrt{1-k^2\sin^2\theta}d\theta$$
$$-\left(1-\frac{k^2}{2}\right)\left[\frac{\pi^2}{12}K(k)-\int_0^{\frac{\pi}{2}}\frac{\theta^2d\theta}{\sqrt{1-k^2\sin^2\theta}}\right]$$

Now

$$\int_0^{\frac{\pi}{2}}\theta^2\sqrt{1-k^2\sin^2\theta}\,d\theta=\frac{\pi^2}{4}E(k)-\int_0^{\frac{\pi}{2}}\phi(\pi-\phi)\sqrt{1-k^2\cos^2\phi}d\phi$$

and

$$\int_0^{\frac{\pi}{2}}\frac{\theta^2d\theta}{\sqrt{1-k^2\sin^2\theta}}=\frac{\pi^2}{4}K(k)-\int_0^{\frac{\pi}{2}}\frac{\phi(\pi-\phi)}{\sqrt{1-k^2\cos^2\phi}}d\phi$$

Hence

$$\frac{4D}{\pi}B_1(k)=\frac{4\pi D}{6}\left[\frac{K(k)-E(k)}{k}-\frac{kK(k)}{2}\right]+DU(k)$$

where

$$U(k) \equiv -\frac{\pi k}{2}\int_0^{\frac{\pi}{2}} \frac{4\phi(\pi-\phi)}{\pi^2}\,\frac{\cos 2\phi}{\sqrt{1-k^2\cos^2\phi}}\,d\phi$$

The factor of the integrand $y(\phi)=\frac{4}{\pi^2}\phi\ (\pi-\phi)$ is represented by a parabola which vanishes when $\phi=0$ and has the maximum value unity when $\phi=\frac{\pi}{2}$, where it also has a horizontal slope. It is therefore very approximately the same as $\sin\phi$. Replacing it by $\sin\phi$ gives the sufficient approximation

$$U(k)=-\frac{\pi k}{2}\int_0^{\frac{\pi}{2}} \frac{\cos 2\phi \sin\phi}{\sqrt{1-k^2\cos^2\phi}}\,d\phi = \frac{\pi\sqrt{1-k^2}}{2k}\left[1-\frac{\sqrt{1-k^2}}{k}\sin^{-1}k\right]$$

$$=\frac{\pi l}{2D}\left[1-\frac{l}{D}\sin^{-1}\frac{D}{\sqrt{l^2+D^2}}\right]$$

Hence

$$\frac{4D}{\pi}B_1(k)=\frac{M}{6}+\frac{l\pi}{2}\left[1-\frac{l}{D}\sin^{-1}\frac{D}{\sqrt{l^2+D^2}}\right] \qquad (11)$$

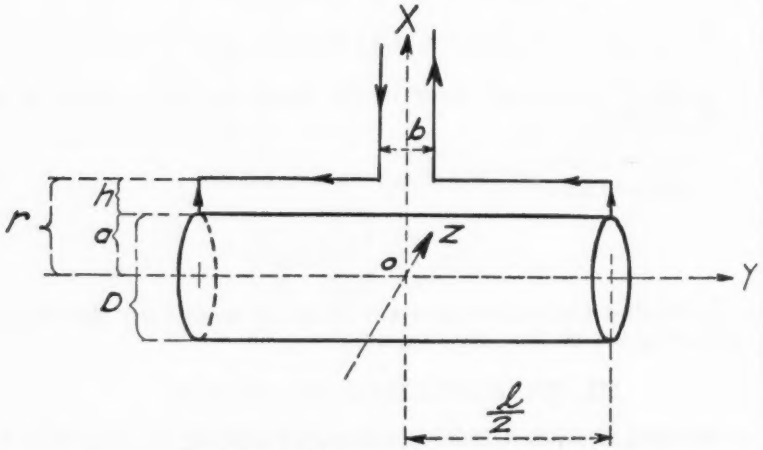

FIGURE 1.—*Arrangements of lead-in wires*

where M is defined by equation (2) and is obviously the mutual inductance between the two end circles of the solenoid. By use of equations (10) or (10)′ and (11), the equation (A) is transformed into formula (3) of this paper.

IV. CORRECTIONS DUE TO LEAD-IN WIRES

The inductance of the helix and lead-in wires together is

$$L'=L+L_1+2M_{hl}$$

where L is that of the helix given by formula (3), L_1 is the self-inductance of the lead-in wires and M_{hl} the mutual inductance between these wires and the helix. In computing M_{hl}, the helix may be considered a current sheet, and only its axial component

of current contributes to M_{hl}. If the leads are disposed as shown in Figure 1, it is evident that these leads which are perpendicular to the axis of the cylinder have no mutual inductance with the cylinder. The latter carries unit current in the $y=$direction so that the current density is $\frac{1}{2\pi a}=\frac{1}{\pi D}$. Consequently, the term M_{hl} is given by

$$M_{hl}=2\int_0^{b/2}A(r,\,y)dy-2\int_0^{l/2}A(r,\,y)dy \tag{12}$$

where

$$A\,(r,\,y)=\frac{1}{2\pi}\int_{-l/2}^{l/2}dy'\int_0^{2\pi}\frac{d\,\phi}{\sqrt{(y-y')^2+a^2+r^2-2\,a\,r\cos\phi}}$$

$$=\frac{2}{\pi}\int_{-l/2}^{l/2}dy'\int_0^{\pi/2}\frac{d\,\theta}{\sqrt{(y-y')^2+(a+r)^2-4\,a\,r\sin^2\theta}}$$

$$=\frac{2}{\pi}\int_0^{\frac{l}{2}+y}dz\int_0^{\pi/2}\frac{d\,\theta}{\sqrt{z^2+(a+r)^2-4\,a\,r\sin^2\theta}}$$

$$+\frac{2}{\pi}\int_0^{\frac{l}{2}-y}dz\int_0^{\pi/2}\frac{d\,\theta}{\sqrt{z^2+(a+r)^2-4\,a\,r\sin^2\theta}}$$

or

$$A\,(r,\,y)=\frac{2}{\pi}\int_{k_y}^{1}\frac{d\,x}{x\sqrt{1-x^2}}\,K\left(\frac{2\sqrt{ar}}{a+r}x\right)+\frac{2}{\pi}\int_{k_{-y}}^{1}\frac{d\,x}{x\sqrt{1-x^2}}\,K\left(\frac{2\sqrt{ar}}{a+r}x\right) \tag{13}$$

where

$$\frac{1}{k_y{}^2}=1+\left(\frac{\frac{l}{2}+y}{a+r}\right)^2 \tag{14}$$

As a special case of this

$$A\,(a,\,o)=\frac{4}{\pi}\int_{k_o}^{1}\frac{K\,(x)\,d\,x}{x\sqrt{1-x^2}}=P\,(\eta_0)\text{ by (7)} \tag{15}$$

Where

$$k_0{}^2=\frac{1}{1+\left(\frac{l}{4\,a}\right)^2}=\frac{1}{1+\left(\frac{l}{2\,D}\right)^2}\text{ and }\eta_0=\frac{l}{2\,D} \tag{16}$$

Now since b and $r-a=h$ are both small, we may write

$$2\int_0^{b/2}A(r,y)dy=2A(a,0)\int_0^{b/2}dy=bA(a,0)=bP(\eta_0) \tag{17}$$

In the first integral of (12) we may write

$$A(ry)=A(a+h,y)=A(a,y)+h\left[\frac{\partial A(r,y)}{\partial r}\right]_{r=a}$$

Computing $\left[\frac{\partial A(ry)}{\partial r}\right]_{r=a}$ from (13), since $\left[\frac{\partial}{\partial r}\frac{2\sqrt{ar}}{a+r}\right]_{r=a}=0$,

one obtains after placing $r=a$

$$\frac{\partial k_y}{\partial r}=\frac{k_y(1-k^2{}_y)}{D} \text{ and } \frac{\partial k_{-y}}{\partial r}=\frac{k_{-y}(1-k^2{}_{-y})}{D}$$

so that

$$-2h\int_0^{l/2}\left[\frac{\partial A(r,y)}{\partial r}\right]_{r=a}dy=\frac{4h}{\pi D}\left[\int_0^{l/2}\sqrt{1-k^2{}_y}\,K(k_y)dy+\int_0^{l/2}\sqrt{1-k^2{}_{-y}}\,K(k_{-y})dy\right]$$

where

$$k^2{}_y=\frac{1}{1+\left(\frac{l/2+y}{D}\right)^2}$$

Changing the variable of integration from y to k_y gives

$$-2h\int_0^{l/2}\left[\frac{\partial A(ry)}{\partial r}\right]_{r=a}dy=\frac{4h}{\eta}\left[-\int_{k_0}^{k}\frac{K(x)dx}{x^2}+\int_{k_0}^{1}\frac{K(x)dx}{x^2}\right]=\frac{4h}{\pi}\int_k^1\frac{K(x)dx}{x^2}$$

$$=\frac{4h}{\pi k}\left[E(k)-k\right] \text{ where } k^2=\frac{D^2}{l^2+D^2} \tag{18}$$

Similarly

$$-2\int_0^{l/2}A(a,y)\,dy=-\frac{4}{\pi}\left[\int_0^{l/2}dy\int_{k_y}^1\frac{K(x)dx}{x\sqrt{1-x^2}}+\int_0^{l/2}dy\int_{k_y}^1\frac{K(x)dx}{x\sqrt{1-x^2}}\right]$$

$$=-\frac{4D}{\pi}\int_k^1\frac{dz}{z^2\sqrt{1-z^2}}\int_z^1\frac{K(x)dx}{x\sqrt{1-x^2}}=-\frac{4D}{\pi}B_0(k) \tag{19}$$

Adding (17), (18), and (19) gives by (12)

$$M_{hl}=\frac{4}{\pi}\left[-DB_0(k)+\frac{h(E(k)-k)}{k}\right]+bP(\eta_0) \tag{20}$$

where

$$k^2=\frac{1}{1+\frac{l^2}{D^2}} \text{ and } k_0{}^2=\frac{1}{1+\left(\frac{l}{2D}\right)^2}$$

By use of (8) this may be put in the general form

$$M_{hl}=\left(1+\frac{h}{D}\right)\sqrt{l^2+D^2}\cdot\frac{4}{\pi}\left[E-k\right]-lP\left(\frac{l}{D}\right)+bP\left(\frac{l}{2D}\right) \tag{21}$$

where $P(x)$ is defined by (4).

WASHINGTON, June 17, 1932.

REGISTER STUDIES IN OFFSET LITHOGRAPHY

By C. G. Weber and R. M. Cobb [1]

ABSTRACT

A serious economic waste in offset lithography results from lack of knowledge of the optimum printing properties of lithographic papers. The most important losses result from register difficulties, and studies of register have comprised a large part of the research on lithographic papers now being carried on at the Bureau of Standards in cooperation with the Lithographic Technical Foundation. Information on factors influencing register was obtained by making experimental printings in a commercial plant under routine operating conditions. The paper samples used were prepared by cooperating manufacturers, knowledge of the history of manufacture of the papers was supplemented by complete laboratory analyses, and their response to offset printing in controlled atmosphere was observed to find the influence of paper characteristics on register of prints. Most satisfactory register was obtained with the papers that had received the least drastic processing of fibers in manufacture. Internal sizing in machine-finish and coated papers appeared essential, but the amount used, within normal limits, was not important. Thorough conditioning of paper to equilibrium with pressroom atmosphere before the first printing was required to obtain register on subsequent printings, and the longest seasoning period practicable between printings was found desirable. Closeness of register was also influenced by variations in pressure, ink, and water used in printing and by uniformity of plates in respect to thickness. An accurate rule of special design for measuring prints and a sword type of hygroscope for determining the hygrometric state of paper were found invaluable in the plant studies.

CONTENTS

	Page
I. Introduction	427
II. Behavior of paper on the offset press	428
III. Description and properties of samples	429
IV. Technique in experimental printings	431
V. Results of studies of factors influencing register	431
1. Atmospheric	432
2. Mechanical	434
3. Water and ink	437
4. Paper properties	437
5. Incidental handling	438
VI. Summary	439
VII. Acknowledgment	440

I. INTRODUCTION

The Bureau of Standards is cooperating with the Lithographic Technical Foundation in a study of the offset lithographic process. The work was undertaken at the request of the foundation. This technical organization of the domestic lithographic industry comprises over 400 members, including lithographic concerns, paper manufacturers and dealers, ink and varnish manufacturers, press and machinery manufacturers, metal lithographers, litho finishers, and photo-composing machine manufacturers. The research is being

[1] Research associate, representing the Lithographic Technical Foundation.

carried on with the advice and active cooperation of an advisory committee from the foundation under the chairmanship of R. F. Reed, director of the department of lithographic research, University of Cincinnati. The study was requested because the industry suffers an enormous annual loss resulting from lack of scientific knowledge concerning the characteristics of paper required for optimum results in offset printing. The principal limiting factor in production is apparently the failure of paper to meet the requirements of the modern high-speed offset press, and it has been conservatively estimated that not over 75 per cent of the theoretical production of the average press is attained for that reason.

Preliminary investigational work was previously done by the bureau[2] for the purpose of finding the principal difficulties in offset lithography for which paper is wholly or partly responsible. A survey was made of 31 lithographic plants, and the results served as a basis for planning the present study. Misregister was the most serious difficulty found; therefore, a study of the register of prints was undertaken first, and this article deals with some results already obtained.

A series of practical printing tests were made in the Buffalo, N. Y., plant of the American Lithographic Co. under routine operating conditions to isolate and study the important factors influencing the closeness of register. An air-conditioned pressroom was selected in order to eliminate variables due to changes in atmospheric humidity. By using specially prepared papers, of which the history of preparation as regards composition, degree and kind of sizing, degree of hydration of fibers, and fiber length were known, information relative to the influence of paper characteristics on closeness of register was developed. Printing identical papers on a press with controlled variations of such factors as pressure, water, and ink gave information on the effects of press variables. The papers used in experimental printings were subjected to complete laboratory tests of physical properties, composition, water penetration, and behavior under tension at different humidities to obtain information for correlation with results developed relative to the response of the papers to the printing tests.

II. BEHAVIOR OF PAPER ON THE OFFSET PRESS

The offset lithographic process is indirect in that the print is transferred from the plate to the paper by means of a rubber blanket. Three cylinders of the same dimensions run one against another in fixed positions with a gear on the end of each engaged with a similar gear on the next. The cylinders are driven through these gears, providing the same speed of rotation for all. They rest one against another with fixed pressure on narrow metal bands, known as bearers, at the ends of the cylinders. The plate with a positive image is clamped around the first or plate cylinder and this bears against the second or blanket cylinder which is covered with a thin rubber blanket. The blanket cylinder bears against a third cylinder known as the impression cylinder. In operation, the plate after being progressively moistened and inked, prints on the rubber blanket which in turn deposits the print on the paper pressed against it by the impression cylinder.

[2] The preliminary work was done by F. H. Thurber, formerly an associate scientist at the Bureau of Standards.

The dimensions of paper may change during passage through the press or between printings, and the nature and extent of such changes determine, largely, the closeness of register in subsequent printings. Changes in length in the short or around-the-cylinder direction are relatively unimportant because any reasonable change in this dimension can be compensated for by press adjustments. However, changes in dimension in respect to the length along the back edge (long direction) always result in register difficulties. In passage through the press, paper does one of three things in respect to length along the back edge before the instant of taking the print. It shortens or "pulls in," remains unchanged, or lengthens by "fanning-out" under stress. If the paper has stretched before taking the impression and recovers afterward with resultant contraction of the printed design, the resulting print will be shorter than the plate image and, if after taking the print the paper expands, the print will be longer than the image.

Register will be obtained regardless of changes in the paper, if at the instant of taking the succeeding print the paper responds in such a manner as to bring the preceding print back to exactly blanket image length. Misregister will occur if the preceding print is not brought to image length. Hence, paper can change in length as measured and the print stay in register; while paper may show no change in length as measured and yet be out of register. A consideration of the mechanics involved indicates that there is much more chance of a short first print stretching or "fanning-out" to plate image length, to obtain register as it takes the next print, than there is of a long print being shortened or "pulled in" to plate image length as it takes the next print. Therefore, papers that expand after taking a print, that is, "print longer than the plate image," are particularly prone to give misregister.

III. DESCRIPTION AND PROPERTIES OF THE EXPERIMENTAL PAPERS

The papers used in the experimental printings were studied in the laboratory in order to obtain complete information for correlation with their response to the printing processes. Through the cooperation of paper manufacturers, four papers of the same composition with different degrees of beating, the same papers with surface sizing, three coated papers differing as to the degree of sizing in the raw stock (paper before coating), and three extra strong machine-finish papers differing as to degree of internal sizing were made available for the studies. The properties of the papers as indicated by the test data for them are given in Table 1. All were chemical wood papers.

Since mechanical deformation of paper is a factor in obtaining register, laboratory studies were made of the elongation of various samples of lithographic papers under tension. Eleven papers were conditioned and tested in atmospheres of 30, 45, 65, and 75 per cent relative humidity. Tensions of from 9 to 455 g were applied to specimens 15 mm wide and the elongation for each increment of tension was observed by means of a horizontal microscope. The results did not indicate any significant differences in elongation between the various samples tested which included machine-finish litho, supercalendered litho, coated litho, and surface-sized paper.

The greatest differences in the elongation of the different papers occurred at 75 per cent relative humidity and there the widest difference was less than 0.1 per cent for the cross direction. Differences for the machine direction were much smaller. Such differences in expansion are not significant; however, the relation of relative humidity to expansion was significant. The minimum variation between the expansions of the different papers occurred at 45 per cent relative humidity and changes in expansion for changes in relative humidity were of smaller magnitude in the vicinity of 45 per cent relative humidity than at other humidities used. These results indicate definite advantages in the selection of an atmosphere of approximately 45 per cent relative humidity for lithographic plants.

TABLE 1.—*Test data of experimental papers*

Sample No.	Weight, 25 by 40 inches, 500 sheets	Thickness	Bursting strength[3]	Folding endurance[1]		Tensile properties[2]				Water resistance (Dry-indicator method)	Ash	Opacity
				Machine direction	Cross direction	Breaking load		Elongation at rupture				
						Machine	Cross	Machine	Cross			
	Pounds	*Inch*	*Points*	*Double folds*	*Double folds*	*kg*	*kg*	*Per cent*	*Per cent*	*Seconds*	*Per cent*	*Per cent*
1	78.1	0.0049	24.3	52	15	6.9	3.3	1.5	3.2	53.7	9.9	96.2
2	74.3	.0042	21.1	18	11	5.5	3.0	1.6	3.7	31.9	11.7	96.2
3	73.8	.0044	21.4	25	10	5.9	3.0	1.1	2.6	44.1	9.9	95.2
4	69.2	.0040	20.7	14	11	5.2	2.9	1.3	3.9	31.5	11.5	94.4
5	79.8	.0048	33.0	62	29	8.5	4.1	1.7	3.7	48.4	9.5	95.2
6	82.0	.0049	25.9	12	15	7.6	3.9	1.5	3.8	63.3	12.1	96.1
7	77.7	.0047	27.9	46	17	8.0	3.8	1.3	3.7	43.4	9.1	94.4
8	76.6	.0047	25.1	14	10	7.1	3.8	1.5	4.2	55.3	10.5	95.6
9	70.2	.0032	21.7	55	10	5.5	2.6	2.3	3.1	19.1	35.7	95.1
10	75.3	.0036	22.8	48	16	5.9	2.8	2.1	3.6	23.1	33.6	95.5
11	76.2	.0037	21.2	38	12	5.4	2.6	2.1	3.4	26.3	35.2	96.4
13	56.3	.0033	20.0	28	12	5.9	2.8	1.5	3.3	12.1	7.2	87.7
14	54.4	.0034	19.6	24	10	5.5	2.5	1.6	3.4	19.3	8.0	88.4
15	53.9	.0032	20.1	26	11	5.5	2.5	1.5	4.0	25.9	8.0	88.9

[1] For test specimen, 15 mm wide and 90 mm between jaws.
[2] For test specimen, 15 mm wide and 100 mm between jaws.
[3] Bursting pressure in pounds per square inch through a circular orifice 1.2 inches in diameter.

Description of special papers

Sample No.	Description
1	Machine-finish litho, light beating, light jordanning.
2	Machine-finish litho, light beating, heavy jordanning.
3	Machine-finish litho, normal beating, light jordanning.
4	Machine-finish litho, normal beating, heavy jordanning.
5	No. 1 surface sized with starch.
6	No. 2 surface sized with starch.
7	No. 3 surface sized with starch.
8	No. 4 surface sized with starch.
9	Coated litho, no sizing in raw stock.
10	Coated litho, one-half normal sizing in raw stock.
11	Coated litho, normal sizing in raw stock.
13	Extra strong machine-finish litho with no sizing.
14	Extra strong machine-finish litho with one-half normal sizing.
15	Extra strong machine-finish litho with normal sizing.
12	Commercial machine-finish litho with which special papers were printed.

NOTE.—The papers were cut 38 by 52 inches with the long dimension in the machine direction of the paper.

IV. TECHNIQUE IN EXPERIMENTAL PRINTINGS

In the experimental printings to determine the relation between paper characteristics and closeness of register, the samples of experimental papers were inserted in the center of the piles and printed with papers being used for regular commercial multicolor printings requiring very close register. To determine the effects of press variables, one press was set aside for experimental work. This press was made ready with the plate at exactly bearer height and with a minimum pressure between the blanket and plate. The printing pressure was varied within closely controlled limits, while printing with a dry plate, with water alone, and with ink and no water to find the extent of effect of each of those factors on register.

Changes in paper dimensions were determined by means of a rule designed for measuring the displacement of reference marks on large sheets of paper. (Fig. 1.) It is equipped with two magnifying glasses, each with a small glass reticule having a vertical cross hair mounted directly underneath. One magnifier may be placed at any point within the range of the scale (24 to 64 inches) and readily set so that its cross hair will coincide with any division on the scale. The other magnifier (fig. 2) is set over the second reference point by means of micrometer adjustment. The distance between the reference points may then be read to 0.001 inch.

Data relative to dimension changes of papers were determined by measuring distances between register marks on the plate, distances between reference marks on the paper before printing and after each printing, and the distances between register prints after each printing. Length of plate image in the around-the-cylinder direction was measured on the press with a thin steel tape.

Since all changes in moisture content of paper are accompanied by dimension changes, a very careful check was maintained on the hygrometric state of the papers, especially in respect to the surrounding atmosphere. The sword type of paper hygroscope [3] was invaluable as a tool for determining quickly whether or not paper was in equilibrium with the pressroom atmosphere. The instrument resembles a sword, the blade of which contains a hygroscopic element. Expansion and contraction of the element actuate the pointer of an indicating device mounted on the handle of the instrument. The hygroscope is first set for the pressroom atmosphere by waving it in the air until the pointer comes to rest and then turning the dial to the position where the zero reference mark is directly under the pointer. The blade is then inserted between the sheets of the pile of paper to be tested, and left until the pointer comes to rest. Movement of the pointer from the zero reference mark indicates that the paper is not in equilibrium with the surrounding atmosphere.

V. RESULTS OF STUDIES OF FACTORS INFLUENCING REGISTER

The results of the printings in respect to permanent dimension changes (figs. 3 and 4), the relation of length of first print to plate image length with subsequent printings (fig. 7), and effects of press variables (figs. 5 and 6), are presented graphically.

[3] Robert F. Reed, The Paper Hygroscope, Sales Bull. No. 1. Research Series No. 6, Lithographic Technical Foundation, 220 East Forty-second Street, New York, N. Y.

A number of important factors were found to affect register in lithographic printing when constant atmospheric conditions were maintained and the response of papers of known history to a number of the factors was studied. Some study of mechanical factors was

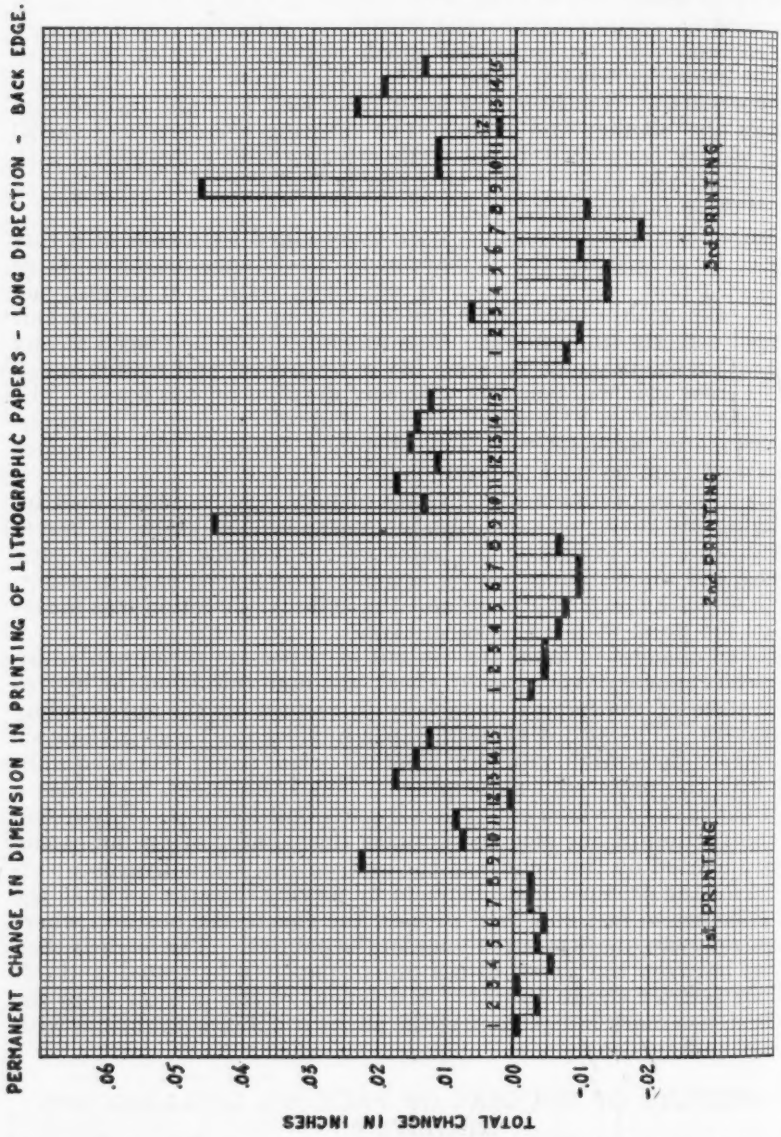

FIGURE 3

necessary in order to eliminate the variables not influenced by paper characteristics.

1. ATMOSPHERIC

The moisture content of the commercial papers as received at the plant was found to vary from 2.8 to 6.2 per cent while that required for hygrometric equilibrium with the press room atmosphere was

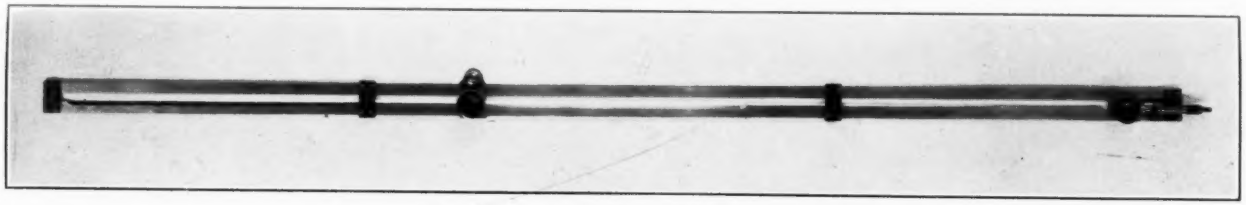

FIGURE 1.—*Special rule for lithography*

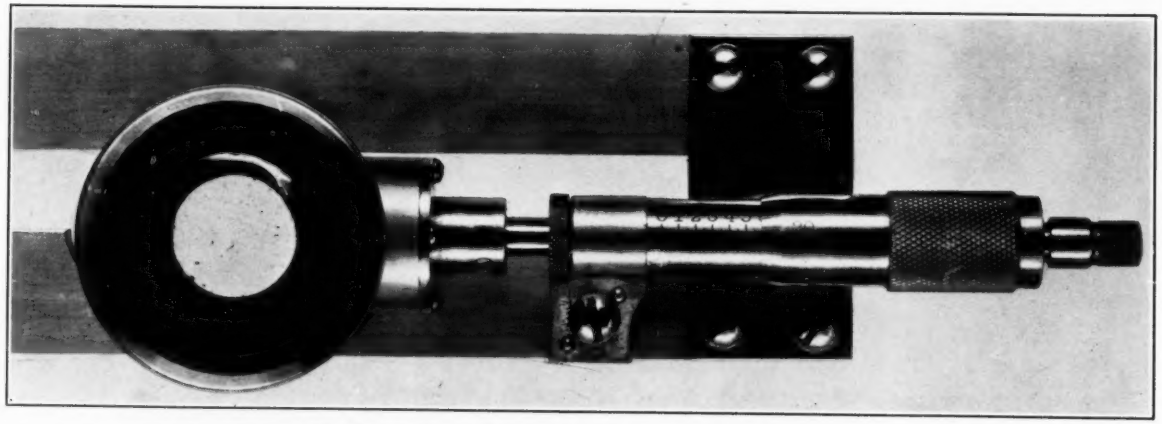

FIGURE 2.—*Rule magnifier with micrometer adjustment*

UNIV OF MICH

approximately 5.0 per cent. When cases of paper having a moisture content more than 1 per cent below room equilibrium were opened and exposed to room atmosphere in the pile, the exposed edges and top of the pile absorbed moisture and waves and wrinkles quickly developed from expansion of those portions. Excessive conditioning

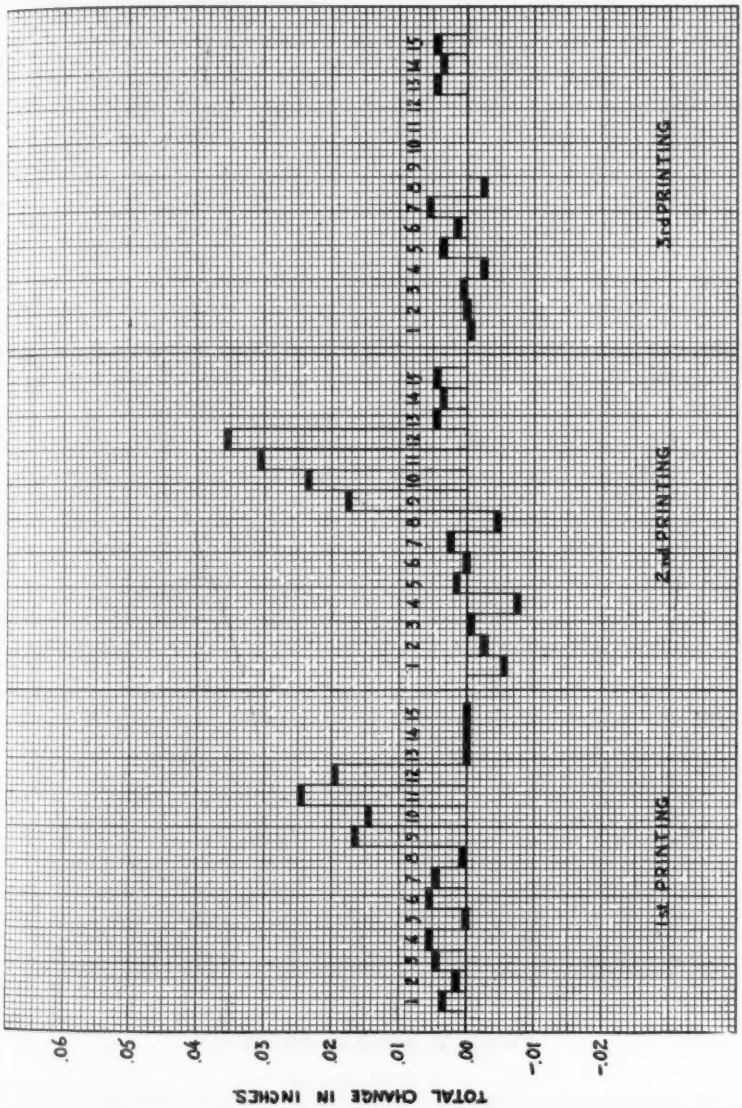

FIGURE 4

time was required for removal of such wrinkles and when they were not removed, misregister resulted as a result of the paper distortion. The benefits of controlled atmosphere in the press room are, of course, lost if the paper is not thoroughly conditioned before the first printing. It is important to remember that papers differ as to time required to

thoroughly condition them. Certain papers, such as moisture-resistant bond paper or paper badly out of equilibrium with press room atmosphere, require extra conditioning time.

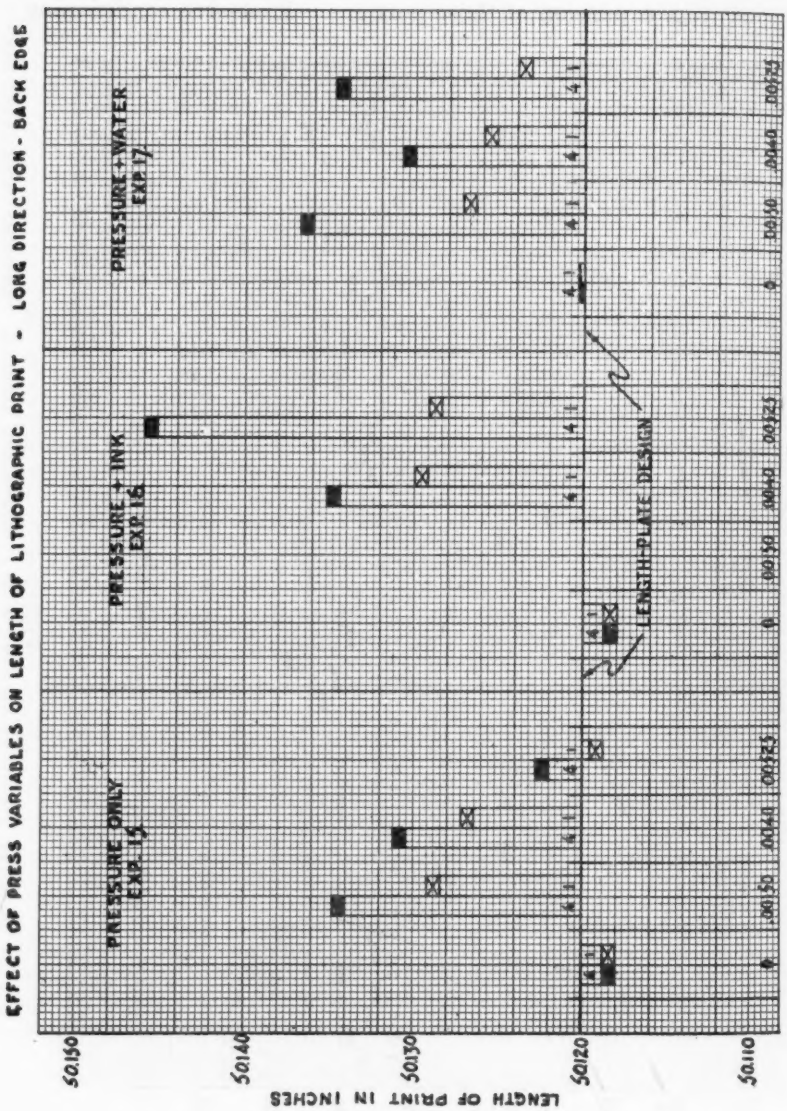

2. MECHANICAL

Thickness of plates and the stress applied in clamping them on the cylinder both influence the effective image length. The length is increased due to curvature in bending the plate around the cylinder and the amount of increase varies with the plate thickness, although no mathematical formula seems to apply. Increase in length of plate due to mechanical stress in clamping it varies inversely with its thick-

ness. All plates measured were from 0.050 to 0.085 inch longer in 35 inches in the around-the-cylinder direction, when clamped on the cylinder than when flat. From these considerations, thickness standardization for plates appears very important.

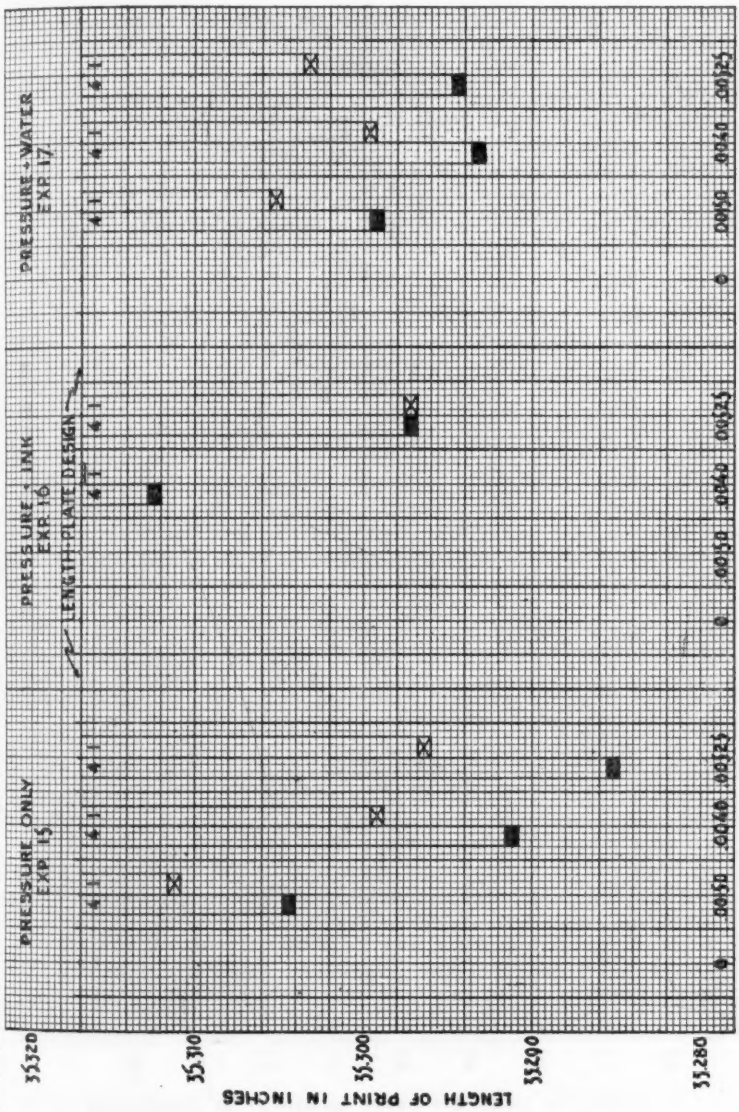

FIGURE 6

Studies were not made to determine the effects of packing under the plate and blanket. In the studies of other factors, the plate was built up to bearer height and the blanket overpacked 0.0025 to 0.003 inch, although it is common practice to build both plate and blanket above bearer heights. The bearers were 18 inches in diameter. With neither ink nor water on the plate, increase in pressure between the

blanket and paper decreased slightly the excess in length of print over plate image along the back. In the short direction, the print was shortened. With ink alone on the plate, the effect of pressure was less along the back edge, but was little changed in the short direction.

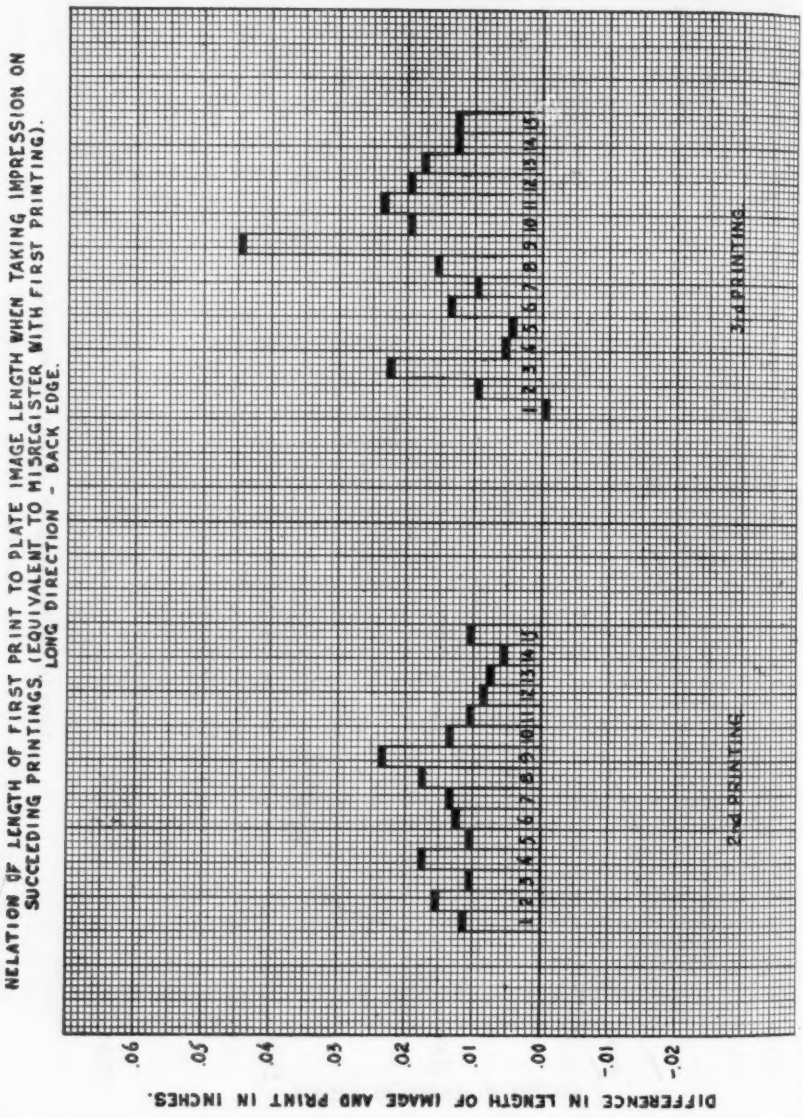

With water alone on the plate, the effects of increased pressure were less in both directions.

A print may be lengthened in the short or around-the-cylinder direction by removing packing from beneath the plate and placing it under the blanket. The increased length is caused by slippage introduced by increasing the circumference and thereby the peripheral

speed of the blanket, and decreasing the peripheral speed of the plate by decreasing its circumference. This slippage is probably taken up largely by blanket creep, but it results in an increase in the length of print corresponding to the difference between the effective cylinder circumferences. Contrary to rather common belief, the increase in plate image length due to change in curvature by removing packing was too slight to require consideration. However, the difference in peripheral speed between plate and blanket introduced by transferring 0.003 inch packing from the plate to the blanket was calculated to be 0.0191 inch in 35 inches. The length of print in the around-the-cylinder direction may also be increased by pasting a sheet of paper on the back cylinder. By this method the peripheral speed of the paper is increased, introducing between the blanket and paper a creeping or slippage which results in a longer print.

3. WATER AND INK

The water used on the press had two effects on the paper passing through the press. The immediate effect, due to absorption of moisture, was an expansion of about 0.005 inch in 50 inches. When conditioned until equilibrium with the atmosphere was again reached, the paper shrank to about 0.005 inch less than its original length, a phenomenon that has not been satisfactorily explained. Ordinarily, paper left in piles between printings is in a condition somewhere between the two extremes at the second printing. The amount of water used is apparently of little importance in respect to action of the paper during passage through the press. During a normal first printing, the moisture content increased about 0.1 per cent. Doubling the amount of water used had no serious immediate effect on the expansion and contraction of the paper.

Ink affects register to a degree contingent on the extent of the area covered. When printing large solid ink areas, the prints were longer than the plate image along the back edge, possibly a result of lubricating action of the ink in permitting the blanket to fan-out without taking the paper with it. Second prints on first prints containing large solid ink areas on which the ink was not entirely dry were short in the around-the-cylinder direction. This may have been due to an effect of the moist ink on the friction between the paper and the blanket, or it may have been due to increased elasticity of the paper, permitting more temporary stretch in the cross direction of the sheet. Ink tackiness was not studied, but is apparently important. These effects of water, ink, and pressure on length of print are shown graphically in Figure 5 (long direction, back-edge) and Figure 6 (short direction).

4. PAPER PROPERTIES

The degree of hydration and length of fibers of paper, which depend on the beating [4] and jordanning [5] the fibers have been given during manufacture, is extremely important. In studying the influence of

[4] Beating is the term applied to mechanical treatment given to paper-making materials, suspended in water, to prepare them for forming a sheet on the paper machine. Beating separates, brushes, and frays out the fibers and causes them to absorb water by a process known as "hydration."

[5] Jordanning is a refining process that usually follows beating to complete the preparation of the materials for forming a paper of the desired character. In the jordan the fibers are freed from lumps and cut to the desired length.

these factors on register, seven of the papers having the same composition, but with different beating, jordanning, and sizing treatments were inserted in the center of a pile of paper on a nine single-color run which required hairline register, and not separated from the pile until the nine printings were finished. The length of the first color (yellow) impression on each paper was measured and compared with those of the regular run. The sample with the least drastic beating and jordanning in its manufacture had the shortest first-color impression along the back edge and was the best as regards register, while the sample with the most drastic treatment in those respects was poorest. The sample with the least beating and jordanning had the longest first-color impression, hence was best in repsect to register in the around-the-cylinder direction, while the sample having the most drastic treatment was again poorest.

Samples of the eight papers (Nos. 1 to 8, Table 1) were also inserted in the center of a pile of commercial paper and printed six colors, two colors each printing. In these tests, as in the preceding, the sample that had the least drastic beating and jordanning was best in respect to register, and misregister increased with increased beating and jordanning. (Figs. 3 and 4.) These results indicate the desirability of manufacturing papers for lithography with the least beating and jordanning necessary to obtain satisfactory strength and printing surface.

The degree of internal sizing and the presence of surface sizing are factors. Surface sizing decreases slightly the dimension changes during printing, but did not have marked effect on the samples available. Increasing the internal (beater) sizing of coated papers reduced the tendency to stretch along the back edge, but was not as effective in the short direction. (Nos. 9, 10, 11, figs. 3, 4, 7.) The effects on register were slight. Paper with one-half normal sizing remained in register best in both directions. With extra strong machine-finished papers, increased degree of internal sizing improved the register on the back edge, but did not improve it in the short direction. (Nos. 13, 14, 15, figs. 3, 4, and 7.) One-half normal sizing was practically as effective as normal sizing. It appears that while internal sizing is desirable for good register, the amount used, within normal limits, was not a very important factor.

5. INCIDENTAL HANDLING

The time that paper is allowed to season between printings will influence results in subsequent printings. In a conditioned plant, it was found that the longest seasoning period practicable is desirable since the seasoning period permits an even distribution of moisture picked up in passing through the press and allows the paper to recover from stresses set up in printing.

Register can be controlled within certain limits by set-up of the feeders. By certain adjustments, a "dip" may be introduced in the sheet that will materially shorten long prints already on the sheet, and at the same time lengthen to somewhat smaller extent the current print. In one case noted, a red color found to be printing 48.866 inches along the back edge was 0.028 inch longer than a succeeding black. By pressing down on the sheet with a 1-inch roller 10 inches inside the edge, while the paper was being fed to the press, the current

black print was lengthened 0.004 inch along the back edge and the paper was drawn in to shorten permanently the preceding red print 0.020 inch. The resulting misregister was therefore reduced to 0.004 inch. Such methods can be employed satisfactorily only on the last printing.

VI. SUMMARY

In the plants having controlled atmosphere, thorough conditioning of paper is essential if the full benefits of atmospheric control are to be obtained. The moisture content of paper to be used in such plants should be adjusted at the paper mill to approach equilibrium with the pressroom conditions in order to facilitate conditioning. Paper badly out of equilibrium should be hung immediately after unwrapping. The hygroscopic condition of paper with reference to pressroom atmosphere in which it is unwrapped can be quickly determined with the sword-type hygrometer. The longest seasoning period practicable between printings is desirable for uniform results, and there appear to be definite advantages in the selection of 45 per cent relative humidity for lithographic plants. For the plant without controlled atmosphere, every precaution should be taken to protect paper from atmospheric changes after starting the first printing. The paper should be protected between printings by covering with waterproof wrappers.

Thickness standardization of plates was found important to insure uniformity of plate stretch in clamping plates in place. With neither ink nor water on the plate, changes in printing pressure affected register only slightly and the effects of pressure variations were even less with ink alone and with water alone. Prints may be lengthened in the around-the-cylinder direction by transferring packing from the plate to the blanket or adding packing to the impression cylinder. The amount of water used did not appear important as doubling the amount used had no serious immediate effects. The effect of ink was contingent on the extent of the area covered, the presence of large solid ink areas resulting in increased register troubles.

Paper characteristics are important. The best register was obtained on the papers that had received the least drastic beating and jordanning in manufacture. Internal sizing was desirable but the amount used, within normal limits, was relatively unimportant. Approximately one-half normal sizing gave best results. The presence of surface sizing had no marked effect on the papers studied.

The closeness with which the imprint length on the paper agrees with the length of the plate design on the first color will indicate the closeness of register that may be expected with subsequent printings. By measuring the first sheets printed on the first color, information may be obtained at the start of any multicolor "job" that will indicate whether register trouble will be encountered in succeeding printings. A first print on the paper longer than the plate design along the back edge is always indicative of register troubles. The special rule described should be of great value to the lithographer for use here in forestalling trouble.

VII. ACKNOWLEDGMENT

Acknowledgment is made of the invaluable assistance in this study of the advisory committee from the Lithographic Technical Foundation; of the Lowe Paper Co., who made the services of Miss R. M. Cobb available; of the American Lithographic Co. in the experimental printings; and of the following paper manufacturers who furnished the experimental papers: Dill & Collins Co., Rex Paper Co., West Virginia Pulp & Paper Co.

WASHINGTON, July 12, 1932.

CREEP AT ELEVATED TEMPERATURES IN CHROMIUM-VANADIUM STEELS CONTAINING TUNGSTEN OR MOLYBDENUM

By William Kahlbaum[1] and Louis Jordan

ABSTRACT

Determinations of creep at temperatures between 750° and 1,100° F. were made on two tungsten-chromium-vanadium and a molybdenum-chromium-vanadium steel. These steels were tested as tempered after mechanical working (rolling) and are compared with steels of similar compositions which had been oil quenched and tempered.

CONTENTS

	Page
I. Introduction	441
II. Method of testing	443
III. Results	444
IV. Discussion and summary	447

I. INTRODUCTION

This paper reports the results of tests of creep in tension made on 3 alloy steels; namely, 2 tungsten-chromium-vanadium steels and 1 molybdenum-chromium-vanadium steel. The chemical compositions of these steels, their mechanical properties at room temperature, and the heat treatments to which they were subjected prior to testing are all listed in Table 1. There are also included in Table 1 three additional steels (a tungsten-chromium-vanadium steel, a chromium-molybdenum, and a molybdenum-chromium-vanadium steel) which had been tested previously for creep.[2] These steels so closely resemble the steels tested in the present work as to make desirable a comparison of the results of creep tests of the two groups.

The two tungsten-chromium-vanadium steels of the present report differ chiefly in carbon content (0.50, and 0.38 per cent). One of the steels previously tested (EE1139) very closely duplicated the two tungsten-chromium-vanadium steels of this report, especially the higher carbon steel. The heat treatments, however, differed in the two cases. The two steels recently tested were simply tempered at a rather high temperature after rolling, while the similar steel of the earlier work was oil quenched and tempered.

The third steel with which this report is primarily concerned is a molybdenum-chromium-vanadium steel (SE208) containing about 1.2 per cent manganese. This steel is compared with two of the steels previously tested, of which one (E1549) was of a very similar composition, also with high manganese (0.95 per cent) but without vanadium; the other was also similar to steel SE208 of the present report, except that this comparison steel (E1490) was of higher carbon and lower manganese content.

[1] Research associate, representing The Midvale Co., Philadelphia, Pa.
[2] H. J. French, William Kahlbaum, and A. A. Peterson, Flow Characteristics of Special Fe-Ni-Cr Alloys and Some Steels at Elevated Temperatures, B. S. Jour. Research, vol. 5 (RP192), p. 125, 1930.

TABLE 1.—*Compositions, mechanical properties, and heat treatment of alloy steels tested for "creep" in tension*

Designation	Chemical composition							Mechanical properties [1]				Mechanical and heat treatment
	C	Mn	Si	Cr	V	W	Mo	Tensile strength	Proportional limit [2]	Elongation in 2 inches	Reduction area	
	Per cent	*Per cent*	*Per cent*	*Per cent*	*Per cent*	*Per cent*	*Per cent*	*Lbs./in.²*	*Lbs./in.²*	*Per cent*	*Per cent*	
EE1546	0.50	0.62	0.76	2.35	0.27	1.66	------	183,500	148,000	13.2	38.5	Rolled; 1,275° F., 1 hour; cooled slowly.
EE1554	.28	.49	.38	2.24	.29	1.92	------	167,500	138,000	16.0	47.8	Rolled; 1,275° F., 1 hour; cooled slowly.
SE208	.34	1.18	.17	1.60	.21	------	0.47	171,500	146,000	18.0	56.3	Rolled; 1,650° F., 30 minutes; air cooled; 1,200° F., 30 minutes; air cooled.
EE1139 [3]	.46	.37	.19	2.2	.25	1.65	------	231,500	207,000 (y. p.) [4]	7.8	22.8	Rolled; 1,400° F., 2 hours; cooled slowly; 1,740° F., 1 hour, oil; 1,000° F., 1 hour; air cooled.
E1549 [3]	.53	.95	.23	1.07	------	------	.44	143,000	124,000 (y. p.) [4]	[5] 18.7	[5] 56.0	Forged; 1,550° F., 1 hour, oil; 1,200° F., 4 hours, cooled slowly.
E1490 [3]	.75	.52	.31	1.45	.27	Ni .15	.54	174,000	------	[5] 7.5	[5] 16.7	Forged; 1,550° F., 1 hour, oil; 1,100° F., 4 hours, cooled slowly.

[1] Determined at room temperature.
[2] Determined on the basis of a strain of 5×10^{-4} indicating departure from a straight line.
[3] Steels previously tested; included for convenience of comparison.
[4] Yield point by drop of beam.
[5] Determined on tensile specimens with a section ⅝ by 0.1565 inch.

II. METHOD OF TESTING

The method employed for determining "creep" was substantially the same as previously described,[3] except that all of the horizontal furnaces and loading machines were replaced by vertical units, as shown in Figure 1. As a result the frictional losses of the mechanical lever loading system were materially reduced.

Figure 1 shows the method of loading the specimen in the vertical furnace. The specimen was 0.250 inch in diameter within the 2-inch gage length. The top adapter was suspended from a spherical seat.

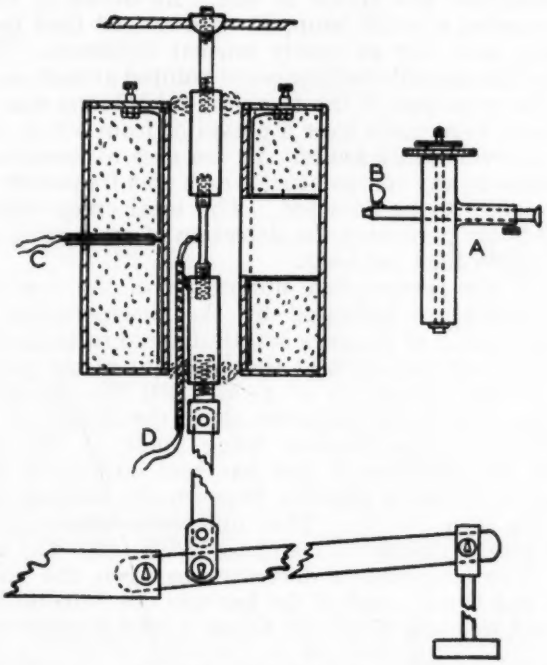

FIGURE 1.—*Diagram of vertical test units for creep tests at elevated temperatures*

A, traveling microscope; *B*, lamp; *C*, furnace control thermocouple; *D*, specimen temperature thermocouple.

The temperature of the specimen was measured by the thermocouple *D*, the hot junction of which was tightly wired to the surface of the specimen at the middle of the gage length. An automatic temperature control which regulated the temperature of the furnace was actuated by the thermocouple *C*, the hot junction of which was placed close to the furnace windings. During operation the top and bottom openings of the furnace around the adapters were tightly packed with asbestos to minimize convection currents within the furnace. A narrow rectangular opening through one side of the furnace (covered except when actually observing the gage marks) permitted measurements of the extension of the specimen during testing.

The gage length of the specimen was defined by cutting a shallow groove close to the fillet at each end of the reduced section of the

[3] See footnote 2, p. 441.

specimen and securing tightly in this groove a loop of 32 B. & S. gage (0.008 inch diameter) platinum wire. The coefficient of expansion of platinum being less than that of steel, the wire did not loosen as the temperature rose.

The expansion was observed by means of a traveling microscope of long focus (*A*, fig. 1) whose motion was governed by a screw of 0.5 mm pitch and a disk carrying 100 divisions. The value of one division on the disk was, therefore, 0.005 mm (2×10^{-4} inch).

The accuracy of the readings depended considerably on the illumination, and therefore the illumination was kept as constant as possible throughout the period of test. As shown in Figure 1, the microscope carried a small lamp, *B*, so arranged that the rays were reflected from the wire at nearly normal incidence. Through the telescope the illuminated spot appeared pointed at each end, and upon the points the cross hair of the traveling microscope was set.

Observations were made over a period of from 400 to 1,000 hours, usually at intervals of 24 hours. In the case of specimens carrying the lower loads at any temperature, there was frequently insufficient creep in 24 hours to be detected. The total creep over periods of 400 to 1,000 hours permitted the detection of creep rates of the order of 10^{-6} inches per inch per hour.

A survey of the temperature uniformity of the specimen showed that the temperature indicated by the thermocouple, *D*, at the surface of the middle of the gage length differed from the temperature at the center of the specimen at the midpoint of the gage length by only 1° F. at 800° F. and by 3° F. at 1,200 °F. Furthermore, the maximum variation in temperature along the length of the test bar (the temperature measurements being made at the ends of the specimen in the shoulder of the bar just outside of the reduced section) was in all cases greatest between the bottom end and the middle of the gage length. This difference amounted to 23° F. (13° C.) at 800° F. (426° C.) and to 18° F. (10° C.) at 1,200° F. (648° C.). The temperature difference between the middle of the gage length and the top end of the bar was not detectable at 800° F. (426° C.), and was only 9° F. (5° C.) at 1,200° F. (648° C.).

III. RESULTS

The time-extension curves for the three steels, showing on each curve the stress in lbs./in.^{2} of original cross section and, in parentheses, the identification number of the specimen, are given in Figures 2, 3, and 4. The two tungsten-chromium-vanadium steels were tested at 750°, 850°, 950°, 1,050°, and 1,100° F.; the single molybdenum-chromium-vanadium steel at 650°, 850°, and 1,050° F.

In Figures 5, 6, and 7 are plotted for the several testing temperatures the stress and the initial flow; that is, the relatively rapid deformation at the time of, or immediately after, loading. Also, there are plotted the stress and the average rates of flow, calculated from the so-called second stage of the time-extension curves; that is, that portion of rather uniform rate of extension following the initial flow.

Figures 8, 9, and 10 show the stress which, at any selected temperature, results in 0.1, 1, 2, or 5 per cent secondary elongation, or creep, in 1,000 hours. These figures also show in some cases the stress resulting in 0.1, 1, or 2 per cent initial elongation preceding the stage of secondary elongation.

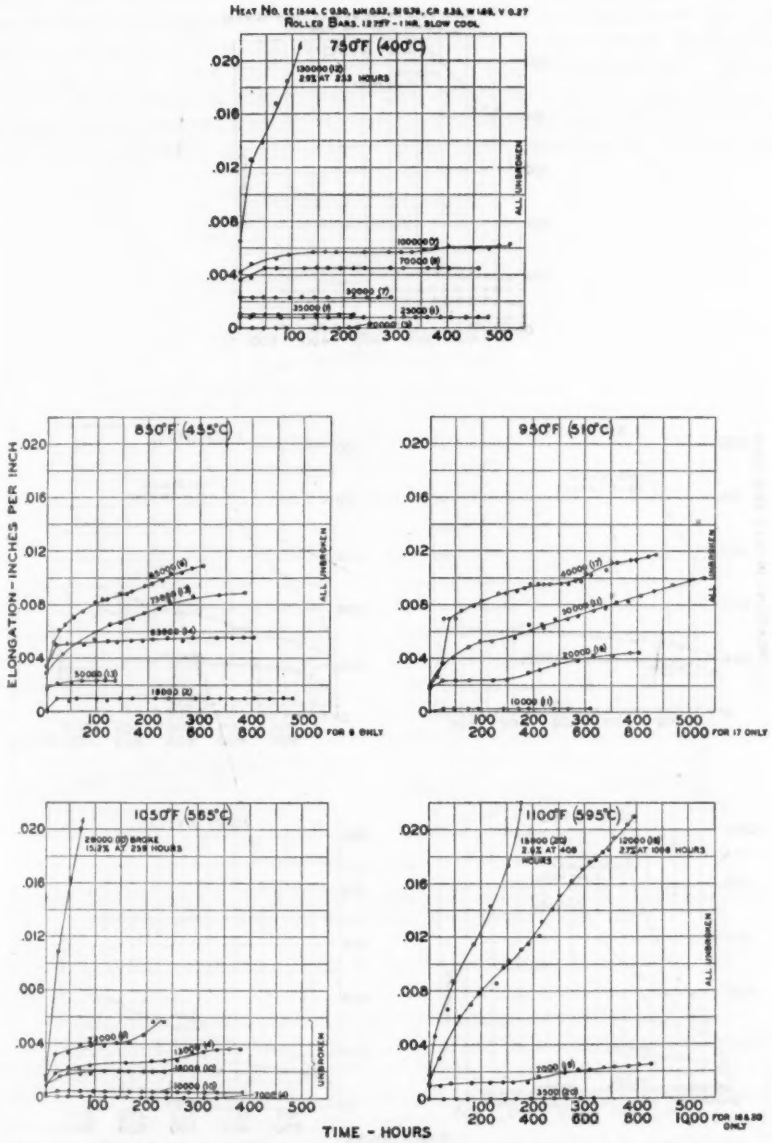
HEAT NO. EE 1546. C 0.50, MN 0.52, SI 0.30, CR 2.35, W 1.65, V 0.27
ROLLED BARS, 1.2"SQ - 1 HR. SLOW COOL
750°F (400°C)
850°F (455°C)
950°F (510°C)
1050°F (565°C)
1100°F (595°C)
ELONGATION - INCHES PER INCH
TIME - HOURS
ALL UNBROKEN
UNBROKEN

FIGURE 2.—*Time-elongation curves of tungsten-chromium-vanadium steel EE1546 under different loads and at different temperatures*

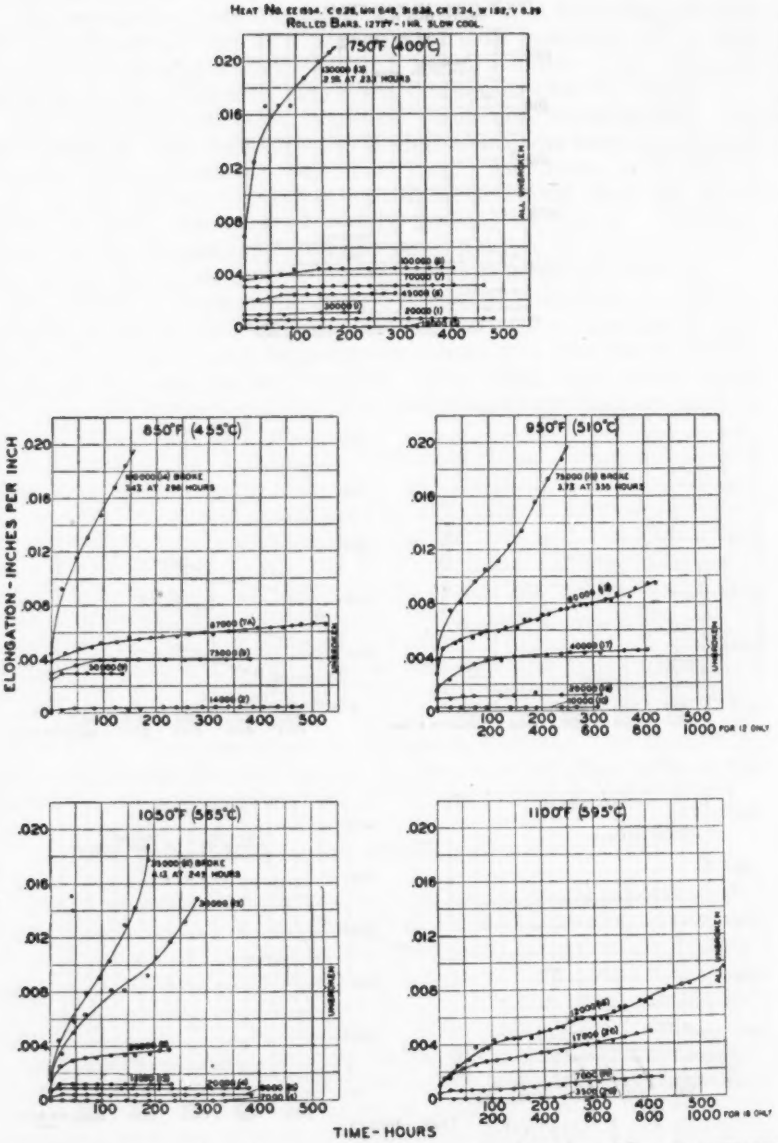

FIGURE 3.—*Time-elongation curves of tungsten-chromium-vanadium steel EE1554 under different loads and at different temperatures*

IV. DISCUSSION AND SUMMARY

The discussion of the results of the present creep tests and correlation of these results with previously tested steels of similar compositions is most conveniently based on Figure 11. In this figure the top and bottom of a solid black rectangle indicate, respectively, the stress producing 1 per cent and 0.1 per cent initial deformation. When there is given only a small solid triangle, the base of the triangle indicates the stress producing 0.1 per cent deformation and there is no value for 1 per cent deformation. Similarly, the open (light) rec-

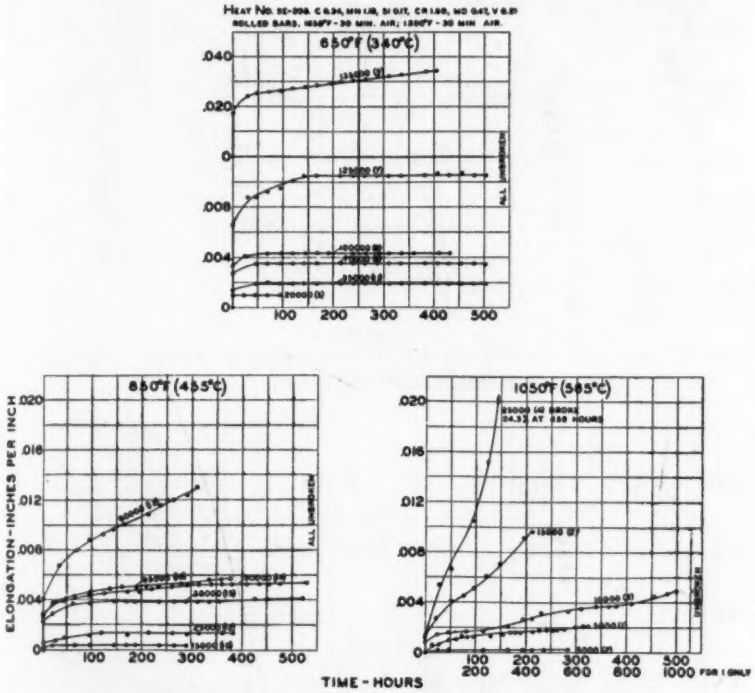

FIGURE 4.—*Time-elongation curves of molybdenum-chromium-vanadium steel SE208 under different loads and at different temperatures*

tangles indicate secondary flow in 1,000 hours of 1 per cent and 0.1 per cent.

A comparison of the two tungsten-chromium-vanadium steels of the present tests (EE1546 and EE1554) shows that appreciably higher stresses are sustained by the steel of lower carbon content (EE1554) at 860°, 950°, and 1,000° F. before 0.1 or 1 per cent creep results than is the case with the higher carbon steel. Also there is for the lower carbon steel a wider range at 950° and 1,000° F. between the stresses producing 0.1 and 1 per cent creep than for the higher carbon steel.

The previously tested tungsten-chromium-vanadium steel (EE1139) was oil hardened and tempered before testing, while steel EE1546 of very similar composition was simply tempered after rolling. From Figure 11 it appears that at the higher testing temperatures, 950°

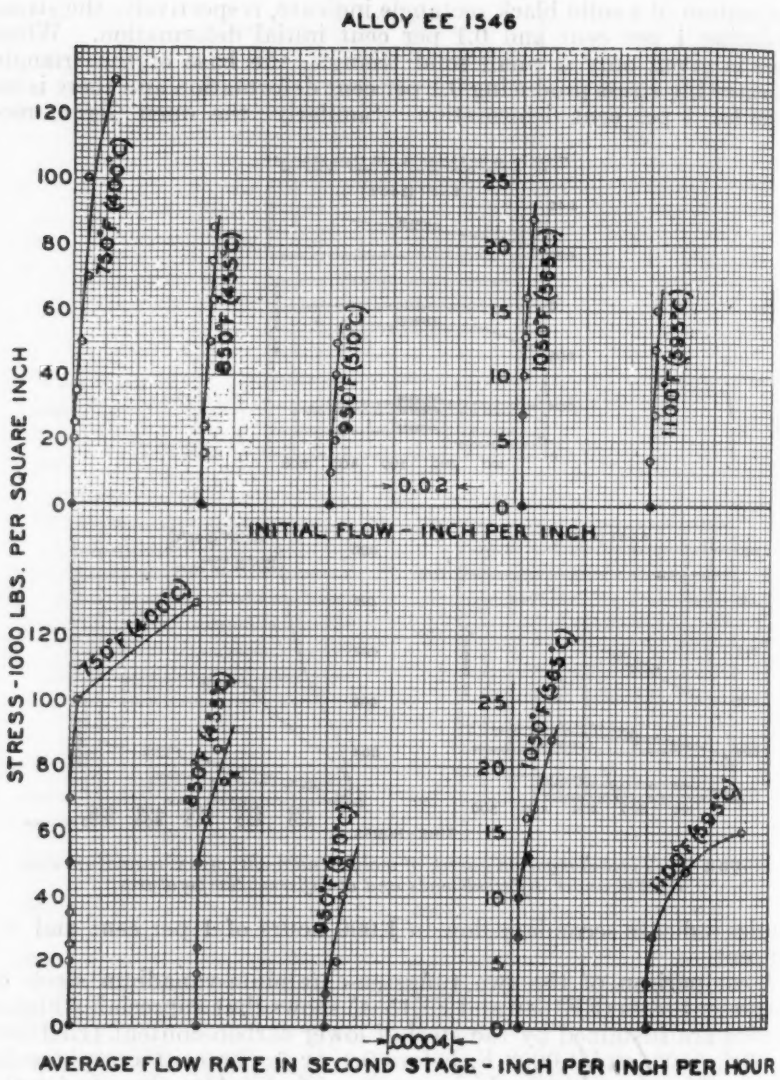

FIGURE 5.—*Flow data for tungsten-chromium-vanadium steel EE1546 at different temperatures*

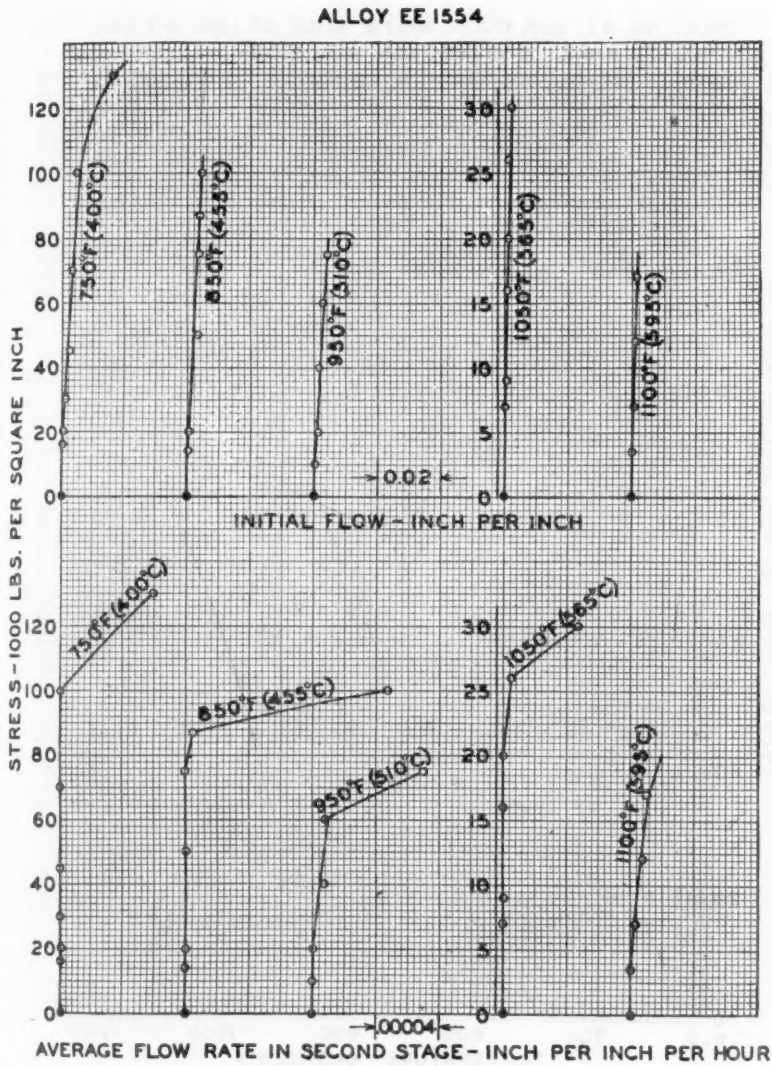

FIGURE 6.—*Flow data for tungsten-chromium-vanadium steel EE1554 at different temperatures*

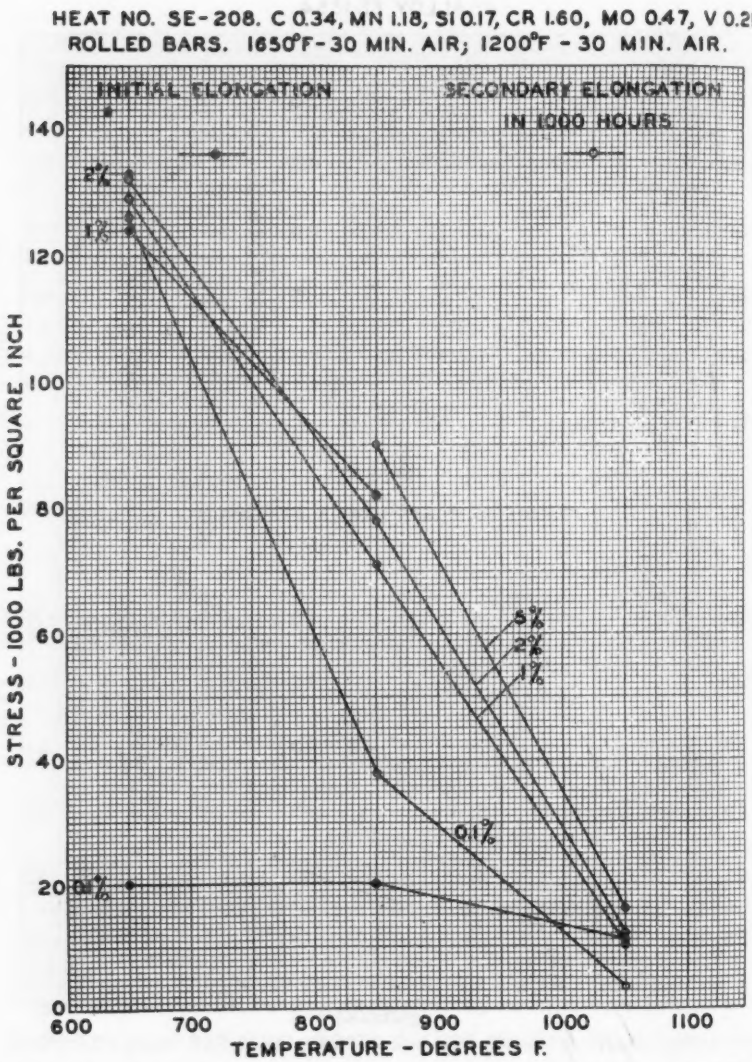

FIGURE 7.—*Flow data for molybdenum-chromium-vanadium steel SE208 at different temperatures*

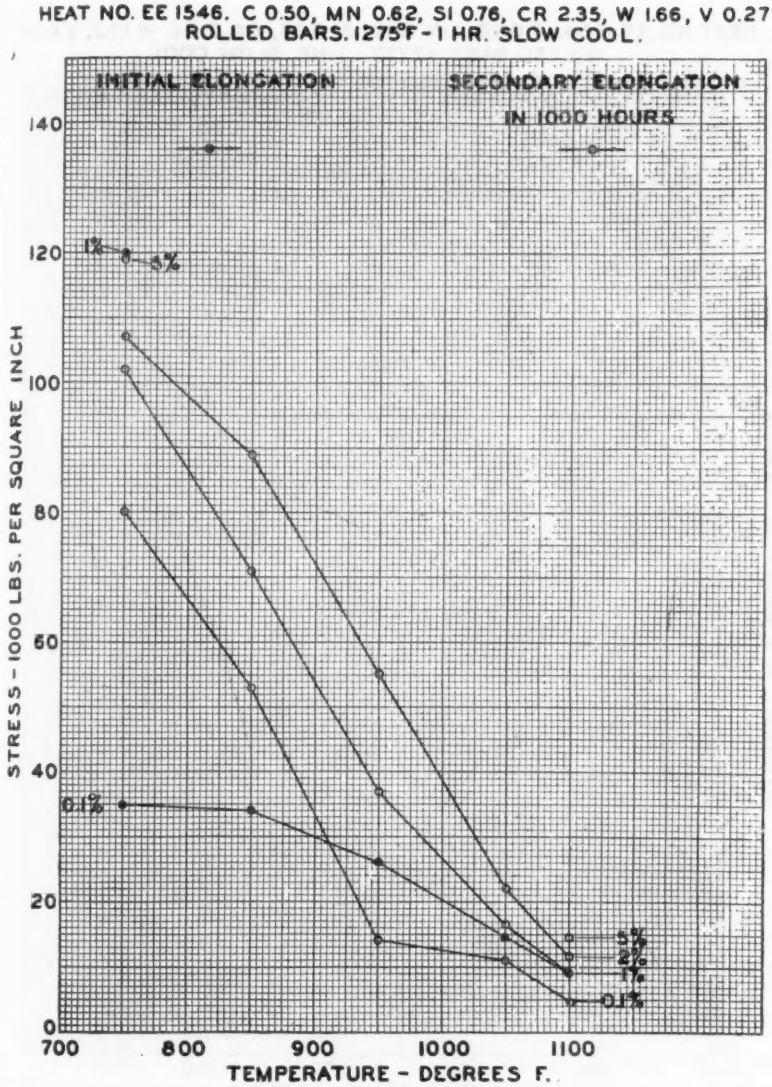

FIGURE 8.—*Flow chart for tungsten-chromium-vanadium steel EE1546 at elevated temperatures*

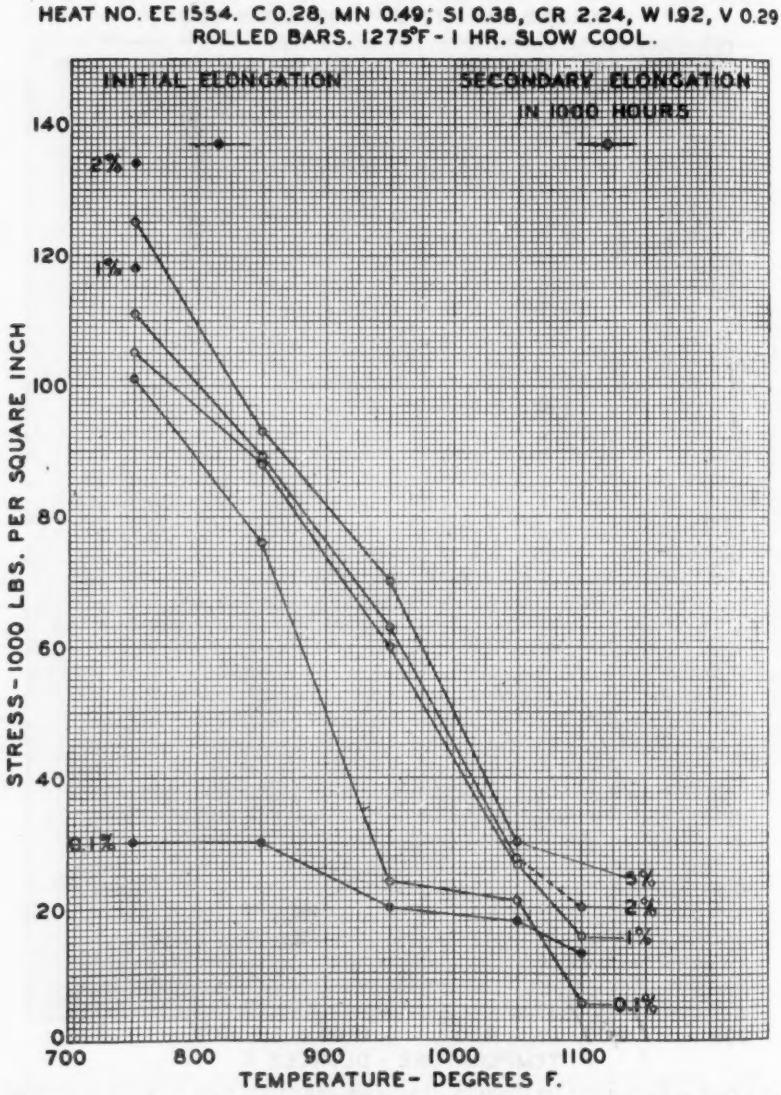

FIGURE 9.—*Flow chart for tungsten-chromium-vanadium steel EE1554 at elevated temperatures*

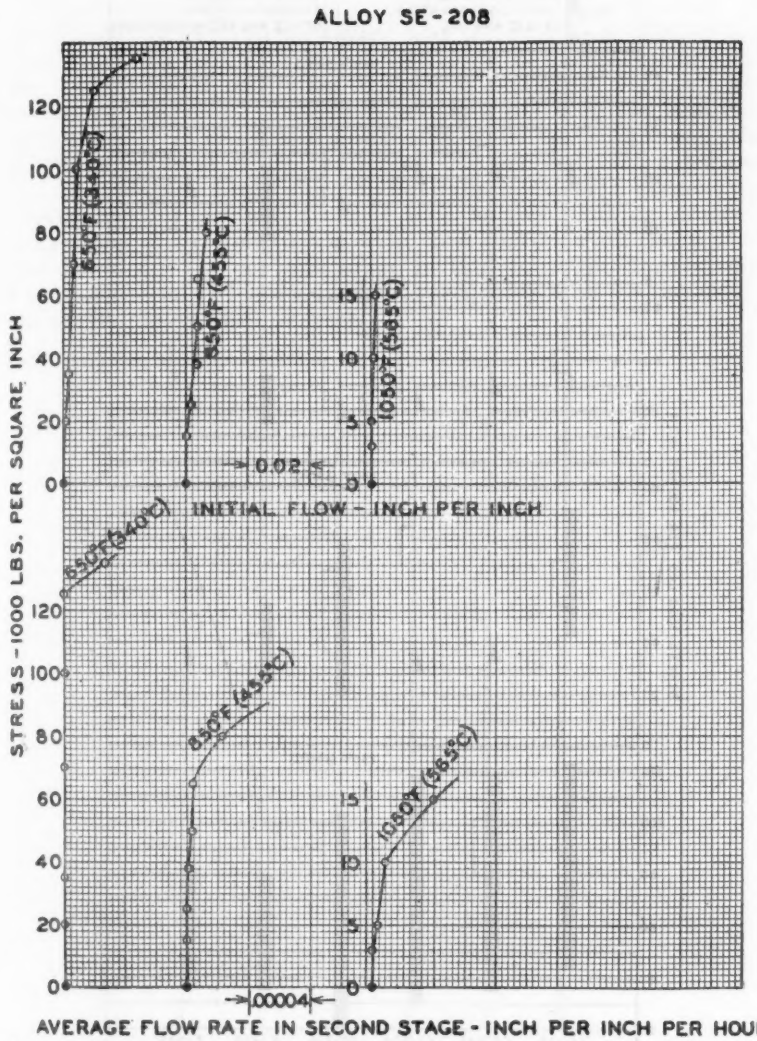

FIGURE 10.—*Flow chart for molybdenum-chromium-vanadium steel SE 208 at elevated temperatures*

132919—32——12

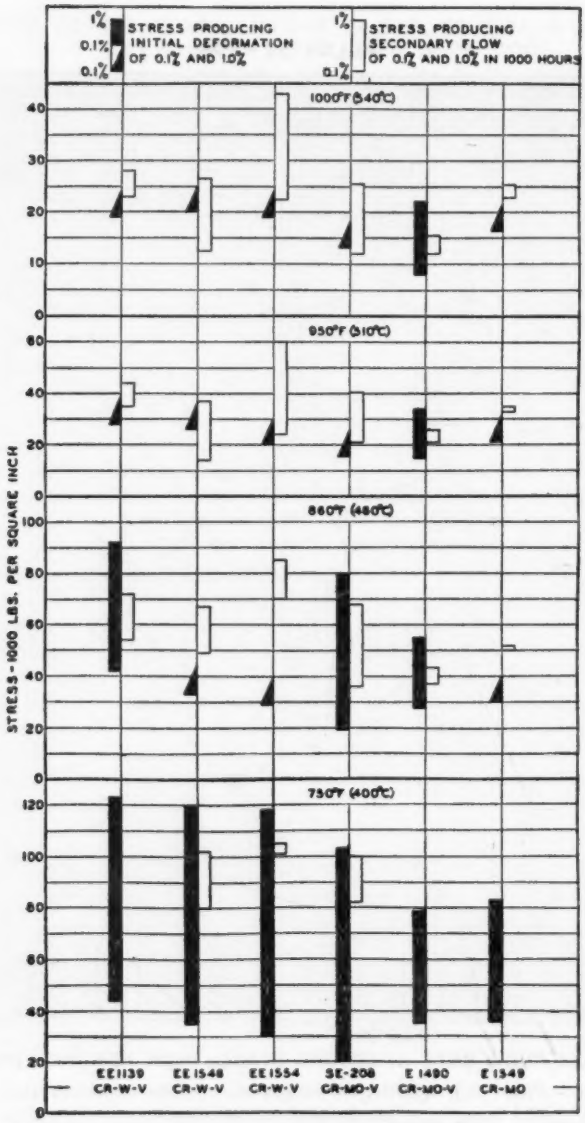
1% 0.1% 0.1% STRESS PRODUCING INITIAL DEFORMATION OF 0.1% AND 1.0%
1% 0.1% STRESS PRODUCING SECONDARY FLOW OF 0.1% AND 1.0% IN 1000 HOURS
1000°F (540°C)
950°F (510°C)
860°F (460°C)
750°F (400°C)
STRESS - 1000 LBS. PER SQUARE INCH
EE1139 CR-W-V
EE1548 CR-W-V
EE1554 CR-W-V
SE-208 CR-MO-V
E 1490 CR-MO-V
E 1349 CR-MO

FIGURE 11.—*Comparison of steels on the basis of the stresses producing both initial deformation and secondary flow (secondary flow is over period of 1,000 hours)*

and 1,000° F., the stress producing 0.1 per cent creep was appreciably higher in the quenched and tempered steel. However, this hardened and tempered steel showed 1 per cent creep at stresses very much lower than the corresponding rolled-and-tempered steel (EE1554) at 860°, 950°, and 1,000° F.

The other comparison to be made in Figure 11 is between the two molybdenum-chromium-vanadium steels, SE208 (normalized and tempered) and E1490 (oil quenched and tempered), the latter steel being considerably higher in carbon and lower in manganese than the former. The greater resistance to creep of the lower carbon higher manganese steel at all of the testing temperatures involved is obvious from Figure 11. It has also a noticeably wider working range; that is, the range between stress producing 0.1 per cent and 1 per cent creep. The simple chromium-molybdenum steel, with about 1 per cent manganese, was found to have such narrow working ranges of stress as to suffer by comparison with steel SE208, even through the stresses producing 0.1 per cent creep in the chromium-molybdenum steel were appreciably higher at all temperatures than for the molybdenum-chromium-vanadium steel.

WASHINGTON, July 13, 1932.

○